NUREG/CR-5418

Near-Surface Neotectonic Deformation Associated With Seismicity in the Northeastern United States

Prepared by S. S. Alexander, D. P. Gold, T. W. Gardner
R. L. Slingerland, C. P. Thornton

Department of Geosciences
Pennsylvania State University

Prepared for
U.S. Nuclear Regulatory Commission

AVAILABILITY NOTICE

Availability of Reference Materials Cited in NRC Publications

Most documents cited in NRC publications will be available from one of the following sources:

1. The NRC Public Document Room, 2120 L Street, NW, Lower Level, Washington, DC 20555

2. The Superintendent of Documents, U.S. Government Printing Office, P.O. Box 37082, Washington, DC 20013-7082

3. The National Technical Information Service, Springfield, VA 22161

Although the listing that follows represents the majority of documents cited in NRC publications, it is not intended to be exhaustive.

Referenced documents available for inspection and copying for a fee from the NRC Public Document Room include NRC correspondence and internal NRC memoranda; NRC Office of Inspection and Enforcement bulletins, circulars, information notices, inspection and investigation notices; Licensee Event Reports; vendor reports and correspondence; Commission papers; and applicant and licensee documents and correspondence.

The following documents in the NUREG series are available for purchase from the GPO Sales Program: formal NRC staff and contractor reports, NRC-sponsored conference proceedings, and NRC booklets and brochures. Also available are Regulatory Guides, NRC regulations in the *Code of Federal Regulations*, and *Nuclear Regulatory Commission Issuances*.

Documents available from the National Technical Information Service include NUREG series reports and technical reports prepared by other federal agencies and reports prepared by the Atomic Energy Commission, forerunner agency to the Nuclear Regulatory Commission.

Documents available from public and special technical libraries include all open literature items, such as books, journal and periodical articles, and transactions. *Federal Register* notices, federal and state legislation, and congressional reports can usually be obtained from these libraries.

Documents such as theses, dissertations, foreign reports and translations, and non-NRC conference proceedings are available for purchase from the organization sponsoring the publication cited.

Single copies of NRC draft reports are available free, to the extent of supply, upon written request to the Office of Information Resources Management, Distribution Section, U.S. Nuclear Regulatory Commission, Washington, DC 20555.

Copies of industry codes and standards used in a substantive manner in the NRC regulatory process are maintained at the NRC Library, 7920 Norfolk Avenue, Bethesda, Maryland, and are available there for reference use by the public. Codes and standards are usually copyrighted and may be purchased from the originating organization or, if they are American National Standards, from the American National Standards Institute, 1430 Broadway, New York, NY 10018.

DISCLAIMER NOTICE

NUREG/CR-5418
RA

Near-Surface Neotectonic Deformation Associated With Seismicity in the Northeastern United States

Manuscript Completed: July 1989
Date Published: October 1989

Prepared by
S. S. Alexander, D. P. Gold, T. W. Gardner
R. L. Slingerland, C. P. Thornton

Department of Geosciences
Pennsylvania State University
503 Deike Building
University Park, PA 16802

Prepared for
Division of Engineering
Office of Nuclear Regulatory Research
U.S. Nuclear Regulatory Commission
Washington, DC 20555
NRC FIN D1150
Under Contract No. NRC-04-85-111-01

ABSTRACT

For the Lancaster, PA seismic zone a multifaceted investigation revealed several manifestations of near-surface, neotectonic deformation. Remote sensing data together with surface geological and geophysical observations, and recent seismicity reveal that the neotectonic deformation is concentrated in a NS-trending fault zone some 50 km in length and 10-20 km in width. Anomalies associated with this zone include distinctive lineament and surface erosional patterns; geologically recent uplift evidenced by elevations of stream terraces along the Susquehanna River; and localized contemporary travertine deposits in streams down-drainage from the inferred active fault zone.

In the Moodus seismic zone the frequency of tectonically-controlled lineaments was observed to increase in the Moodus quadrangle compared to adjacent areas and dominant lineament directions were observed that are perpendicular and parallel to the orientation of the maximum horizontal stress direction (N80-85E) recently determined from in-situ stress measurements in a 1.5 km-deep borehole in the seismic zone and from well-constrained earthquake focal mechanisms.

One of the most important results of this study was the identification of travertine as a promising new indicator of neotectonic fault movements in areas underlain by limestone and dolomite. Using the theory, which predicts that travertine deposits will occur downstream from the surface projection of active faults in carbonate-rich terranes, contemporaneous travertine deposits were discovered just downstream from the Fruitville fault which is associated with the major recent earthquake activity in the Lancaster area.

TABLE OF CONTENTS

LIST OF FIGURES

LIST OF FIGURES (continued)

LIST OF TABLES

NEAR-SURFACE NEOTECTONIC DEFORMATION ASSOCIATED WITH SEISMICITY IN THE NORTHEASTERN UNITED STATES

EXECUTIVE SUMMARY

The main objectives of this investigation were (1) to examine systematically the available imagery for selected seismically active areas of the northeastern United States for evidence of near-surface deformation; (2) to determine, via field geologic studies, the nature of these anomalies; and (3) to look for manifestations on the imagery or in the field of specific types of near-surface deformation expected from tectonic models of seismogenic structures.

The two geographic areas of investigation chosen for detailed study were the Lancaster, Pennsylvania seismic zone and the Moodus, Connecticut seismic zone. Rather than investigate a third specific site it was decided to focus on the generic problem of evaluating a new indicator of neotectonic deformation, travertine deposits in small streams.

For the Lancaster seismic zone the multifaceted investigation revealed several manifestations of near-surface, neotectonic deformation. Remote sensing data together with surface geological and geophysical observations, and recent seismicity reveal that the neotectonic deformation is concentrated in a NS-trending fault zone some 50 km in length and 10-20 km in width. Anomalies associated with this zone include distinctive lineament and surface erosional patterns; geologically recent uplift evidenced by elevations of stream terraces along the Susquehanna River; and localized contemporary travertine deposits in streams down-drainage from the inferred fault zone. Details of these results appear later in this report, especially in the appendices.

In the Moodus seismic zone results of previous ground-based geological studies were combined with remote sensing observations (aerial photography, SLAR imagery, and SPOT imagery) and used to look for evidence of near-surface deformation associated with the zone of recent seismicity. Lineament frequency was observed to increase in the Moodus quadrangle compared to adjacent areas and dominant lineament directions were observed that are perpendicular and parallel to the orientation of the maximum horizontal stress direction (N80-85E), recently determined from in-situ stress measurements in a 1.5 km-deep borehole in the seismic zone and from well-constrained earthquake focal mechanisms. These dominant lineament orientations are those expected in the present thrust stress regime which has generated recent

earthquakes in the Moodus area. No geochemical anomalies or travertine deposits were found to be associated with the zone of seismicity. The only potential source of travertine in the area is one metamorphic rock unit, which upon weathering produces calcium carbonate. However concentrations necessary to cause precipitation of travertine were not found in any of the streams sampled. Details of the Moodus investigation appear as an appendix to this report.

One of the most important general results of this study was the identification of travertine as a possible new indicator of neotectonic fault movements in areas underlain by limestone and dolomite. The working hypothesis (developed originally by C.P. Thornton) is that water reaching the surface along fault gouge zones will emerge saturated or supersaturated in carbon dioxide and then will quickly precipitate in nearby small streams to produce readily-observed travertine (tufa) deposits. No such deposits are expected to be associated with dormant faults because the high surface area to volume carbonate material in the fault gouge will have been dissolved and carried away shortly after the last fault movement. If this hypothesis is correct and generally applicable, then recently-active faults should be found just upstream from observed trevertine deposits. Alternatively stated, travertine deposits are predicted to occur downstream from the surface projection of active faults in carbonate-rich terranes. Guided by this theory a ground-based survey was carried out in the Lancaster seismic zone and contemporaneous travertine deposits were discovered just downstream from the Fruitville fault which is associated with the major earthquake activity in the area; none had previously been reported for this area. The travertine is presently being deposited at all the sites where it was found.

The possibility of age-dating travertine deposits suggests that the time history of nearby fault activity might be reconstructed as well. Late in this study an attempt was made to age-date a travertine deposit from the Quicksburg, VA area using a radiocarbon method. The date obtained was 4210 ± 60 years, which represents a lower bound for the age of last fault movements producing the deposit. However, travertine is presently being deposited approximately 5 km upstream indicating recent fault movement there. This area has experienced historic earthquake activity indicating that neotectonic deformation is occurring. The travertine found in the Lancaster seismic zone is currently being deposited as evidenced by twigs and other debris entrained in the deposit and by its coating of stream pebbles. Further investigation of this new indicator of neotectonic fault movement is clearly warranted.

INTRODUCTION

Rationale for Choices of Areas of Concentrated Study

The Lancaster Seismic Zone

The area around Lancaster, PA historically has been one of the most active areas in Pennsylvania. The largest instrumentally-recorded event in that area was the recent Easter Sunday m_{bLg} 4.2 earthquake on April 23, 1984, which was felt as far south as Washington, DC and northern Virginia, as far north as Connecticut and as far west as Pittsburgh. Because of the available data for this event and other smaller events in the area, it was possible to characterize the active tectonic environment in this area and better interpret potential near-surface indicators of neotectonic deformation. The approach to looking for such indicators was to carry out an integrated study using geophysical, geological and remote sensing observations. Finally this active seismic area was chosen because there are nearby operating nuclear power plants (Three Mile Island, Peach Bottom) for which this zone constitutes part of the seismic hazard.

The Moodus, Connecticut, Seismic Zone

The area around Moodus, CT is also one that has experienced a significant history of earthquake activity and it is an area where considerable geological, geophysical, and remote sensing data are available to characterize the tectonic environment. From a tectonic point of view this area may mark the transition from the ubiquitous ENE maximum compressive stress to the south and west to WNW (or mixed) stress domain that characterizes much of New England. A large EPRI study recently completed shows that there are mixed results from focal mechanism solutions (some ENE, some WNW maximum horizontal compressive stress directions) from Moodus northward through New England; direct stress measurements also give mixed results. Two borehole stress measurements recently made near Moodus under NRC sponsorship (NUREG/CR4623 EI-1126) indicate high horizontal stresses and WNW maximum compression. If these results reflect the tectonic stress near Moodus, then there must be a significant change between this region and the nearby Ramapo system to the southwest. Recently-completed deep (1 km) borehole stress measurements at Kent Cliffs, NY (about 80 km from Moodus) together with a large number of well-constrained focal mechanism solutions in southeastern New York clearly establish a dominant ENE orientation for the maximum compressive stress in this neighboring region. The nature of near-surface neotectonic deformation near Moodus is anticipated to be different, depending on which of these stress orientations is active. In particular, geomorphic evidence such as terraces and stream patterns and gradients should be sensitive to the prevailing stress conditions.

Another reason for focusing on the Moodus area was that a 1.5 km deep borehole was planned to be drilled in the Moodus seismic zone during early to mid-1987 for the purpose of measuring the tectonic stress at greater depths than the shallow NRC boreholes sampled and determining whether this zone is truly anomalous with respect to the neighboring seismically active area in southeastern NY. This experiment, jointly sponsored by the Empire State Electric Energy Corporation, Northeast Utilities, and EPRI, is highly relevant to the present study of near-surface neotectonic deformation.

As in the Lancaster case there are nearby operating plants for which this zone constitutes part of the seismic hazard.

A Potential New Indicator of Geologically Recent Fault Movement

As the initial work on this project developed, discussions with a colleague at Penn State, Prof. Charles Thornton, revealed that he had observed the distribution of travertine deposits in northern Virginia in his Ph.D. field area and concluded that they were uniquely associated with nearby, active faults. He postulated that water coming to the surface along a fault gouge zone in limestone becomes saturated with calcium carbonate and upon entering a nearby surface stream quickly becomes supersaturated and precipitates to form the travertine (tufa) deposits that he observed. They do not occur upstream of the faults even though limestone rock units do, and this process is postulated to occur only when there is freshly brecciated limestone to provide a large surface area to volume ratio for limestone to interact with the groundwater.

Localization of the travertine downstream from mapped fault traces is taken to indicate that the source of the calcium carbonate-saturated waters was the fault zones along which crushing of the limestones has resulted in their higher-than-normal solubility. However, it seems unlikely that this crushing dates from the time of origin of these faults some 250 m.y. ago--the supply of crushed limestone produced at that time should long since have been exhausted. The more probable alternative is that geologically-recent movement has occurred along these faults, producing a new supply of crushed limestone for the circulating ground water to act on. On this hypothesis, the ages of the travertine deposits would reflect the times of movement along these faults.

Thus, it was postulated that travertine deposits may be used to identify nearby zones of geologically-recent fault movement and that, if true, there is a possibility of age dating the sequence of local travertine deposits to fix the intervals of past active faulting. Travertine (or tufa) deposits are located along many streams in the Shenandoah Valley of Virginia, in many (and perhaps in all) instances just downstream from the points where these streams cross the outcrops of thrust faults. The closest reported travertine deposit to the Lancaster seismic zone at the start of this study was near McConellsburg, PA, approximately 30 km to the west.

If this technique proves to be generally applicable, it would be possible to search for such deposits elsewhere in the northeast using remote sensing techniques, because the deposits are distinctive in appearance and will not be obscured by vegetation along the streams. A systematic ground-based search of small streams in areas of interest would also be an effective means of locating such deposits.

NEOTECTONIC DEFORMATION IN THE LANCASTER SEISMIC ZONE

Summary

This study is focused on the contemporary tectonics of the Lancaster County in southeastern Pennsylvania. The neotectonic deformation associated with recent seismicity in this zone is inferred from the source mechanism of the largest recent event in the region, the April 23, 1984, magnitude 4.2, maximum intensity VI earthquake. In addition, the principal stresses thus derived, historical seismicity, and geological and geophysical observations are utilized in defining a north–south–trending zone of recent faulting, the Lancaster seismic zone. This zone is approximately 50 km in length and 10–20 km in width, encompassing the city of Lancaster.

Introduction

Lancaster County is the most seismically active area in Pennsylvania, with several magnitude 3.0 or greater earthquakes in the past 25 years. The goal of this part of the investigation was to understand the present tectonic conditions and associated neotectonic features of the region, and thus shed light on the cause of contemporary seismicity.

A multi–disciplinary approach toward the identification and analysis of neotectonic sites was applied to the Lancaster County region. This approach utilizes six different paths of investigation, simultaneously, in order to arrive at the best possible interpretation. The six areas of investigation are: recent seismicity; structural geology; geomorphology; lineaments and remote sensing; applied geophysics; and historical seismicity. Appendix A contains a complete description of this investigation represented by a M.S. thesis completed by David Stockar as part of the project.

Recent Seismicity

On April 23, 1984 at 1:36 U.T. (6:36 pm, 22 April EST), Lancaster County experienced one of the largest recorded earthquakes in Pennsylvania. The region of maximum intensity (MM = VI) for the event occurred south of the city of Lancaster, near Marticville (Figure 1). Seismic records of the event give a magnitude of 4.2, with a strong audible component (Scharnberger and Howell, 1985).

A foreshock of magnitude 3.0 occurred on April 19, at 4:55 U.T. (11:55 pm EST, 18 April). The region of maximum intensity (MM = IV) for this event was centered 8–10 km south of the mainshock. Both of these mainshock and

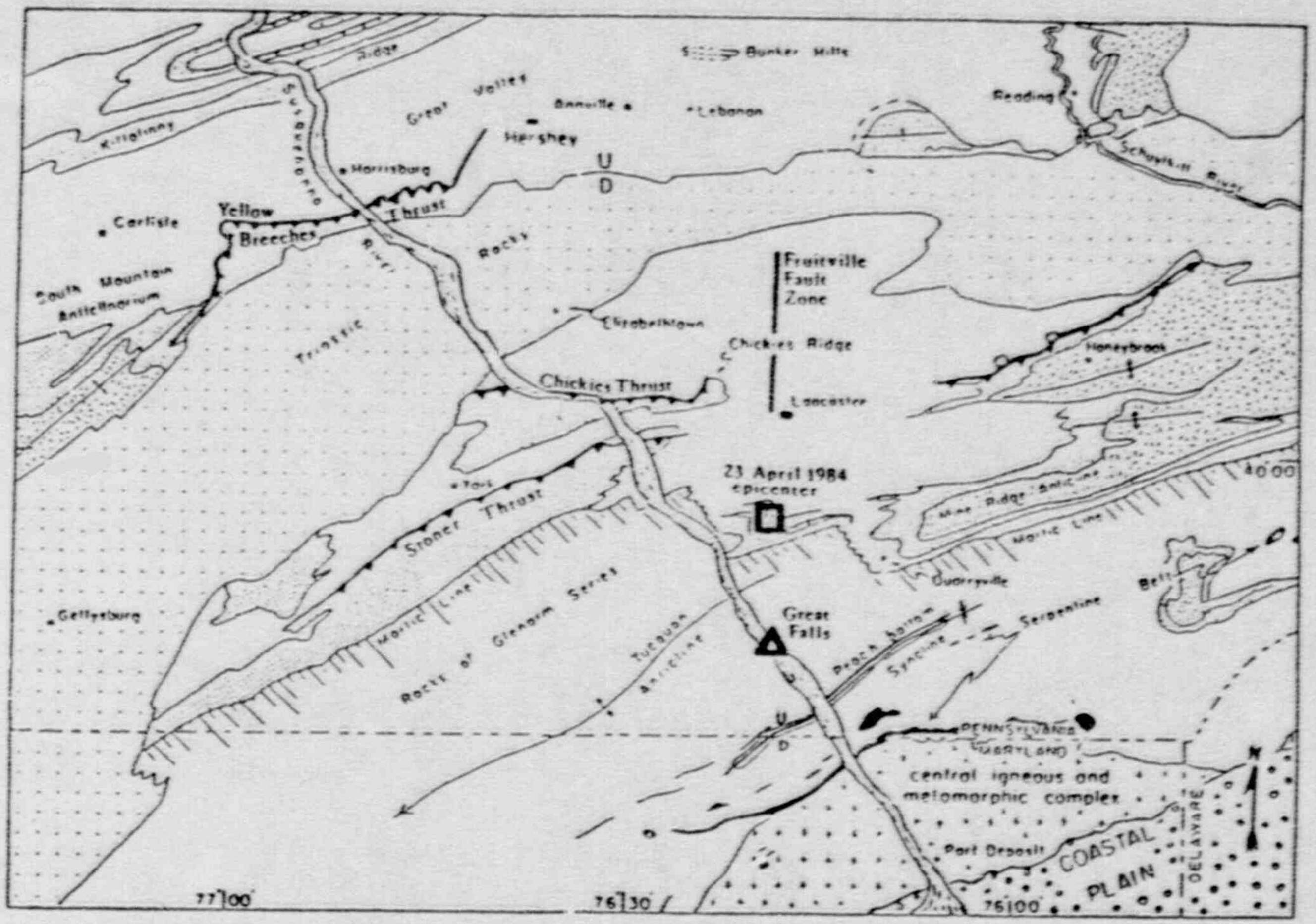

FIGURE 1 Geologic index map of the Appalachian Piedmont along the Susquehanna River of Pennsylvania and Maryland. (modified after Wise, 1967)

foreshock epicenters were verified by the hypocenter location program HYPOINVERSE (Klein, 1978; Lahr, 1980) and a relative location algorithm (Baumgardt 1977, 1985).

The April 23, 1984 earthquake had numerous aftershocks which lasted well into September, 1984. The largest of these was a magnitude 2.1 event (Scharnberger and Howell, 1985). Ten of the earliest of these aftershocks were recorded by a temporary seismic network set up within a day of the mainshock. The network consisted of 9 portable seismographs (3 from Pennsylvania State University and 6 from Lamont-Doherty Observatory) including smoked paper and digital recorders. The ten recorded aftershocks defined a 3 km long, N-NNE striking zone of activity within the region of the April 23 mainshock. The length of the zone was significantly larger than the location error of $\pm$ 0.5 km. Therefore, the N-S trending fracture suggested by the aftershocks appeared to be real. Equally real was the 4.5 km depth obtained from the aftershocks (Armbruster and Seeber, 1985). This depth was later verified by a modified cepstral analysis applied to a series of seismograms for the mainshock (Stockar, 1986).

The north-south fracture orientation indicated by the aftershocks was further supported by a double-couple fault plane solution based on 57 first motions from the mainshock and the aftershocks. This well-constrained solution indicates a seismogenic fault with a NNE strike of N 10^{o}E, dipping 60^{o}E, with reverse and right-lateral displacement. It has a P-axis which is nearly horizontal and striking ENE. This is consistent with the ENE maximum compressional stress for this part of the United States, based on other earthquake generated focal mechanisms, geological data, and in situ crustal stress measurements (Zoback and Zoback, 1980; Zoback, 1986).

Geological Structures

Central Lancaster County, the area of interest, is within the Lancaster or Conestoga Valley of the Piedmont. This carbonate valley is dominated by recumbent folding and thrusting in the north, and tight isoclinal folding in the south. Its southern terminus is the Martic Line where the Wissahickon Schist of the Glenarm Series is in contact with the Lower Paleozoic Conestoga limestone of the Lancaster Valley. The Martic Line and all of the Paleozoic folds and thrusts, as well as the Triassic Basin, follow the general east-west structural grain of the region (Figure 1) (Wise, 1967).

However, detailed geological mapping within central Lancaster County revealed the youngest faults to be north–south striking. As early as 1930, Stose and Jonas mapped several N–S striking faults which offset all the E–W striking faults and folds. According to the study, the most dominant of these N–S striking faults is the Fruitville fault (Figure 1, 2 and 3) which offsets all surrounding lithologies and structures right laterally in outcrop. In 1971, Meisler and Becker remapped this region and broke the Fruitville fault into a zone of smaller cross faults due to a lack of outcrop in this dominantly agricultural region (Figure 2). However, both studies agree that the youngest faults are N–S trending and that the dominant of these is the Fruitville fault zone.

The youngest rocks in the Lancaster County Piedmont are radiometrically-dated Late Triassic to Early Jurassic (180–200 m.y.) diabase dikes (VanHouten, 1969) which are associated with the diabase sills or sheets of the Newark–Gettysburg Triassic Basin north of Lancaster Valley (Figure 4). These diabase dikes are of three separate intrusive events based on composition (Smith et al, 1973). They are all N– to NE–striking within the Lancaster region (Figure 4). They typically are steeply–dipping features that extend over long distances. They appear to be parallel or subparallel to the N–S cross–faults, and cross-cutting contacts between the two sets are unknown. This may suggest a similar origin.

Several sets of Precambrian metadiabase dikes occur east and northeast of Lancaster County (Figure 4). They, too, have a predominantly N–NE strike and indicate zones of weakness within the Precambrian basement which underlies the Paleozoic sediments of the Lancaster Valley. These zones may have been reactivated by the Mesozoic igneous activity and its associated normal faulting.

Geomorphology

A preliminary look at the drainage pattern of the Lancaster area indicates a predominantly north–south drainage orientation (Figure 2). A study of over 300 straight segments of stream channels in central and southern Lancaster County reveals two major channel directions. One direction (approximately N 80°E) is parallel to bedding. The other direction (approximately N 10°W) is nearly perpendicular to bedding and parallels the general N–S trend of the youngest cross faults such as the Fruitville fault (Meisler and Becher, 1971). In northern Lancaster County, in the narrow neck of the Newark–Gettysburg

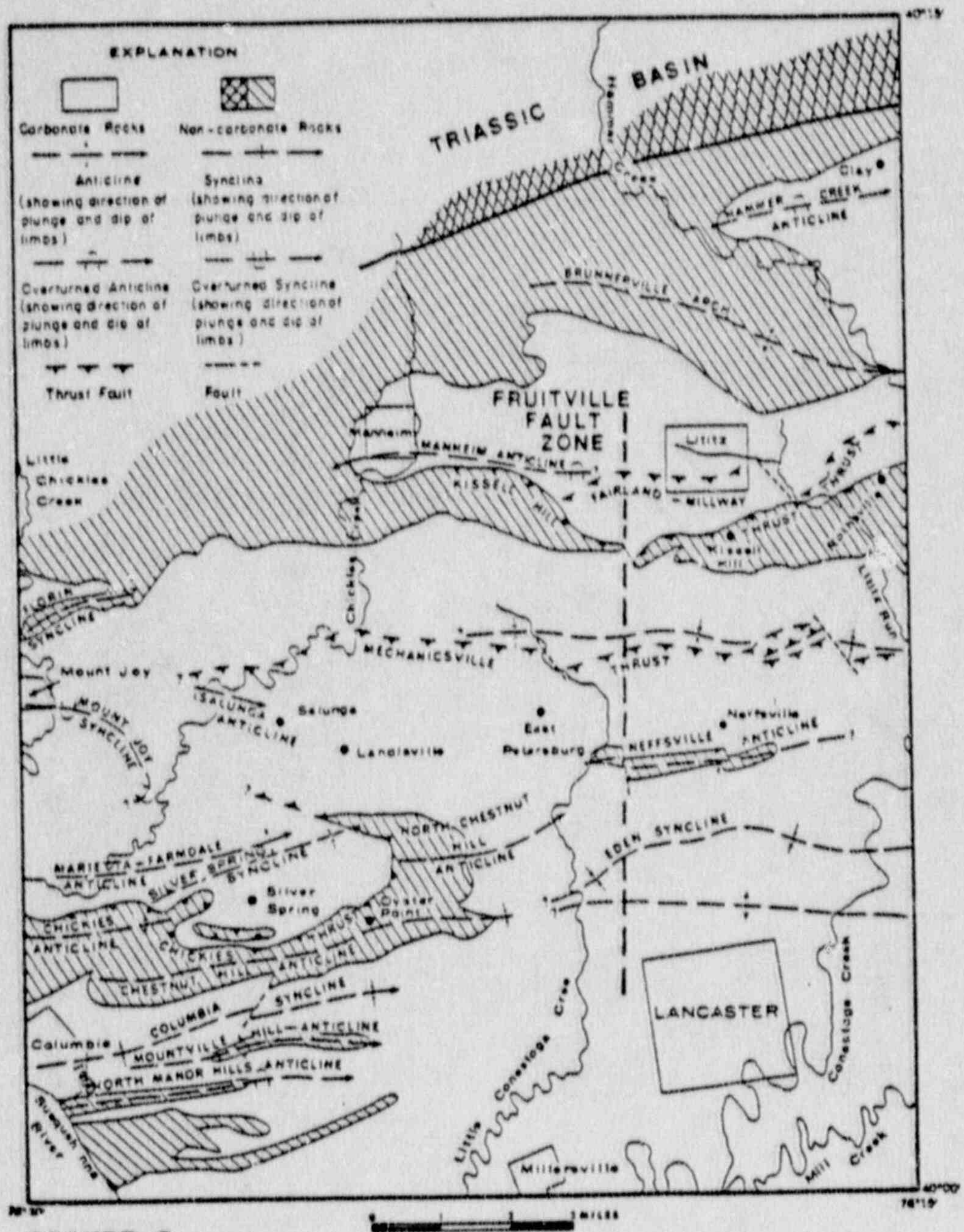

FIGURE 2

Structural map of the northern Lancaster County area. The Fruitville Fault Zone mapped by Stose & Jonas (1930) is superimposed on to the map as a dashed line. (modified after Meisler & Becher, 1971)

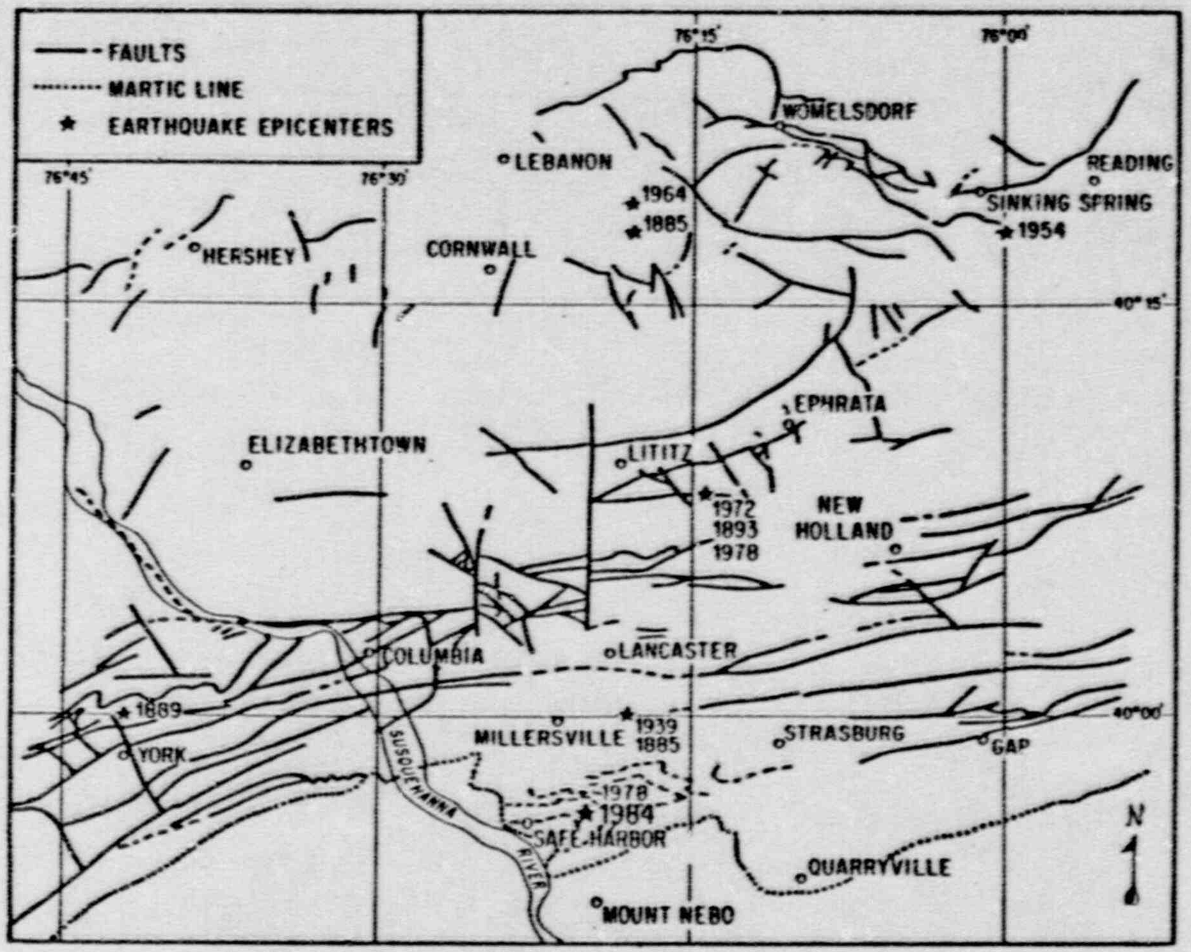

FIGURE 3 Map of the faults and the seismicity in the Lancaster Region. The faults appear as mapped by Stose & Jonas (1930). (after Scharnberger & Howell, 1985)

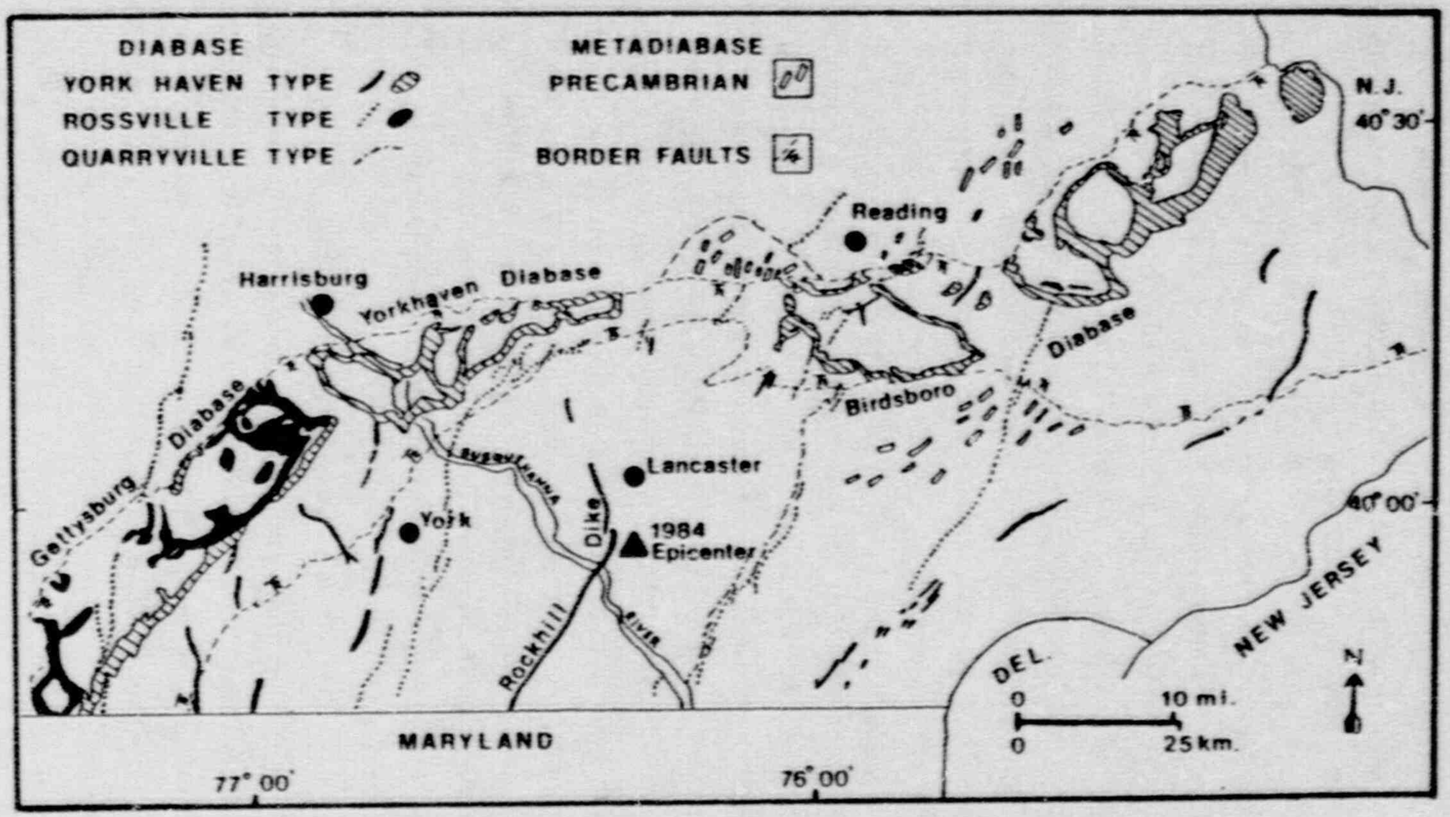

FIGURE 4 Hap of the Hesozoic diabase and Precambrian setadiabase of southeastern Pennsylvania. (modified after Saith, et al., 1975)

Triassic Basin, the drainage pattern is trellis, utilizing the N–S striking cross-faults. An example is Hammer Creek which flows south for several kilometers along a fault-induced straight segment which is a direct continuation of the Fruitville fault zone (Figure 2) (Gray et al, 1958; Meisler and Becher, 1971). There is also a set of springs in central Lancaster County which align with the southern projection of the Fruitville fault (Figure 5).

Finally, as early as 1929, Knopf and Jonas observed that "the Holtwood Dam (on the Susquehanna River) has utilized a natural falls or rapids known as Cullys Falls." Recently, Thompson (1985) has observed evidence for large preglacial falls on the Susquehanna in this area of Holtwood, Pennsylvania. He calls them "the Great Falls of the Susquehanna." These falls are directly south of the N–S striking Fruitville fault zone and its associated N–S trending seismic zone, (Figure 1, Figure 3) which is discussed below. Preliminary evidence suggests that the falls are due to preglacial faulting and/or flexuring in the area, possible preglacial uplift along the Fruitville fault zone.

Lineaments and Remote Sensing

Intermediate lineaments (10 – 80 km) and long lineaments (greater than 80 km) in southeastern Pennsylvania appear to be underlain by zones of fractured and jointed rocks and represent zones of deformation that transgress Precambrian through Traissic age lithologies. They are often reflected by straight valley segments, abrupt changes in valley alignment, gaps in ridges, gully and sink hole alignment, localized springs, diffuse seepage areas, localized vegetation differences, and drainage patterns (Gold, et al., 1973, 1974).

Kowalik and Gold (1975) studied the intermediate lineaments in Pennsylvania, based on Earth Resource Technology Satellite – 1 (ERTS–1) images. In Lancaster County, they identified several lineament directions with the north–south direction dominant.

Wise (1967) used topographic maps to identify topographic linears of the Susquehanna Piedmont (Figure 6). He found that the orientations of these lineaments (rosette B, Figure 6), did not match the strikes of the 1400 ground-measured master joints (rosette A). Thus, the lineaments represent an "apparently different system" (Wise, 1967) of fractures. It is noteworthy that Wise identified a set of N–S striking topographic lineaments as clearly dominent within the Lancaster region (Figure 6). In fact, his topographic lineaments clearly define the Fruitville fault (Figure 1) and the Lancaster seismic zone (Figure 3), (note the location of the 1984 earthquake in Figure 6).

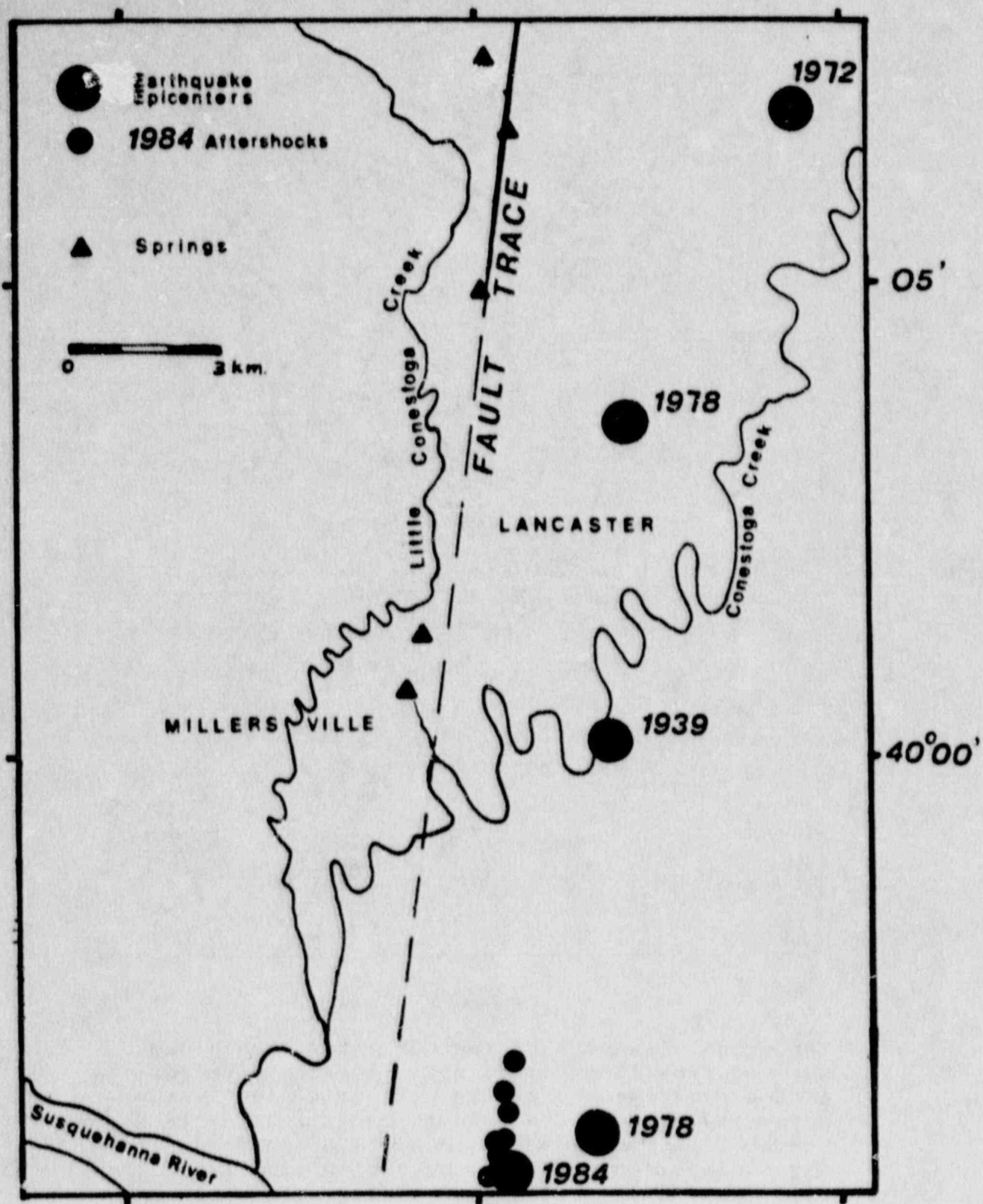

Figure 5. Map springs in relation to recent earthquake epicenters along the southern trace of the Fruitville Fault near Lancaster, Pennsylvania.

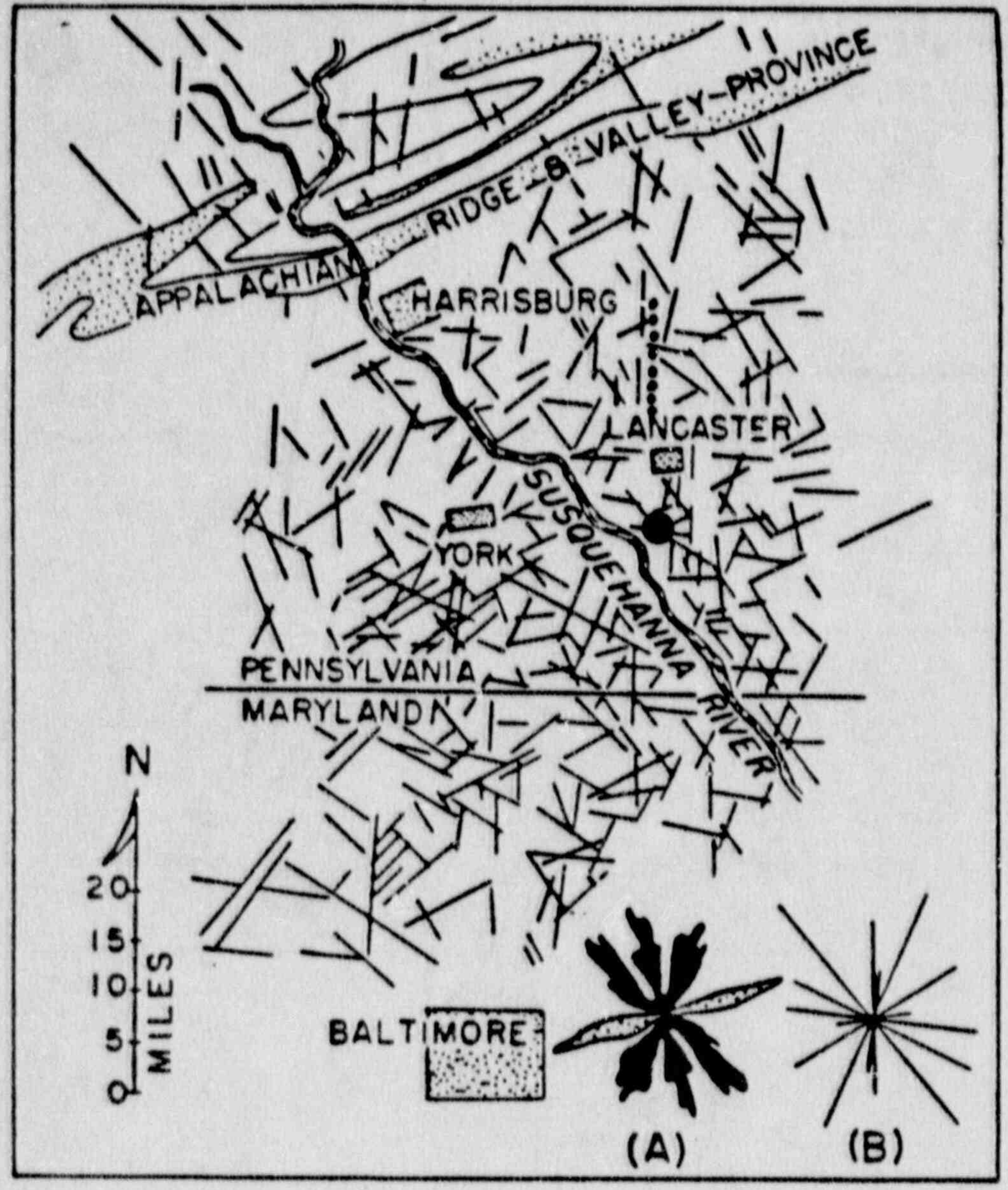

FIGURE 6

Topographic linears of the Lancaster County area derived from topographic maps. Rosette A represents ground measurements of the strikes of 1400 master joints related to the late stage of folding in the Piedmont of Pennsylvania. Rosette B represents the eight directions of the topographic linears on this map, apparently a different system from Rosette A. The dotted line represents the Fruitville Fault Zone, and the large solid dot is the epicenter of the April, 1984 earthquake. (modified after Wise, 1967)..

An investigation of LANDSAT-4 imagery (30 m resolution) carried out in this study reveals that clearly the dominant lineaments in Lancaster County are those of the Appalachian structural trend (nearly E-W striking) and those defining the Fruitville fault zone which trend N-S (Figure 7). The latter are defined by gaps and drainage through the Triassic rocks, stream drainage within the Paleozoic rocks, and the right-lateral offsets in the E-W striking ridges of the Conestoga Valley (Figure 2).

A Morphotectonic Study of the Lancaster Area*

Although the Lancaster area has been known for its seismic activity (see Figure 8) ever since it was settled, little is known of the source, and almost nothing of the surface expression of any fault(s) associated with these seismic events. Not only is the ground-based geological mapping hampered by the paucity of exposed bedrock, except along the Susquehanna River, but agricultural practice (thick lowland soils, intensively cultivated, with forest cover the hilly areas) tend to subdue and mask the normal geomorphic expression of fault displacement, e.g., scarplets on the surface. The search in this aspect of the study was focussed on the more-subtle manifestations of surface movements in the drainage pattern, and in the density and rate of gully development, using a photogeologic approach.

A search for fault-related topographic features, such as scarps, sag ponds, as well as displacements and deflections of drainage, failed to reveal the presence at the surface of an active fault of moderate to large displacement. A more sensitive indicator is likely to be in the orientation, position, and density of the 4th order streams and gullies, especially those developed on a short time scale in cultivated fields. Because of other variables that are cultural in nature (e.g., ploughing direction) we have rationallized that density data are less ambiguous than strictly orientational data. The search was not limited to co-linear patterns of gully concentrations or orientations, because it is possible that the strains associated with neotectonic deformation may reflect a broad fault zone, or more likely, an en echelon pattern of faults rather than a single break.

---

* Air-photo analysis by Haiyan Hu, with data manuplation by Hue-Chung Chou. Supervised by D. P. Gold and T. Gardner.

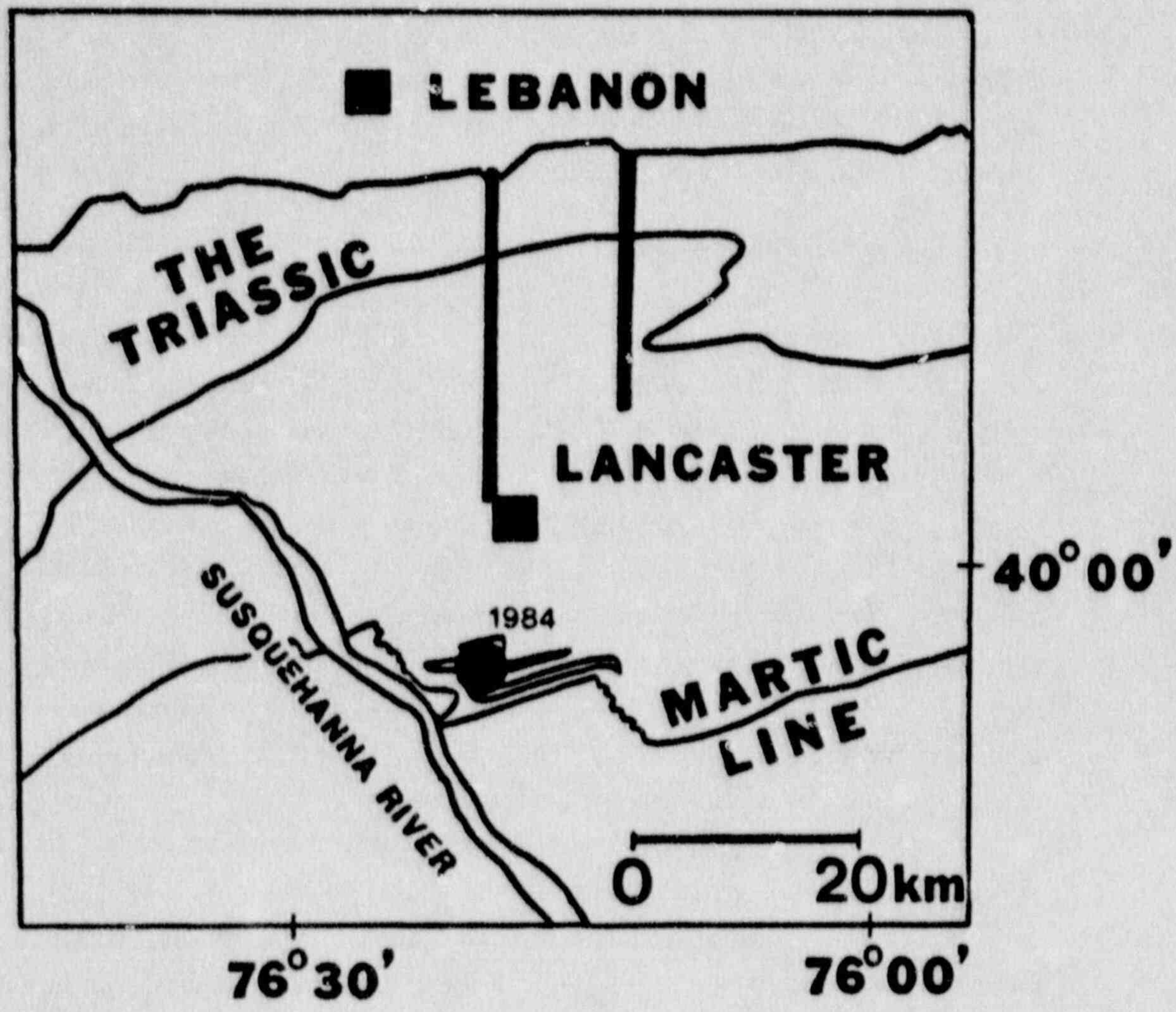

FIGURE 7

Map showing major LANDSAT-4 lineaments (dark lines) obtained in a preliminary survey of the Lancaster County area. The solid dot is the epicenter of the April 23, 1984 earthquake.

LINEAMENTS OF PENNSYLVANIA

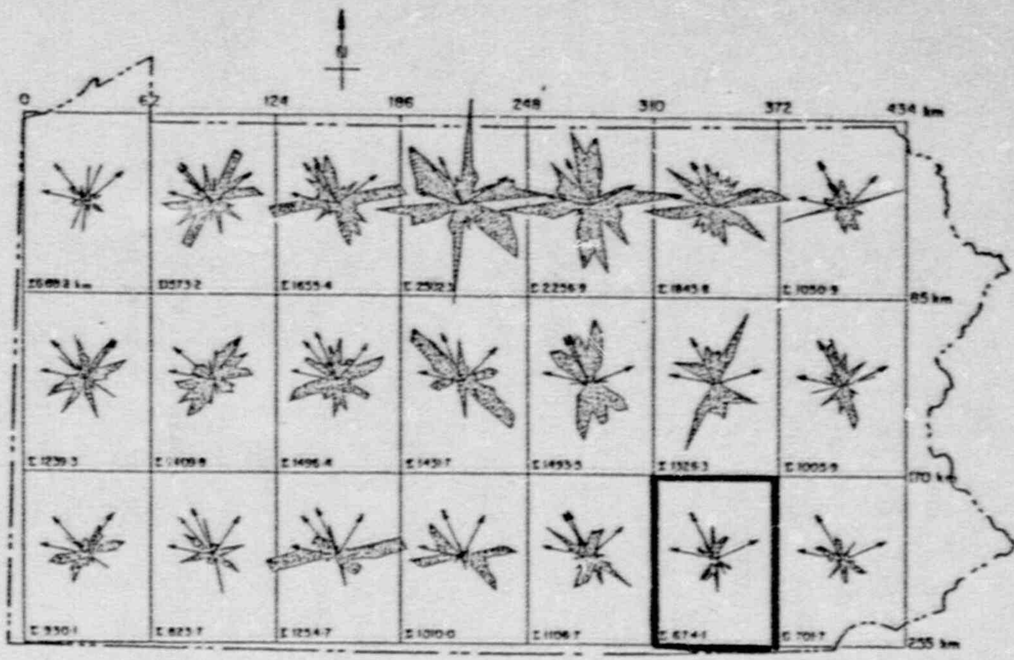

LANCASTER COUNTY

● EPICENTERS

— LINEAMENTS

▲ 1984 EARTHQUAKE EPICENTER

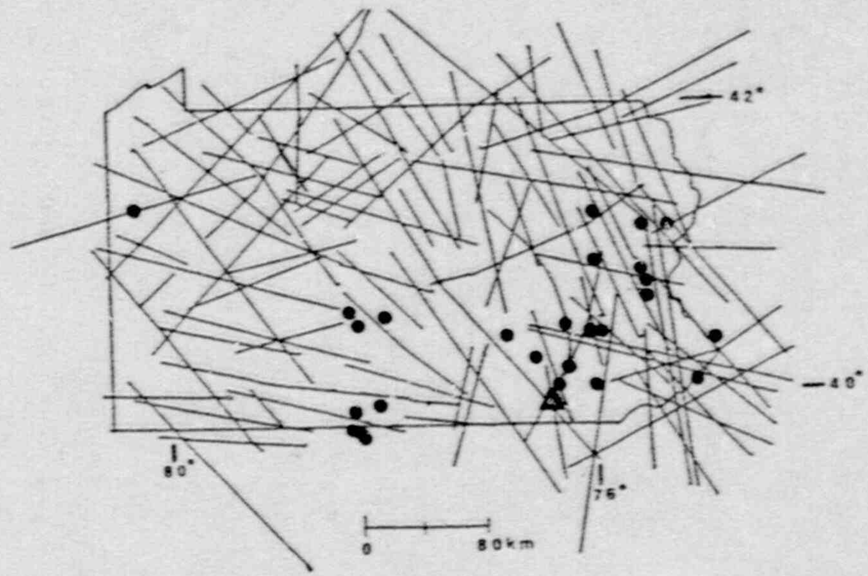

(AFTER KOWALIK & GOLD,1974)

Figure 8.

In addition to a lineament analysis (Figure 9) using Landsat imagery two scales of aircraft overflights were used for most of the detailed mapping and analysis, viz., low altitude photographs (1:20,000) flown during 1964, and high altitude (1:48,000) flown during 1978. All of the small features were mapped on 265 of the higher-resolution, low-altitude photographs. As part of a terrain analysis, the headward segments of rills and gullies were mapped on acetate overlays on alternate frames (see index on Figure 10) in a stereo-model, and transferred onto a base map. To avoid biasing the data by mapping the same area more than once only the central portion (5" x 7") of each photograph was transferred. The county boundary, reference coordinates, and the end points of the "gullies" were transferred from the base map to magnetic tape on a source bed plotter. This digital data bank was used in subsequent computer assisted statistical analyses for density and orientation parameters. Data pertinent to each frame mapped were plotted at the location of the principal point of the appropriate photograph (Figure 11). Cells of area slightly less than that covered by the aerial photograph were superimposed on the base map in order to develop density contour diagrams (Figure 12). They also facilitated the comparison of density and orientation of "gullies" and gully patterns among different areas.

The criteria and parameters in distinguishing and mapping gullies on aerial photographs are:

(1) they appear as thin, dark-grey to black lines in the checkered or striped agricultural pattern of the arable lands;

(2) gully expressions commonly are from 100 to 250 feet, but range in length from less than 50 feet to more than 100 feet;

(3) most of the gullies are either oblique or perpendicular to the topographic contour, rarely parallel to it;

(4) gully patterns vary with topography and bedrock attitude and lithlogy;

(5) the density of gullies per photo-cell* is highly variable. A value of 15 to 20 per photo-cell was considered to be background, and more than 30 as anomalous. The largest anomalies approach values of 60 gullies per cell.

---

* The central 5" x 7" rectangle used on each aerial photograph to minimize the amount of radial distortion.

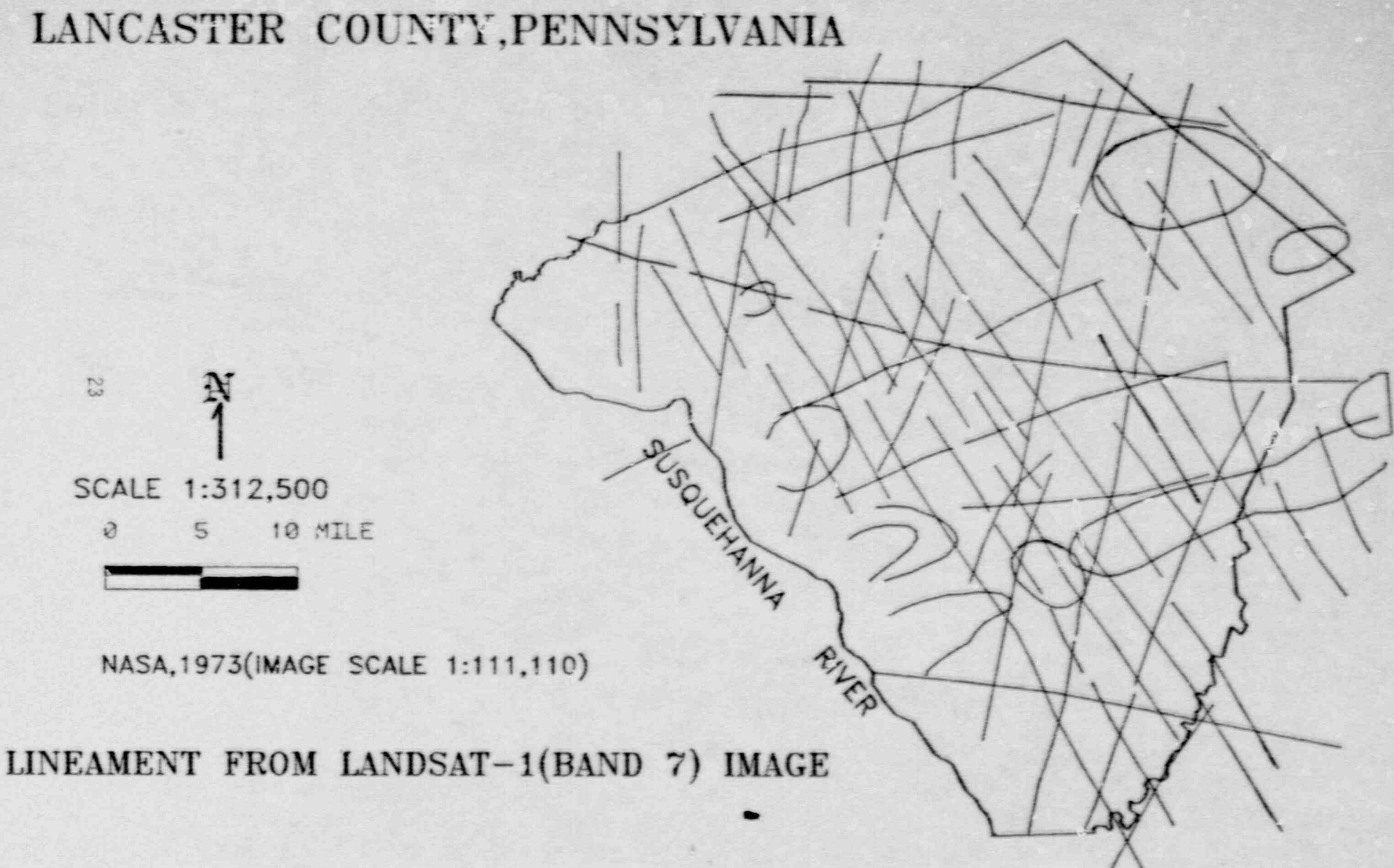
LANCASTER COUNTY,PENNSYLVANIA
N
SCALE 1:312,500
0 5 10 MILE
NASA,1973(IMAGE SCALE 1:111,110)
LINEAMENT FROM LANDSAT-1(BAND 7) IMAGE
SUSQUEHANNA RIVER

Figure 9.

LANCASTER COUNTY

N

SCALE 1:312,500

0 5 10 MILE

ROCK TYPE

PHOTO INDEX AT CENTER

AERIAL PHOTOGRAPHS(1:20,000)

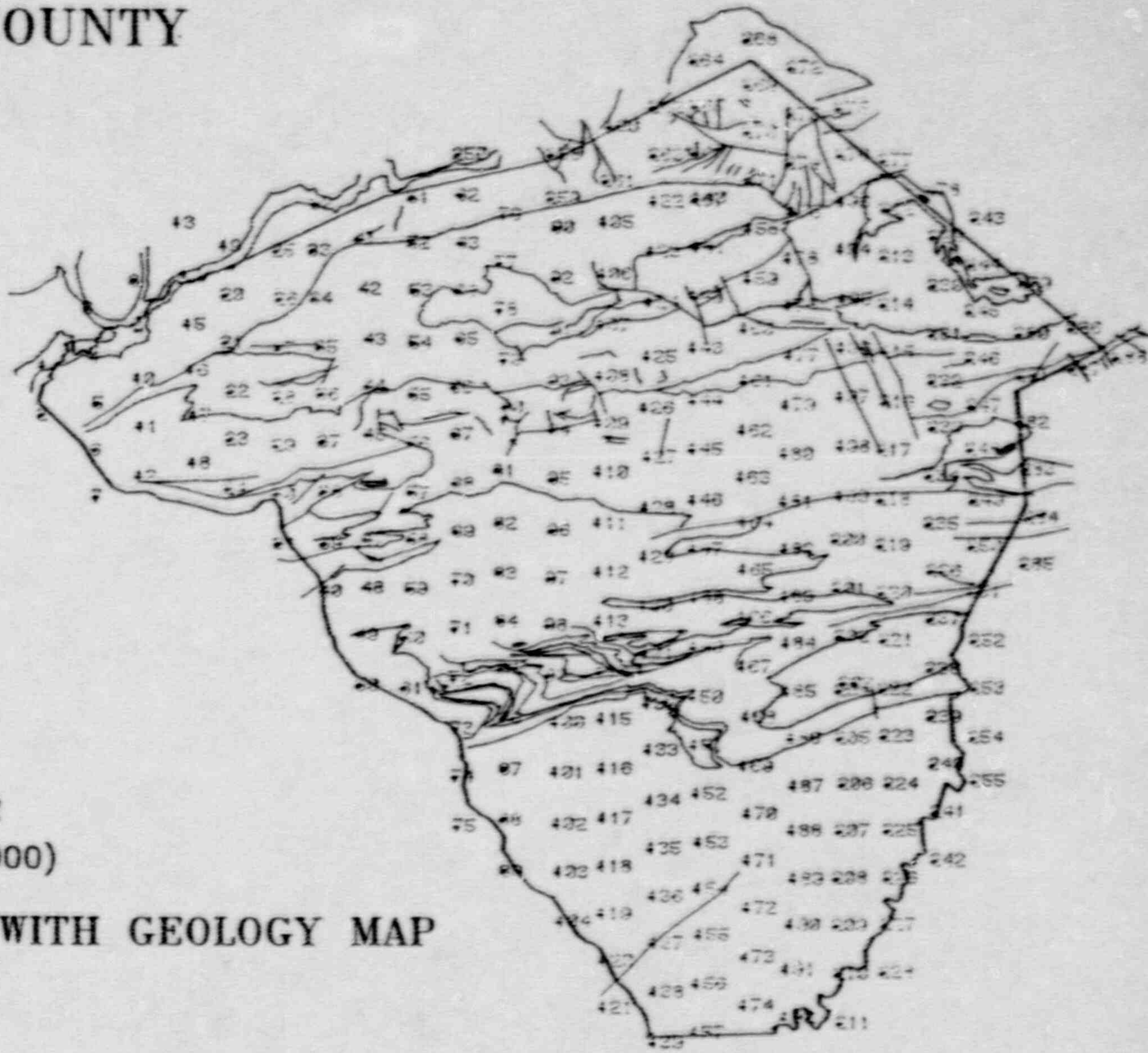

OVERLAY PHOTO CENTER WITH GEOLOGY MAP

Figure 10.

LANCASTER COUNTY, PENNSYLVANIA

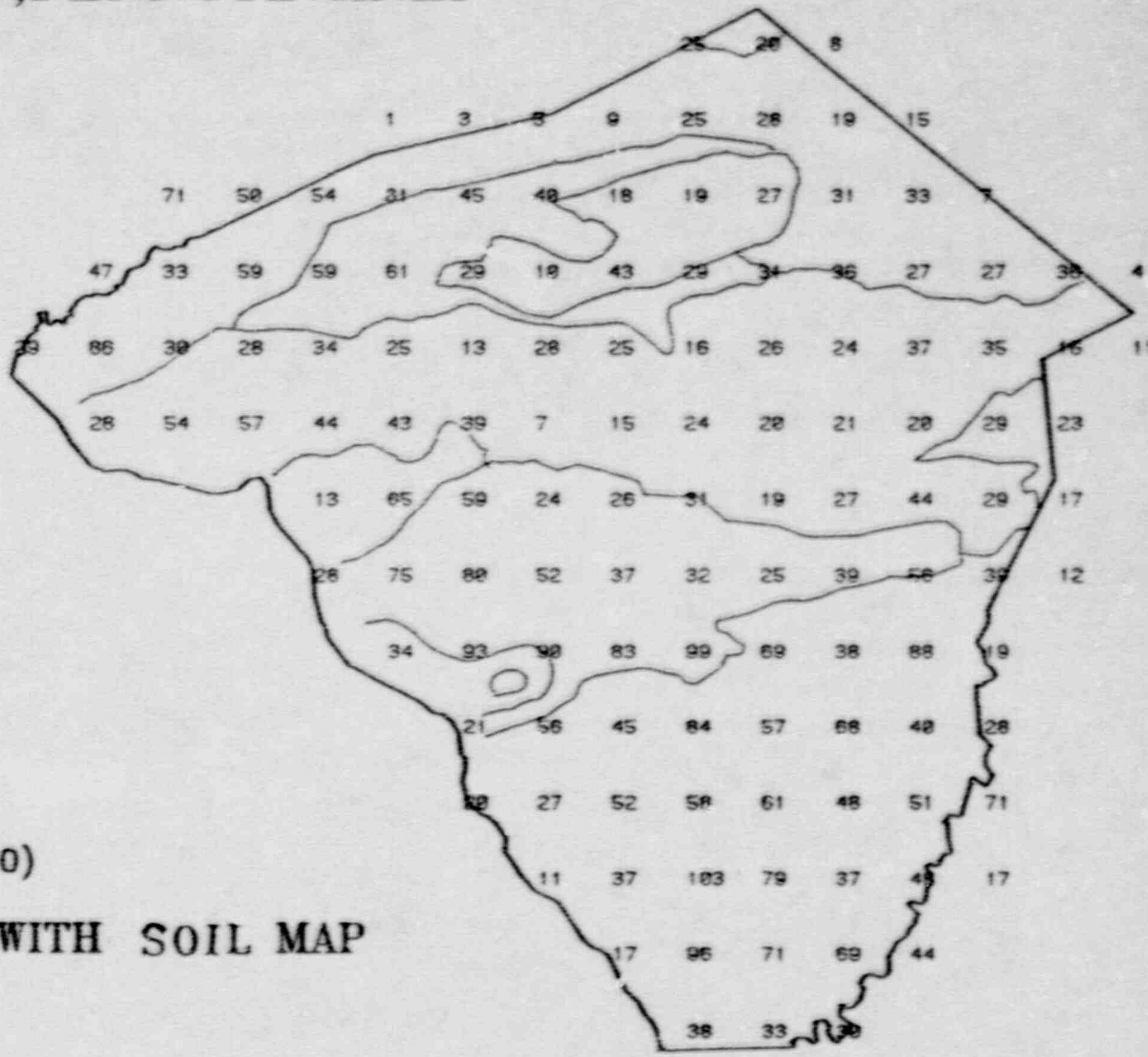

N

SCALE 1:312,500

0 5 10 MILE

SOIL TYPE

AERIAL PHOTOGRAPHS(1:20,000)

OVERLAY GULLY DENSITY WITH SOIL MAP

Figure 11.

LANCASTER COUNTY, PENNSYLVANIA

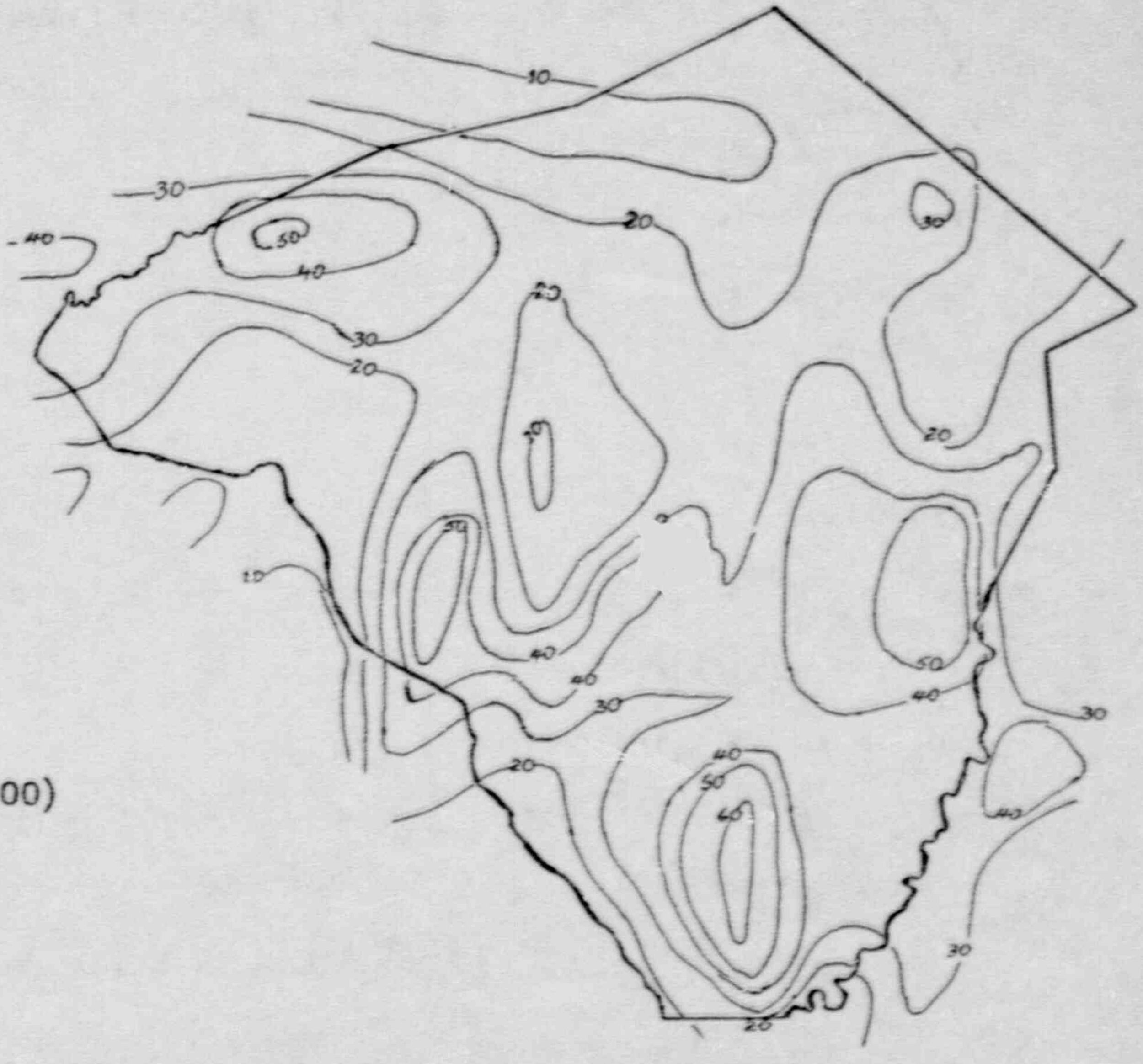

N

SCALE 1:312,500

0 5 10 MILE

SOIL TYPE

AERIAL PHOTOGRAPHS(1:40,000)

GULLY DENSITY

Figure 12.

The main factors controlling gully development, distribution and density are:

(1) climate, including rainfall distribution;
(2) farming practice, especially direction of plough furrows, i.e., commonly the long axis of field;
(3) time-duration for natural processes to supercede anthropomorphic adjustments, e.g., ploughing to remove rills;
(4) soil thickness and type;
(5) bedrock composition;
(6) orientation and nature of bedrock fractures;
(7) slope aspect and gradient;
(8) tectonic activity (e.g. differential uplifts etc.)

The first three factors can be considered to have been constant on the scale of the county for at least the last 5 to 100 years (Custer et al., 1985). The latter factors are sensitive to local changes, and because they are site-specific, they need to be considered independently.

A total of 5154 gullies were mapped on 265 low altitude (1:20,000) aerial photographs of Lancaster County. These were transferred to the base map on a scale of 1:48,000, and then transduced to provide a digital data base from which frequency and orientation parameters could be deduced (i.e. a contour map of density (Figure 12), and histograms rose diagrams (Figure 13), depicting the degree of local anisotrophy in fracture orientations.

The gully density distribution (Figures 11 and 12) indicates three anomalously high areas in Lancaster County. The southern areas is underlain mainly by schists and micaceous gneisses of Precambiran age. The middle anomaly is located in the west-central part of the county, around the city of Lancaster. It is underlain by clastic sediments and limestones of Cambrian age, which are deformed by folds and thrust faults (see Figure 10). Epicenters of modern earthquakes cluster along the western side of this anomaly. The third anomaly is located in the northwestern part of the country, where Ordovician sandstones and limestones are overlain by Triassic Redbeds, intruded by diabase dikes and Triassic/Jurassic age. A common feature to these three anomalous areas is the presence of generally north-south trending diabase dikes.

Except for the anomalously low "gully-density" swath across the northern part of Lancaster county, which correlates with the forested terrain underlain

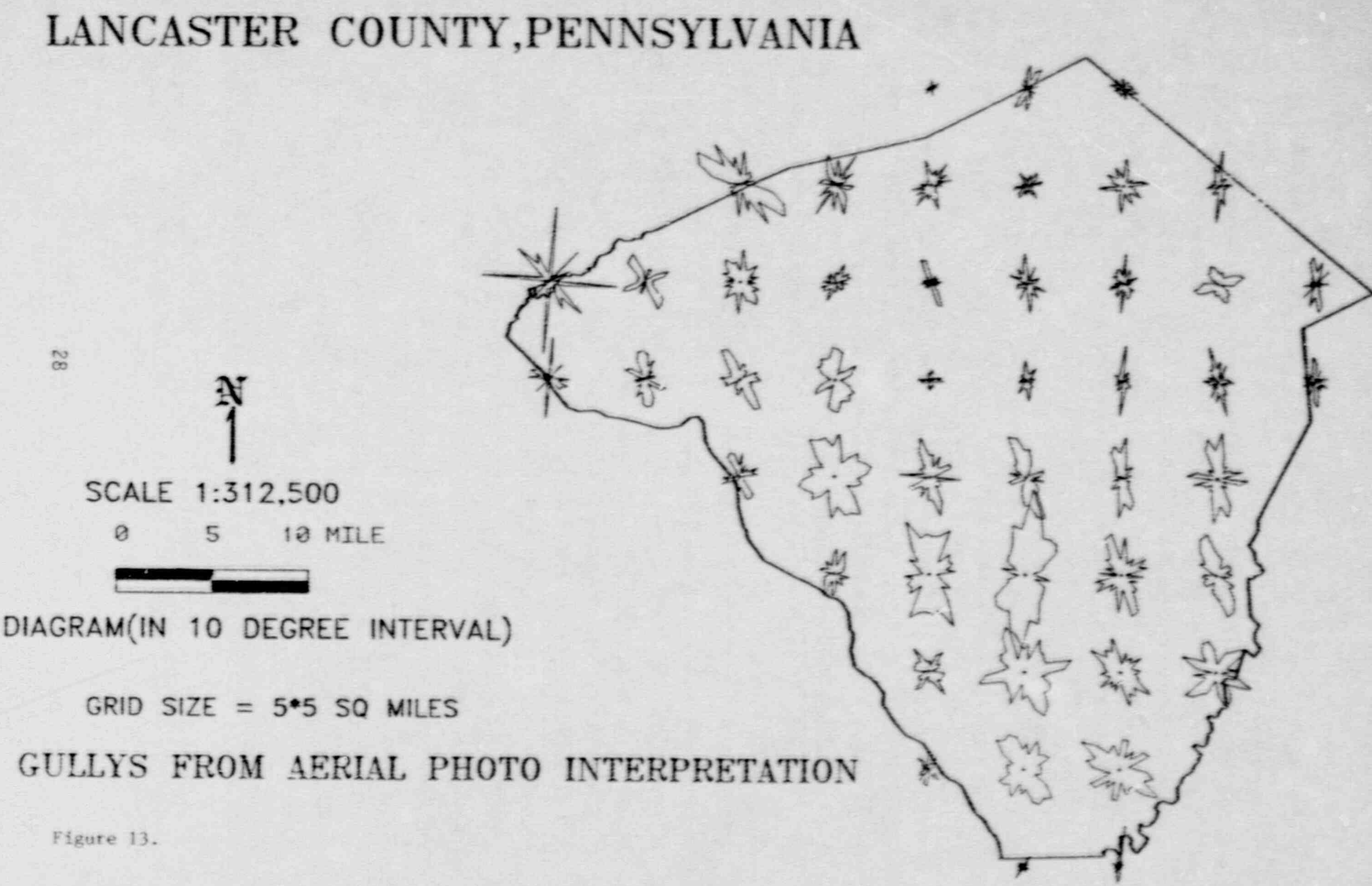
LANCASTER COUNTY,PENNSYLVANIA
N
SCALE 1:312,500
0 5 10 MILE
DIAGRAM(IN 10 DEGREE INTERVAL)
GRID SIZE = 5*5 SQ MILES
GULLYS FROM AERIAL PHOTO INTERPRETATION

Figure 13.

mainly by Triassic rocks, gully development is not as strongly influenced by lithology as it is by bedrock structure and attitude.

In the central area, the paucity of gully development is reflected by the low contour value (10 gullies/4 square miles) on the density contour map, and the small size of the rosette in the cell/rose diagram plot. In the southern part, the general background value for gully density is high. This is reflected in the trend surface, and in particular in the size of the rosettes in the corresponding cells. These anomalies are correlated with bedrock, and soil types.

An unusually high uplift rate has been established for the southern part of the county by Gardner (this study) through dating and levelling of a series of terraces along the Susequehanna River. As a result of rapid uplift, headward erosion and downward incision are promoted until an equilibrium grade is reestablished. Bedrock conditions (e.g. the well-jointed Peters Creek Schist Formation), with only a thin soil cover also enhance the gully development.

Other factors can be eliminated as a cause for the "high density" anomaly that occurs in the southern part of the county because its north-south trend is transverse to the lithology, soil types, and uplift axis. The remaining factor of importance is a tectonic control of some sort. The north-south spike in the rose diagrams (see Figure 13) for the cells within this anomaly are transverse to bedding dip and slope and major drainage directions, suggesting a superimposed fracture control. The breadth of this anomalous belt suggests the presence of multiple north-south oriented fractures in a zone rather than a single fault. These suppositions are consistent with the location of recent earthquake epicenters, spring, and travertine dams in the Lancaster area (Stockar, 1986; Stockar et al., 1987), which indicate an active north-south trending zone of weakness subparallel to north-northeast trending diabase dikes of Triassic age.

The principal conclusions from this morphotectonic analysis are:

(1) The northwest trend of high "gully-density" anomalies reflects the geomorphic influence of the Susquehanna River, while the north-south trends in the "gully density" contours, rose diagrams of gully direction and joints, (Figure 14) coincide with regional (diabase dikes and faults) and local structures.

(2) The fossil strain reflected in the orientation of the diabase dikes and thrust faults is similar to the modern strains manifest by gully development and the clustering of epicenters.

TOPOGRAPHIC LINEARS AND JOINTS OF LANCASTER AREA

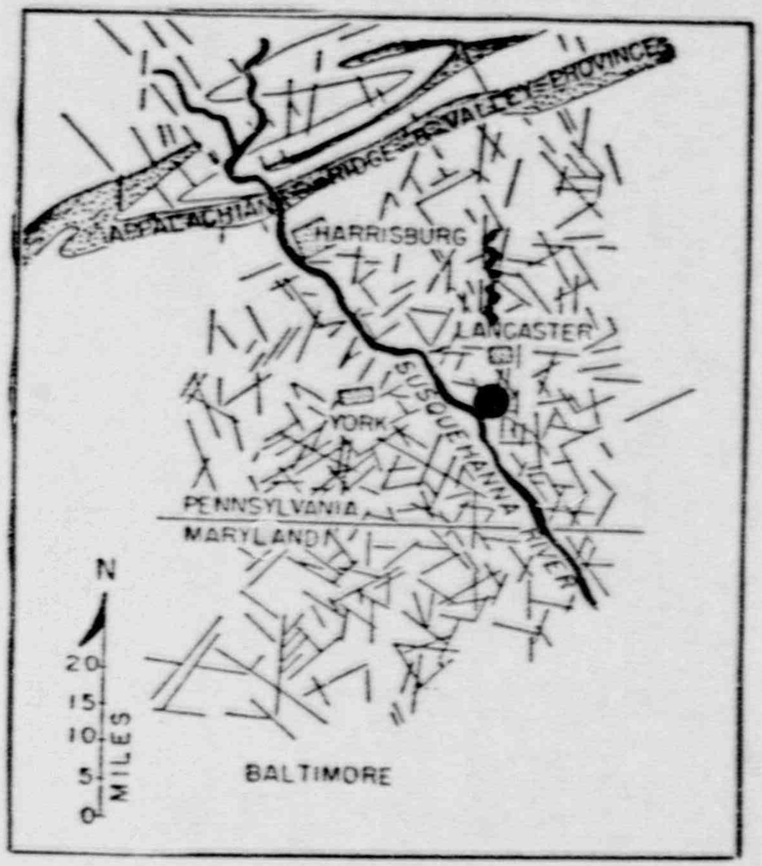

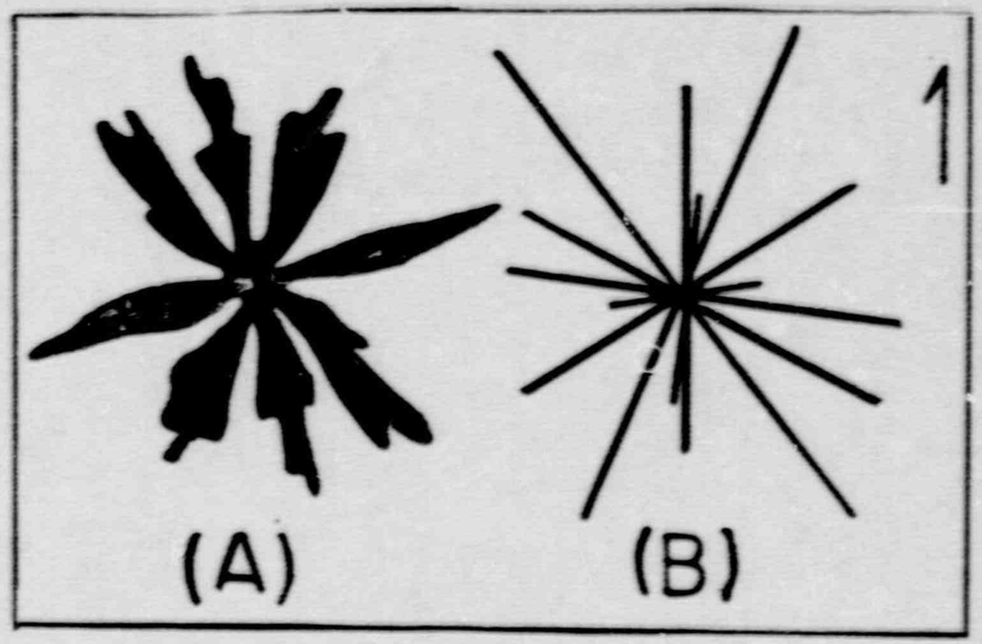

ROSETTA A : STRIKES OF 1400 MASTER JOINTS

ROSETTA B : TOPOGRAPHIC LINEARS – 8 SETS

FRUITVILLE FAULT ZONE ● 1984 EARTHQUAKE EPICENTERS

(MODIFIED AFTER WISE, 1967)

(3) We conclude that two areas of anomalously high gully development in Lancaster county are due to near-surface deformation caused by local uplift and a seismically active fault zone. Moreover, the morphotectonic techniques developed for this study were able to discriminate between the two causes when the local fracture (gully) orientation fabric is considered. In summary, the high gully density zones coincide with areas of anomalous uplift, and an active seismic zone. Aligned spikes in rose diagrams from the active seismic zone provide information on the strike of the crypto-fractures.

Gravity and Magnetics

Sumner (1975) compiled gravity data for the Newark-Gettysburg basin and contoured a simple Bouguer gravity map (Figure 15). 4500 gravity stations were plotted with a station spacing of 1-5 km over the basin and 2-10 km over adjacent areas. The standard error is about 0.2 mgals.

The density contrast between the various Triassic and Paleozoic rocks underlying the area is very small, with the exception of the diabase (Sumner, 1976, 1977). Therefore, it is difficult to detect near-surface faulting within these rocks. Nevertheless, on the simple Bouguer map (Figure 15), there is some evidence for a N-S fault zone in the area of the Fruitville fault of Lancaster County. The contour lines appear warped within this area, in contrast to their parallel, equally spaced regional trend on both sides of the proposed fault zone (Figure 15).

Bromery and Griscom (1967) compiled an aeromagnetic map of SE Pennsylvania based on several 15-minute quadrangle surveys. The quadrangles of interest, within the proposed Lancaster seismic zone (Figure 3), are, north to south, the Lititz quadrangle (Bromery and Zandle, 1961), the Lancaster quadrangle (Bromery and Zandle, 1961), and the Conestoga quadrangle (Bromery and Zandle, 1959). The flight paths are N-S with a contour interval of 25 gammas. These three quadrangle maps have been combined in Figure 9.

Despite the large, regional scale of this aeromagnetic survey, there is clear evidence of a disturbance in the magnetic contours as they cross the area of the Fruitville fault and its N-S extension (Figure 16). Further south, in the Conestoga quadrangle, the Martic Line contact creates an approximately 800 gamma, steeply dipping, shallow magnetic contrast (Figure 16) (Socolow, 1974). Along the southern extension of the Fruitville fault, this contact (as well as the Martic Line) trends N-S. This is also the area of the 1984 earthquake.

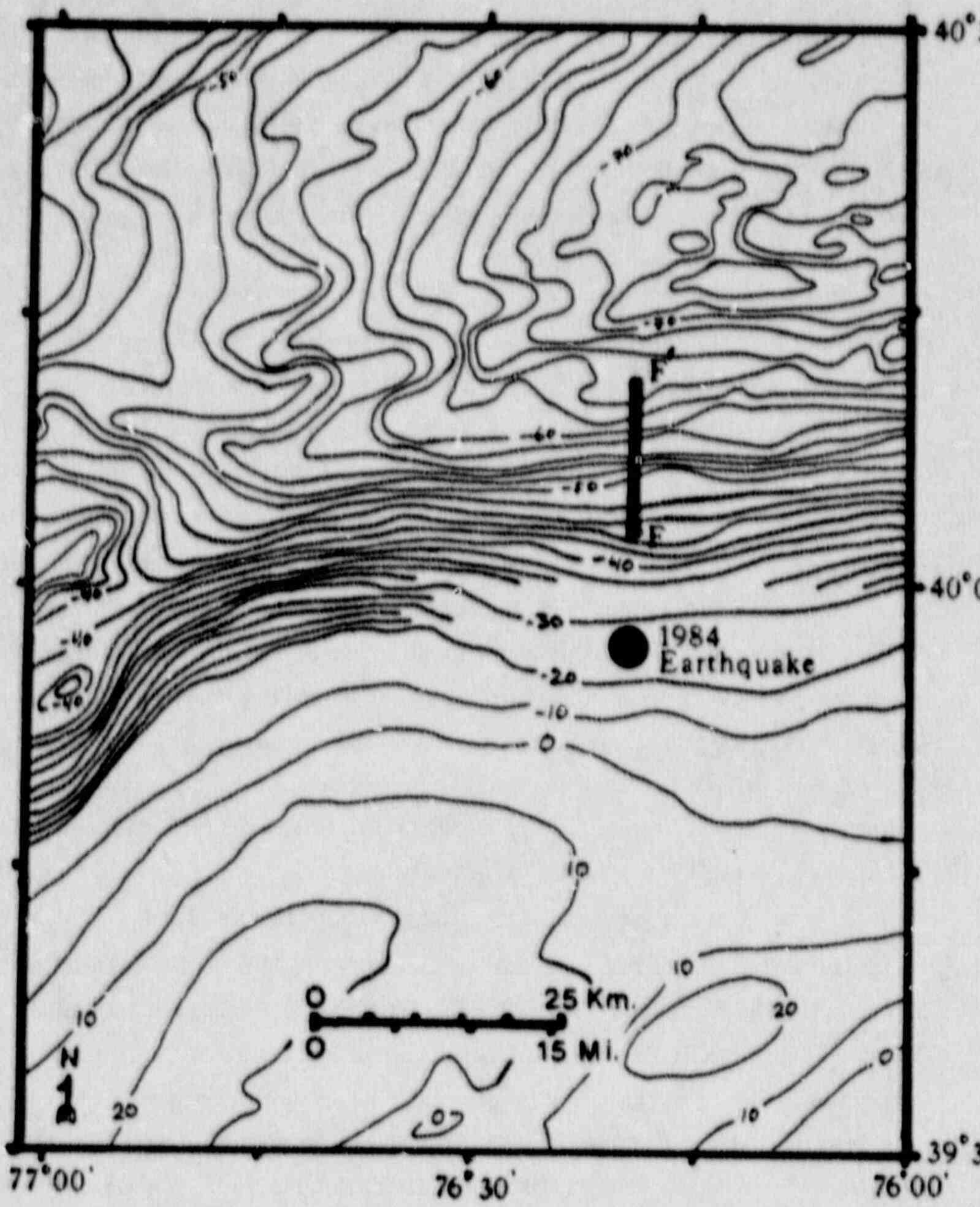

FIGURE 15. Simple Bouguer Gravity map of southeastern Pennsylvania and northern Maryland, contoured at 2 and 10 mgals. The dark line labelled FF' is the schematic representation of the Fruitville Fault Zone. Also shown is the April, 1984 earthquake epicenter. (modified after Sumner, 1975)

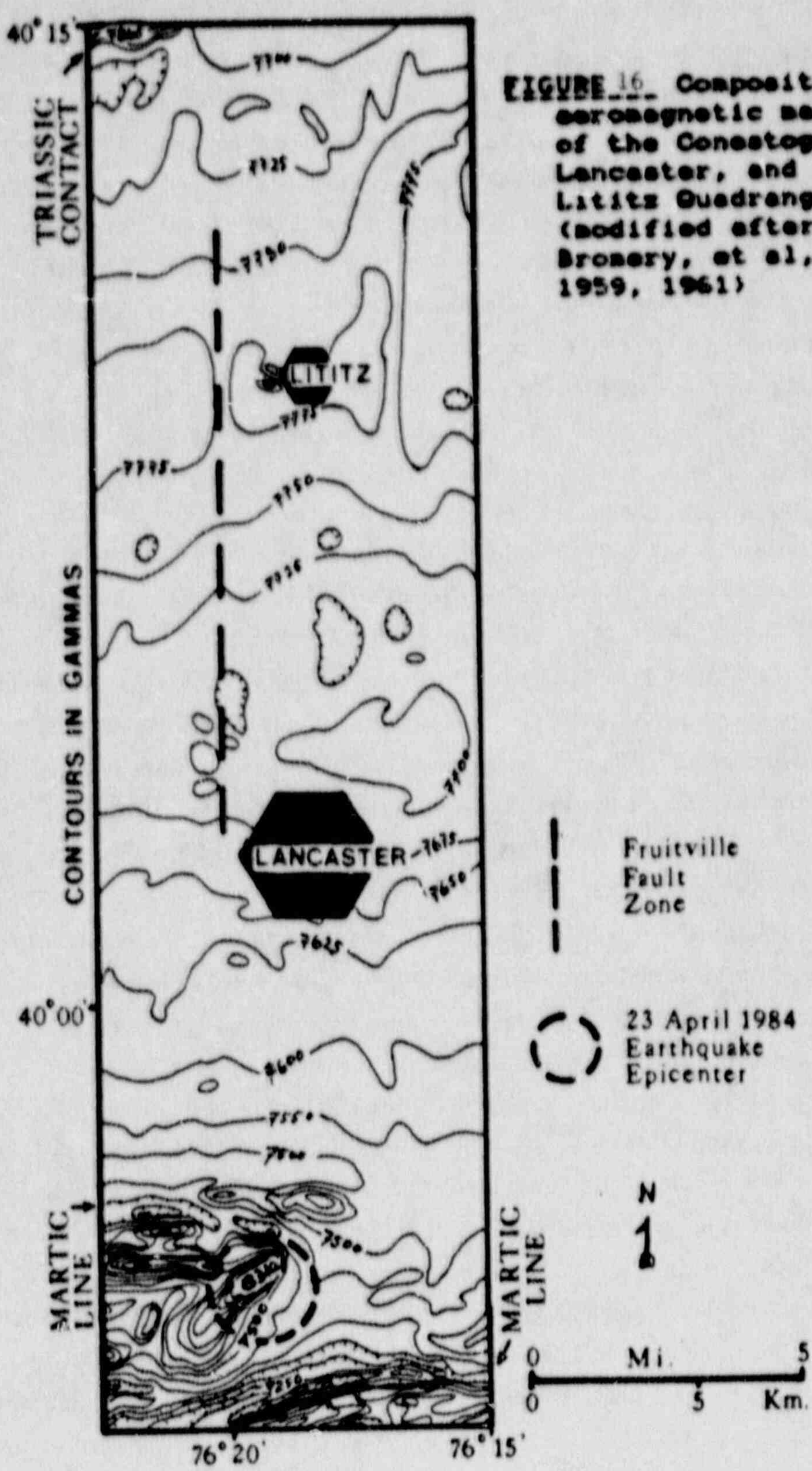

FIGURE 16 Composite aeromagnetic map of the Conestoga, Lancaster, and Lititz Quadrangles. (modified after Bromery, et al, 1959, 1961)

Likewise, this area in Conestoga is the part of the Martic contact of Pennsylvania which is most highly folded, and offset in two step-like features (Figure 1) (Berg, et al, 1980). These step offsets are in harmony with the right-lateral displacement along the Fruitville fault and other N-S trending faults of the area. However, at this point no causal relationship can be established.

Finally, one must keep in mind that, as in the gravity case, the uniform lithology of the Lancaster valley area makes it very difficult to identify structural features on the aeromagnetic data. The magnetization of the Paleozoic and Triassic rocks, with the exception of the diabase, is very uniform and low because of the relatively uniform composition of these clastics and carbonates (Sumner, 1977). Thus, the aeromagnetic data for the Triassic and Paleozoic sedimentary rocks has a range of less than 100 gammas.

Historical Seismicity

Sharnberger and Howell (1985) did a study of the historical seismicity of Lancaster County and obtained the results of Figure 3 and Table 1. However, there is evidence that the location of the October 6, 1978 event near the town of Lititz (Figure 3) is in error. The preferred location of this event is on the northern outskirts of the city of Lancaster (Figure 17). This is based on Scharnberger's (1978) intensity maps for the two 1978 Lancaster earthquakes (Figure 18), and on the results of applying a relative location algorithm which used the locations of the July 16, 1978 and the April 23, 1984 earthquakes to locate the October 6, 1978 event (Figure 18). Furthermore, although traditionally the March 8, 1889 event, of intensity MM = V, has been located in York, Pennsylvania, new studies of newspaper records have been used to relocate the event within the area around the city of Lancaster (Nottis, 1983; Armbruster and Seeber, 1985). Based on these historical locations, it is clear that a N-S trending seismic zone dominates Lancaster County (Figure 10).

The earthquakes of largest instrumentally-recorded magnitude within this zone of seismicity, the Lancaster seismic zone (LSZ) are the recent April 23, 1984 event with a magnitude 4.2, and the May 12, 1964 event which had a published magntidue 4.5, but which was recalculated in this study to be of magnitude 3.6 (Figure 17). The other instrumentally-recorded events in the LSZ are: The December 8, 1972 event (magnitude 2.1; Dewey and Gordon, 1984) at a depth of about 3.5 km; the July 16, 1978 event (magnitude 3.0; Scharnberger, 1978) at a depth of about 5.0 km; and the October 6, 1978 event (magnitude 3.1, Scharnberger, 1978).

TABLE 1

HISTORICAL SEISMICITY OF THE LANCASTER REGION

Date	Location	Mercalli Intensity	Comments
1885	Lancaster/ Lebanon	II-III	
Mar. 8, 1889	York or Lancaster	V-VI	strongly felt in both locations
Apr. 26, 1893	Lancaster	III	
Apr. 1, 1939	Lancaster	II	
May 12, 1964	Lebanon	VI	M = 3.6
Dec. 7, 1972	Lancaster	V	
Jul. 16, 1978	Lancaster	V	
Oct. 6, 1978	Lancaster	V	

(modified after Sharnberger & Howell, 1985)

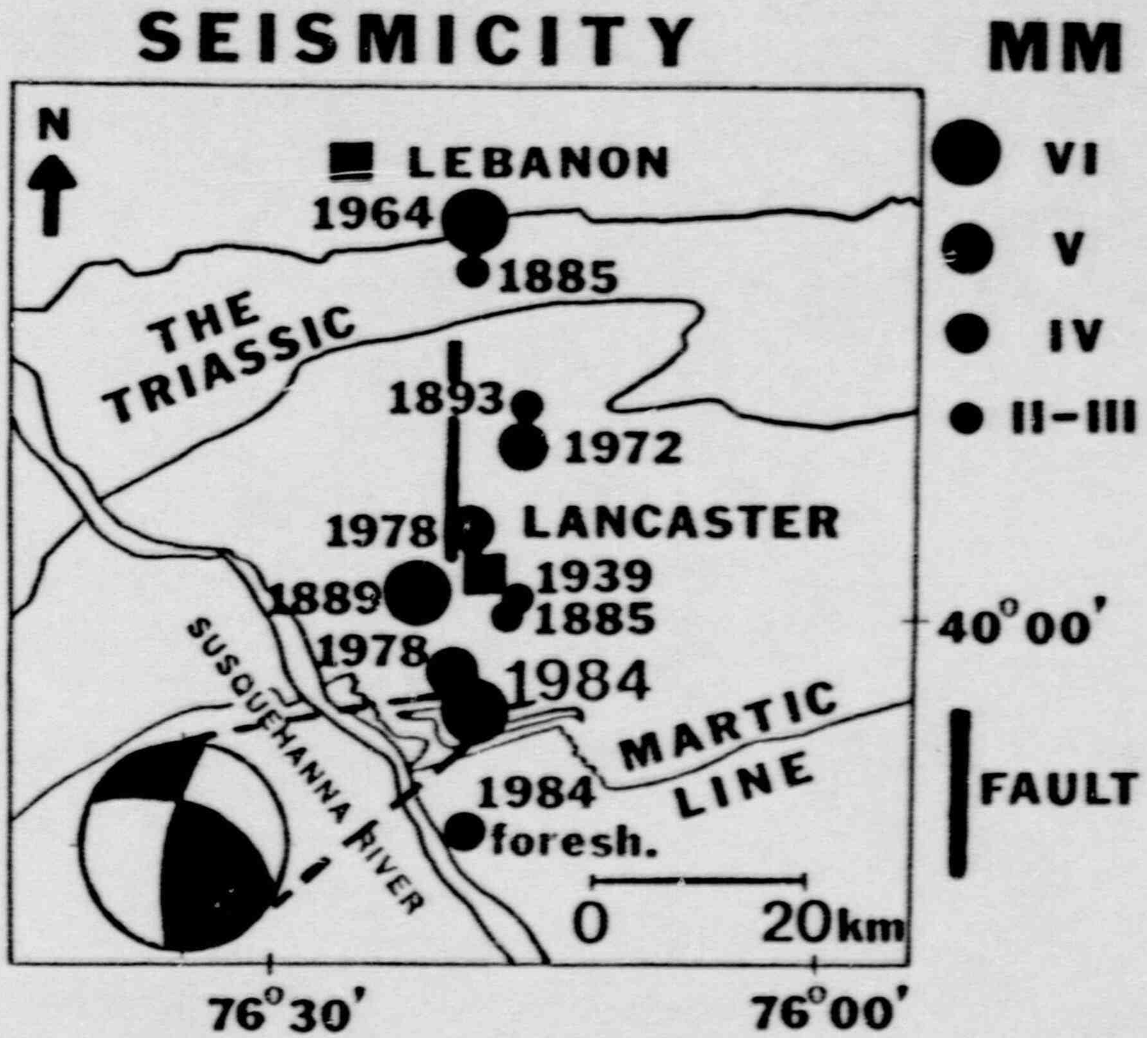

FIGURE 17 Map of the seismicity of Lancaster County in relation to the Fruitville Fault Zone (dark line). Inserted is the upper hemisphere projection of the fault plane solution obtained by Armbruster and Seeber (1985) for the April 23, 1984 earthquake. (modified after Scharnberger & Howell, 1985)

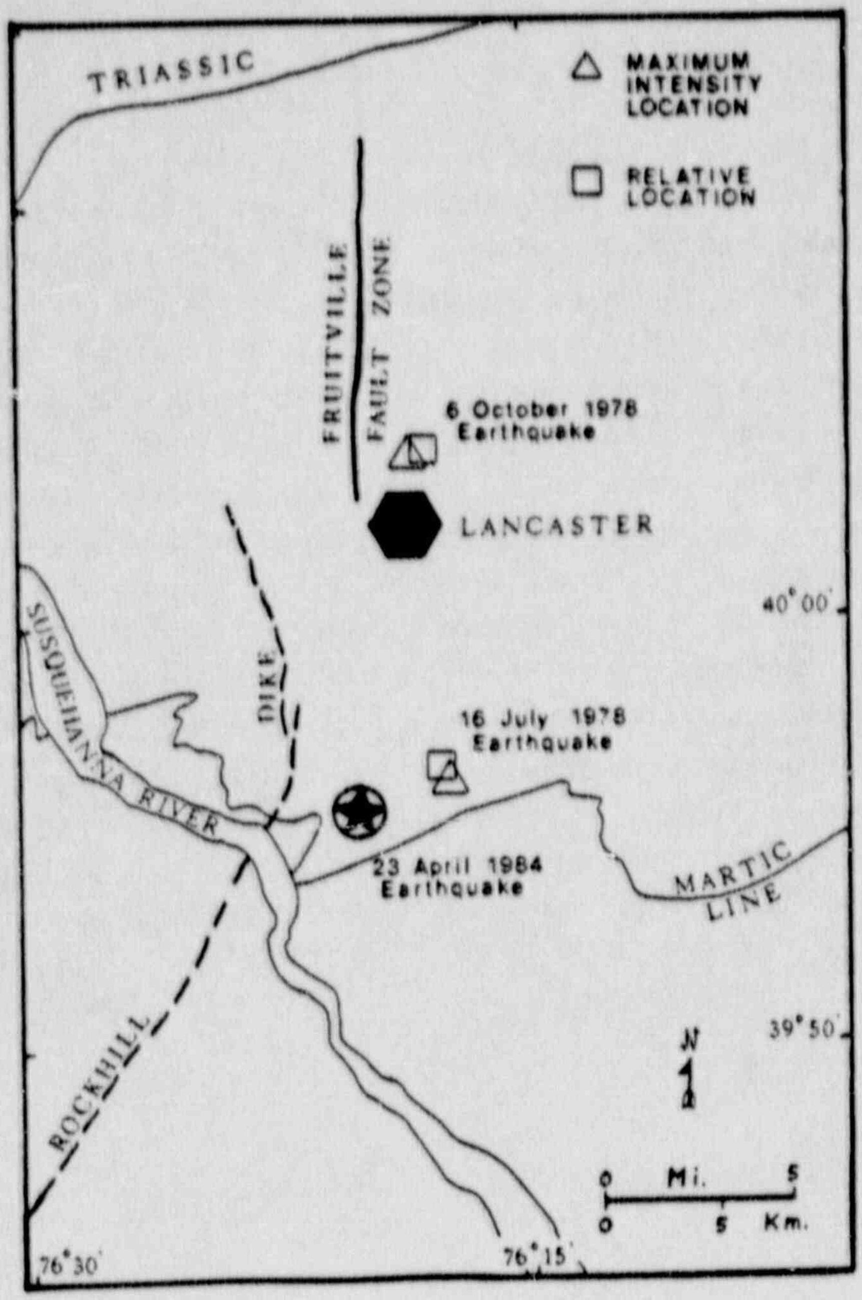

FIGURE 18 Maximum intensity locations and relative locations for the July 16, 1978 and the October 6, 1978 Earthquakes. (modified after Gray, et al., 1960).

Thus, it is apparent that historically the seismicity is clustered in a N-S striking zone along the Fruitville fault. The zone appears to be about 50-60 km long, in the N-S direction, and 10-20 km wide, in the E-W direction. It runs directly through the center of Lancaster County, Pennsylvania and parallels the most recent faulting in the area, such as that of the Fruitville fault zone (Figure 2).

Conclusions

Based on a multi-disciplinary approach, a neotectonic zone of deformation, the Lancaster seismic zone (LSZ), is identified in southeastern Pennsylvania. Historically several earthquakes have occurred in the N-S striking, 50 km to 60 km long, 10 km to 20 km wide zone. The largest recent event of April 23, 1984 was located in the southern end of the zone at a depth of 4.5 - 5.0 km. The fault plane solution for the event indicates a N 10°E striking fault plane with a 60°E dip, and a right-lateral sense of motion. Field geology identifies a N-S striking fault zone, the Fruitville fault zone (FFZ), which is coincident with the LSZ. The FFZ is in agreement with the location, the sense of motion, and the fault plane solution for the April 23, 1984 event. Furthermore, it has proven to be the youngest structural feature in the area, offsetting all surrounding structures and lithologies, except one. These are the Triassic-Jurassic diabase dikes. They parallel the youngest faults, such as the FFZ, and may be genetically related to them. Finally, a preliminary study of the drainage patterns, lineaments, and potential field data in central Lancaster County suggests the presence of a N-S trending fracture system within the LSZ and coincident with the FFZ.

FLUVIAL TERRACES ALONG THE LOWER SUSQUEHANNA RIVER*

Introduction

Fluvial terraces are preserved along the lower Susquehanna River from Harrisburg to Havre de Grace at the mouth of the Susquehanna. The lower course of the Susquehanna and the preserved terrace remnants transect the southern area of historic seismisity in the Lancaster, Pennsylvania area. It was therefore postulated that these terrace remnants could record any slow, long-term, regional, crustal deformation resulting from neotectonic activity in the Lancaster area.

As many as six gravel-capped terraces (Figure 19) occur along the lower Susquehanna (Stose, 1928). To constrain rates of crustal deformation across the Lancaster seismic area, these terrace remnants must be accurately correlated and subsequently dated. Uplift rates can then be calculated by two possible methods. The first method estimates the uplift rate from the difference in elevation between terraces or between a terrace and the modern stream level. It assumes that stream incision to the present level is only a result of tectonic uplift and neglects stream incision caused by either eustatic sea-level change or changes in sediment load resulting from climatic change, among others. However, along the lower Susquehanna all three processes have operated during the Quaternary to affect stream incision. Uplift rates calculated from the first method could only yield maximum values if the terrace age is well constrained.

The second method estimates uplift magnitude and rate by calculating the difference in terrace elevation along any <u>one</u> terrace. This method is most useful where individual terraces actually develop an upstream slope as a result of tectonic deformation. In that case, the magnitude and rate of crustal deformation can be accurately estimated if the terrace age is well constrained.

Although terrace remnants are preserved along the lower Susquehanna, two significant problems must be addressed in order to estimate magnitude, rate, and age of crustal deformation; the terrace remnants must be correctly correlated along the length of the river and the terraces must be accurately dated.

---

* This analysis was carried out by T. Gardner.

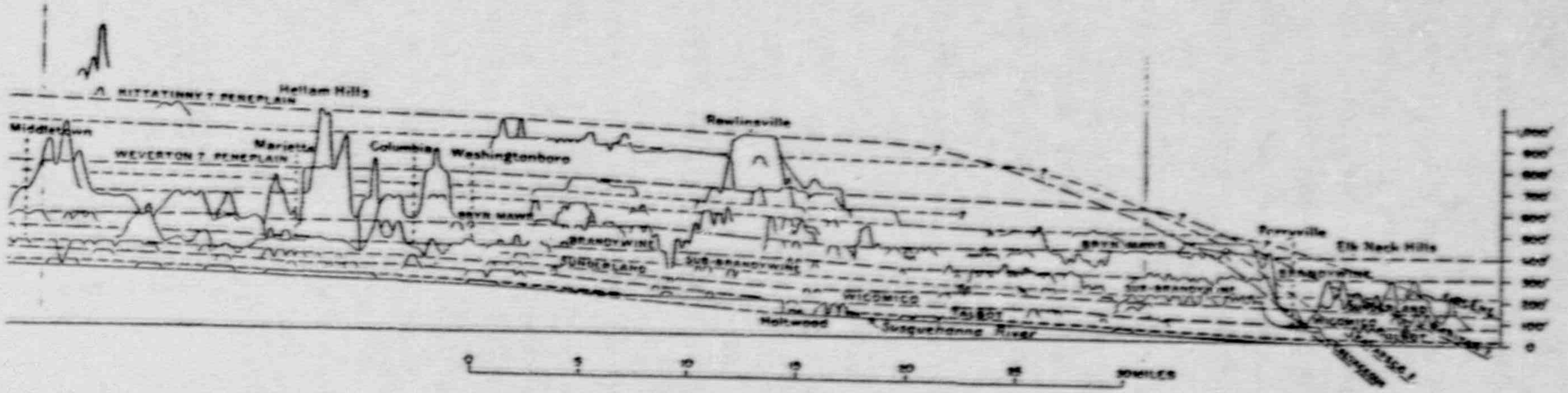

Figure 19. Composite terrace correlations for the lower Susquehanna River from Middletown to Haure de Grace (from Stose, 1928).

Distribution and Age of Terraces

Two detailed studies reporting the distribution of terrace remnants along approximately 100 kms. of the lower Susquehanna have been reported by Stose (1928, 1930) and Campbell (1929). At least six, gravel-capped terrace levels that are of potential use in this study have been mapped (Figure 19) and tentatively dated. These include, from lowest to highest, the Talbot, Wicomico, Sunderland, Sub-Brandywine, Brandywine, and Bryn Mawr. They range in elevation above the river from less than 20 feet (Talbot) to approximately 300 feet (Bryn Mawr).

The three lowest terraces (Talbot, Wicomico and Sunderland) which are also the best preserved and most continuous have generally been assigned a late Pleistocene age (Stose, 1928; Schlee, 1957) and tentatively related to glacial and periglacial processes in the headwaters of the Susquehanna. These terraces generally have a longitudinal profile that is parallel to the modern river profile. Therefore, in calculating uplift rate, the first method can be used to estimate possible maximum uplift rate.

The upper two terraces (Brandywine and Bryn Mawr) commonly referred to as the "Upland Gravels" occurs as scattered remnants of boulder strewn, flat uplands that can be found up to three miles from the modern river course. These gravel are mineralogically distinct from the lower terraces. Clast composition consists of a mature suite of orthoquartzites and cherts quite distinct from the less mature glacial gravels of the lower terraces.

The Upland Gravels generally consist of isolated, rounded, exotic boulders and cobbles preserved in a residual soil developed on local bedrock. Because these terrace deposits are poorly preserved and deeply weathered, no dateable materials have been found in them. Tentative age assignments are based on degree of weathering and possible correlation to related marine units in the coastal plain. Assumed ages range from earliest Pleistocene to middle Pliocene (Schlee, 1957) or late Tertiary (Stose, 1928).

An attempt was made to constrain the age of these Upland Gravels using a micropaleontologic method. Samples were collected from nearshore marine sediments from the head of Chesapeake Bay that are correlated to these Upland Gravels. These include samples from the Sand Hill Quarry (elevation 60 ft., Rte. 7 north of Hauredegrace), Cecil Brothers Quarry(elevation 420 ft., Rte. 275), and York Brothers Quarry (elevation 400 ft., Belevedere Rd.). However, all samples were devoid of palynomorphs (see letter from Travspore Inc.). Other studies have also reported similar unsuccessful results. Therefore, the age of these "Upland Gravels" is very poorly constrained at this time. The poorly constrained age estimates will not affect estimates of magnitude of crustal deformation, but will affect all rate calculations based upon these Upland Gravels.

Terrace Correlation

To estimate the magnitude and distribution of possible crustal deformation along the lower Susquehanna River, terrace remnants must be accuratley correlated along the length of the river. Because of the poor preservation of Upland Gravel terrace remnants along the lower Susquehanna, the only two detailed studies of that area (Campbell, 1929 and 1933; Stose, 1928, 1930) have produced rather disparate views on the nature of the correlation. The relevant controversy involves correlation and inferred deformation of the oldest gravel-capped terrace remnants, the Bryn Mawr Terrace of assumed earliest Pleistocene or Pliocene age (Schlee, 1957). Campbell's (1929) correlation of the Bryn Mawr Terrace remnants shows a distinct upward bulge in the Bryn Mawr surface (Figure 20) centered near Safe Harbor, in the general vicinity of historic seismic activity around Lancaster. Contours drawn on this warped surface produced the Westminster Anticline (Figure 21) with nearly 100 feet of closure that extended from the Potomac River in the southwest to the Schuylkill River in the northeast. However, Stose (1930) questioned the accuracy of the terrace correlations, suggesting that the Bryn Mawr was miscorrelated by Campbell. Stose's (1930) correlation showed no deformation along the Bryn Mawr surface. Given the poor preservation of the Bryn Mawr terrace gravels, it is not possible to determine the correct correlation at the present time. Therefore, uplift rates based on both correlations will be calculated for the lower Susquehanna.

Neotectonic Deformation Along The Lower Susquehanna

Given the above limitations on age and correlation of terrace remnants, uplift and possible uplift rates have been calculated for the lower Susquehanna. (Table 2). Maximum possible uplift rates vary over an order of magnitude, but are consistantly quite low ranging from 6.5×10^{-2} mm/yr to 2.8×10^{-1} mm/yr. However, these low rates could be expected for crustal deformation along a passive, continental margin. Importantly, uplift rate calculated from closure on the Westminster Anticline is centered in the vicinity of historic seismic activity near Lancaster and may reflect deformation associated with that activity over the last several million years. However, uplift rates calculated with the first method, using terrace elevation above modern stream level, may reflect a more regional uplift pattern, extending along the entire course of the lower Susquehanna. This type of broad crustal deformation may be more reasonably related to regional isostatic uplift resulting from slow but steady erosion of the Piedmont. However, the presence of distinct convex-up tributary stream segments (Thompson, 1985) and associated geomorphic features (Hack, 1982) support the notion that neotectonic uplift may be occurring over a more narrow region of the Piedmont upstream from the Coastal Plain. This would tend to support the deformation model suggested by Campbell (1929).

Table 2. Possible Uplift Rates along the lower Susquehanna River.

Method	Terrace	Elevation Difference ΔZ(meters)	Time Interval Δt(years)	Uplift Rate (mm/yr)
Closure on Westminster Anticline (Campbell, 1929)[1].	Bryn Mawr	65	1 million	6.5×10^{-2}
Elevation of Bryn Mawr above modern river level[2]. (Stose, 1930).	Bryn Mawr	100	2 million	1.0×10^{-1}
Elevation of Sunderland above modern river level[2]. (Stose, 1930).	Sunderland	38	100,000	3.8×10^{-2}
Elevation of Wicomico above modern river level[2]. (Stose, 1930).	Wicomico	20	70,000	2.8×10^{-1}

1. using method 2 in text
2. using method 1 in text

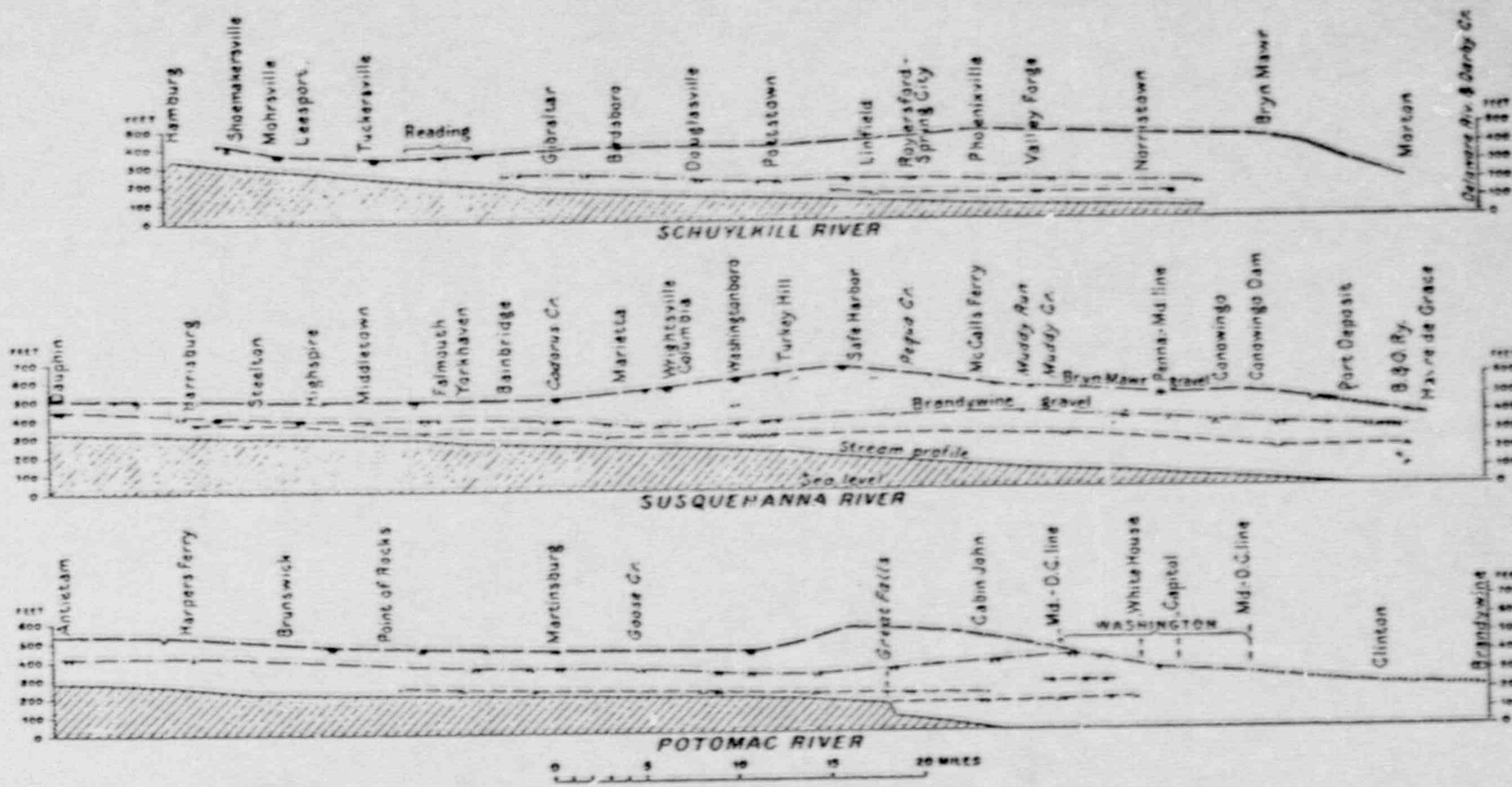

Figure 20. Terrace profiles of Bryn Mawr (or equivalent) and lower surfaces for three major rivers in the northern Appalachian Piedmont. Note inferred deformation on the Susquehanna in the vicinity of Safe Harbor. (from Campbell, 1929).

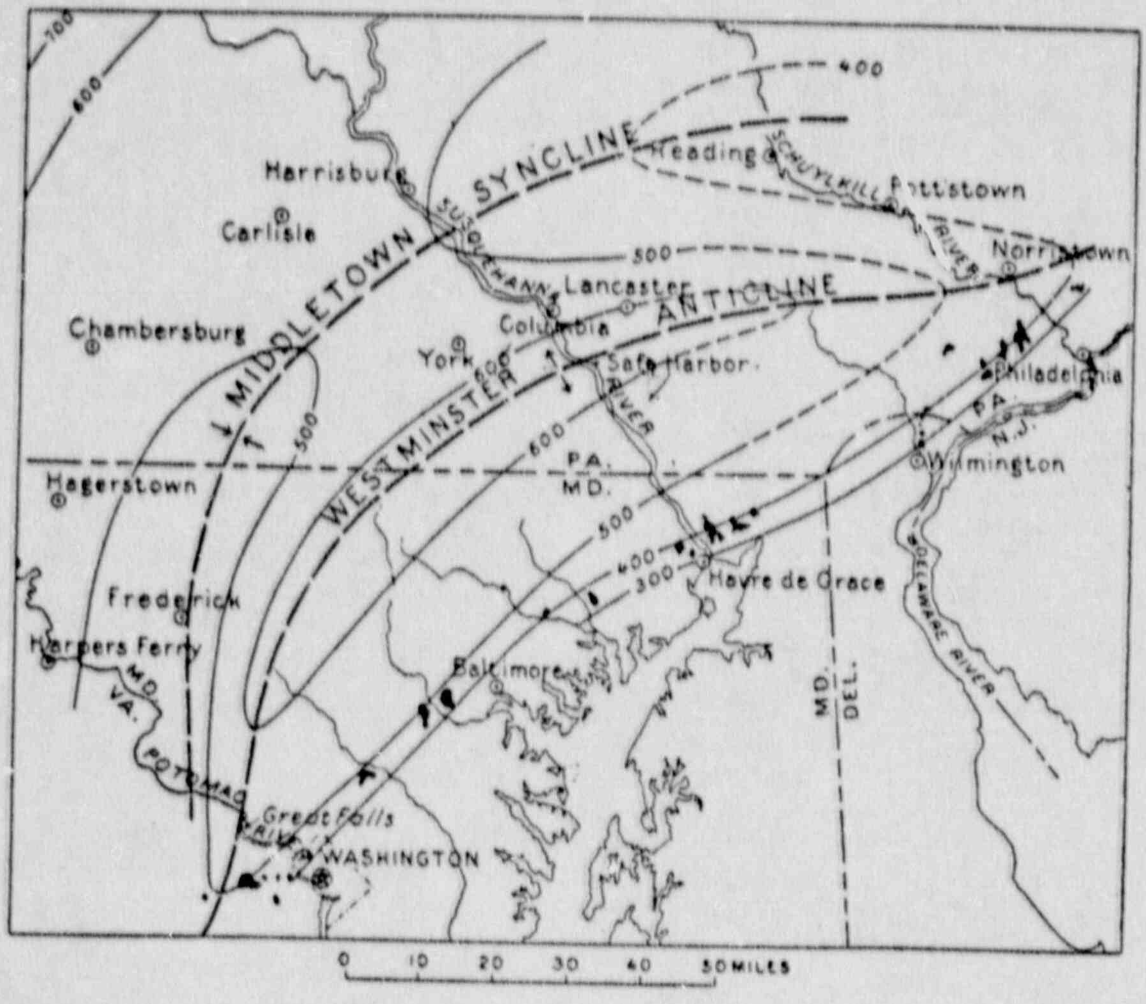

Figure 21 Distribution of the Westminster Anticline shown by contour lines on the surface of the Bryn Mawr gravel. Data from Figure 20. Contour interval 100 ft; datum near sea level. (from Campbell, 1929).

TRAVSPORE, INC.
R. D. 2, BOX 390
HUNTINGDON, PA 16652
U.S.A.

22 December, 1986

Dr. Thomas Gardner
Dept. of Geosciences
303 Deike Building
University Park, PA 16802

Dear Tom:

We have completed our study of the four (presumably) Neogene samples you gave us to work on, per your letter of 16 October.

I very much regret to report that the samples are utterly devoid, not only of palynomorphs, but of organic matter at all. The samples consist primarily of clean clay--kaolinite or montmorillonite probably. There are some silt-size particles which I assume must be quartz from the observed reactions:

1.no reaction in 15% HCl (therefore no carbonates)

2.violent reaction (explosive) in 52% HF

3.no $ZnCl_2$ (sp. gr. 2.1) float (this is really quite unusual for silty clay samples).

I believe you should look for a darker gray color in the field (these are practically white)--in my experience, this would indicate the probability of organic matter being present. Also, be sure to look for siltstone (these present samples are barely gritty to the teeth but are probably mostly clay?). It might be helpful to have me help do the collecting?

Per my original quote (my letter of 23 October, 1986), I enclose an invoice at $50/sample = $200.

Yours very truly,

Alfred Traverse
President

AT/et
encl: invoice

TRAVERTINE AS AN INDICATOR OF RECENT FAULT MOVEMENT

Summary

Based on Thornton's hypothesis travertine deposits such as those found in central Virginia, are associated with recent fault movements in carbonate terranes. Therefore, travertine deposits should now be forming in the Lancaster seismic zone. As predicted a ground-based survey revealed the presence of travertine deposits on small streams crossing the Lancaster fault zone in Lancaster, PA. Present deposition occurs downstream from the inferred fault trace which cuts the carbonate bedrock. This suggests that the seismically active fault may be mylonitizing the country rock and acting as a conduit for the calcium-carbonate-rich groundwater which supersaturates the runoff streams. It appears that this causative association of travertine with neotectonic fault movement can be used to locate and identify recently active faults in the northeastern U.S.

Background

Travertine (or tufa) deposits are located along many streams in the Shenandoah Valley of Virginia, in many (and perhaps in all) instances just downstream from the points where these streams cross the outcrops of thrust faults. Most of the deposits with which have been investigated (by Thornton) are not forming at the present time, but are being cut into by the streams that they have dammed. Along Holman Creek, between Forestville and Quicksburg, deposition of travertine was followed by a period of alluviation, so that some of the deposits are overlain marginally by stream sand and silts. This indicates that the period of travertine deposition there ended some time ago, yet the travertine is still younger than the origin of the present valley of Holman Creek. Appendix B gives further details concerning the nature and origin of these deposits.

Localization of the travertine downstream from the fault traces is taken to indicate that the source of the calcium carbonate-saturated waters was the fault zones, along which crushing of the limestones has resulted in their higher-than-normal solubility (Thornton's hypothesis). However, it seems unlikely that this crushing dates from the time of origin of these faults some 250 m.y. ago—the supply of crushed limestone produced at that time should long since have been exhausted. The most probable alternative is that geologically-recent movement has occurred along these faults, producing a new supply of crushed limestone for the circulating ground water to act on. On this hypothesis, the ages of the travertine deposits would reflect the times of most recent movement along these faults.

A number of large and rather spectacular examples of these deposits are known in Virginia, such as along Tumbling Run south of Strasburg, along Marl Creek just east of Steeles Tavern, along South River near Cornwall, and at Falling Springs north of Covington (Thornton, 1959). However, the stratigraphic and chronologic relationships are probably better displayed in some of the less spectacular occurrence such as those along Holman Creek mentioned above and those along Smith Creek east of Tenth Legion.

Discussion

Lancaster, Pennsylvania has been the region of recent seismic activity (Figure 17). The earthquakes, with a maximum magnitude of 4.2 (April 23, 1984), appear to be concentrated within a seismic zone which is 10–20 km wide and 50 km long. As discussed earlier, the Lancaster seismic zone, is associated with a reverse fault, the Fruitville fault, which strikes NNE through central Lancaster County (Figure 17).

As discussed earlier, on April 23, 1984 a magnitude 4.2, intensity VI earthquake occurred at a depth of 4.5 km along the southern extent of the fault zone (Figure 17). The main event was followed by several aftershocks which clearly indicated a NNE strike of the rupture (Figure 22). However, the faulting did not break the surface.

Ground surveys in the area carried out as part of this project revealed that the southern trace of the Fruitville fault zone is associated with preferential north–south drainage of the major streams in the area, the occurrence of springs, and presently active travertine deposition (Figure 22).

The ground surveys revealed four locations of present travertine deposition (Figure 22). Site 1 is located on a small stream at the southeast boundary of Millersville University campus. The source of the stream appears to be a spring near the inferred fault trace (Figure 22). The travertine is depositing within a small waterfall created by an outcrop of bedrock. The deposit is up to 1 cm thick and covers the bedrock and presently-growing algae. Site 2 is at the mouth of Stehman Run where a very thin coat (less than 0.2 cm) of travertine is being deposited on cobbles, logs, and algae within the turbulent parts of the stream. Site 3 is on the north branch of Stehman Run.

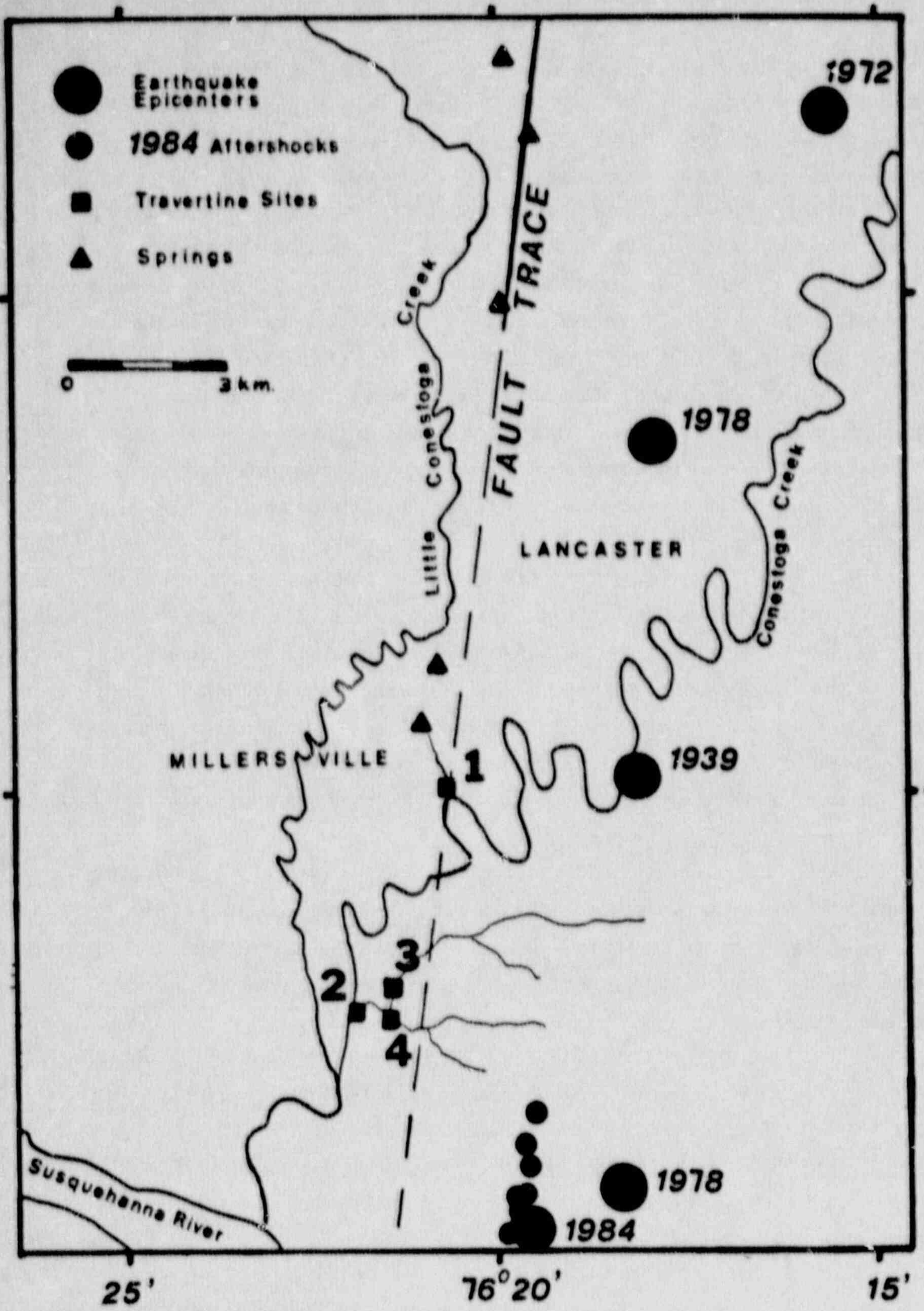

FIGURE 22 Map of travertine sites and springs in relation to recent earthquake epicenters along the southern trace of the Fruitville Fault near Lancaster, Pennsylvania.

The travertine forms a layer up to 0.5 cm thick on tops of cobbles which form small dams and agitate the stream. It is also depositing on growing algae. Site 4 is on the south branch of Stehman Run where a travertine layer of similar thickness covers dead branches and cobbles within small waterfalls.

All of the locations have several common traits. In all cases the travertine is precipitated in agitated water, such as a small falls within the stream. It always appears downstream from the inferred fault trace of the Gruitville fault. Finally, in this region the travertine forms only thin veneers up to 1 cm thick which coat rocks, organic debris, and actively growing plants and algae. In other regions of Pennsylvania (Carlisle and Chambersburg) and in Virginia recent ground surveys revealed dams of travertine up to tens of meters high associated with faulted carbonates. However, most of these indicated nc present deposition as did the above-mentioned sites in the Lancaster seismic zone.

Although this survey is not extensive or exhaustive, the occurrence of the travertine deposits downstream from the Fruitville fault trace, the presence of springs aligning with the fault trace, and the recent seismic activity (Figure 22), suggest the following possible explanation. The seismically active faults in the LSZ may be mylonitizing the country rock and acting as a conduit for calcium-carbonate-rich groundwater which supersaturates the runoff streams and precipitates travertine near points of exit where there is turbulent flow downstream from the active fault.

Thus, association of travertine with active faults suggests that by locating travertine deposits in the northeastern U.S. (or elsewhere) one can identify nearby faults which are associated with neotectonic deformation. The technique should be tried in other zones of recent seismicity where carbonate rocks exist.

It should be noted that after this project was completed travertine deposits were discovered (by C.P. Thornton) in Giles County, VA, the site of one of the largest (about magnitude 6) historic earthquakes in the eastern U.S. This deposit was discovered based on the prediction that travertine should be present in this area of major earthquake activity, although it had not previously been reported.

While the presence of travertine implies nearby neotectonic fault movement it does not necessarily imply seismogenic faulting. F sumably slower (non-seismic) fault movements would allow the same travertine-generating process to operate. However, the identification of those faults in eastern North America which are experiencing activity of any type vs dormant faults is very important in understanding the nature and origin of neotectonic deformation and associated hazard.

Age Dating of Travertine Deposits

If the association of travertine deposits with fault movements is correct then the ages of these deposits should represent the periods of past fault activity. Hence age dating of travertine deposits should provide a time history of active faulting in each area. Towards the end of this project an initial attempt was made to date the travertine deposit on Holman Creek near Quicksburg, VA described originally by Thornton (1959 and Appendix B). This site was chosen because the travertine's development is well-constrained geologically. The sequence of development was: valley cutting, followed by travertine deposition, followed by valley filling with alluvial deposition over the travertine, followed by the re-excavation by streams. There was no further travertine deposition after the alluvial cover was deposited. Therefore, to fix a minimum age for the last travertine deposition at this site samples of the gastropod shells (calcium carbonate) found in the overlying, layered alluvium were sent to a radiocarbon age dating laboratory for analysis. The carbon in the gastropod shells would represent atmospheric carbon and hence not be potentially biased by the carbon in carbon dioxide derived from host rocks. This age determination gave 4210 $\pm$ 60 years which means that the most recent nearby fault movement would have occurred earlier than this date. Because of time and budget constraints, age determinations on the travertine deposit itself were not made. It remains to be determined whether the carbon in the travertine reflects the age of deposition, the age of the parent carbonate rock or some combination of the two. If it is the former, then one must use carbonaceous material entrained with the travertine when it was deposited or material in underlying and overlying alluvial deposits as in the case just described. It is quite possible that bimodal ages will be found, one representing the age of deposition of the travertine and the other the age of deposition of the parent carbonate rock. Follow-on studies of this nature are clearly needed to establish the potential for reconstructing the history of neotectonic activity areas where travertine deposits are found.

However, in all cases where travertine deposition is presently occurring (e.g. Lancaster) associated geologically-recent movement on nearby faults (upstream) can be inferred.

NEOTECTONIC, GEOCHEMICAL AND LINEAMENT STUDIES OF THE MOODUS SEISMIC AREA

In an attempt to identify neotectonic, geochemical, and lineament characteristics of a second seismically active area in the northeastern United States, studies were conducted during the late summer and fall of 1987 in and around the Moodus, Connecticut, area. This project focused on a six quadrangle region centered on the "Moodus seismic area," an area of anomalously high seismic activity in recent and historic times.

The study included a review of the relevant literature, particularly with regard to features that might be related to the seismic activity, and field work to locate and examine those neotectonic features. Also, the local drainage network was examined and water samples were taken to assess their degree of saturation by chemical species which might indicate deep fluid movement along active faults or fractures. Finally, remote sensing imagery at four scales (1:250,000 SLAR radar imagery, 1:100,000 SPOT satellite image, 1:80,000 high-altitude photography, and 1:18,000 low-altitude photography) were examined for the presence of lineaments on other features that may reveal bedrock fracturing and tectonic stress orientations.

No unambiguous evidence of neotectonic features has previously been reported for this area. No evidence of tectonically disturbed glacial drift or stream deposits appeared in previous reports covering the area, except possibly in one study where the critical outcrop was regraded and obscured. The geochemical studies in the present study revealed no evidence of mineral precipitates or supersaturated species in 33 stream bottom samples and 8 water samples. Lineament analysis of the six-quadrangle area at the three smaller scales and the Moodus quadrangle at the 1:18,000 scale produced varying distributions of feature orientation, frequency, and length. These orientations are concentrated in the northwest quadrant, although secondary peaks occur in the north-northeast and east directions. The similar distribution of lineament orientations produced from the SPOT imagery and high-altitude photographic images, indicates that these similarly-scaled remote-sensing products are sampling a common set of lineaments. The differences between the distributions may be a result of stereoscopic viewing of the aerial photographs. The prominent lineament orientation peaks at azimuths of 80°-90° and 340°-350° are nearly parallel and perpendicular, respectively, to the direction of the maximum compressive stress (σ_1) as determined from in situ stress and earthquake focal mechanisms in the area (Woodward-Clyde Consultants, 1988). This association suggests a causal association with the present thrust stress regime. Lineament frequency was observed to increase in the Moodus quadrangle relative to adjacent study quadrangles, suggesting an increase in fracture density in the vicinity of the seismic zone.

The variation in the orientation of lineament features appears to be compatible with a first-, second-, and third-order shear couple model. Lineament frequency was observed to increase on the radar, SPOT, and high-altitude photography in the Moodus quadrangle block relative to adjacent quadrangles. This indicates that a higher degree of fracturing may be present in the vicinity of the active seismic area. In addition, scale phenomena functions related to the lineament analysis were developed. They show: 1) an exponential decay in lineament frequency per unit area with increasing scale number, and 2) a linear increase in average lineament length with increasing scale number.

Details of this study are contained in a report by C. Shuman presented in Appendix C.

SUMMARY AND CONCLUSIONS

For the Lancaster seismic zone the multifaceted investigation revealed several manifestations of near-surface, neotectonic deformation. Remote sensing data together with surface geological and geophysical observations, and recent seismicity reveal that the neotectonic deformation is concentrated in a NS-trending fault zone some 50 km in length and 10-20 km in width. Anomalies associated with this zone include distinctive lineament and surface erosional patterns; geologically recent uplift evidenced by elevations of stream terraces along the Susquehanna River; and localized contemporary travertine deposits in streams down-drainage from the inferred fault zone.

In the Moodus seismic zone results of previous ground-based geological studies were combined with remote sensing observations (aerial photography, SLAR imagery, and SPOT imagery) and used to look for evidence of near-surface deformation associated with the zone of recent seismicity. Lineament frequency was observed to increase in the Moodus quadrangle compared to adjacent areas and dominant lineament directions were observed that are perpendicular and parallel to the orientation of the maximum horizontal stress direction (N80-85E), recently determined from in-situ stress measurements in a 1.5 km-deep borehole in the seismic zone and from well-constrained earthquake focal mechanisms. These dominant lineament orientations are those expected in the present thrust stress regime which has generated recent earthquakes in the Moodus area. No geochemical anomalies or travertine deposits were found to be associated with the zone of seismicity. The only potential source of travertine in the area is one metamorphic rock unit, which upon weathering produces calcium carbonate. However concentrations necessary to cause precipitation of travertine were not found in any of the streams sampled.

One of the most important general results of this study was the identification of travertine as a possible new indicator of neotectonic fault movements in areas underlain by limestone and dolomite. The working hypothesis (developed originally by C.P. Thornton) is that water reaching the surface along fault gouge zones will emerge saturated or supersaturated in carbon dioxide and then will quickly precipitate in nearby small streams to produce readily-observed travertine (tufa) deposits. No such deposits are expected to be associated with dormant faults because the high surface area to volume carbonate material in the fault gouge will have been dissolved and carried away shortly after the last fault movement. If this hypothesis is correct and generally applicable, then recently-active faults should be found just upstream from observed trevertine deposits. Alternatively stated, travertine deposits are predicted to occur downstream from the surface projection of active faults in carbonate-rich terranes. Guided by this theory a ground-based survey was carried out in the Lancaster seismic zone and contemporaneous travertine deposits were discovered just downstream from the Fruitville fault which is associated with the major earthquake activity in the area; none had previously been reported for this area. The travertine is presently being deposited at all the sites where it was found.

The possibility of age-dating travertine deposits suggests that the time history of nearby fault activity might be reconstructed as well. Late in this study an attempt was made to age-date a travertine deposit from the Quicksburg, VA area using a radiocarbon method. The date obtained was 4210 ± 60 years, which represents a lower bound for the age of last fault movements producing the deposit. However, travertine is presently being deposited approximately 5 km upstream indicating recent fault movement there. This area has experienced historic earthquake activity indicating that neotectonic deformation is occurring. The travertine found in the Lancaster seismic zone is currently being deposited as evidenced by twigs and other debris entrained in the deposit and by its coating of stream pebbles. Further investigation of this new indicator of neotectonic fault movement is clearly warranted.

Appendix D contains copies of published abstracts of papers presented at technical meetings describing the results of this study.

REFERENCES

Armbruster, J. G., and Seeber, L., 1985, Marctic April 23, 1984 earthquake and the Lancaster seismic zone in eastern Pennsylvania: (unpubl.).

Baumgardt, D. R., 1977, The application of differential travel-time residuals for the study of mantle heterogeneities (abstr.): Earthquake Notes, v. 48, p. 9-10.

Baumgardt, D. R., 1985, Personal communication.

Berg, T., et al., 1980, Geologic map of Pa.: Pa. Geol. Surv., 1:250,000.

Bromery, R. W., and Zandle, G. L., 1959, Aeromagnetic map of the Conestoga quadrangle, Lancaster County, Pa: U.S. Geol. Survey, Geophys. Invest. Map GP-218.

Bromery, R. W., and Zandle, G. L., 1961, Aeromagnetic map of the Lititz quadrangle, Lancaster County, Pa.: U.S. Geol. Survey, Geophys. Invest. Map GP-257.

Bromery, R. W., and Griscom, A., 1967, Aeromagnetic and generalized geologic map of S.E. Pennsylvania: U.S. Geol. Survey, Geophys. Inv. Map GP-577.

Campbell, M. R., 1933, Chambersburg (Harrisburg) peneplain in the Piedmont of Maryland and Pennsylvania, Geological Society of America, v. 44, p. 553-573.

Campbell, M. R., 1929, Late geologic deformation of the Appalachian Piedmont as determined by river gravels, Proc. National Academy of Sciences, v. 15, p. 156-161.

Custer, B. H., Merkel, E. J., Yaworski, M., Knight, W. R., and Holzer, D. B., 1985. Soil Survey of Lancaster County, Pennsylvania. U.S. Dept. Agriculture, Soil Conservation Service., 152 p.

Dewey, J. W., and Gordon, D. W., 1984, Map showing recomputed hypocenters of earthquakes in the eastern and central U.S. and adjacent Canada: U.S. Geol. Survey Map MF-1699.

Gold, D. P., Parizek, R. R., and Alexander, S. S., 1973, Analysis and Application of ERTS-1 data for regional geological mapping: Technical presentations of symposium on significant results obtained from the earth resources techn. satellite-1, v. 1, p. 231-246.

Gold, D. P., Parizek, R. R., and Alexander, S. S., 1974, Applications of remote sensing to natural resources and environmental problems in Pennsylvania, Earth and Mineral Sci. Bull., v. 3, no. 7.

Gray, C., Geyer, A. R., and McLaughlin, D. B., 1958, Geology of the Richland quad., S.E. Pa.: Pa. Geol. Soc., Atlas 167D.

Hack, J. T., 1982, Physiographic division and differential uplift in the Piedmont and Blue Ridge, U.S. Geological Survey Prof. Paper No. 1265, 49 p.

Klein, F. W., 1978, Hypocenter location program, HYPOINVERSE: U.S. Geol. Surv. Open-file Report 78-697.

Knopf, E. B., and Jonas, A. I., Geology of the McCalls Ferry - Quarryville district, PA Geol. Survey Bull. No. 799.

Kowalik, W. S. and Gold, D. P., 1974, Use of Landsat-1 imagery in mapping lineaments in Pa.: 1st. Internat. Conf. on the New Basement Tectonics; Utah Geol. Assoc. Publ. #5, ed. R. A. Hodgson, et al. p. 236-249.

Kowalik, S. W. and Gold D. P., 1975, Lineaments and mineral occurrences in Pa.: NASA Tech. Rept., ORSER/SSEL Rept. 14-75 in M.S. thesis, Kowalik, W. S., Penn State Univ., University Park, PA.

Kowalik, W. S., and Gold, D. P., 1976. The use of Landsat-1 imagery in mapping lineaments in Pennsylvania. Proc. 1st Int. Conf. on the New Basement Tectonics (Utah Geol. Assoc., #5, 236-249.

Lahr, J. C., 1980, Hypoellipse/multics: A computer program for determining local earthquake hypocentral parameters, magnitude, and first motion pattern: U.S.G.S. Open File Rept. 80-159, revised April 1980 for version II, 59 p.

Mackir, J. H., 1934, Terraces in the Susquehanna valley below Harrisburg, PA, Science, v. 80, p. 140-141.

Meisler, H., and Becher, A. E., 1971, Hydrology of the carbonate rocks of the Lancaster 15-min. quad., Pennsylvania: Pa. Geol. Soc. Progress Report 171.

Nottis, H. N., 1983, Epicenters of N.E.U.S. and S.E. Canada, onshore and offshore, time period: 1534-1980: Map and Chart Series #38, N.Y. State Museum.

Scharnberger, C. K., 1978, Lancaster County earthquake, July 16, 1978; and Another Lancaster County earthquake: Pennsylvania Geology, v. 9, #5 & #6.

Scharnberger, C. K., and Howell, B. F., 1985, Intensities and Structural setting of the earthquake of 19 April and 23 April, 1984 in Lancaster County, Pennnsylvania: Earthquake Notes, 56(2), p. 43-46.

Schlee, J., 1957, Upland gravels of southern Maryland, Geological Society of America, v. 68, p. 1371-1410.

Smith, R. C., et al., 1975, Geology and Geochemistry of the Triassic diabase in pennsylvania: G.S.A. Bull., v. 86, p. 943-955.

Socolow, A. A., 1974, Geologic interpretation of the aeromagnetic maps of southeastern Pennsylvania: Pa. Geol. Survey Inform. Circ. #77.

Stockar, D. V., 1986, Contemporary tectonics of the Lancaster Pennsylvania seismic zone: M.S. thesis, the Pennsylvania State University, University Park, Pennsylvania, 226 pp.

Stockar, D. V., C. P. Thornton, D. P. Gold and S. S. Alexander, 1987, Travertine deposits within the Lancaster Seismic Zone, preliminary report, The Pennsylvania State University, 5 pp.

Stose, F. W., 1928, High gravels o Susquehanna River above Columbia, Pennsylvania, Bulletin Geological Society of America, v. 39, p. 1073-1086.

Stose, G. W., 1930, Is the Bryn Mawr peneplain a warped surface, American Journal of Science, v. 219, p. 177-184.

Stose, G. W. and Jonas, A. I., 1930, Lancaster quadrangle atlas: Pa. Geol. Surv., Atlas #168.

Sumner, J. R., 1975, Geophysical interpretation of the structural configuration of the Newark-Gettysburg Triassic basin: Report Geol. Surv. Grant 14-080001-G150, Dept. of Geol. Sc., Lehigh Univ., Pa.

Sumner, J. R., 1976, Residual gravity anomaly map of the Newark–Gettysburg Triassic basin, G.S.A. Abst. w/Prog., v. 8, p. 280.

Sumner, J. R., 1977, Geophysical investigation of the structural framework of the Newark–Gettysburg Triassic basin, Pennsylvania: G.S.A. Bull., v. 88, p. 935–942.

Thompson, G. H., 1985, The preglacial great falls of the Susquehanna River, Geological Society of America Abstract with Programs, v. 17, p. 734.

Thornton, C. P., 1953, The geology of the Mount Jackson quadrangle, Virginia, Ph.D. thesis, Yale University, 211 pp.

Van Houten, F. B., 1969, Late Triassic Newark Group, northcentral N.J. and adjacent Pa. and N.Y., in Geology of Selected Areas in N.J. and Eastern Pa. and Guidebook of Excursions: G.S.A. Annual Meeting, Rutgers Univ. Press, p. 314–330.

Wise, D. U., 1967, Radar Geology and pseudo geology on an Appalachian Piedmont Cross-section, Photogrammetric Eng., 752–761.

Woodward–Clyde Consultants, 1988, Regional Crustal Stress Study 3: Tectonic Stress in South–Central Connecticut, Empire State Electric Energy Corp. Research Report No. EP86–46, 32 pp. + 9 appendices.

Zoback, M. L., and Zoback, M. D., 1980, State of stress in the continental U.S.: J.G.R., v. 85, p. 6113–6156.

Zoback, M. D., 1986, In–situ stress measurements in the Kent Cliff research well: prepared for the Empire State Electric Energy Corp., N.Y., N.Y.

APPENDIX A

CONTEMPORARY TECTONICS OF THE LANCASTER, PENNSYLVANIA SEISMIC ZONE

David W. Stockar

Department of Geosciences

The Pennsylvania State University

TABLE OF CONTENTS

CHAPTER

Page

LIST OF FIGURES

LIST OF TABLES

ACKNOWLEDGMENTS

I would like to give special thanks to Dr. Shelton S. Alexander, for his guidance; Dr. Roy J. Greenfield, Dr. Peter M. Lavin, Dr. David P. Gold, Dr. Benjamin F. Howell, and Dr. Charles K. Scharnberger, for their expertise; Roger Felch, Kristin Vogfjord, John Barry and Lily Tang, for their insights; Tess Altland for her advise; and Dr. Ernst Zurfleuh for his interest and support.

This research was supported by the U.S. Nuclear Regulatory Commission under contracts # NRC-04-85-111-01 # NRC-04-83-021 and # NRC-04-85-113-04.

ABSTRACT

This study is focused on the contemporary tectonics of the Lancaster Seismic Zone in southeastern Pennsylvania. The neotectonic deformation associated with recent seismicity in this zone is inferred by consideration of source mechanisms of recent earthquakes and the inferred principal stresses, and geological and geophysical observations in the Lancaster area.

The hypocenter of the largest recent event in the Lancaster, Pennsylvania region, the magnitude 4.2, MM VI earthquake that occurred on April 23, 1984, was at a depth of 4.7 km, determined through cepstral analysis, and at a latitude and longitude of 39.94° N, 76.325° W near Marticville, about 10 km. south of Lancaster. The event was preceded by a magnitude 3.0, MM IV foreshock located near McCalls Ferry, about 8 km directly south of the mainshock. It was followed by several aftershocks oriented in a north-south trend over a 2 km zone. The focal mechanism of the mainshock also indicates a NS-striking fault plane. This strike is perpendicular to the dominant EW structural grain of the Appalachians within the Pennsylvania salient and of the Martic Line. Upon closer observation it is revealed that the youngest structures in the Lancaster region are all north-south trending and not EW-striking like the dominant Paleozoic features. Based on cross-cutting relationships, the youngest rocks present are the NS-striking Triassic-Jurassic diabase dikes, and the youngest faults present are the NS-trending cross-faults which offset all other structural features and lithologies of the area. The April, 1984 event is within the dominant zone of these faults. The historical seismicity and relocated, instrumentally recorded, events also define a NS-trending zone, the Lancaster Seismic Zone. It is approximately 50-60 km in length and 10-20 km in width. The seismic zone is parallel to the fault zone. The drainage pattern of the major streams is also predominantly NS-trending near Lancaster. Potential field (aeromagnetic and gravity) anomalies and prominent remote sensing lineaments provide further evidence of the presence of the cross-structural zone inferred from the geology and seismicity, including evidence for large scale basement features.

INTRODUCTION

Lancaster County is the most seismically active area in Pennsylvania, with several magnitude 3.0 or greater earthquakes in the past 25 years. The goal of this investigation is to understand the present tectonic conditions and associated neotectonic features of this region, and, thus, shed light upon the cause of this seismicity.

On April 23, 1984 Lancaster County, Pennsylvania experienced one of the largest earthquakes in its recent history. It registered a magnitude of 4.2 and a maximum intensity of MM VI. This mainshock was preceded by a magnitude 3.0, MM IV foreshock, on April 19 of the same year, and followed by several aftershocks which lasted until September, 1984. Immediately after the mainshock, the Pennsylvania State University and the Lamont-Doherty Observatory set up a temporary network of seismometers to record the aftershocks, and for six days recorded 10 events, the largest being a magnitude 2.1 (Armbruster and Seeber, 1985). These aftershocks lined up in a N-S trending zone approximately 2 km long near Marticville, about 10 km south of the city of Lancaster. Armbruster and Seeber (1985) obtained a fault plane solution based on the first arrivals from the mainshock and the aftershocks, which appeared to have the same epicenter. The fault plane solution suggested a N 10° E preferred fault plane with a dip of about 60 degrees toward the east. The motion on the fault plane appeared to be right-lateral reverse, with the maximum axis of compression in the ENE direction, analogous to the maximum principal stress orientation predicted by Zoback and Zoback (1980) and Zoback (1986) for this region.

This information prompted an investigation of the region, and of the possible source of the April 23, 1984 earthquake. The findings of this investigation are summed up in this paper. They were obtained by a thorough search of some 200 publications dealing with the geology, structure, geomorphology, gravity, magnetics, remote sensing and the seismicity of the Lancaster region, and of S.E. Pennsylvania, in general. Furthermore, the April 23, 1984 event, and the April 19, 1984 foreshock were located independently and relative to each other through a HYPOINVERSE (Klein, 1978; Lahr, 1980) absolute location algorithm and through a relative location algorithm (Baumgardt, D.R., 1977 & 1985). These locations were compared to the maximum intensity locations for the two events obtained by Scharnberger and Howell (1985), and were found to match within the 95% confidence error ellipses for the location algorithms.

The findings of the above investigation indicate a N-S striking zone of seismic activity, approximately 50-60 km in length and 10-20 km in width, through the center of Lancaster County. This zone, the Lancaster Seismic Zone, appears to be associated with N-S trending dikes and faults in the area, in particular the Fruitville Fault Zone (Figure 1). Furthermore, cross-cutting relationships, along with radiometric dating of the dikes, indicate that the N-S striking features are the youngest.

Thus, these youngest, N-S faults may be presently reactivated, in a reverse right-lateral sense, by the ENE maximum compressional stress predicted by Zoback and Zoback (1980, 1986), for this region. This would create earthquakes such as the April 23, 1984 event. If the ENE maximum compressional stress regime is ubiquitous for the entire region, such N-S trending faults may act as seismic source zones in other regions of the northeastern U.S.

Finally, in order to get a better idea of the source depth for the April 23, 1984 event, a cepstral analysis was conducted on data from this event received at 13 stations in New York State. The cepstral analysis predicted a 4.7 km depth for the mainshock which was in general agreement with the 4.4-4.7 depth for the aftershocks obtained through local monitoring by the Pennsylvania State University and the Lamont-Doherty Observatory in the epicentral area (Armbruster and Seeber, 1985).

GEOLOGY

General Appalachian Tectonics

The tectonic provinces of the Eastern United States are outlined and described by King (1951) as three separate regions. They are the central stable region, the Appalachian orogenic system, and the Coastal Plain. King's outline of the three regions is as follows:

- I.) Central stable region
  - a.) Laurentian shield (part of Precambrian Canadian shield)
  - b.) Interior lowlands (bordering platforms covered by younger rocks)
- II.) Appalachian orogenic system or tectonic province
  - a.) Fold belt (roughly the Valley and Ridge physiographic province)
  - b.) Blue Ridge belt (Blue Ridge physiographic province)
  - c.) Piedmont belt (Piedmont physigraphic province and part of the Blue Ridge physiographic province)
  - d.) New England - Maritime belt
- III.) Coastal Plain (post-orogenic deposits overlapping the Appalachian system)

from (Hadley & Devine, 1974)

The central Appalachians, in which Lancaster County, Pennsylvania is located, were affected by three Paleozoic orogenies. The first was the Taconic orogeny which occurred in the middle to late Ordovician (450-470 m.y.), followed by the Acadian orogeny of the early and middle Devonian (360 - 400 m.y.) and the Alleghenian orogeny of the Pennsylvanian and/or Permian (230 - 280 m.y.). The South Mt. anticlinorium and the lower Paleozoic rocks of the Great Valley and the Conestoga Valley (region surrounding Lancaster in Figure 1) were mainly deformed by the Alleghenian orogeny. This event was composed of several stages of deformation. The first was the thrust along a decollement of Precambrian rocks over lower Paleozoic ones in the Martic line region. This contact (Figure 1) strikes east-west through southern Lancaster County. This was followed by the folding of the decollement, and finally flat thrusting of the decollement terrane in the western margins of the Blue Ridge (Drake, 1980).

This type of deformation may be quite similar to that of the Southern Appalachians. Gwinn (1964) claims that "the tectonic style of the Central Appalachians is entirely analogous to that of the Southern Appalachians". According to this popular idea, the Valley and Ridge and the Appalachian Plateau are folded, NW moving, thin, thrust sheets, allochtonous for hundreds of kilometers on a sole thrust (decollement zone), which occurs largely within incompetent strata of middle Cambrian, upper Ordovician, upper Silurian, and middle and upper Devonian age.

General Geology of the Lancaster Area

The Lancaster area is within the major salient of the Appalachians. The tectonic grain in the region has a east-west strike (Figure 1) (Wise and Kauffman, 1960). Crystalline carbonate rocks underlie nearly half of the county (Meisler and Becher, 1971), and clastic sedimentary rocks and schists dominate south of the Martic line (Bria, 1978). Quartzites, carbonates, and pelitic sediments comprise the general stratigraphy from the basement upward within the lower Paleozoic rocks of the Conestoga Valley. However, in the middle Ordovician there is a gradual change from dominantly carbonate to dominantly clastic sediments (Wise and Kauffman, 1960). These Paleozoic rocks are strongly folded by at least two generations of folding. Further to the north, near the border of Lebanon County are the clastic sediments of the Newark - Gettysburg Triassic basin. These are intruded by large diabase sheets and dikes. These diabase dikes, which are predominantly N - NE striking (Figure 4), intrude all surrounding rocks of the region and are thus the youngest (Bria, 1978).

Poth (1977) offered a more detailed summation of the local geology. He mentioned that Lancaster County lies in the Piedmont physiographic province (Figure 1), which he divided into three sections, as follows:

Triassic lowlands section - This region occupies the northern tenth of Lancaster County. It is underlain by the shales and sandstones of the Gettysburg-Hammer Creek formation and the New Oxford-Stockton formation, as well as diabase sheets and dikes.

Conestoga Valley section - This section occupies the central half of the county. It is chiefly composed of carbonate rocks and shales, with minor amounts of quartzite, phyllite, and schist, as mentioned above.

Ordovician rocks (youngest to oldest)
- Cocalico formation : a fissile shale
- Conestoga formation : crystalline limestone containing clayey, graphitic, and micaceous laminae, and a basal carbonate-rock conglomerate
- Beekmantown Group : limestones, interbedded limestones and dolomites, and dolomites

Cambrian rocks (youngest to oldest)
- Conococheaque Group
- Elbrook-Cooks Corner formation : interbedded limestones and dolomites

- Ledger formation : dolomite
- Kinzers formation : shales with beds of limestone and dolomite
- Vintage formation : dolomite
- Antietam, Harpers & Chickies formations : Quartzite, phyllite, and schist

Piedmont Uplands section - This region is the southern part of the county. It is underlain by Precambrian and lower Paleozoic metamorphic rocks of the Peters Creek Schist, and the Wissahickon formation. These are schist and quartzite, and schist, respectively.

Newark - Gettysburg Triassic Basin

The Triassic sedimentary rocks of the Newark Group outcrop in elongated basins along the Atlantic coast from Nova Scotia to South Carolina. Two of the largest of these basins are in Connecticut along the Connecticut River, and in Pennsylvania and New Jersey. They are thought to share a common structural history, the Palisades disturbance (King, 1961; Bria, 1978). The Newark-Gettysburg Basin of Pennsylvania (Figure 1) is approximately 225 km. long and 6-50 km wide. It trends in the ENE direction across the SE corner of the state. It is the largest Triassic basin in the United States. It has a possible aggregate thickness of more than 6 km (Stose, 1932; Beck, 1965; Bria, 1978). The sediments of the Newark Group were deposited by streams and rivers from nearby uplands. Variation in topography and climate resulted in mostly poorly sorted lenticular beds. The fluviatile formations are red in color and the lacustrine formations are grey shales. These formations include conglomerates, shales, sandstones, siltstones and argillite. Furthermore, they contain Triassic-Jurassic sills, dikes, and irregular cross-cutting bodies whose thickness varies from less than 1 m to 1000 m. Igneous activity occurred in the late stage of deposition with some dikes being intruded after deposition ceased (Stose, 1932; Johnston, 1966; Shaub, 1975; Bria, 1978). The sedimentary rocks themselves are upper Triassic in age, based on faunal data (Willard et al, 1959).

The Newark-Gettysburg Basin follows the regional grain of the Appalation structures (30°-50°NE), although in the Lancaster County area it strikes due east-west. The dip of the Triassic sediments is on average 10°-20°NW., but locally it may differ widely due to warping and faulting (Van Houten, 1969). A set of faults in the basin's NW border indicate as much as 5,500 m of stratigraphic displacement. This is possibly due to gradual subsidence of the basin during sedimentation, culminating in block faulting immediately after the diabase intrusion (Stose, 1949; Bria, 1978).

However, it is more likely that this stratigraphical displacement along the northern border fault was caused by tensional crustal thinning and graben formation (Beck, 1972; Bott, 1976). This conclusion is reinforced by evidence that much stratigraphical displacement also occurred along flanks of the SE border of the basin. This probably occurred along a fault zone, possibly a set of faults, not clearly expressed in the exposed rock terrain (Van Houten, 1969). A 864 ft. borehole (core) in Thomasville, west of York, Pennsylvania, was taken on the SE border of the basin. It drilled through an apparent growth fault which is covered by the overlapping New Oxford formation. Cloos and Pettijohn (1973) concluded that this was evidence that the SE border of the basin was not a simple onlap, but probably a major faulting border, as appears to be the case along the northern border. Thus, they supported the full graben model for the origin of the Newark-Gettysburg Basin.

In fact, the origin of the Triassic basins has been very controversial up to the present. The three dominant theories are:

1. Full graben (Sanders, 1963)
2. Half graben faulted on the north side (Stose & Jonas, 1939)
3. Crustal downwarp with no major fault boundaries (Faill, 1973)

Since this is a very extensive debate that is not too pertinent to the Lancaster Seismic Zone, we shall not dwell on it any longer. Some useful references on the subject are: (Stose & Jonas, 1939; Stose, 1949; Willard et al, 1959; Sanders, 1960, 1963; Beck, 1965; DeBoer, 1967; Van Houten, 1969; Phillips & Forsyth, 1972; Faill, 1973; Cloos & Pettijohn, 1973; Shaub, 1975; Bott, 1976; Bria, 1978; Olsen, 1980; Daniels et al, 1983; Klitgord et al, 1983). However, one thing most of these authors do agree on is that the Triassic basins of the eastern United States, like the Newark-Gettysburg Basin, formed during the onset of the rifting of the present day Atlantic Ocean and are somehow associated with it.

The Piedmont

The Piedmont physiographic province in the Lancaster area is composed of metamorphic rocks in the south and sedimentary rocks, mostly carbonates, in the north. The exact stratigraphy of the region is given in Appendix 1, according to Wise and Kauffman (1960).

The bulk of the recrystallization of the Piedmont appears to be around 300-350 m.y. ago, in the early to middle Paleozoic, based on radiometric dating. The presence of 'alpine' peridotites and of serpentinites in the Inner Piedmont suggests that the region is part of the axial zone of the Appalachian mountains. Such serpentine belts follow the Appalachian trend along the entire length of the mountain chain . The western limit of these serpentine belts crosses the Susquehanna River in SE Pennsylvania at about the Maryland state line (Wise & Kauffman, 1960).

There is a decreasing metamorphic intensity across the Piedmont from SE to NW. The gradient of metamorphism in the Piedmont of this region is as follows (from greatest degree of metamorphism to the least degree):

1. A zone of extensive granitization and/or intrusion, with extensive basement flowage and mantle gniess domes in the Baltimore area
2. A schist belt with serpentine bodies in it
3. A zone with tightly folded Cambro-Ordovician carbonates with steeply dipping axial planes in the Lancaster Valley, accompanied by some basement uplift
4. A zone of NW recumbent folds and flowage, accompanied by some basement uplift
5. The Triassic basin, graben-like structure (not part of Piedmont)
6. The Valley and Ridge Province of folded Appalachians (not part of Piedmont)

from (Wise & Kauffman, 1960)

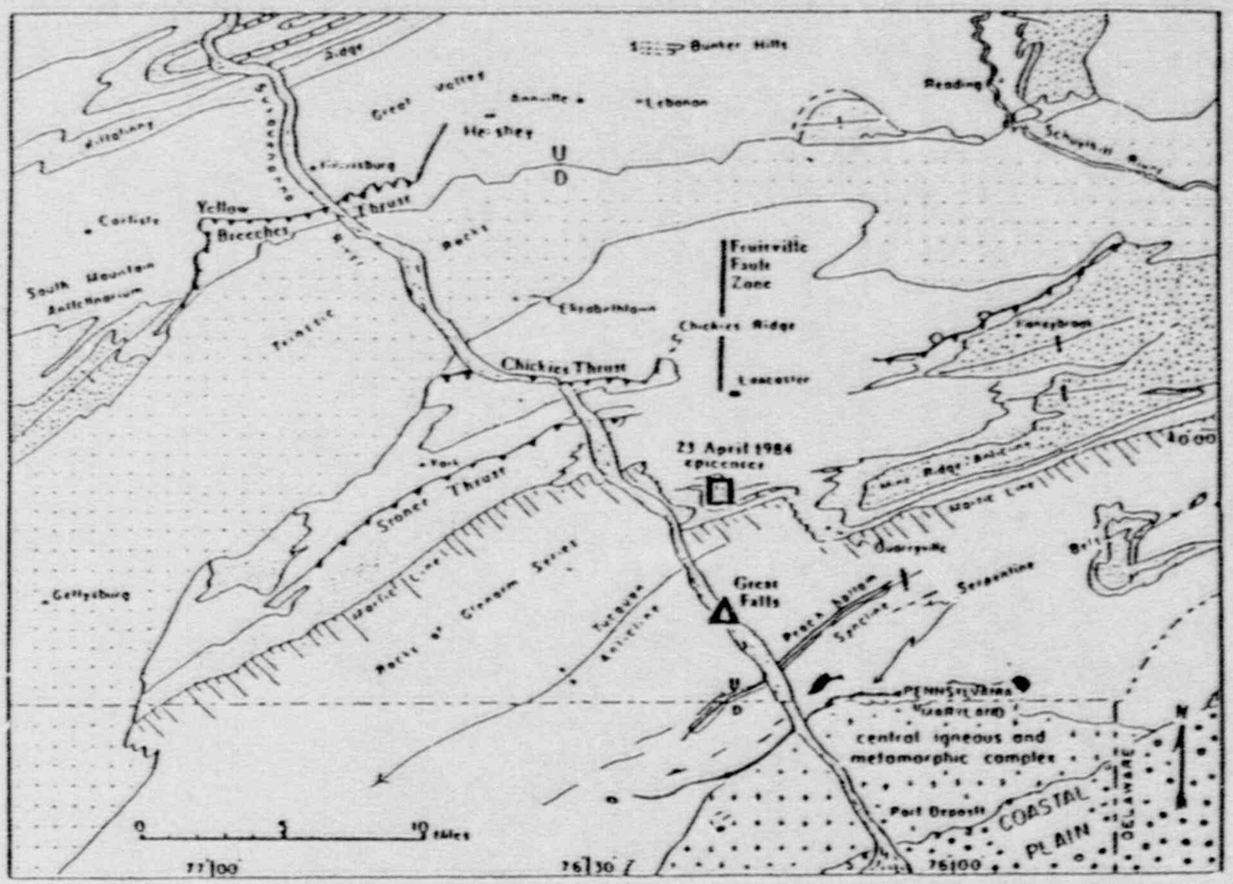

FIGURE 1 Geologic index map of the Appalachian Piedmont along the Susquehanna River of Pennsylvania and Maryland. (modified after Wise, 1967)

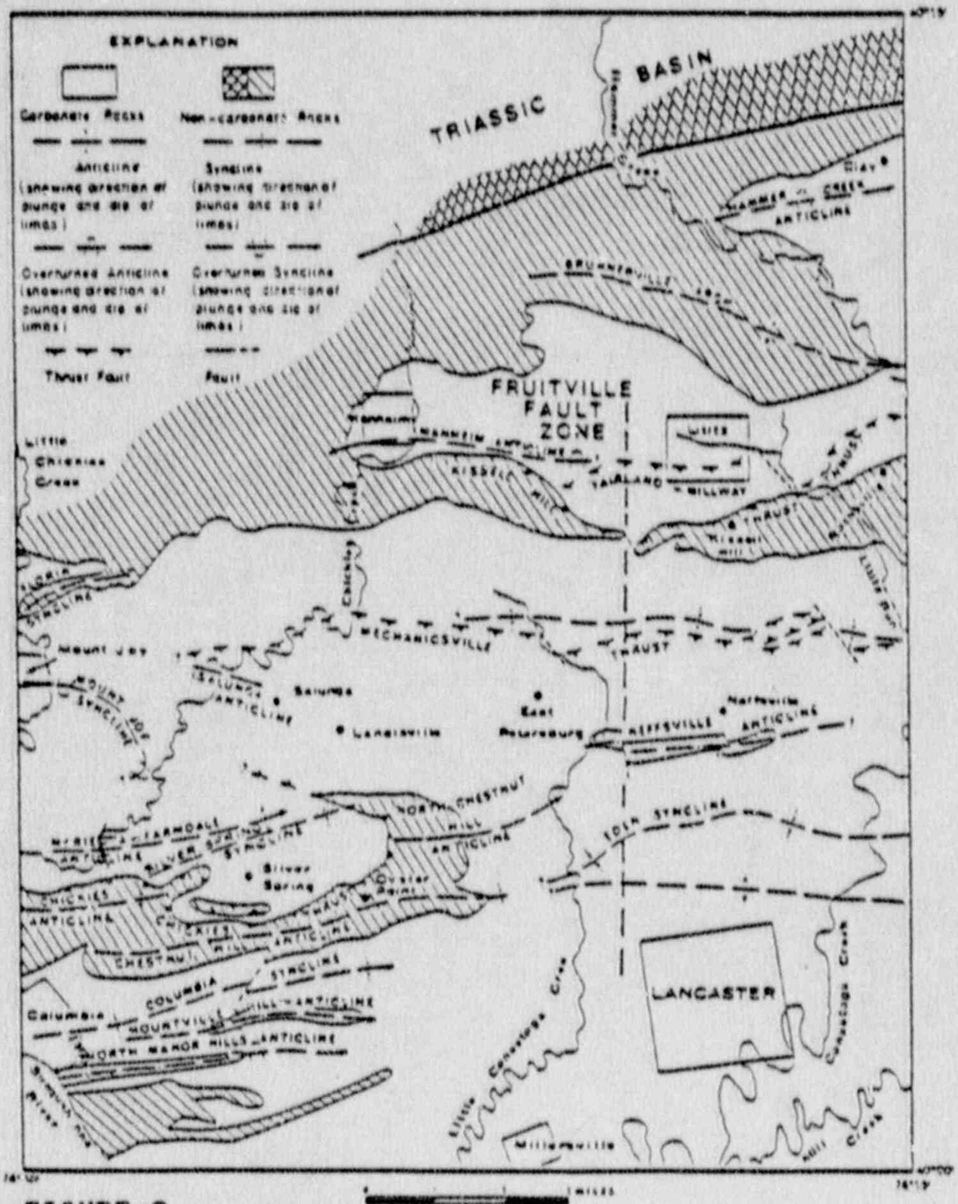

FIGURE 2

Structural map of the northern Lancaster County area. The Fruitville Fault Zone mapped by Stose & Jonas (1930) is superimposed on to the map as a dashed line. (modified after Meisler & Becher, 1971)

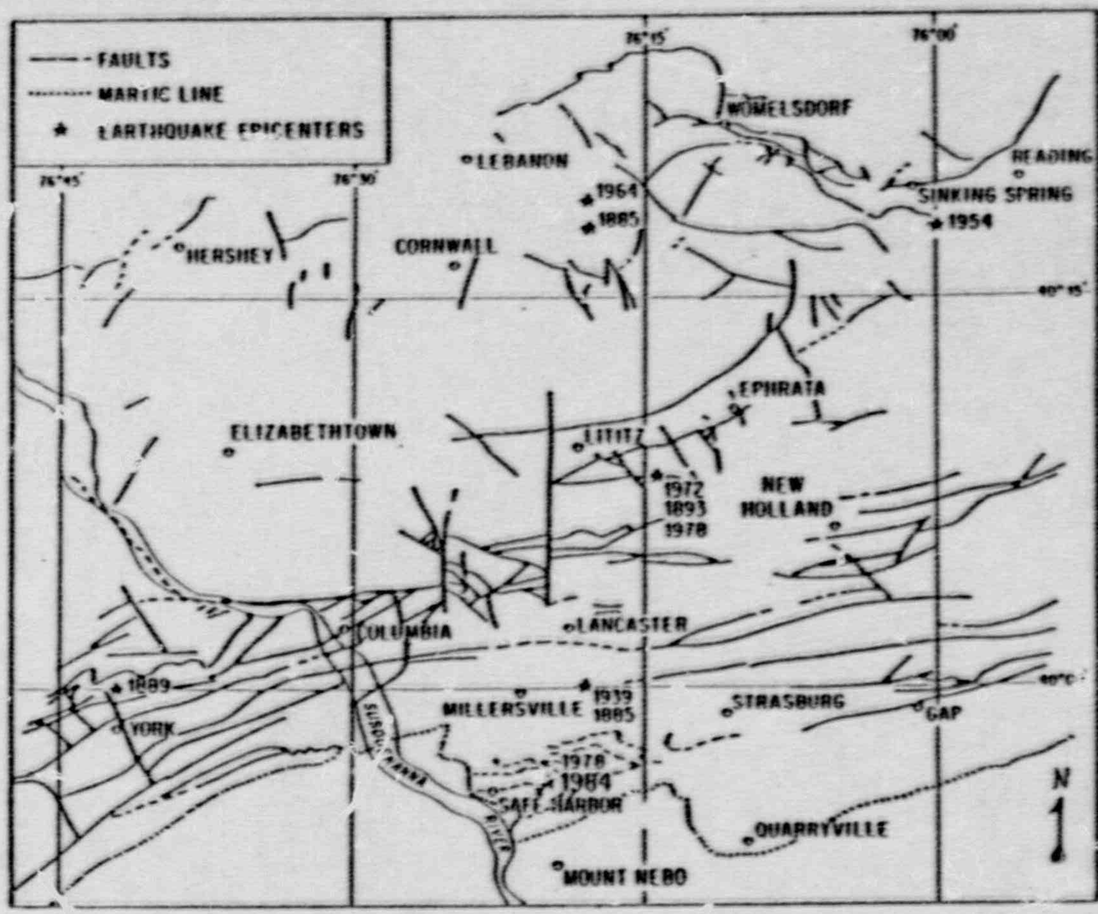

FIGURE 3 Map of the faults and the seismicity in the Lancaster Region. The faults appear as mapped by Stose & Jonas (1930). (after Scharnberger & Howell, 1985)

STRUCTURE

Major Structures of Lancaster County

The geology of the Lancaster area can be divided into several structural provinces. Starting at the northern part of the overall region (Figure 1), we encounter the Great Valley. This geological province is one large synclinorium with its southern limb overturned (Grey et al, 1958). South of the Great Valley is the Newark-Gettysburg Triassic Basin. This trough appears to be confined by normal, border faults on the north and south end. The Triassic basin, which is narrow and highly faulted in the Lancaster County region, follows the east-west trending structural grain of the region. It is dominated by several large diabase sheet intrusives within its red beds. South of the Triassic basin is the Lancaster or Conestoga Valley. This carbonate valley is dominated by recumbent folding and thrusting in the north, and tight isoclinal folding in the south. As in the Triassic basin, the youngest faulting in the region is north-south striking and the youngest rocks are the north-south striking Triassic-Jurassic diabase dikes. South of this carbonate valley is the Martic Line contact where the Wissahickon schist of the Glenarm series overlaps the Conestoga limestone of the Lancaster Valley. This Martic Line contact appears to be an early Paleozoic zone of imbricate thrusting which has later been folded (Jonas & Stose, 1930; Cloos & Heitanen, 1941; Meisler & Becher, 1971; Bria, 1978).

More locally the Lancaster Valley region surrounding the city of Lancaster (Figure 2), can be subdivided into three regional, structural domains (Meisler & Becher, 1971). The northern regional domain is characterized by nappe structure consisting of recumbent folds, thrust faults, and gentle south-dipping axial plane cleavage. The central regional domain has variable fold-geometry and intricate faulting in which the north-south striking faults are the youngest. Finally, the southern regional domain is dominated by upright, near-isoclinal folds and steeply dipping axial plane cleavage.

Based on their field observations, Meisler and Becher (1971) postulate the structural history of the area. They suggest that multiple events occurred beginning early in the Paleozoic and continuing up to at least the Triassic and Jurassic. Thus, epeirogenic movements caused pre-Conestoga and pre-Cocalico unconformaties. These are the earliest structural events (mid-Cambrian to mid-Ordovician) recorded in the carbonate rocks of the Lancaster Valley. This was followed by the deposition of the Conestoga and Cocalico formations in the early Paleozoic (Meisler and Becher, 1971).

The first period of deformation resulted in the development of the nappe structures and the axial plane cleavage, which dominate the northern zone of recumbent folding. This was accompanied by thrust faulting, minor thrusting and shearing on the overturned limb of the Manheim Anticline (Figure 2). Furthermore, in the initial stages of deformation, there occurred some strike-slip faulting and local warping of the axial plane cleavage (Meisler and Becher, 1971).

The second major deformation, which may have overlapped the first, produced the following results. In the southern part of the Lancaster Valley it produced isoclinal or near isoclinal folds, steeply dipping axial plane cleavage, and reverse faults with fairly constant strike and steep dip across the Maryland and Pennsylvania Piedmont. This deformation also formed more open folds such as the Eden Syncline and Chestnut Hill Anticline in the south (Figure 2). In the recumbent folding region it seemed to produce open folds in the cleavage and the bedding, or broad arches such as the Brunnerville Arch (Figure 2). The variability of the fold types, ranging from broad, open folds to tight isoclinal ones, is probably due to the different lithologies, and to the locally different intensity of basement deformation. Finally, "faults as late as the Triassic age are probably present in the carbonate rock" (Meisler & Becher, 1971).

Diabase Intrusions

Triassic-Jurassic Diabase Sheets

Within the Newark-Gettysburg basin of southeastern Pennsylvania are various diabase intrusions varying from dikes, flows, and irregular cross-cutting bodies to the dominant sheet (sill) form with its contact metamorphism of dark hornfels (Beck,1965). These Triassic sheets occur in three predominant bodies (Figure 4), the Gettysburg, the York Haven, and the Birdsboro Diabase. They have oval and elliptical outcrop patterns, and are commonly discordant with the surrounding sedimentary rocks. Therefore, they rarely represent true sills (Hotz, 1952). The few sills that do exist appear as west-dipping ring structures in the southeastern part of the basin and change into cross-cutting bodies in the north and northwest parts of the basin. They extend to the northwest edge of the basin where they are terminated by a boundary fault (Kauffman, 1967; Smith et al.,1975). At depth they appear saucer shaped with a thickness of 60 - 600 m. (Smith et al, 1975; Bria, 1978). This curved, basin shaped form may be due to near horizontal fractures in the Triassic sediment (Hotz, 1952; Bria, 1978).

The diabase is believed to have originated from deep reservoirs below the Triassic sedimentary rocks, ascending in vents such as stocks, dikes, and cross-cutting features (Smith, 1931; Bria, 1978). The main feeder fissures are thought to be concentrated near the northwest edge of the basin, where it is the deepest, and where the cross-cutting features and the faulting is more abundant (Kauffman, 1967).

Triassic-Jurassic Diabase Dikes

Dikes in the Lancaster County region are marked by long, low-lying, often forested ridges known as "ironstone ridges", and the presence of scattered diabase boulders known as the "float". In fields which have been cleared, they appear as soil coloration changes. Furthermore, there are steeper slopes in the vicinity of the dikes due to the differential weathering between the diabase and the surrounding carbonates. Some streams are also diverted by the dikes in the area (Lanning, 1973; Bria, 1978).

The diabase dikes usually are at most few tens of meters wide and fine grained. Some have flow differentiation and minor alteration to chlorite and sericite (Smith et al.,1975), but on the whole the Pennsylvania diabases are essentially unaltered (Bria, 1978).

These dikes and associated stocks have a large content of their original magnetite, which is a component of deep seated magma. This suggests that the magma rose up direct channels produced by faults, which extended at least some 6-7 km. to the bottom of the thick sedimentary accumulation in the region (Van Houten, 1969). The dikes that filled these fissures cut across the Triassic and Paleozoic rocks. Thus, they are of late Triassic age or younger (Jonas and Stose, 1930). In fact, the dikes are the only form that the diabase intrusives take in the older rocks that border the Triassic basin in Pennsylvania (Bria, 1978).

The dikes occupy steeply dipping fractures with a predominantly north to northeast strike and extend over long distances (Van Houten, 1969; Bria, 1978). "Most of the outlying dikes intrude the metamorphic and plutonic rocks of the Piedmont province, although a few extend northward into the Paleozoic rocks of the Valley and Ridge province near Harrisburg, Pa. Southeastward many of the dikes extend to the edge of the Atlantic Coastal Plain, where they pass unconformably beneath Cretaceous and younger strata." (King, 1961). Several dikes trend in the N-S direction for

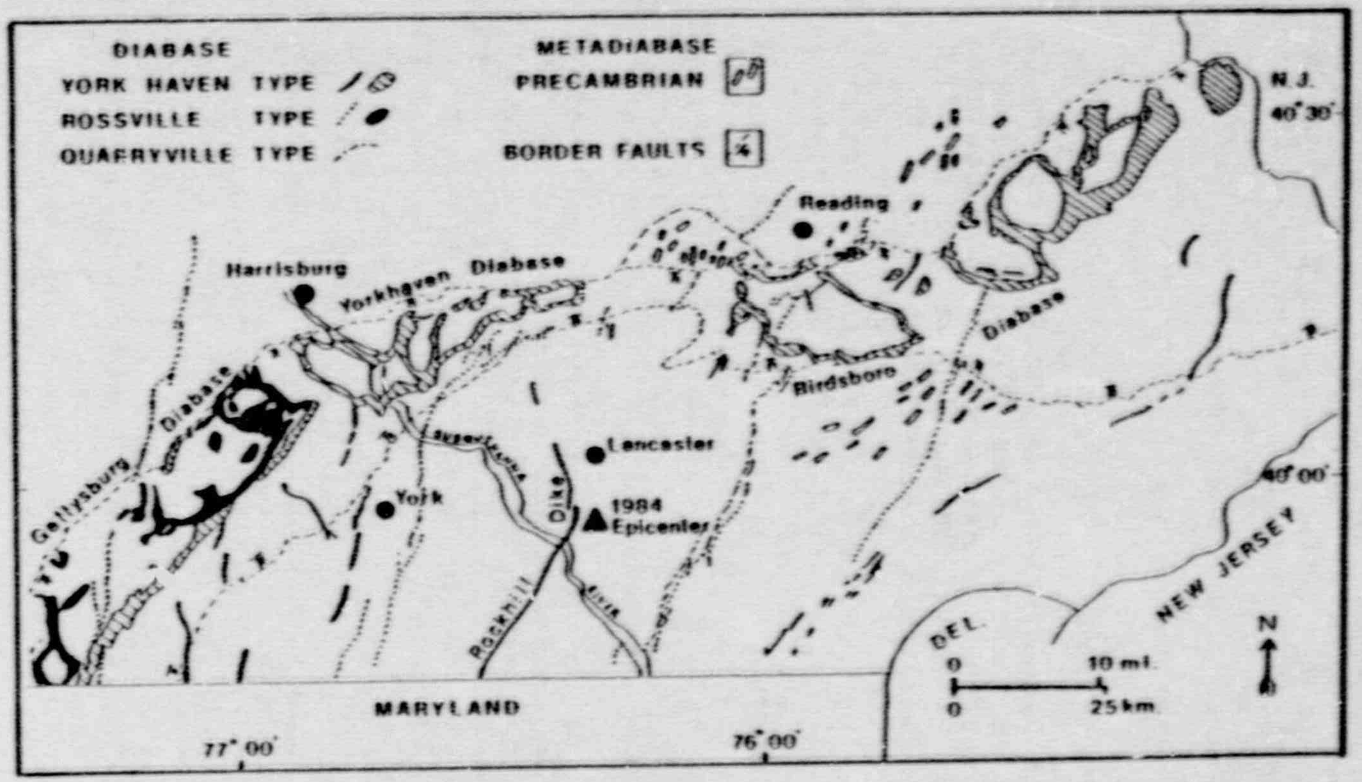

FIGURE 4 Map of the Mesozoic diabase and Precambrian metadiabase of southeastern Pennsylvania. (modified after Smith, et al., 1975)

more than 150 km., and magnetic surveys indicate that many continue at depth (DeBoer, 1967). Van Houten (1969) sums it up as follows: "within the Triassic basin in SE Pennsylvania, long, slender steep-dipping, N to NE trending dikes are common throughout. These are discordant to enclosing rocks,....much straighter than the sinous basin trends, and commonly extend beyond the basin border but are not offset by its faulted margin". Furthermore, some of the dikes appear as offshoots of massive diabase stocks and sheets within the basin (King, 1971).

Ages of the Mesozoic Diabases

Most of the diabase sills and dikes in southeastern Pennsylvania appear to be late Triassic to early Jurassic in age (180-200 m.y.) (Van Houten, 1969). Although this general age for all the intrusions is well agreed upon, the exact sequence of emplacement for the various sheets and dikes, and thus their relative ages, is not.

A late Triassic date for the diabase sills in the Gettysburg Basin is supported by faunal evidence (Willard et al.,1959) and radiometric K-Ar dating (DeBoer, 1968). However, paleomagnetic evidence suggests that the "fossil magnetic directions of the dikes coincide neither with the late Triassic nor the early Cretaceous paleomagnetic directions, which suggests a Jurassic age for the intrusions" (DeBoer, 1967). This opinion, that the N-S trending diabase dikes are the youngest rocks in the region is echoed by many authors. Lapham and Gray (1972) observe that the dikes intrude Precambrian, Paleozoic and Triassic rocks of SE Pennsylvania, and appear to be the last phase of magmatic activity which was preceded by the flows and sheets. Likewise, Van Houten (1969) stated that the dikes " commonly extend beyond the (Triassic) basin borders but are not offset along its faulted margin. Thus, these dikes are younger than the sills and flows, their subsequent tilting, and the major faulting of the basin ". Because the dike trends and distribution appear to be structurally independent of the sheets (sills), King (1961) concluded that the dikes were intruded after the sheets.

However, most of the above reasoning was based on the popular half-graben models for the origin of the Triassic basin. There was one obvious hint in the geology, which pointed toward a more complex age relationship between the dikes and the sheets, than the simple sequence of sheet intrusion followed by dike intrusion. Although the dikes appear to transect all the igneous and sedimentary units of the Triassic basin and the sedimentary and metamorphic rocks of the Peidmont, there are very few chilled margins where the dikes are in contact with the sheets (Gray et al., 1960). Furthermore, Smith (1973) found an absence of crustal contamination in all the diabases. This suggested that the magma was not ponded in the crust for long periods of time, but rather that the sheets, dikes, and flows appeared synchronous. Thus, the prevailing theory, is that the diabase sheets and dikes are the youngest rocks in SE Pennsylvania, but that they were intruded synchronously, in three consecutive phases, during the late Triassic and early Jurassic (Smith et al, 1975).

These are the three types of Triassic diabase in SE Pennsylvania based on chemical composition (Figure 4) (Smith et al., 1975):

Quarryville type	- oldest - occurs as an olivine tholeiite dike swarm
York Haven type	- intermediate in age - quartz tholeiite sheets, dikes, and flows
Rossville type	- youngest - quartz tholeiite sheets and dikes

Within the same diabase type, there is a very uniform composition. Based on calculated cooling rates, homogeneities in each magma type, and paleomagnetics, Smith et al (1975) concluded that there was a short period of intrusion for each diabase type.

Field evidence in the form of cross-cutting relationships supports the above age classification. The Quarryville dike group (Figure 4) partially intrudes the Triassic basin. Therefore, it is younger than late Triassic age (Smith et al., 1975). It also contains a cleavage structure at, at least, half the locations (Lanning, 1972). This deformational structure is not present in the approximately 500 samples of Rossville and York Haven dikes, sheets, swarms, or flows (Smith et al., 1975). The Rossville type dike intrudes the Quarryville swarm. Based on float distribution, Lanning (1972) concluded that a Quarryville dike is cut by a Rossville dike. Therefore, the Quarryville diabase type is older than the Rossville diabase type. Likewise, in the Gettysburg sheet near the town of Gettysburg (Figure 4), "the chilled contact of Rossville (type diabase) cutting across York Haven diabase shows that the Rossville is younger then the York Haven by at least the few thousands of years required for the cooling of the York Haven magma as found from heat flow calculations" (Smith et al., 1975). Just south of Gettysburg, near Greenmount, a York Haven diabase sheet is cut by a Rossville diabase dike with chilled contact. Southwest of Birdsboro (Figure 4) a NE-trending dike of Rossville age also cuts a T-shaped York Haven type dike. All the sheet intrusives of the Triassic basin are of York Haven age, except for the inner part of the Gettysburg sheet, which is of Rossville age (Figure 4) (Smith et al., 1975), and the St. Peters - Birdsboro sheet (Figure 4), which approaches the age of the Rossville intrusives based on radiometric aging (Beck, 1965).

The age distribution above is also supported by paleomagnetic data for the Lancaster region. The Rossville and the York Haven type diabase differ in their respective magnetic domain structure. Paleomagnetic studies place Rossville type diabase at a 185 m.y. age which is approximately the late Triassic and early Jurassic boundary. The study reveals that it is the youngest recognized diabase in the area (Volk, 1977).

Fanale and Kulp (1962) used muscovite from a contact zone, chlorite schist to date the York Haven type sheets at 195 m.y. Thus, they are older than the Rossville type diabase.

Orientation of the Mesozoic Dikes

The diabase dikes are distributed along the entire length of the Appalachian mountains. Locally the dikes have a common trend, but regionally it varies with latitude (Figure 5). In the 400 mile segment of the Appalachians from Alabama to North Carolina the dikes trend NW. In southern Virginia this trend changes to NNW, in Virginia to N, in Maryland and SE Pennsylvania to NNE, and continues NE through New England. In eastern Canada, northern Maine, and Nova Scotia the diabase dikes extend for large distances in the ENE direction (King, 1961,1971; DeBoer, 1967).

The dikes are nearly vertical,and have not intruded into rocks of Cretaceous age or younger. They occur in relatively narrow zones, and their trend is everywhere discordant to older structures. In fact, they are often cutting perpendicularly across the Appalachian trend (King, 1961; DeBoer,1967; Bria, 1971).

Likewise, "in Pennsylvania and adjacent states, the dikes are not deflected by the marked sinuosities in the trend of the Newark rocks and their associated faults"(King, 1961), but trend across them (Figure 4). They have thicknesses from about 10 m to 80 m in the Triassic basin, and often extend into the surrounding Paleozoic rocks (Socolow, 1966).

In general, the dikes in the Lancaster area strike N - NNE (Figure 4) (Socolow, 1966; Smith, 1973; Olsen, 1980). There are several of these diabase dike swarms in Lancaster County and eastern York County. They are of all three ages (types), thus proving that this N - S zone of crustal weakness was reactivated during all three of the intrusive events (Figure 4). The strike of the three separate diabase types can be seen in Rose diagrams of Figure 6, (Smith, 1973) with the average values as follows:

Quarryville dikes strike = N 27° E

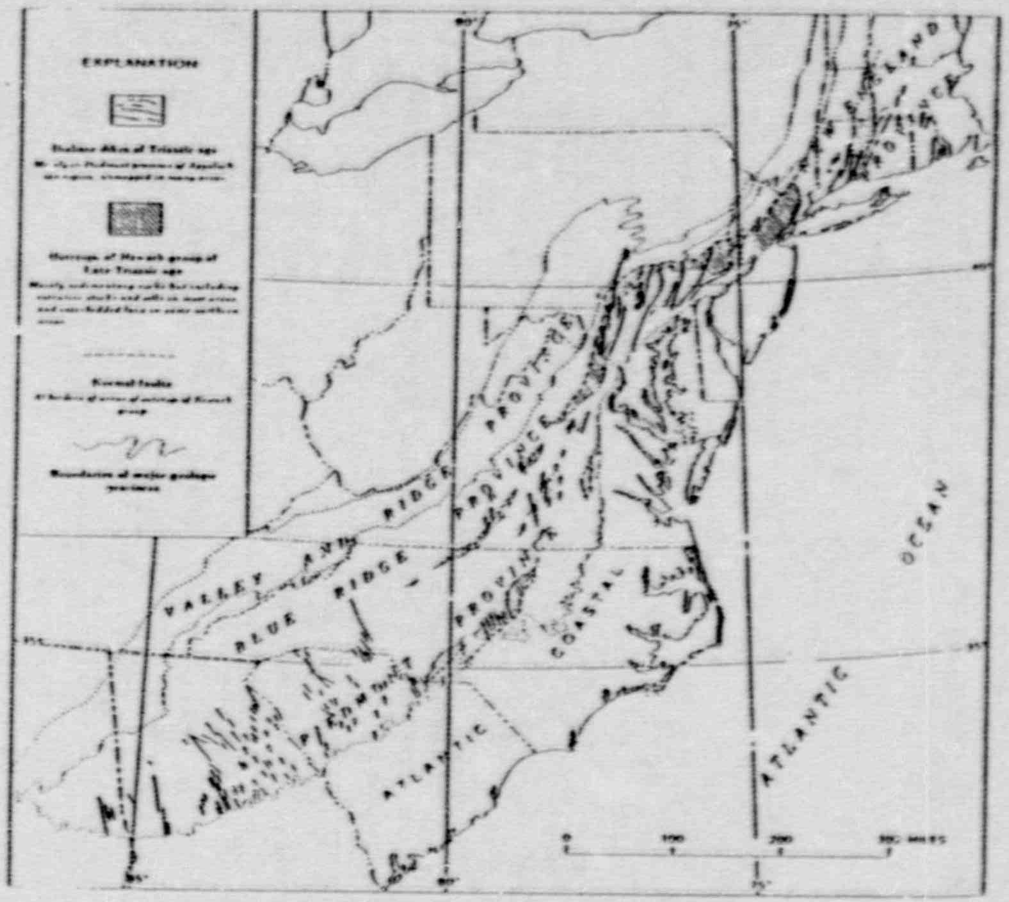

FIGURE 5 Map of the Late Triassic and Early Jurassic diabase dikes, and Triassic basins of the eastern United States. (after King, 1961)

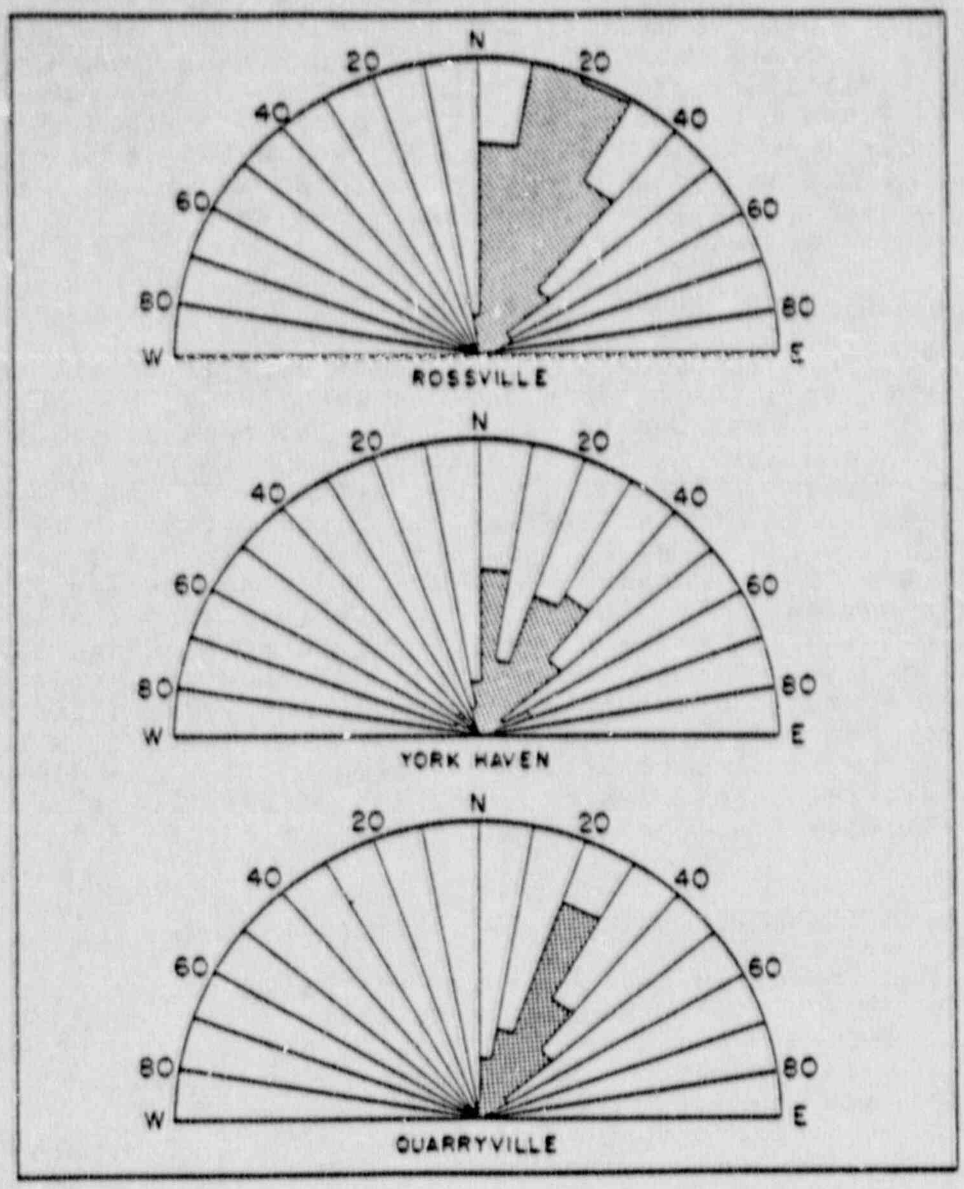

FIGURE 6 Rose diagrams for the strikes of Rossville, York Haven, and Quarryville-Type Dikes. The scale is 0.1 cm per 1.6 km of dike for Rossville and York Haven, and 0.1 cm per 0.48 km of dike for the Quarryville-type. (after Smith, 1972)

York Haven dikes strike = N 5° E , N 32° E (bimodal)

Rossville dikes strike = N 20° E

Thus, all three types of dikes have a NNE strike with the York Haven ones having a bimodal distribution. This is misleading because one of the main York Haven dikes, the Rockhill (Safe Harbor) dike, with its 65 km length of exposure (into Maryland), strikes approximately N 20° E, which fills the minimum between the two maxima in the Rose diagram. It is this dike which is worth considering in more detail because of its proximity to the area of interest, within Lancaster County.

The Rockhill (Safe Harbor) Dike

As mentioned above, this diabase dike is of the York Haven type. It is 65 km long and changes strike from NNE in Maryland and York County to N in the area of interest (south of the city of Lancaster) to NNW in northwestern Lancaster County (Figure 4) (Smith et al., 1975; Grey et al., 1980). The overall variation in its strike is from N 14°W to N 13°E and in width from 2 - 12 m (Bria, 1978).

In the area of interest (Figure 4), near the April 23, 1984 earthquake, the Rockhill dike is in a wooded area of ironstone with a maximum relief of 42 m (Lanning, 1973; Bria, 1978). In outcrop, it dips 65-80 degrees to the west.

A magnetic ground survey by Bria (1978), using ten traverses perpendicular to the structure, suggests a 10 m wide, nearly vertical dike in this region. The dike diverts the Conestoga Creek, which runs N - S, parallel along it until it enters the Susquehanna River (Bria, 1978; Grey et al.,1980).

Theories on the Emplacement of the Mesozoic Dikes

Many theories abound on the intrusion of the diabase dikes in the Late Triassic and early Jurassic. Most of these theories associate the dike intrusion with the opening of the present Atlantic Ocean. However, much of the agreement ends there.

One popular theory is that well after the initiation of rifting and basin formation along the proto-Atlantic margin, a set of basic dikes was injected radially, with its center located off of the coast of the S.E. United States in the vicinity of the Bahama platform and the Blake plateau (Figure 7). This is in agreement with the radial distribution of these diabase dikes along eastern North America, northwestern Africa, and the coast of northern South America (Figure 7) (May, 1970, 1971; King, 1971; Klitgard, et al., 1983; Armbruster and Seeber, 1985).

There are several other theories which are also based on diabase intrusion due to the extensional stress regime

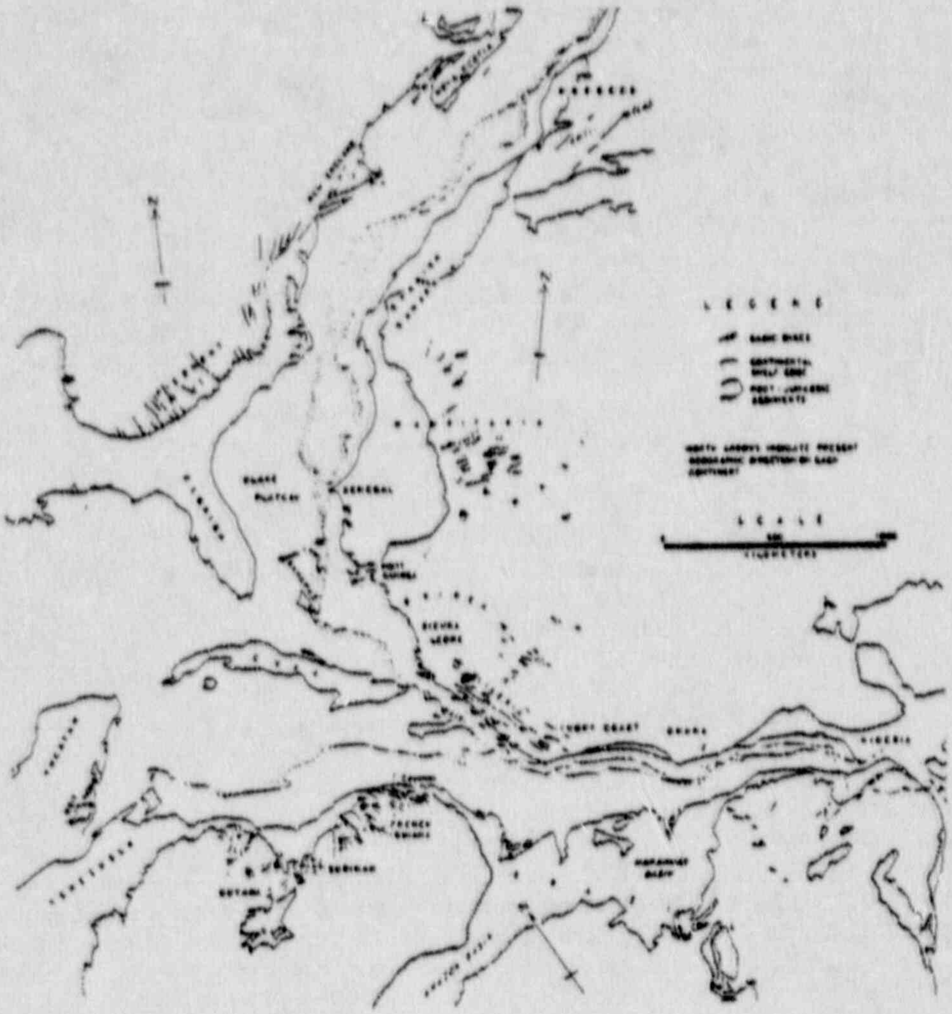

FIGURE_7 Mesozoic diabase dikes in eastern North America, West Africa, and northeastern South America, with the continents restored to their relative position in the Triassic. (after May, 1970) associated with rifting, (King, 1961; Siedner and Miller, 1968; Van Houten, 1969; Dietz and Holden, 1970; Smith and Hallam, 1970; Rogers, 1970; Lapham and Gray, 1972; Bria, 1978). All these are basically a variation on the first idea.

An alternative theory is proposed by DeBoer, (1967). He believes that the dikes may have been intruded in a regime dominated by shearing stresses, rather than an extensional regime. The pure shear system would be associated with sinistral rotation along NE trending fault zones. The idea is backed by paleomagnetic rotations in Newfoundland and New Brunswick (Block, 1964).

Finally, in a more local study, Volk (1977) proposed a reconstruction of the tectonic history and diabase intrusion of S.E. Pennsylvania, through paleomagnetic data in association with the geochemical and relative ages obtained by Smith, et al.,(1975). Her reconstruction is as follows:

1. Deposition of sediments, probably in a crustal downwarp
2. York Haven type diabase dikes and sheets intruded while Triassic sediments remained relatively undeformed
3. Approximately a 10 degrees NW tilting of the Triassic basin and possibly of the surrounding area by rotation on small fault blocks.
4. Rossville type diabase intruded in dikes and sheets
5. Folding along NW trending axis and continued NW tilt of blocks

The folds in the last phase are temporally and spatially related to the N to NE trending dikes, suggestive of a NE to SW axis of principle compression which persisted during the rifting of the North American and European plates. The fault block rotation model (step 3, above) can explain the nonuniform rotations observed within the basin that neither the full, the half graben, nor the downwarp models for the Triassic basin formation can explain. The NW tensional stress, during dike intrusion and early Atlantic rifting, is in agreement with that found by Dietz and Holden (1970) in their reconstruction of the continents during the late Triassic, the period of the initial breakup of the Pangean supercontinent.

Precambrian Metadiabase of S.E. Pennsylvania

Precambrian metadiabase occurs in the form of batholiths, lenses, and especially dikes (Bascom and Stose, 1938). These metadiabase dikes are dark gray, fine grained intrusives. Locally, in S.E. Pennsylvania, their minerology is altered, and they appear greenish in color. They are located in the Precambrian granitic and hornblende gniesses of the Reading Prong, and within a small exposure north of the town of Lancaster, just north of the thin neck of the Newark-Gettysburg Triassic basin (Figure 4). Here, they strike primarily in the N and NNE directions. They also appear in the Precambrian gniesses within an exposure just north of Downington, Pa. (Figure 4). Here in Chester County they have a more NE to NNE trend (Berg, et al., 1980).

These metadiabase dike swarms, with their N to NE strike, are ancient zones of weakness which seem to underlie the Paleozoic and Triassic sedimentary rocks of Lancaster County and vicinity. They appear to cut all of the Precambrian rocks. Thus, they are probably associated with a period of diabase intrusion in the late Precambrian (Breg, et al., 1980).

The N to NE strike of the Precambrian metadiabase dikes of the Lancaster area is the same as that of the Triassic-Jurassic diabase dikes of the same region (Figure 4). This parallel trend suggests a possible reactivation of a preexisting structural zone of weakness within the basement and the cover rock. The Triassic-Jurassic diabase could have utilized these weakness planes, and could have been confined to them (Smith, et al., 1975).

Similar intrusions are found associated with Precambrian gniesses throughout the Atlantic belt. They form important parts of the Precambrian complex of the Adirondacks. They, also, appear in the Highland of New Jersey where they are described as Losee gniess (diorite) and Pohuck gniess (gabbro) (Bascom and Stose, 1938).

Faults

Introduction to Faulting in the Lancaster County Region

Most of the known faults in the Appalachian area are believed to extend to relatively shallow depths, probably less than 7 to 8 km (Hadley and Devine, 1974). Therefore, they are not projected into the basement (Hadley and Devine, 1974). However, these "presently inactive faults, associated with past tectonic occurrences, may indicate an inherent weakness in the area. An active surface trace is not required inasmuch as a fault may tend to be active at depth without surface evidence." (Fox, 1970).

The first set of faults in Lancaster County is a E-W striking set of thrust faults of Paleozoic age. The largest of these appears to be the the Martic Line contact in southern Lancaster County (Figure 1). However, it is not the only one. Several other E-W striking thrust fault occur north of the Martic line (Figure 2).

The second and younger set of faults in Lancaster County is the N-S striking set. These faults are perpendicular to the geologic trend, and offset all the lithologies as well as structural features, including the

E-W striking thrust faults (Figure 2). Thus, they are often termed "cross faults" in the literature. They appear to have formed initially as normal faults associated with the period of extension in the late Triassic and early Jurassic. Subsequently they appear to have been reactivated as oblique reverse faults in the present stress regime.

It is important to remember that faults in the Lancaster area are difficult to confirm and many more may be present. This difficulty results from the sparsity of bedrock exposures in this well farmed region, and the lack of distinctive mappable lithologic units (Socolow, 1966).

The Martic Line

The Martic line is a contact which is traced for hundreds of kilometers along the Appalachians (Wise and Kauffman, 1960). In Lancaster County, it separates rocks of known Paleozoic age in the north from uncertain age rocks of the Glenarm series to the south (Figure 1) (Anderson, et al., 1965).

There are two major opinions on the nature of the contact, stemming from the undetermined age of the Glenarm series. The first theory is that the Glenarm series is Precambrian, and that the Martic Line is a large, far travelled overthrust separating Precambrian rocks from Lower Paleozoic ones. The second theory is that no major overthrust exists, and that the Wissahickon schist of the Glenarm series is a highly metamorphosed facies of the Ordovician Martinsburg shales which rests normally above the Ordovician limestones. Thus, both of these theories try to explain the fact that the Wissahickon schist clearly rests on top of the metamorphosed Conestoga limestones and other Lower Paleozoic formations (Cloos and Heitanen, 1941). In recent years the thrust fault theory has become popular in much of the literature but this may change.

This theory, that the Martic Line is a major thrust, is the older of the two ideas. When the area was first mapped in detail, in 1929, Knopf and Jonas (1929) described it as the "Martic overthrust". They said that it was the major fault of Lancaster County, which "seems to place Wissahickon schist (Precambrian or Lower Paleozoic) of the S.E. Piedmont northwestward over the Paleozoic sediments of the Lancaster Valley" (Knopf and Jonas, 1929). They also estimated the displacement along this thrust to be about 33 km.

The Paleozoic structures associated with the Martic Line strike E-W (Armbruster and Seeber, 1985). These structures are folds and small scale thrust faults, which result in a five-fold repetition in the stratigraphic sequence. However, in the field, there appears to be no evidence of mylonitization, brecciation, or any other trace of extensive movement. In stead, "the repeated section has been thoroughly deformed after repetition by a uniform act of folding which overturned all folds southward and produced a unique cleavage which dips to the north" (Cloos and Heitanen, 1941). Thus, all the deformations cross the Martic Line without change, indicating that this thrust zone predates all the major folding in the Lancaster region (Cloos and Heitanen, 1941; Freedman, et al., 1964). Thus, the Martic Line does not separate structural provinces, since all structures transgress it or are parallel to it.

The stages in the development and deformation of the Martic line are best summed up by Wise (1970) as:

1. Thin-skinned imbricate thrusting
2. Regional metamorphism and flow to the NW, with major basement folding and thrusting
3. Brittle movement of large basement blocks near the line, with folding of earlier basement thrusts
4. More brittle behavior with locally intense folding
5. Development of kink bands and joints

Thus, the Martic Line is either a Lower Paleozoic facies change or a Lower Paleozoic thrust zone which has been extensively deformed in the later Paleozoic, and which has been inactive ever since.

<u>Paleozoic E-W Trending Thrust Faults</u>

There are several E-W trending thrust faults, in the Lancaster County region, which are Paleozoic in age. They appear to be associated with the formation of the Appalachian Mountains, and thus, of the same age as the E-W trending folds of the region (Berg, et al., 1980).

The first of these major E-W trending thrust faults is the Stoner Thrust (Figure 1). It lies on the south side of York valley and crosses the Susquehanna River into Lancaster County west of the town of Lancaster (Figure 1). Here, in the Susquehanna River gorge, the lower beds of the Chickies formation are thrust against the Conestoga limestones. Thus, there is considerable horizontal shortening. All the rocks of the Stoner thrust are closely folded. Furthermore, the fault's sinuous outline (Figure 1) indicates a low angle dip, which was folded during and after thrusting. This deformation involved all the Paleozoic rocks. The magnitude of these folds and thrusts, and their parallelism with those of the Great Valley, indicates that they were formed during the Alleghenian orogeny (Kauffman, 1967).

A second major thrust fault in the area is the Chickies thrust (Figure 1). This fault emerges from under the Gettysburg Triassic basin in northern York County and crosses the Susquehanna River, with an E-W strike, into Lancaster County. There, as in the case of the Stoner

Thrust, it becomes unrecognizable in outcrop within the Conestoga limestone, west of the city of Lancaster. The fault is diagonal to the regional folding, truncating the Chickies Rock, Accomac, and Trout Run anticlines (Figure 1). Based on the outcrops, the diagonal movement is in part a thrust, and in part a horizontal shear along the bedding. The Chickies thrust cuts out several thousand meters of section, and apparently marks a major line of demarcation between the sedimentary facies to the north and to the south. There is no exposure of Conestoga limestones north of this zone (Figure 1)(Gray, et al., 1960; Kauffman, 1967; Grey, et al., 1980).

The third major Paleozoic thrust fault in the area is the Yellow Breeches thrust, just south of Harrisburg, and just north of the Triassic basin (Figure 1). It truncates the plunging nose of the South Mountain anticlinorium, strikes E-W across the Susquehanna River, and disappears in the carbonates of the Great Valley. It separates the lithology and structure of the Cumberland Valley from that of the Lebanon Valley to the east. There are vast differences in the facies across the trust, but only minor differences within each sequence. The thrust is nearly horizontal, even north dipping at times, with thrusting juxtaposing distant sequences of a pre-deformational, depositional basin. The thrust is associated with minor steep faults (Gray, et al., 1960; Kauffman, 1967; Berg, et al., 1980).

On the more local map of the north-central part of Lancaster County (Figure 2), there are several smaller thrusts which may be associated with the larger Stoner and Chickies thrusts mentioned above. They, too, strike E-W with the south side allochthonous and are accompanied by overturned folding.

In the northern section of Figure 2, between Manheim and Lititz are the Kissell Hill thrust and the Fairland-Millway thrust. The Kissell Hill thrust dips south and strikes E-W, and has a maximum stratigraphical throw of about 1300 m, with the displacement established at several kilometers. Some of this displacement may be due to reactivation of the fault in the Triassic. North of this fault is the Fauland-Millway thrust which also dips to the south, and strikes E-W. It has a displacement of about 1.7 km. To the south is another E-W striking thrust, the Mechanicsville thrust, which is also south dipping and E-W striking. All of these faults are offset by N-S striking cross faults which will be discussed below (Gray, et al., 1960; Meisler and Becher, 1971; Berg, et al., 1980).

Triassic Border Faults

The faults bordering the Triassic basin are E-W striking, parallel to the structural grain. Although the amount of displacement along them, and thus their importance in relation to the Triassic basin is still disputed, a northern border fault is well documented (Figure 1). The southern border fault, if it exists at all, is not as clear in outcrop, for most of it appears to be covered by sediments. It is typically thought to be a few kilometers north of the end of the Triassic onlap (Sumner, 1975). For more details on the geology of the Triassic basin see the section titled "Newark-Gettysburg Triassic Basin" above.

Post-Triassic Cross Faults

The youngest structural features of the Lancaster, Pennsylvania region are the north-south trending, post-Triassic normal faults. They offset all of the lithologies in the region, as well as the east-west striking Paleozoic folds and thrust faults (Gray, et al., 1960; Berg, et al., 1980). The strike of these youngest faults is analogous to that of the Triassic-Jurassic dikes, and the faults appear to be associated with the dike swarms (Smith, et al., 1975).

These normal faults run continuously through the Triassic rocks of the Newark-Gettysburg basin and the surrounding Paleozoic rocks. Their formation appears to be contemporaneous with the Mesozoic rotation of the Triassic basin during the initial opening of the Atlantic Ocean. The downthrown side of these faults is on the SE side (Root and MacLachlan, 1978).

Jonas and Stose (1930) first described the cross faults of Lancaster County as follows: " The northerly system (of faults) is apparently the most recent, for the faults of this system offset all the others. This is very strikingly shown by the north-south fault through Fruitville." This Fruitville fault is the largest of the cross faults mapped by Jonas and Stose (1930), with a right lateral separation of about a quarter of a mile (400 m). Furthermore, it is located at the center of the north-south trending zone of seismicity (Figure 3), and is thus of considerable interest in this study.

A smaller fault, the Marietta Junction fault of Jonas and Stose (1930), parallels the Fruitville fault to the west, and also displays right lateral separation (Figure 3).

The above interpretations of the post-Triassic faulting, done by Jonas and Stose (1930), were used on the 1960 Geologic Map of Pennsylvania (Gray, et al., 1960)

(Figure 3). However, Meisler and Becher (1971) mapped several smaller cross faults, with strikes varying from NW to NE, in place of the larger faults of Jonas and Stose (1930). These faults were mapped within the more resistant ridges of clastic rock, but along the same north-south fault zone as the Fruitville fault, and with the same right lateral separation (Figure 2). This is the interpretation placed on the 1980 Geologic Map of Pennsylvania (Berg, et al., 1980). In short, the lengths of the cross faults differ on the two maps, but both agree that they are the youngest structural features, associated with primarily right lateral separation, and striking in a predominantly north-south direction (Figure 2).

The apparent discrepancy in the two maps is rather to be expected considering the lack of outcrop in this historically very agricultural region. Furthermore, as Fox (1970) states, " Although active faults are not common in the eastern U.S., presently inactive faults associated with past tectonic occurrences may indicate an inherent weakness in the area. An active surface trace is not required inasmuch as earthquakes originate at depth; a fault may tend to be active at depth without surface evidence." The inherent weakness, which Fox (1970) mentions above, is indicated by the predominantly north-south strike of not only the post-Triassic normal faults, but also the predominantly north-south strike of the Precambrian and Triassic-Jurassic diabase dikes swarms associated with them (Gray, et al., 1960; Berg, et al., 1980).

Further evidence for a north-south trending zone of weakness within the Lancaster area is the large density of cross faults, of a N-S strike, within the narrow neck of the Newark-Gettysburg Triassic basin. This area is within the northern part of the seismically active region of Figure 3 (Gray, et al., 1960; Berg, et al., 1980).

When the Triassic basin is divided into domains, based on areas where the bedding attitude is relatively constant, there is a region, within the narrow neck, where the bedding domains are small , numerous and very random in dip direction. This area coincides with the area of highest faulting, mentioned above (Faill, 1973).

Most of the faults in this block faulted, narrow neck of the basin are steeply-dipping, N-S striking, normal faults which are nearly at right angle to the E-W trending basin (Kauffman, 1967; Faill, 1973; Bria, 1978). As early as 1938, Bascom and Stose (1938) noticed that " the faulting presumably involved in some degree both the underlying and the adjacent Paleozoic and Pre-Paleozoic rocks. Such faults have been traced in the Paleozoic formations, but because of the absence of well-defined beds, it is not possible to trace them for any great distance in the Pre-Paleozoic crystalline rocks." They identified one fault in the region where movement occurred after the red Triassic sediments were deposited and intruded by the diabase, since " the Triassic rocks here adjacent to the diabase are red and are not baked by the diabase, as they would be if the diabase intruded them." Likewise, north of Manheim (Figure 2), in the northwestern part of the seismically active area of Figure 3, is a north-south trending fault which offsets, with a right lateral separation of a few hundred meters, both a York Haven type diabase sheet and a Triassic border fault (Johnston, 1966). Finally, in the Cornwall area (Figure 3), several small faults, and one major fault, offset all the lithologies including the diabase. The major fault is 3 km in outcrop. Therefore, the crosscutting relationship indicates that the north-south trending normal faults are generally younger than the surrounding late Triassic sedimentary and igneous rocks (Lapham and Gray, 1972).

All the drainage of the region, within the narrow neck of the Triassic basin and within the northern part of the seismic zone (Figure 3), including Hammer Creek (Figure 2) appears to follow the N-S striking faults. Most of these faults have displacements of a few hundred meters but two have throws of thousands of meters (Gray, et al., 1958). The largest displacement in the area is associated with a N-S striking diabase dike, about 1.7 km west of Hammer Creek. The strata is offset about 2.4 km in a right lateral direction across the dike, with a throw of about 1,500 m upward on the west side. The strike of the Triassic ridges on either side of the dike is discordant by fully 30 degrees (Gray, et al., 1958).

Lanning (1973) found petrographic evidence that shear displacement occurred along the Quarryville and York Haven type diabase within the Piedmont. Due to the lack of shearing in the youngest diabase of the Rossville type, he concluded that the shearing accompanied the intrusion of the Rossville. This is further supported by evidence of offset of 100 m of beds along a large Rossville dike near Doe Run, east of Lancaster. The fracture cleavage within the Quarryville and York Haven diabase is in the north-south direction, which parallels the orientation of the dikes and youngest cross faults of the region (Lanning, 1973).

Coastal Plane Faulting

Due to a lack of post-Triassic rocks in the Lancaster region of Pennsylvania, it is difficult to date more recent movement along the faults observed in outcrop. However, there is evidence within the Coastal Plain sediments that faulting is a continuous, ongoing process along the Eastern U.S.

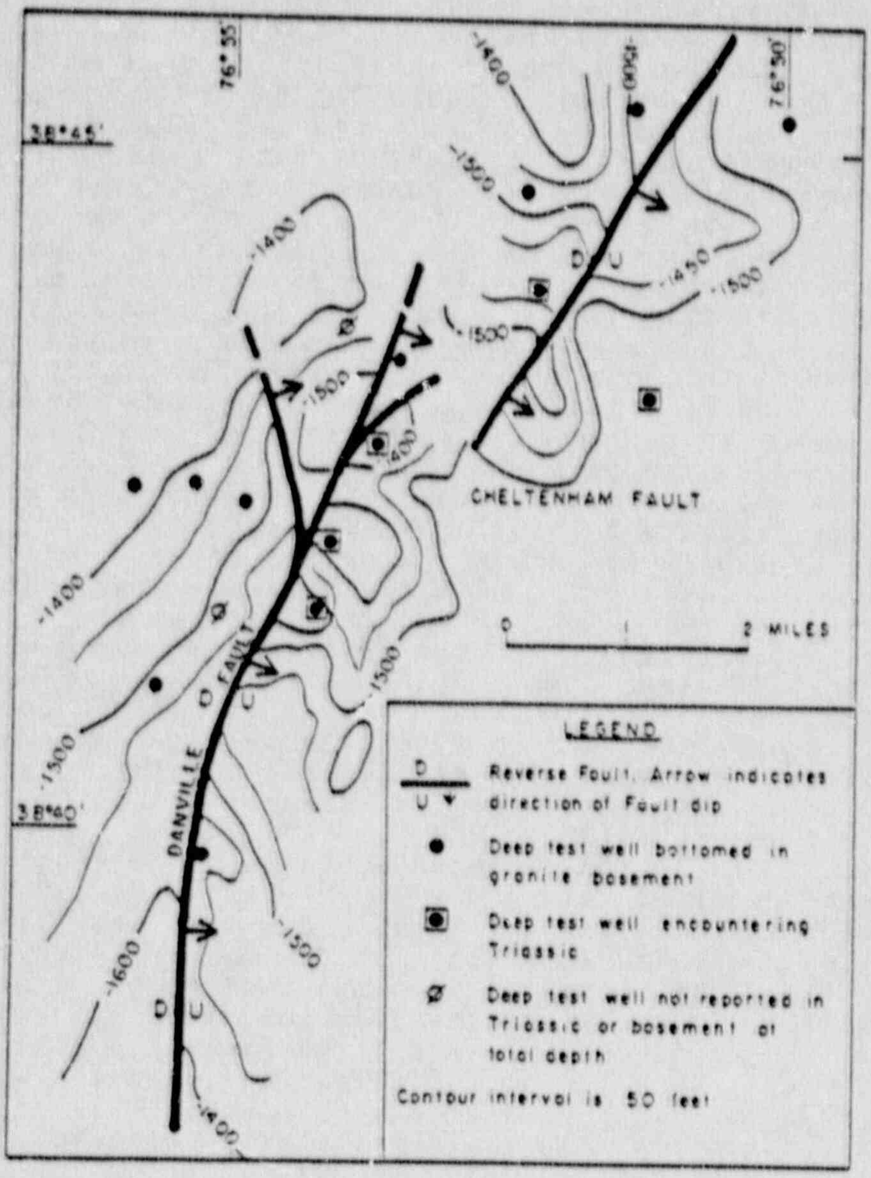

FIGURE 8 Top of the basement map of recent Coastal Plain faulting in Georges County, central Maryland, about 20 km southeast of Washington D.C. (after Jacobeen, 1972)

The geographically closest example of recent faulting within the Coastal Plain comes from a study done in Prince George and Charles Counties of Maryland, about 15 to 25 km SE of Washington D.C. (Jacobeen, 1972). Seismic evidence indicates two east dipping, north-south trending, high angle, reverse faults within the Coastal Plain. This system, the Brandywine system (Figure 8), is divided into two enechlon faults, both extending to the north and to the south beyond the study area. The maximum throw on the southern fault, the Danville fault, is over 75 m at the top of the granitic basement and the top of the lower Cretaceous Arundel formation (Figure 8). The throw on the northern fault, the Cheltenham fault, is about 30 m. Both of the faults indicate reverse faulting with the SE block upthrown. Stream anomalies and lineaments are clues to the fault location at the surface. However, recent drilling shows no rupture reaching the surface. The fault displacement is absorbed upward, and only folding occurs in the Tertiary sediments (Jacobeen, 1972). However, based on seismic profiles across the area, the Danville fault comes very close to the surface, since near surface beds appear to be offset. Furthermore, it was clear that the faulting occurred from the Cretaceous to the Miocene, since the fault cuts basement and Cretaceous rocks, and flexes Eocene and Miocene sediments. These sediments are up to 550 m thick. Coastal Plain faulting activity is not unique to these two faults. Other faults cutting upper Potomac and younger sediments have been observed at the surface in the Washington, D.C. area (Jacobeen, 1972).

Joints

The jointing pattern observed in the Lancaster, Pennsylvania region is fairly consistent with the fold pattern. Wise and Grauch (1967) examined 100 master joints in 14 different areas of the Piedmont in Lancaster County. Their findings are shown in the Rose diagram of Figure 9. The cross joints, which are perpendicular to the nearly east-west fold axis, strike N 15-35°W. They are the major symmetry plane of Figure 9, with conjugate fractures which strike NNE and NW. The strike joints, which parallel the trend of the folds, strike N 65-80°E (Wise and Grauch 1967).

The dynamic interpretation of this joint pattern is based on traditional brittle yield theory. Wise and Grauch (1967) state that "the conjugate pair of joint sets represent conjugate shears with their acute bisector pointing in the direction of maximum compression (N 15-20°W). Any pure shearing parallel with the compression direction would tend to form fractures parallel with the acute bisector (N 15-20°W). With relaxation of

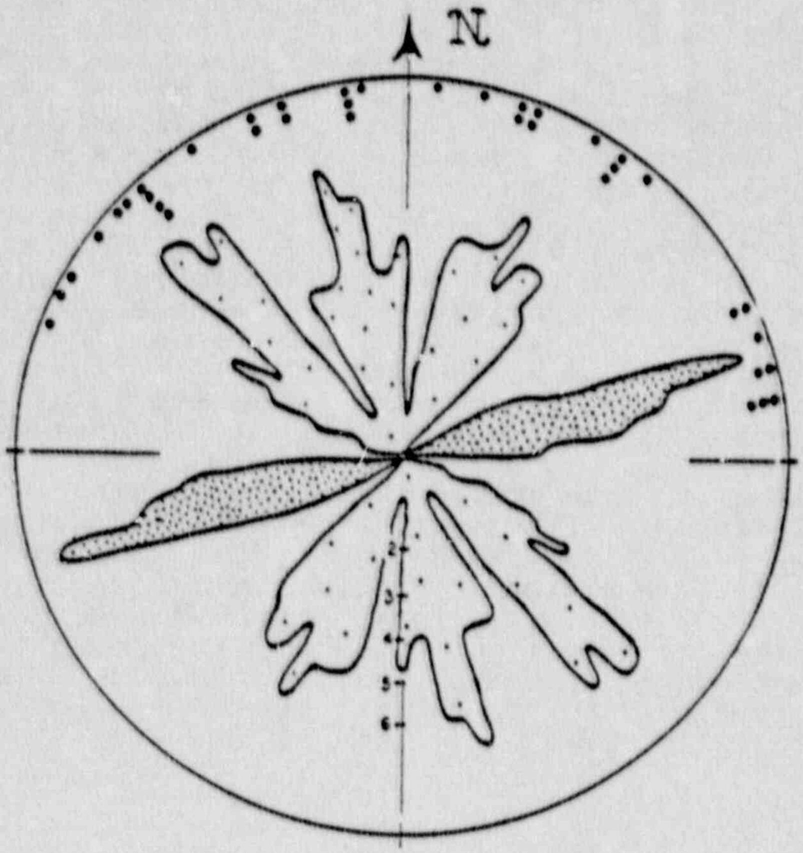

FIGURE 9 Strike of major joint sets in the inner Piedmont of Pennsylvania. Dots represent the strike of 38 major joint sets. Numbers indicate population of dots falling within a 15 degree sector. Obtuse bisector joint is indicated by closer spaced dot pattern. (after Wise & Granch, 1967)

compression, expansion fracturing would occur at right angles to the former compression, producing the distinctive set of obtuse bisector joints at N 65-80°E."

Cloos and Heitanen (1941) examined 200 joints randomly throughout southern Lancaster County. They found a dominant joint set striking at N 10°W and conjugate joint sets to the NW and NE, analogous to those of Wise and Grauch (1976) above. Rios (1966) looked at jointing in Quarryville, Pennsylvania, SE of the city of Lancaster, within Lancaster County (Figure 1). He found a well defined pair of joint sets which dominated the Glenarm series and the Paleozoic rocks near the Martic Line. The joint sets had strikes of N 8°W and N 32°W with dips of 76°E and 88°E respectively. Kink planes were associated with the joints but the displacement sense may have been considered normal or reverse.

Therefore, the joint sets seem to reflect the Paleozoic deformation associated with the last stage of folding in the region (Rios, 1966). However, since they are zones of weakness within the rock fabric, it is important to note their dominant strike directions.

The Relative Ages of the Structural Features of Lancaster County

The cross-cutting relationships between the main structural features of the area, the E-W striking faults, the N-S striking faults, and the diabase, suggest the following relative ages (oldest to youngest):

1. The E-W striking, predominantly thrust faults are cut by all the Mesozoic diabase intrusives and offset by the N-S striking cross faults. They are, therefore, the oldest structural features, other than the few Precambrian metadiabase intrusives. These E-W striking faults appear to be the result of the Paleozoic orogenies which formed the Appalachian mountains.
2. The Mesozoic diabase bodies were intruded in three separate episodes within the Late Triassic-Early Jurassic period of rifting. The oldest is the Quarryville diabase, then the York Haven diabase, and finally the Rossville (Smith, 1972). They are all predominantly N-S trending and cut across all the E-W striking features. Of the three diabase types, only the youngest, the Rossville, is not clearly offset by the N-S striking cross faults. Although, it is on occasion bordered by them (Johnston, 1966; Lapham and Gray, 1972). Therefore, the diabase sills and dikes are older than the N-S striking faults, with the possible exception of the Rossville

diabase, which may be contemporaneous.

3. The N-S striking cross faults appear to be the youngest structural features based on the cross-cutting relationships. They are consistently right lateral in offset (Berg, et al., 1980), and appear to be originally normal faults, associated with post-Triassic rifting.

In the area of seismicity within Lancaster County (Figure 3), the Fruitville fault zone runs north-south, parallel to the 76°20' longitude line. This fault offsets all the lithologies. Spacifically, it outcrops on a quartzite ridge, in the Neffsville anticline, 3 km north of the city of Lancaster, where it right-laterally displaces the ridge (Figure 2) (Jonas and Stose, 1930; Meisler and Becker, 1966). Further north it offsets the Cocalico shales (Ordovician) and the Kissell Thrust, just SW of the town of Lititz (Figure 2) (Jonas and Stose, 1930; Meisler and Becher, 1966). This displacement is also right lateral. Thus, this is the youngest fault in the region, and the one along whose length the historical seismicity clusters (Figure 3).

It may be possible that at least some of the youngest, N-S trending faults may be currently reactivated as high angle, right-lateral, reverse faults by the present ENE striking maximum compressional stress derived by Zoback and Zoback (1984) for this region of the country.

GEOMORPHOLOGY

The Topography and the Drainage of Lancaster County

Carbonate rocks dominate the Lancaster County region, and so does the gentle rolling topography. The maximum relief in the carbonate rocks is approximately 75 m with local relief of 6 m - 60 m. The relief is controlled by the erosional resistivity of the various rocks. The dominant carbonate group in the area, the Conestoga formation, has greater relief than the surrounding formations, and is more finely dissected by streams. These differences may be due to lithologic contrast and emphasized by the near-vertical dip of the cleavage and the bedding within the Conestoga (Meisler and Becher, 1971).

A preliminary look at the drainage pattern of the Lancaster area shows the larger streams generally flowing in the north-south direction (Figure 2). A study of over 300 straight segments of stream channels in central and southern Lancaster County, the area dominated by carbonates, shows two major channel directions. One direction (approximately N 80°E) is parallel to bedding, the other direction (approximately N 10°W) is nearly perpendicular to the strike of the beds (Figure 10) (Meisler and Becher, 1971).

In the northern part of the Lancaster region, within the area of the Lebanon County line, the drainage pattern is distinctly trellis in the north-south direction. It is clearly controlled by the N-S striking cross faults within this narrow neck of the Newark-Gettysburg Triassic basin. Here, the streams flow along the N-S faults which offset all other features in the area. This region is north of the towns of Lititz and Manheim. The dominant stream, the Hammer Creek, also has a several-kilometer-long N-S trending straight segment in this area (Gray, et al., 1958; Meisler and Becher, 1971). Interestingly, it is a direct continuation of the Fruitville fault zone (Figure 2).

As early as 1929, Knopf and Jonas (1929) observed that "the Holtwood Dam (on the Susquehanna River) has utilized a natural falls or rapids known as Cullys Falls". Recently, Thompson (1985) has observed evidence for large preglacial falls on the Susquehanna in this same area of Holtwood, Pennsylvania. He calls them the "Great Falls of the Susquehanna". These falls are directly south of the N-S striking Fruitville fault zone and its associated N-S trending seismic zone (Figures 1 & 3). Preliminary evidence suggests that the falls may be due to preglacial faulting or flexuring in the area (Thompson, personal communication) indicating recent uplift along the Fruitville Fault zone.

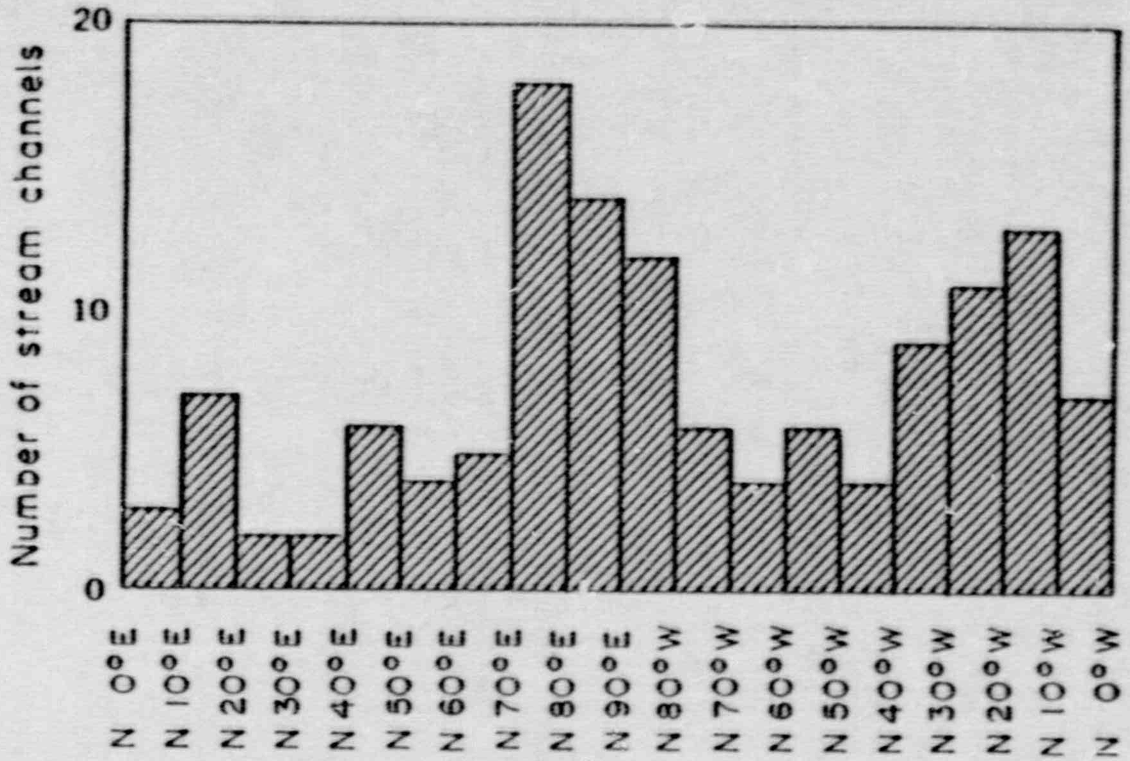

FIGURE 10 Orientation of stream channel segments in central Lancaster County, Pennsylvania. (after Meisler & Becher, 1971)

GRAVITY AND MAGNETICS

Gravity Survey of Lancaster County

Sumner (1975) compiled gravity data for the Newark-Gettysburg basin and contoured a simple Bouguer gravity map (Figure 11). Over 4500 gravity stations were plotted with a station spacing of 1-5 km over the basin and 2-10 km over adjacent areas. The standard error was about 0.2 mgals.

The density contrast between the various Triassic and Paleozoic rocks is very small, with the exception of the diabase (Table 1) (Sumner, 1976,1977). Therefore, it is difficult to pick up near surface faulting within these rocks. Nevertheless, on the simple Bouguer map (Figure 11), there is some evidence for a N-S fault zone in the area of the Fruitville fault of Lancaster County. The contour lines appear warped within this area, in contrast to their parallel, equally spaced regional trend on both sides of the proposed fault zone (Figure 11) (Sumner, 1975).

Magnetic Survey of Lancaster County

Bromery and Griscom (1967) compiled an aeromagnetic map of S.E. Pennsylvania based on several 15-minute quadrangle surveys. The quadrangles of interest, within the proposed Lancaster seismic zone (Figure 3), are, north to south, the Lititz quadrangle (Bromery, et al., 1961), the Lancaster quadrangle (Bromery, et al., 1961), and the Conestoga quadrangle (Bromery, et al., 1959). The flight paths are N-S with a contour interval of 25 gammas. These three quadrangle maps have been combined in Figure 12.

Despite the large, regional scale of this aeromagnetic survey, there is clear evidence of a disturbance in the magnetic contours as they cross the area of the Fruitville fault and its N-S extension (Figure 12). Further south, in the Conestoga quadrangle, the Martic Line contact creates an approximately 800 gamma, steep dipping, shallow magnetic contrast (Figure 12) (Socolow, 1974). Along the southern extension of the Fruitville fault, this contact (as well as the Martic Line) trends N-S. This is also the area of the 1984 earthquake.

Likewise, this area in Conestoga is the part of the Martic contact of Pennsylvania which is most highly folded, and offset in two step-like features (Figure 1) (Berg, et al., 1980). These step offsets are in harmony with the right lateral displacement along the Fruitville fault and other N-S trending faults of the area. However, at this point no causal relationship can be established.

Finally, as in the gravity case, the uniform lithology of the Lancaster valley area makes it very difficult to

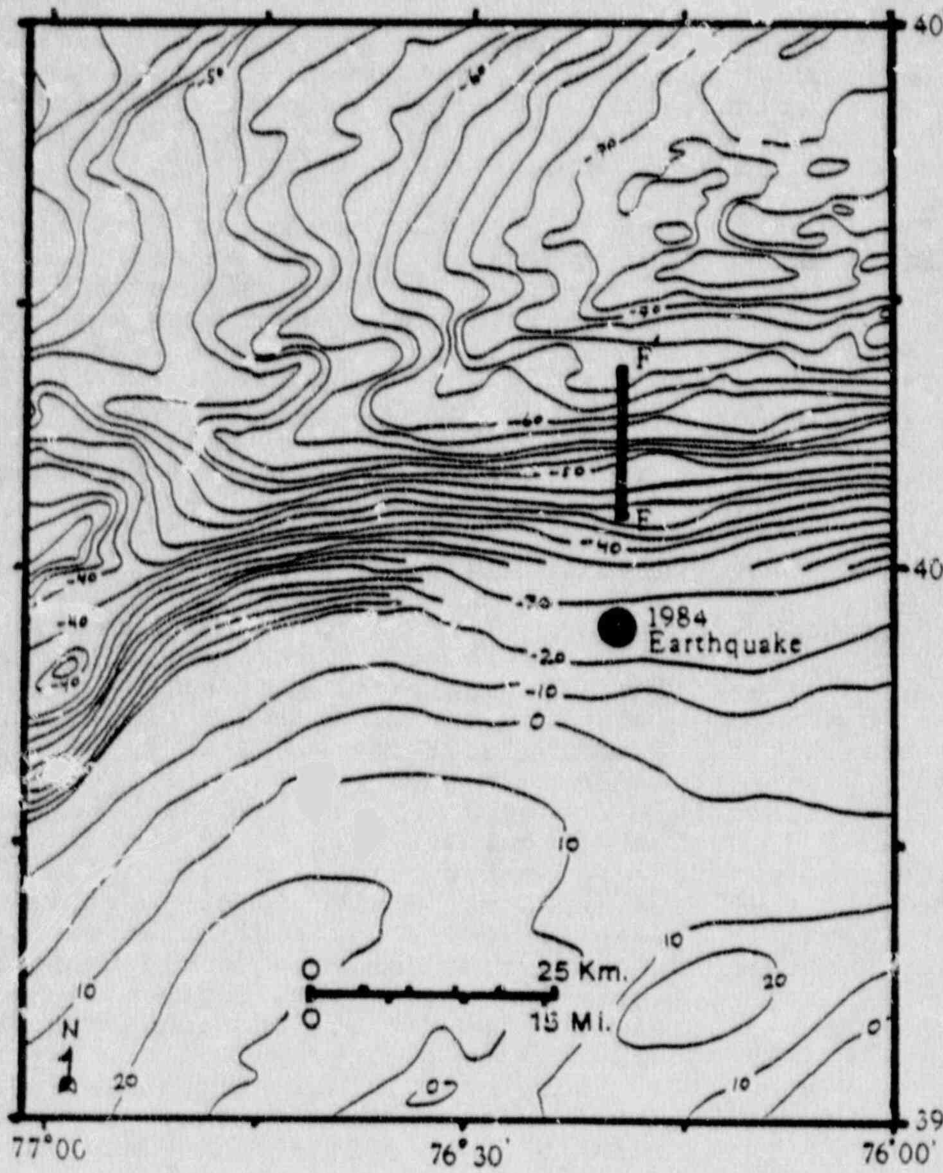

FIGURE 11 Simple Bouguer Gravity map of southeastern Pennsylvania and northern Maryland, contoured at 2 and 10 mgals. The dark line labelled FF' is the schematic representation of the Fruitville Fault Zone. Also shown is the April, 1984 earthquake epicenter. (modified after Sumner, 1975)

TABLE 1. DENSITY, MAGNETIZATION, AND STRATIGRAPHY OF MAJOR ROCK UNITS IN EASTERN PENNSYLVANIA

Rock unit	Rock type	Density (g/cm^3), with no. of samples	Magnetizations ($\times 10^{-6}$ emu/cm³), with no. of samples
Precambrian gneiss of Reading Prong	Hornblende gneiss	2.8–3.0,[*] > 5	1000–10,000, 5
	Granitic gneiss	2.56–2.7,[*] > 5	100–1,000, 5
Hardyston Quartzite, Cambrian	Gray sandstone	2.63,[*] > 5	~100, 2
Leithsville Formation, Cambrian	Sandy dolomite	2.7,[*,†] >5, 3	< 10, 2
Allentown Group, Cambrian	Limestone and dolomite	2.7–2.75,[*,†] >5, 6	< 10, 2
Beekmantown Group, Ordovician	Dolomite	2.81,[*,†] >5, 6	< 10, 2
Jacksonburg Formation, Ordovician	Argillaceous limestone	2.67,[*] > 5	< 10, 2
Martinsburg Formation, Ordovician	Gray shale, slate	2.63–2.77[*] (varies with metamorphic grade), > 10	~50, 2
Triassic sedimentary rocks	Red mudstone, siltstone, sandstone, conglomerate	2.43–2.73,[*,§] 2.65 mean, 87	~100, 73
Triassic diabase	Dark gray diabase	2.92–3.10,[*] 95	3,000–7,000,[*] 95

[*] Hersey (1942).
[†] Sumner and others (1973).
[§] Sumner (1975).
[#] Beck (1965).

(after Sumner, 1977)

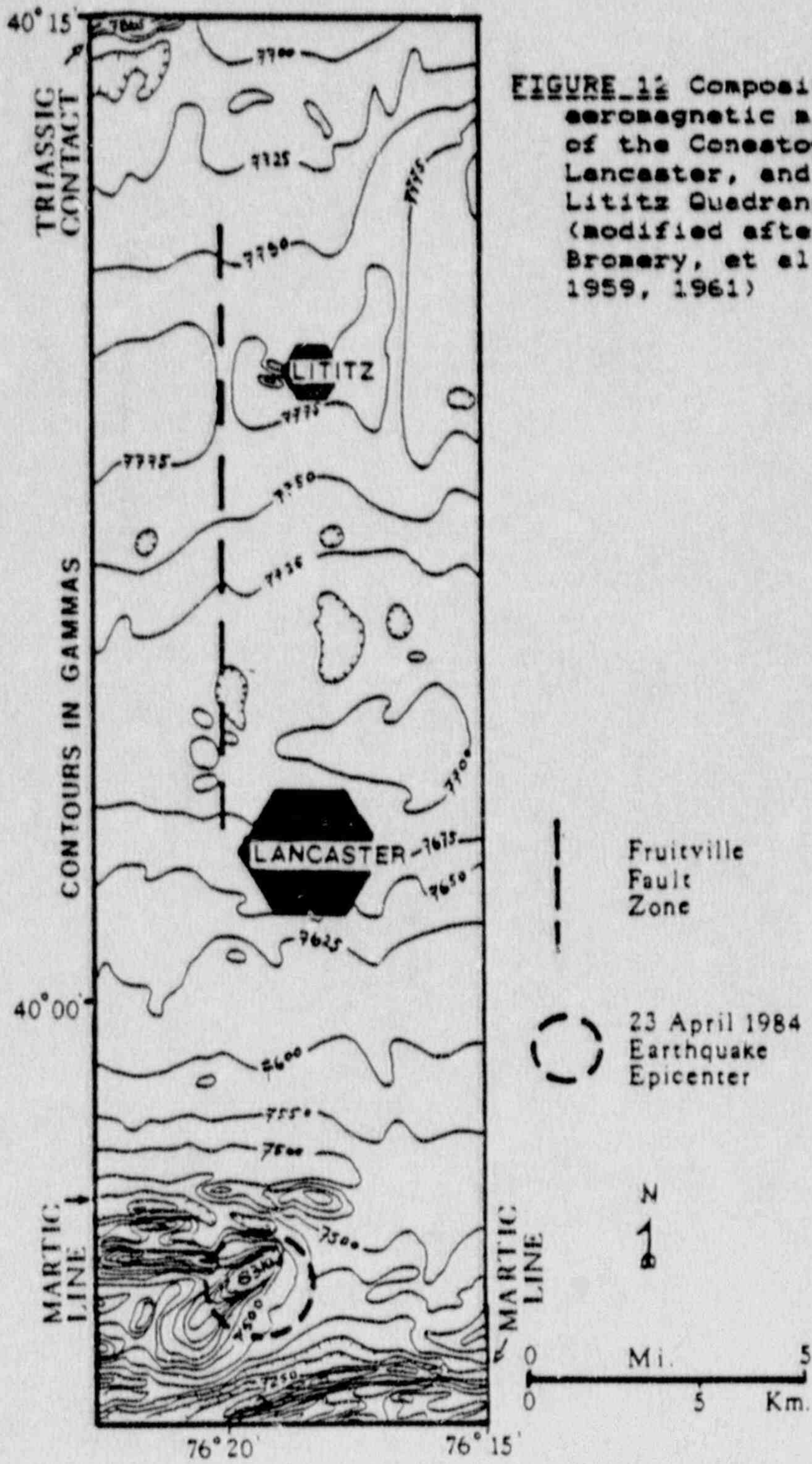

FIGURE 11 Composite aeromagnetic map of the Conestoga, Lancaster, and Lititz Quadrangles. (modified after Bromery, et al, 1959, 1961)

identify structural features on the aeromagnetic data. The magnetization of the Paleozoic and Triassic rocks, with the exception of the diabase, is very uniform and low (Table 1) because of the relatively uniform composition of these clastics and carbonates (Sumner, 1977). Thus, the aeromagnetic data for the Triassic and Paleozoic sedimentary rocks has a range of less than 100 gammas.

Socolow (1974) sums up the problem, in the Lancaster region, well, when he says, "Considerable faulting and folding are involved in the area, but the sediments have such similar magnetic properties that the structures are not indicated by the magnetic data." A ground magnetic survey, with its higher resolution, may be useful to help verify the proposed fault zone.

Basement Structures

There is mounting geophysical evidence that the eastern U.S. is characterized by large, NW striking, basement blocks. Regional gravity, magnetics, LANDSAT imagery, and geological information suggest several such blocks in the Pennsylvania and New York area (Gold, et al, 1974; Lavin and Alexander, 1981; Lavin, et al., 1982). The major lineaments defining the block boundaries can be seen in the simple Bouguer anomaly map of the area (Figure 13) (Lavin and Alexander, 1981; Lavin, et al., 1982). They are defined according to offsets in the gravity anomalies. These inferred fracture zones appear to penetrate deep into the crust, possibly the mantle. This is suggested by their continuation through a variety of geological terrains and geophysical expressions, as well as their great length and linearity. The more prominent of these inferred fracture zones are the Tyrone-Mount Union (TMU) and the Pittsburgh-Washington (PW) lineaments (Figure 13). "The extensions of the Tyrone-Mount Union and the Pittsburgh-Washington lineaments bound a distinct crustal block (the Lake Erie-Maryland block) over 100 km wide and probably more than 600 km in length" (Lavin, et al., 1982). During the Precambrian to Lower Ordovician, this block may have moved NW at least 60 km, with later movements being predominantly vertical with respect to the surrounding blocks. Similar structures are identified in New York State (Diment, et al., 1980).

Further evidence for the Lake Erie-Maryland crustal block comes from an offshore gravity and magnetic study by Taylor et al., (1968). They found a major magnetic feature which runs offshore, down the east coast, approximately parallel to the coast line, and located directly over the continental slope. This magnetic feature coincides with the +30 mgal Bouguer gravity anomaly. However, the magnetic feature deviates from the continental slope between the

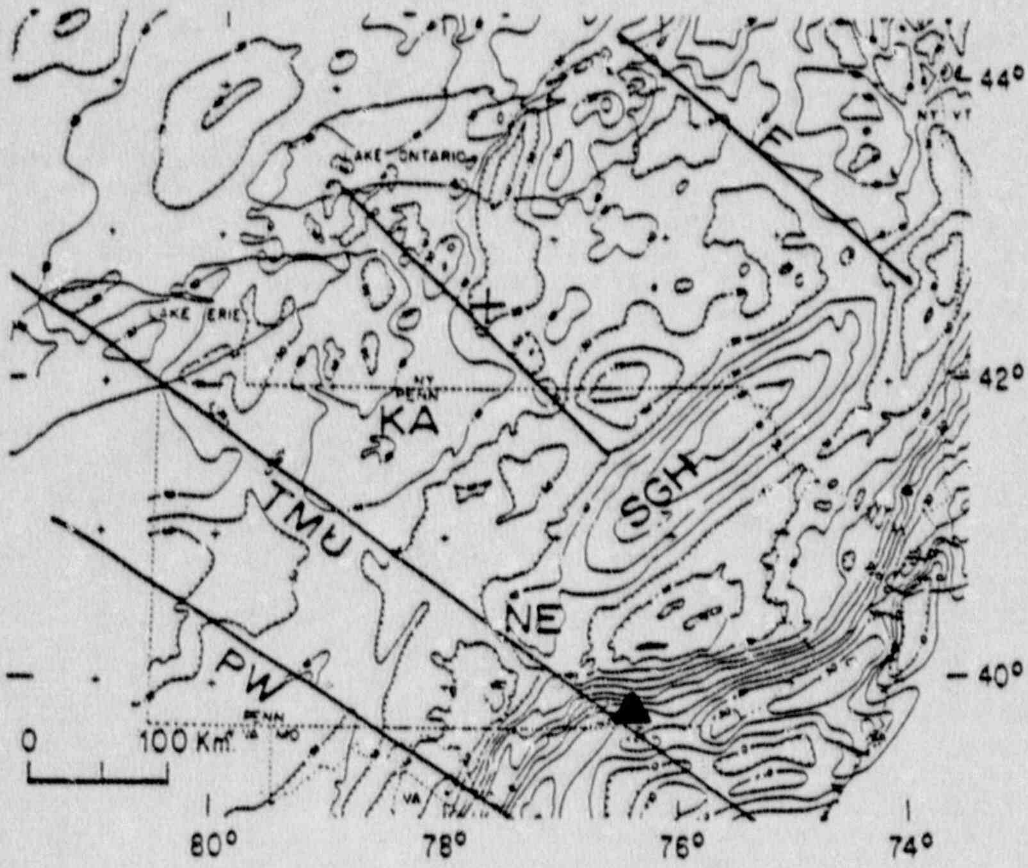

FIGURE 13 Simple Bouguer anomaly map (contour interval equal to 10 mgal) of Pennsylvania showing large crustal lineaments. Heavy lines are the Tyrone - Mt. Union (TMU) and Pittsburgh - Washington (PW) crustal lineaments. The Kane (KA), Scranton (SGH), and Newport (NE) gravity highs are labeled. The triangle is the approximate location of the April 23, 1984 earthquake. (modified after Lavin et al, 1982)

39th and 40th parallel, where it takes a bend landward, and is possibly offset. This offset is consistent with the NW offset on the Lake Erie - Maryland crustal block mentioned above.

Kimberlite structures in Pennsylvania, New York, Kentucky, and Tennessee appear to be at intersections of the Rome Trough (NE trending), with its down-to-the-east basement faulting, and the major structural (NW trending) lineaments mentioned above. The kimberlites' radiometric ages decrease from Mississippian-Permian in Tennessee to mid-Jurassic in New York "perhaps reflecting the gradual opening of the modern day Atlantic Ocean" (Parrish and Lavin, 1982).

It is noteworthy that the dominant of these NW trending lineaments, the Tyrone-Mount Union lineament, runs through the vicinity of the Lancaster area (Figure 13). As yet there has been no direct correlation of the seismicity of this region and the lineament. However, it represents a crustal-wide inhomogeneity that may serve to concentrate stresses in the area. This remains to be investigated.

LINEAMENTS

Lineaments in the Northeastern United States

As early as 1904, Hobbs (1904) fou[illegible] NW trending lineaments, by observing that many of th[illegible] large scale rivers and lakes in the NE U.S. aligned themselves in a given direction for several hundreds of kilometers (Figure 14). He defined a set of NNE striking linear features and a set of NW striking ones. The NW lineaments are very analogous to the NW lineaments geophysically identified by Lavin, et al., (1982) (Figure 13), above. Likewise, Wheeler, et al., (1974) used detailed mapping and structural analysis to describe 17 NW striking lineaments in the Plateau Province. They discovered 5 lineaments in Pennsylvania, and 12 in West Virginia. They varied in length from 13 km to 172 km, averaging 71 km. They strike from N 9°W to N 91°W, with an average of N 53°W (Wheeler, et al., 1974). Based on field studies, all these cross-structures in the NE U.S. are not simple tear faults or joints, but rather complex zones of closely fractured rocks (Wheeler, et al., 1978).

Wise (1974) used shadow methods on raised plastic relief maps of the NE U.S. to produce psuedo-radar photo maps, and to analyze them for linear components. He concluded that " the most pervasive fracture systems, striking N 20°E, N 25°W, and N 70°E, extend at least from Lake Ontario to Pennsylvania to Maine. These topographic linears, ranging from 20 km to 200 km in length, are ubiquitous, independent of rock type, local geological provinces or curvatures of the mountain system, and do not change patterns near the coastlines." (Figure 15). This suggests that these linears are the latest deformation superimposed on all the structures. A detailed area in NW Massachusetts was used to compare these linears to ground measured brittle fractures and to ERTS (Earth Resource Technology Satellite) imagery lineaments (Wise, 1974). The study concluded that a strong correlation in the strike directions of the fractures and the linears does exist.

In the Lancaster, Pennsylvania area Wise (1974) identified three lineament directions using the above method (Figure 15). One N-NNE in strike, the second ENE in strike, and a weaker striking NW. The ENE striking lineaments seem to reflect the Paleozoic structural trend of the Appalachian mountains in the region. The weaker NW trending lineaments are possibly those described by Wheeler et al, (1978) and Lavin, et al., (1982), above. Finally, the N-NNE lineament may be associated with the cross faults of the region, such as the Fruitville fault and the seismic zone around it (Figure 3).

Lineaments in the Lancaster County Region

Lineaments have the same morphological characteristic as fracture traces except that they are wider, longer, not at all obvious in the field, and exert a major influence on the topography (Gold, et al., 1973). This is also the case for the lineaments identified in Pennsylvania.

Gold, et al. (1973,1974) located major lineaments (greater than 80 km) in Pennsylvania based on ERTS-1 (Earth Resource Technology Satellite - 1) images. Most of these lineaments were straight and appeared independent of regional structural trends. Many are nearly perpendicular to the NE-SW Appalachian belt (Figure 16).

Kowalik, et al. (1975) studied the intermediate lineaments (10 - 80 km) in Pennsylvania, also based on ERTS-1 data. In the Lancaster region (the thick bordered square of Figure 17), they recognized several lineament directions with the N-S direction dominant.

Both the intermediate and long lineaments in SE Pennsylvania appear to be "underlain by zones of fractured and jointed rocks and represent zones of deformation" (Gold, et al., 1973). They transgress Precambrian through Triassic age lithologies, and "must represent either a rejuvenated crustal fracture system..., and in a sense are a reflection through the cover rocks of active crustal "joints"" (Gold, et al., 1973). They are often reflected by straight valley segments, abrupt changes in valley alignment, gaps in ridges, gully and sink hole alignment, localized springs, diffuse seepage areas, and drainage patterns (Gold, et al., 1973, 1974).

Wise (1967) used topographic maps to identify topographic linears of the Susquehanna Piedmont (Figure 18). He found that the orientations of these lineaments (Rosette B, Figure 18), did not match the strikes of the 1400 ground measured master joints (Rosette A). Thus, the lineaments represent an "apparently different system" (Wise, 1967) of fractures. It is noteworthy that Wise identified a set of N-S striking topographic lineaments as clearly dominant within the Lancaster region (Figure 18). These topographic lineaments clearly define the Fruitville fault (Figure 1) and the Lancaster seismic zone (Figure 3), (note the location of the 1984 earthquake in Figure 18).

The preliminary investigation of LANDSAT-4 imagery (30 m. resolution) reveals that clearly the dominant lineaments in Lancaster County are those of the Appalachian structural trend (nearly E-W striking) and those defining the Fruitville fault zone which trend N-S (Figure 19). The latter are defined by gaps and drainage through the Triassic rocks, stream drainage within the Paleozoic rocks, and the right lateral offsets in the E-W striking ridges of the Conestoga Valley (Figure 2).

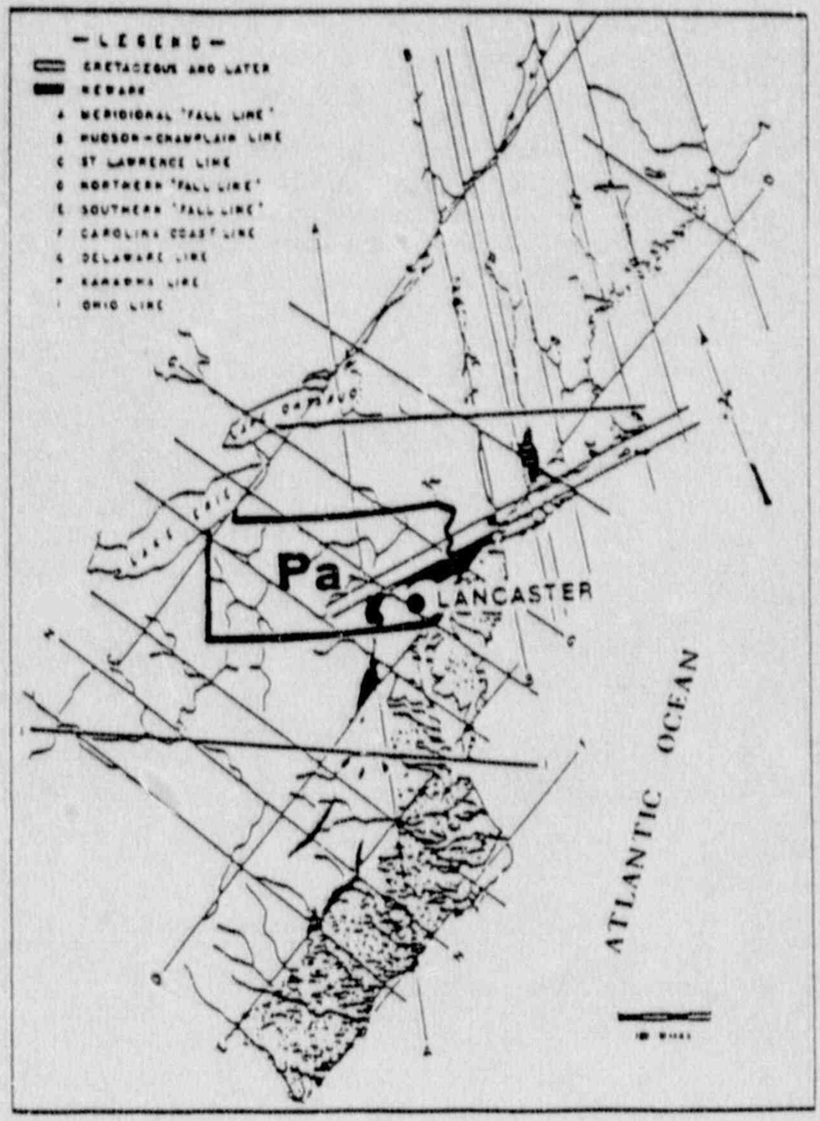

FIGURE 14 Topographic lineaments of the Atlantic Border Region in relation to Lancaster, Pennsylvania (after Hobbs, 1904).

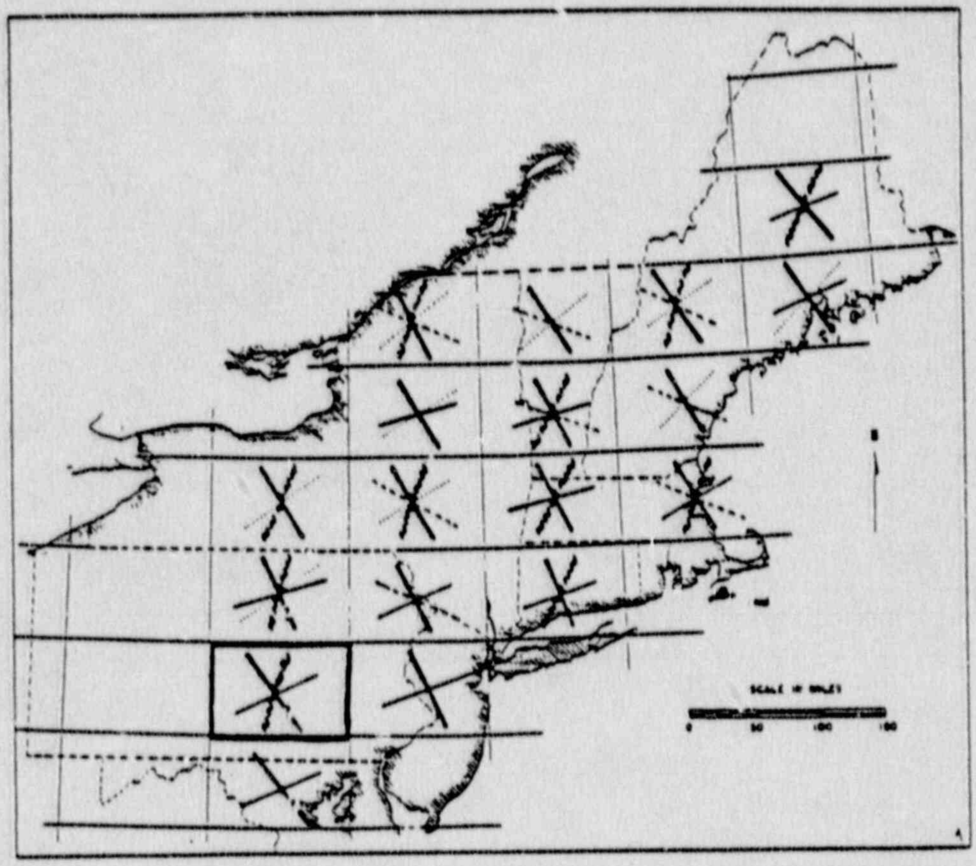

FIGURE 15

Major Fracture Orientations of the Northeastern United States on a quadrangle-by-quadrangle basis using a topographic shadow technique. The contrasting line types are used to suggest correlations among the various fractures. The quadrangle with the dark borders is the one which includes Lancaster, Pennsylvania. (after Wise, 1974)

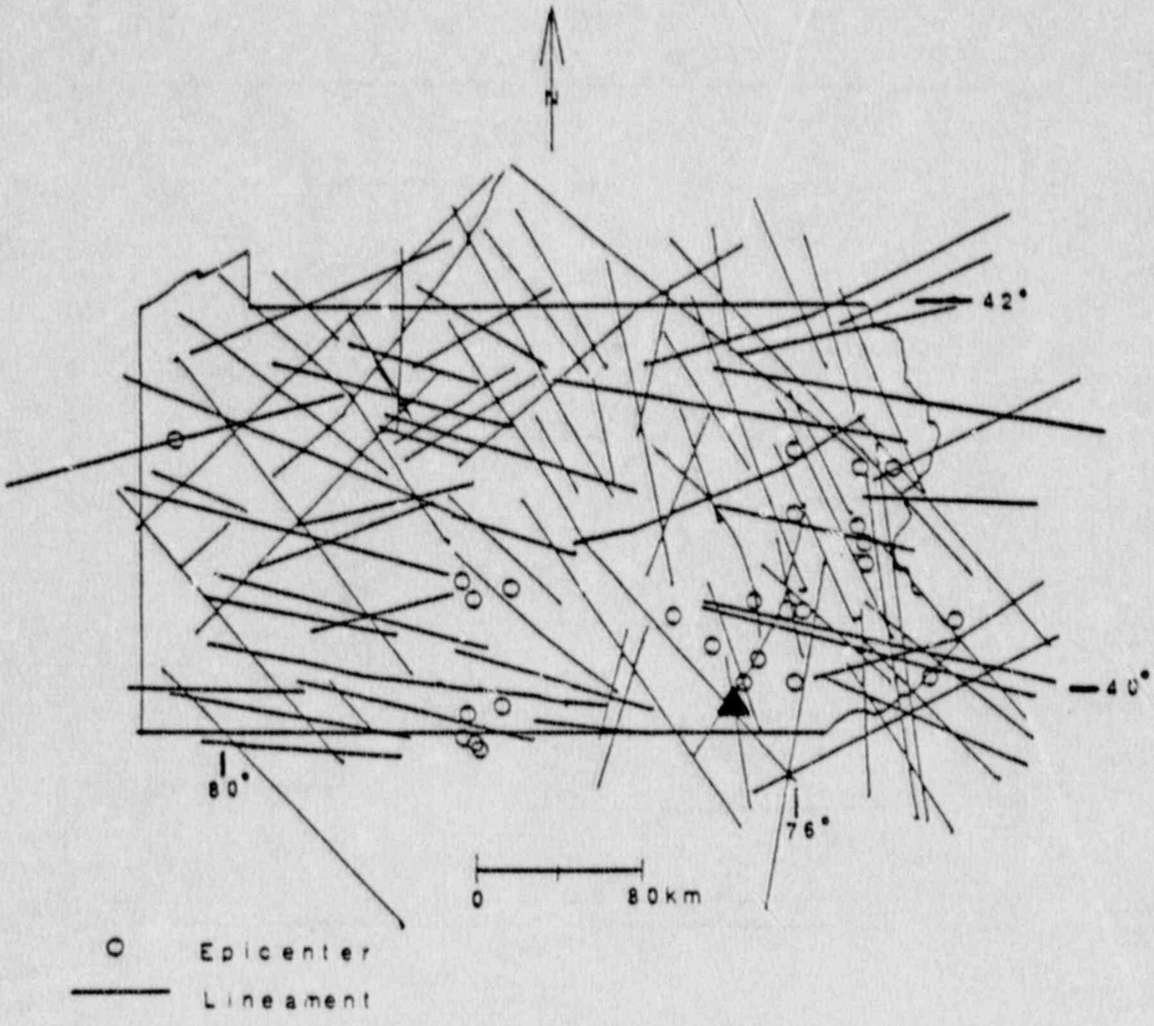

FIGURE 16

ERTS-1 satellite lineaments of Pennsylvania and the location of historic epicenters of earthquakes, including the April 23, 1984 event shown by the triangle. (after Gold, et al., 1974)

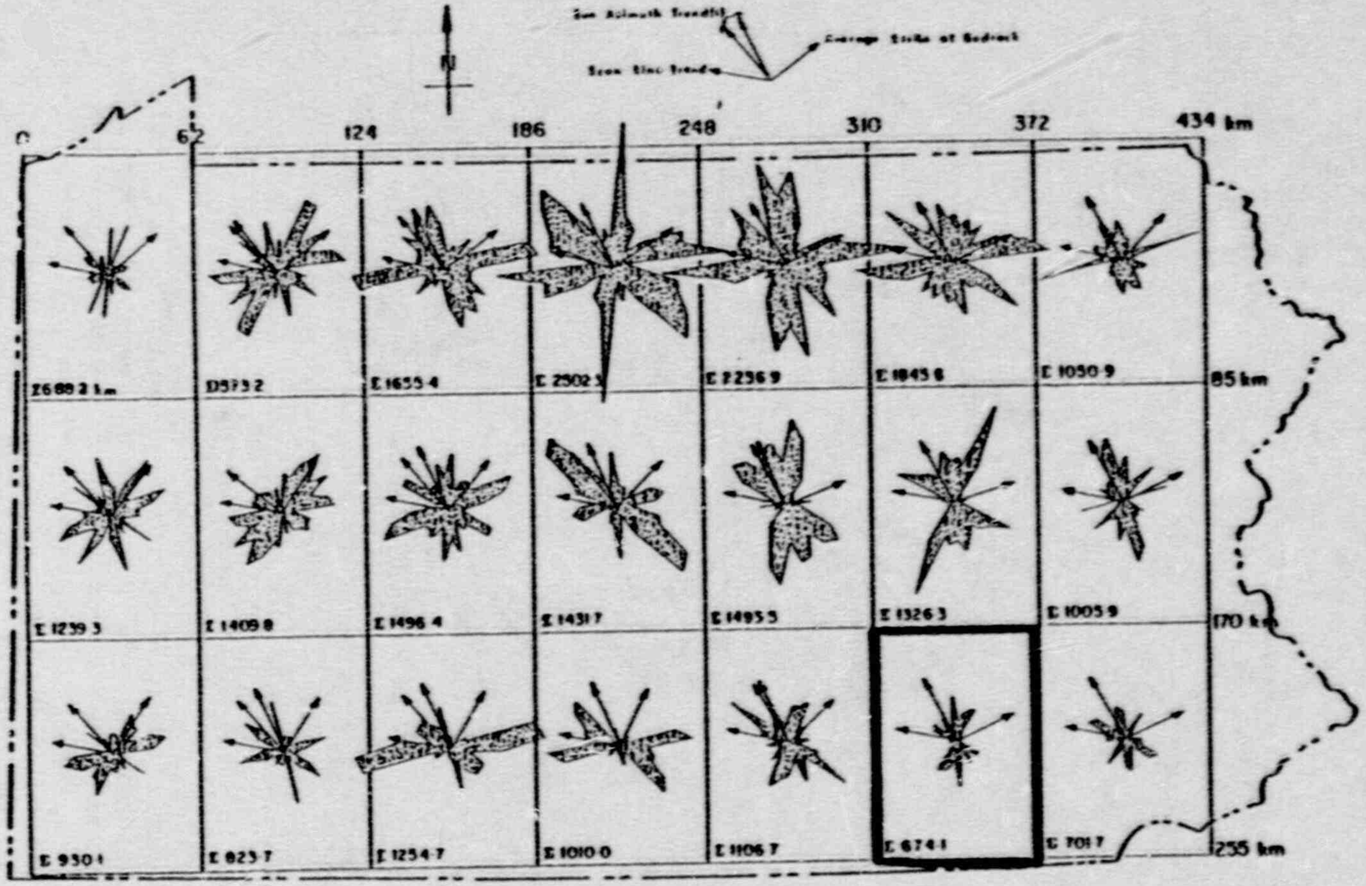

FIGURE 17 LANDSAT-1 intermediate length lineament orientations summarized in rose diagrams for cells on a grid across Pennsylvania. The dark bordered cell is the one for the Lancaster area. The scan line direction, sun azimuth, and general strike of bedrock are superimposed on the diagram. The density of lineaments in one cell can be judged by the sum of their lengths, recorded in kilometers in the lower corner. (after Kowalik & Gold, 1974).

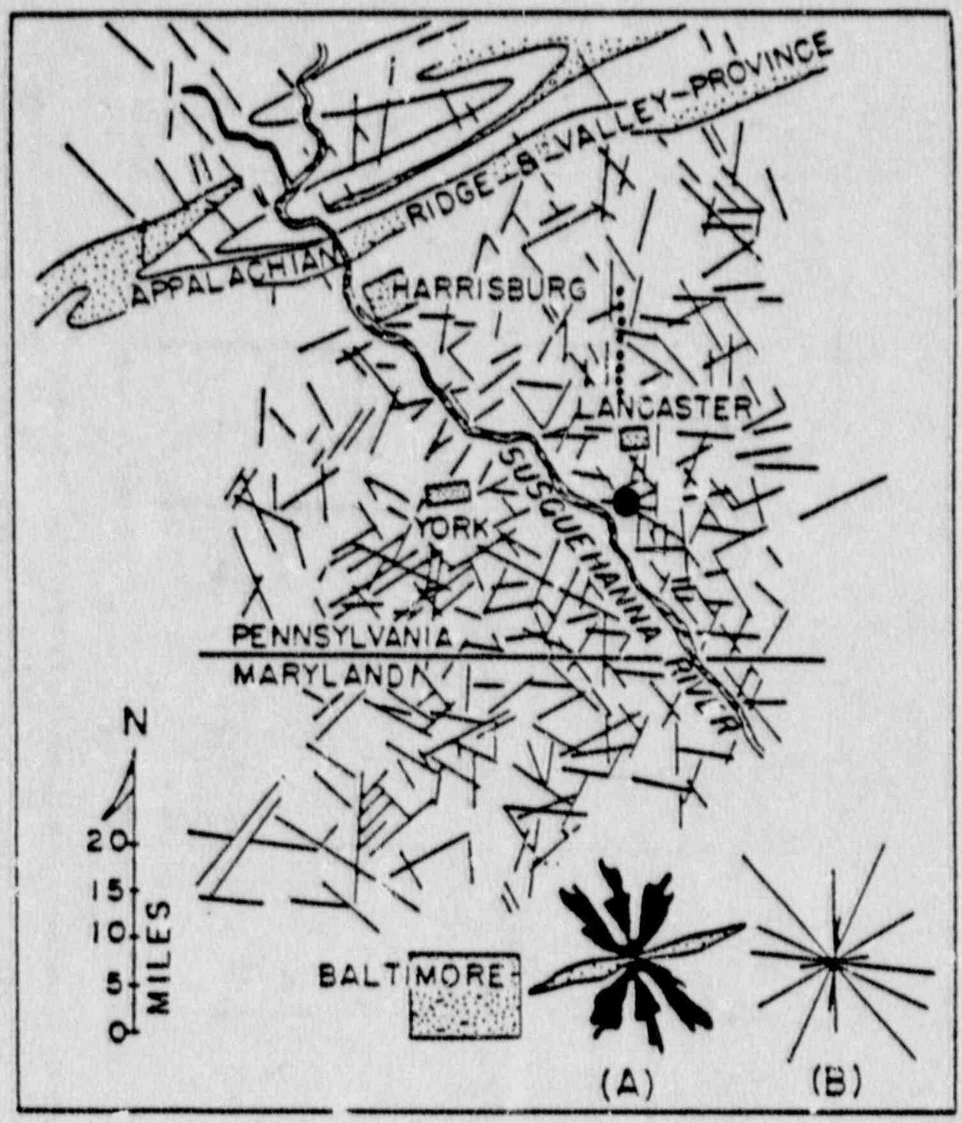

FIGURE 18

Topographic linears of the Lancaster County area derived from topographic maps. Rosetta A represents ground measurements of the strikes of 1400 master joints related to the late stage of folding in the Piedmont of Pennsylvania. Rosetta B represents the eight directions of the topographic linears on this map, apparently a different system from Rosetta A. The dotted line represents the Fruitville Fault Zone, and the large solid dot is the epicenter of the April, 1984 earthquake. (modified after Wise, 1967)..

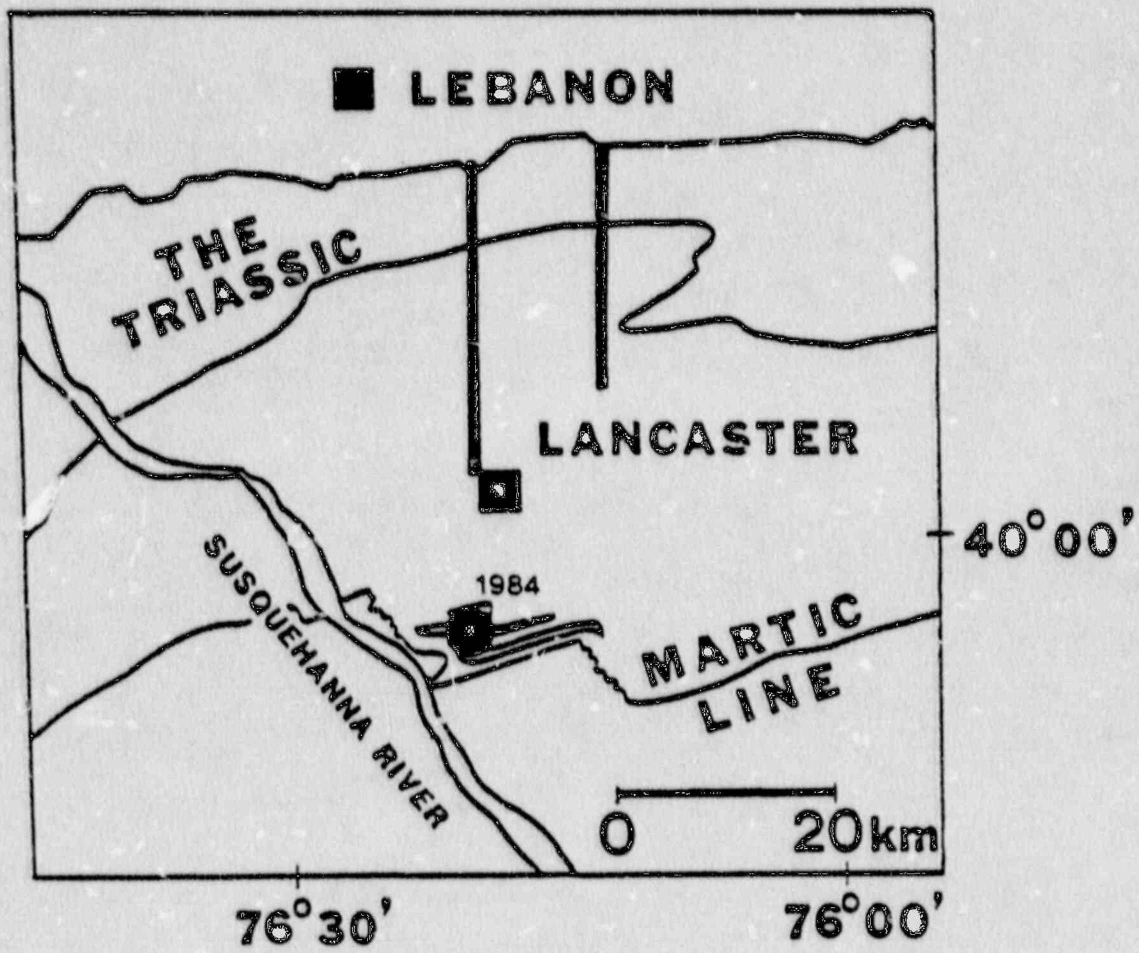

FIGURE 19

Map showing major LANDSAT-4 lineaments (dark lines) obtained in a preliminary survey of the Lancaster County area. The solid dot is the epicenter of the April 23, 1984 earthquake.

HISTORICAL SEISMICITY

Seismicity in the Northeastern United States

It appears that the historical earthquake activity and the present seismic events bear no consistent relationship to tectonic provinces. Rather, seismic zones usually cut across their boundaries (Hadley and Devine, 1974). Furthermore, "for small magnitude events, about half of the instrumentally recorded earthquakes that have been studied, are in persistant source zones. The remainder are more than 20 km from other earthquakes" (Diment, et al., 1983). There is mounting evidence that one of these source zones is the area of Lancaster County in the vicinity of the Fruitville fault (Figure 3).

Seismicity in the Lancaster County Region

The Lancaster area has been shaken by several distant earthquakes (Table 2), the largest of which have had intensities of up to MM IV. However, Pennsylvania has had a fair amount of seismicity of its own (Table 3; Table 4) (Nottis, 1983; Scharnberger and Howell, 1985), and it is the local activity that has created the highest intensities felt in Lancaster (intensity MM VI).

Sharnberger and Howell (1985) did a study of the historical seismicity of Lancaster County and obtained the results of Figure 3 and Table 5. However, there is evidence that the location of the October 6, 1978 event near the town of Lititz (Figure 3) is in error. The preferred location of this event is on the northern outskirts of the city of Lancaster (Figure 20). This is based on Scharnberger's (1978) intensity maps for the two 1978 Lancaster earthquakes (Figure 21), and on the results of applying a relative location algorithm which used the locations of the July 16, 1978 and the April 23, 1984 earthquakes to locate the October 6, 1978 event (Figure 22). Furthermore, although traditionally the March 8, 1889 event, of intensity MM V, has been located in York, Pennsylvania, new studies of newspaper records have been used to relocate the event within the area around the city of Lancaster (Nottis, 1983; Armbruster and Seeber, 1985).

Thus, it is apparent that the seismicity is clustered in a N-S striking zone along the Fruitville fault. The zone appears to be about 50-60 km long, in the N-S direction, and 10-20 km wide, in the E-W direction. It runs directly through the center of Lancaster County and the city of Lancaster, Pennsylvania (Figure 20). Armbruster and Seeber (1985) have called this zone, the Lancaster Seismic Zone (LSZ).

The earthquakes of largest instrumentally recorded magnitude within the LSZ are the recent April 23, 1984 event with a magnitude 4.2, and the May 12, 1964 event which had a previous magnitude 4.5, but which was recalculated, in this study, to be of magnitude 3.6 (Figure 20). The other instrumentally recorded events in the LSZ are: the December 8, 1972 event (magnitude 2.1, Dewey and Gordon, 1984) at a depth of about 3.5 km; the July 16, 1978 event (magnitude 3.0, Scharnberger, 1978) at a depth of about 5.0 km; and the October 6, 1978 event (magnitude 3.1, Scharnberger, 1978).

Armbruster and Seeber (1985) conducted a systematic search of newspapers from the years 1750-1900, and found 13 new epicenters for known and previously unknown earthquakes. They showed a N-S trending seismic zone (the Lancaster Seismic Zone) which completely overlaps and matches the one identified by Scharnberger and Howell (1985) in Figure 3. However, they presented the new location of several events not on Scharnberger and Howell's map. They are as follows:

29 November 1800 - magnitude 4.1
21 August 1820 - magnitude 3.4
5 February 1834 - magnitude 4.0
8 March 1889 - magnitude 4.3 (new location).

The location of these earthquakes is seen in Figure 23 & Figure 24. It is clear that a N-S trending seismic zone dominates Lancaster County (Figure 20 & Figure 24) and parallels the most recent faulting in the area, such as that of the Fruitville fault zone (Figure 20).

TABLE 2

CHRONOLOGICAL LISTING OF DISTANT EARTHQUAKES WHICH HAVE AFFECTED THE LANCASTER REGION OF PENNSYLVANIA

Date	Lat. (N)	Long. (W)	Epicentral Intensity	Distance from Lancaster (Mi.)	Site Intensity	
Feb. 5, 1663	47.6	70.1	X	610 NE	III-IV	•
Dec. 18, 1737	40.8	74.0	VII	150 E	IV	•
Nov. 18, 1755	42.9	70.6	VIII	360 ENE	III	•
Dec. 16, 1811	36.6	89.6	XI-XII	720 WSW	IV	•
Jan. 23, 1812	36.6	89.6	XI-XII	720 WSW	IV	•
Feb. 7, 1812	36.6	89.6	XI-XII	720 WSW	IV	•
Mar. 9, 1828	37.5	78.0	VI	210 SW	III	#
Aug. 10, 1884	40.6	74.0	VII	145 E	IV	#, $
Aug. 31, 1886	32.9	80.0	IX-X	540 S	III-IV	#, $
May 31, 1897	37.3	80.7	VIII	290 SW	II-III	#
Apr. 9, 1918	38.7	78.4	V-VI	140 SW	II-III	#
Nov. 1, 1935	45.8	79.1	VII	475 NNW	II-III	#, $
Sept. 4, 1944	44.9	74.9	VIII	340 NNE	II-III	#, $

• Intensity estimated.

Intensity determined from isoseismal maps.

$ Intensity determined from local accounts.

(after Holt, 1972)

TABLE 3

EARTHQUAKES OF PENNSYLVANIA

Day	Year	Place	Mercalli Intensity	Reference
Oct. ?	1728	Philadelphia	?	Winkler, 1978
Dec. ?	1738	Dauphin Co.	?	Winkler, 1978
Oct. 30	1763	Bucks County	?	Stone, 1943
Apr. 25	1772	Delaware Valley	IV	Winkler, 1978
Nov. 22 & 23	1777	Philadelphia	?	Winkler, 1978
Nov. 29	1780	Bucks County	?	Stone, 1978
Nov. 29	1783	Philadelphia	IV-V	Winkler, 1978
Nov. 30	1783	Philadelphia	IV	Winkler, 1978
Mar. 17	1799	Philadelphia	?	Winkler, 1978
Mar. 17	1800	Philadelphia	?	Coffman, Von Hake, 1973
Mar. 29	1800	Philadelphia	?	Winkler, 1978
Nov. 20	1800	Dauphin County	?	Winkler, 1978
Nov. 29	1800	Philadelphia	IV	Coffman, Von Hake, 1973
Nov. 12	1801	Philadelphia	?	Winkler, 1978
Dec. 8	1811	Philadelphia	VII	Winkler, 1978
Mar. 14	1828	Pittsburgh	III-IV	Winkler, 1978
Nov. 11 & 14	1840	Philadelphia	IV	Winkler, 1978
Aug. 17	1873	Sharon, Pa.	IV	Frederick, 1979
May 31	1884	Allentown	V	Coffman, Von Hake, 1973
Mar. 8	1889	York	V	Landsberg, 1938b
Mar. 9	1889	York	?	Landsberg, 1938b
May 31	1908	Allentown	VI	Coffman, Von Hake, 1973
Oct. 29	1934	Erie	V	Coffman, Von Hake, 1973
Nov. 5	1934	NW Pa.	III	Neumann, 1936
Aug. 26	1936	Mercer County	III	Neumann, 1936
June 8	1937	Reading, Pa.	?	Neumann, 1940
July 15	1938	Blair County	VI	Landsberg, 1938a
Aug. 28	1938	Philadelphia	?	Stone, 1943
Apr. 1	1939	Lancaster	?	Bodle, 1941
Nov. 15	1939	Philadelphia	?	Stone, 1943
May 28	1940	Harrisburg	?	Neumann, 1942
Oct. 16	1941	Centre County	?	Stone, 1943
Nov. 23	1951	Allentown	?	Murphy, Cloud, 1953
Jan. 7	1954	Sinking Spring (many aftershocks)	VI	Murphy, Cloud, 1956
Feb. 21	1954	Wilkes-Barre	VII	Murphy, Cloud, 1956
Feb. 23	1954	Wilkes-Barre	VI	Murphy, Cloud, 1956
Jan. 19	1955	Berks County	IV	Murphy, Cloud, 1957
Sept. 14	1961	Lehigh Valley	V	Lander, Cloud, 1963
Dec. 27	1961	Pa.-N.J. Border	V	Lander, Cloud, 1963
Sept. 7	1962	Fulton County	?	U.S.C.G.S. list
Oct. 10	1963	Fulton County	?	U.S.C.G.S. list
Feb. 13	1964	Blair County	V	News reports
May 12	1964	Cornwall	VI	Von Hake, Cloud, 1966
Dec. 7	1972	Lancaster County	V	Coffman, Von Hake, 1974
Feb. 28	1973	NJ & S. Phila.	V-VI	Sbar et al. 1975
July 16	1978	Lancaster County	V	Person, 1979
Oct. 6	1978	Lancaster County	V	News reports

Where intensity is not listed, it was small.

(after Howell, 1979)

TABLE 4

HISTORICAL SEISMICITY OF PENNSYLVANIA

DATE			ORIGIN TIME (GMT)			EPICENTER		DEPTH		MAGNITUDE		INTENSITY		LOCALITY
YEAR	MONTH	DAY	HR.	MIN.	SEC.	N. LAT.	W. LONG.	(KM.)	REF.	VAL.	TYPE	(MM)	REF.	
1800	MAR	17	—	—	——	39.80	75.20	——	10	——	-	F	10	PA PHILADELPHIA
1800	MAR	29	—	—	——	39.80	75.20	——	118	——	-	F	118	PA PHILADELPHIA
1800	NOV	29	—	—	——	39.80	75.20	——	10	——	-	F	10	PA PHILADELPHIA
1884	MAY	31	—	—	——	40.60	75.50	——	10	——	-	6	10	PA ALLENTOWN
1889	MAR	08	23	40	——	40.00	76.00	——	10	——	-	5	10	PA LANCASTER
1907	JAN	10	10	00	——	41.20	77.10	——	101	——	-	4	101	PA WILLIAMSPORT
1908	MAY	31	17	42	——	40.60	75.50	——	10	——	-	6	10	PA ALLENTOWN
1921	SEP	27	04	32	——	42.10	80.20	——	101	——	-	3	101	PA ERIE
1934	OCT	29	20	07	——	42.00	80.20	——	69	——	-	5	69	PA ERIE
1936	AUG	26	09	08	——	41.40	80.40	——	71	——	-	3	102	PA GREENVILLE
1937	JUN	09	00	04	——	40.30	75.90	——	72	——	-	2	102	PA READING
1938	JUL	15	22	45	——	40.40	78.20	——	51	——	-	5	51	PA CLOVER CREEK
1939	APR	02	03	00	——	40.00	76.30	——	3	——	-	2	102	PA LANCASTER
1940	MAY	28	20	05	——	40.30	76.90	——	74	——	-	2	102	PA HARRISBURG
1942	OCT	24	17	27	——	41.00	75.30	——	102	3.4	G	——	——	PA STROUDSBURG
1944	FEB	05	16	22	——	40.80	76.20	——	102	3.7	G	——	——	PA SHENANDOAH
1946	OCT	28	20	36	——	41.50	76.40	——	102	3.6	G	——	——	PA LAPORTE
1950	MAR	20	22	55	——	41.50	75.80	——	102	3.3	G	——	——	PA NW. OF SCRANTON
1951	NOV	23	06	45	——	40.60	75.50	——	10	——	-	4	10	PA ALLENTOWN
1954	JAN	07	07	25	——	40.30	76.00	——	102	——	-	4	102	PA SINKING SPRINGS
1954	JAN	24	03	30	——	40.30	76.00	——	102	——	-	3	102	PA SINKING SPRINGS
1954	AUG	11	03	40	——	40.30	76.00	——	102	——	-	4	102	PA SINKING SPRINGS
1954	SEP	24	11	00	——	40.30	76.00	——	102	——	-	2	102	PA SINKING SPRINGS
1955	JAN	20	03	00	——	40.30	76.00	——	102	——	-	4	102	PA SINKING SPRINGS
1960	JAN	22	20	53	——	41.50	75.50	——	61	3.4	G	——	——	PA CARBONDALE
1961	SEP	15	02	16	——	40.80	75.50	——	79	——	-	5	79	PA LEHIGH VALLEY
1963	MAR	02	20	24	——	41.50	75.70	——	64	3.4	G	——	——	PA SCRANTON
1964	FEB	13	19	46	40.80	40.38	77.96	——	32	3.2	D	——	——	PA MARKLESBURG
1964	MAY	12	06	45	10.70	40.30	76.41	——	32	3.2-	D	6	107	PA LANCASTER —
1965	OCT	08	02	17	——	40.10	79.80	——	120	3.3	G	——	——	PA SOUTHWESTERN
1972	DEC	08	03	00	33.30	40.14	76.24	——	32	3.5	D	——	——	PA LANCASTER
1978	OCT	06	19	25	47.40	40.05	76.09 •	——	133	3.8	H	6	23	PA LANCASTER
1980	MAR	02	11	54	47.90	40.21	75.08	——	112	2.0	H	——	——	PA ABINGTON
1980	MAR	05	17	06	56.50	40.17	75.07 •	——	112	3.5	r	3-4	140	PA ABINGTON
1980	MAR	05	17	20	32.40	40.18	75.0[illegible] •	——	112	3.1	H	——	——	PA ABINGTON
1980	MAR	11	06	00	26.90	40.15	75.09 •	——	112	3.7	H	4-5	140	PA ABINGTON
1980	MAR	11	16	16	05.50	40.25	74.99 •	——	112	2.8	H	4-5	140	PA ABINGTON
1980	MAY	02	15	23	23.50	40.16	74.99 •	——	113	2.8	H	——	——	PA LANGHORNE
1980	MAY	02	19	02	24.40	40.24	75.03 •	——	113	3.0	H	——	——	PA JAMISON

(after Nottis, 1983)

TABLE 5

HISTORICAL SEISMICITY OF THE LANCASTER REGION

Date	Location	Mercalli Intensity	Comments
1885	Lancaster/ Lebanon	II-III	
Mar. 8, 1889	York or Lancaster	V-VI	strongly felt in both locations
Apr. 26, 1893	Lancaster	III	
Apr. 1, 1939	Lancaster	II	
May 12, 1964	Lebanon	VI	M = 3.6
Dec. 7, 1972	Lancaster	V	
Jul. 16, 1978	Lancaster	V	
Oct. 6, 1978	Lancaster	V	

(modified after Sharnberger & Howell, 1985)

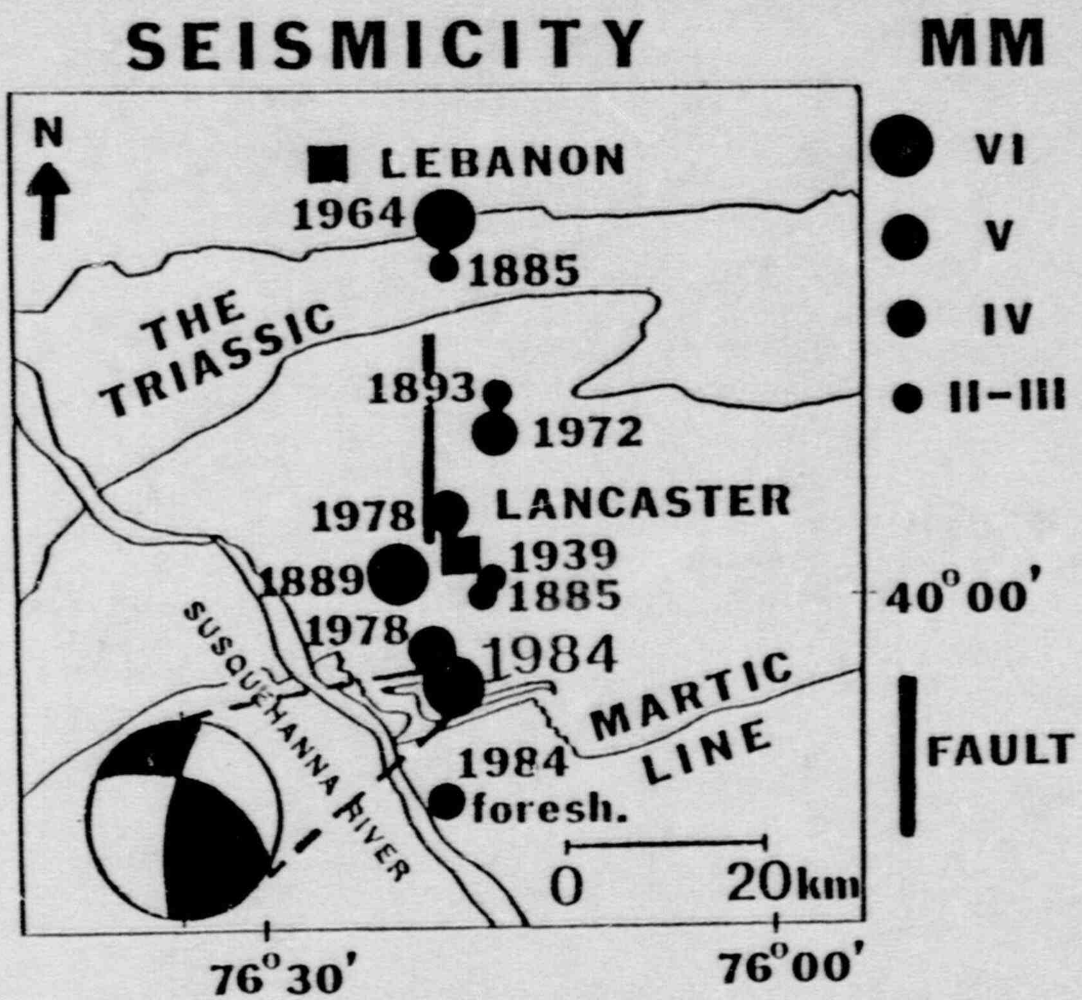

FIGURE 20 Map of the seismicity of Lancaster County in relation to the Fruitville Fault Zone (dark line). Inserted is the upper hemisphere projection of the fault plane solution obtained by Armbruster and Seeber (1985) for the April 23, 1984 earthquake. (modified after Scharnberger & Howell, 1985)

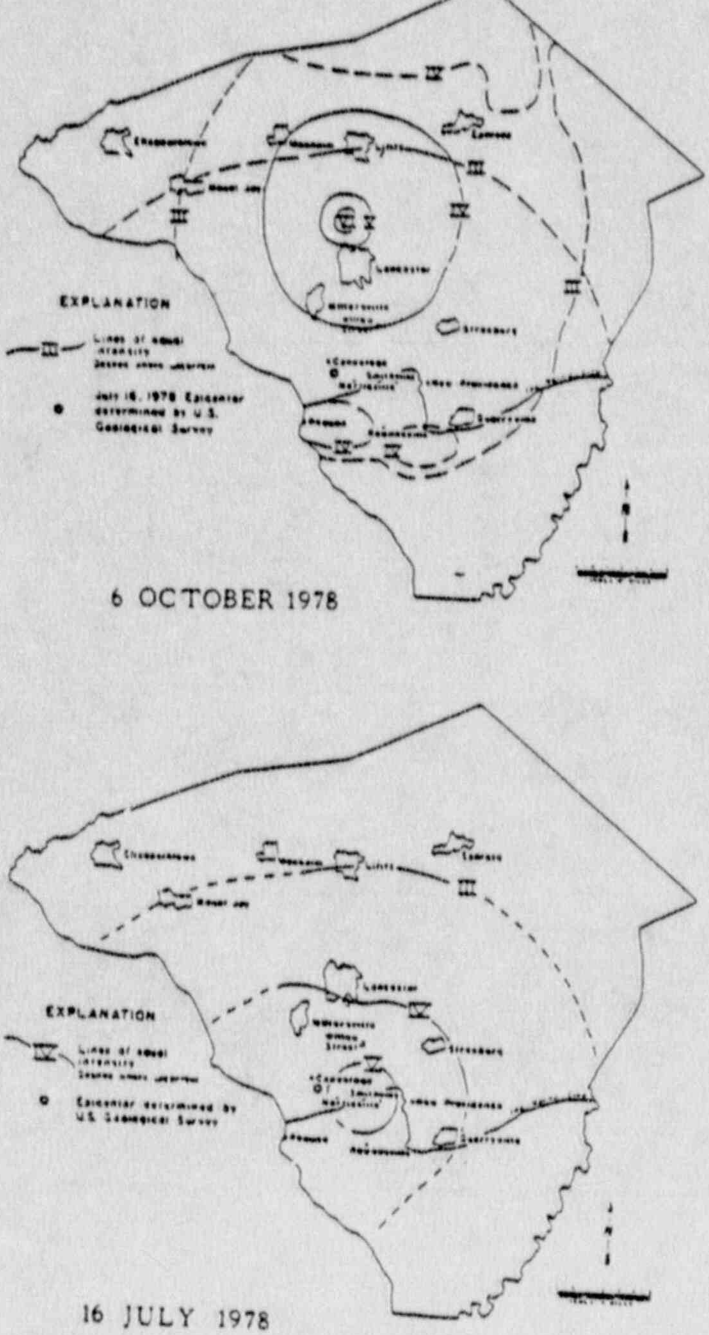

FIGURE_21 Intensity map for the July 16, 1978 and the October 6, 1978 earthquakes in Lancaster County, Pennsylvania. (after Scharnberger, 1978)

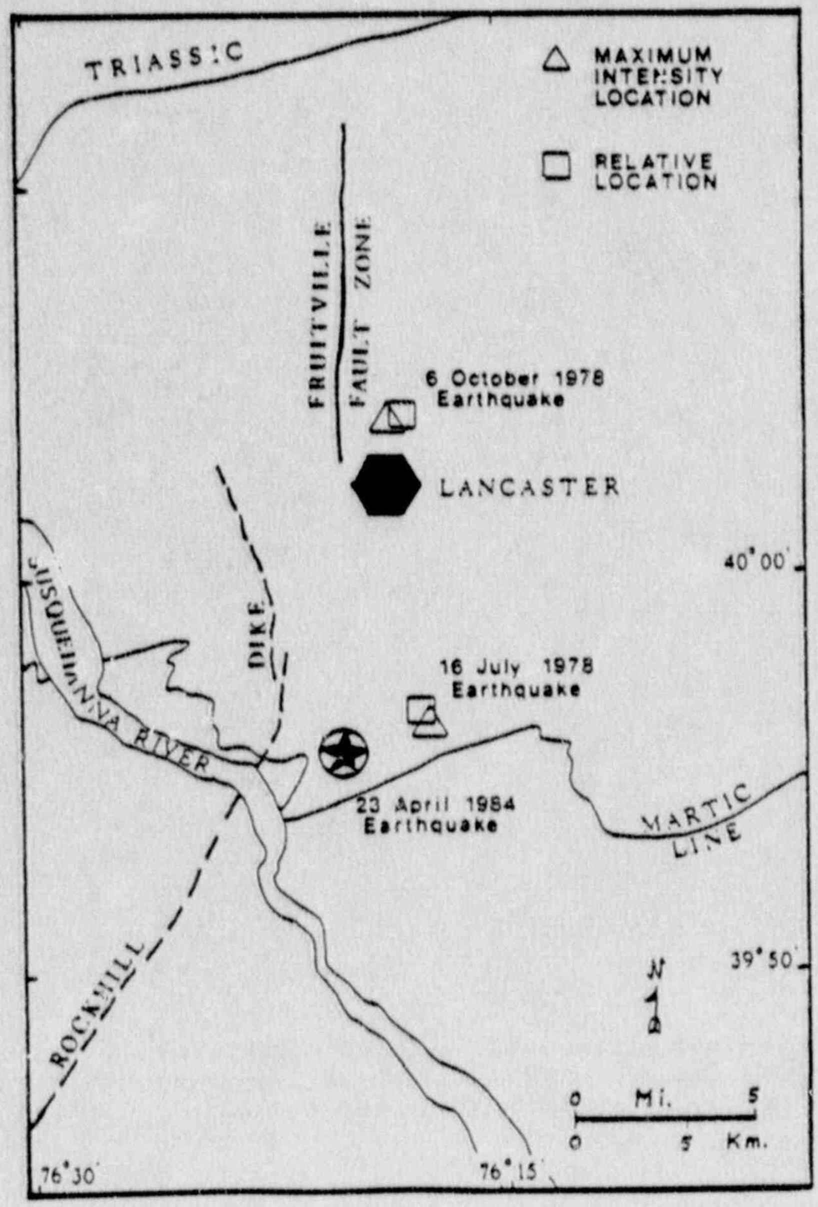

FIGURE 22 Maximum intensity locations and relative locations for the July 16, 1978 and the October 6, 1978 Earthquakes. (modified after Gray, et al., 1960).

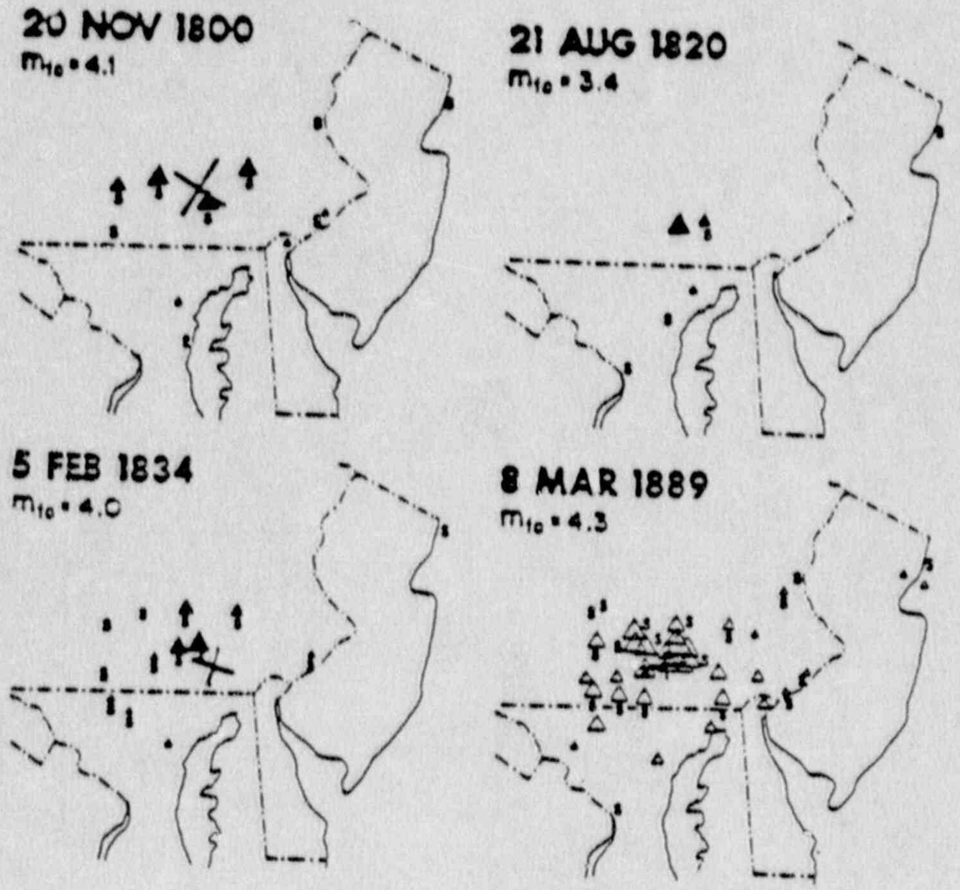

FIGURE 23 Maximum intensity locations obtained by Armbruster and Seeber (1985) for four large events during the 1800's. (after Armbruster & Seeber, 1985)

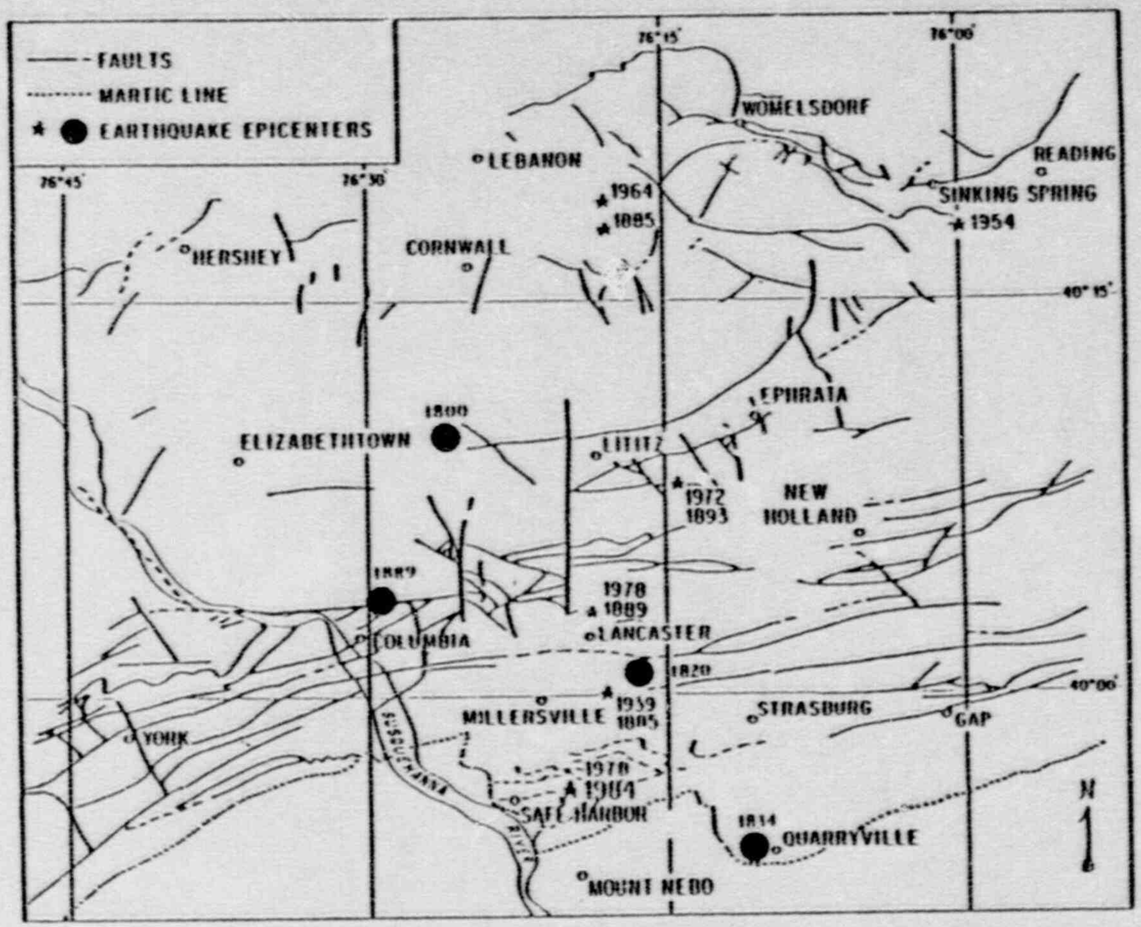

FIGURE 24 Modified seismicity map for the Lancaster area. The July, 1978 and the March, 1889 events have been relocated, and fall north of the city of Lancaster. The solid dots indicate the approximate locations of the four events in Figure 23. (modified after Scharnberger & Howell, 1985)

LANCASTER EARTHQUAKE -APRIL, 1984-

On April 23, 1984 at 1:36 U.T. (6:36 pm, 22 April EST), Lancaster County experienced one of the largest recorded earthquakes in Pennsylvania. It was felt from Westchester County, New York to Cambria County, in western Pennsylvania, to Washington, D.C. and Sussex County, Delaware. The region of maximum intensity (MM = VI) for this event occurred south of the city of Lancaster, near Marticville (Figure 25). Seismic records of the event give a magnitude of 4.2, with a strong audible component (Scharnberger and Howell, 1984).

This mainshock was preceded by a foreshock of magnitude 3.0 on April 19, at 4:55 U.T. (11:55 pm, 18 April EST). The region of maximum intensity (MM =IV) occurred in the southern portion of the mainshock maximum intensity area, south of Marticville (Figure 25). The epicenter for the foreshock based on all the intensity data, appears to be several kilometers south of the mainshock (Scharnberger and Howell, 1984).

The April 23 mainshock was followed by many aftershocks which lasted well into September, 1984. They were of varying magnitude, the largest a magnitude 2.1 (Scharnberger and Howell, 1984). Ten of the earliest of these aftershocks were recorded by a temporary seismic network, set up in the mainshock region, within a day of the event, and operated for several days by the Pennsylvania State University and the Lamont - Doherty Geological Observatory (Armbruster and Seeber, 1985). The network consisted of 9 portable seismographs (3 from Penn State and 6 from Lamont-Doherty), including smoked paper and digital recorders. The location of these 9 stations and the location of the 10 recorded aftershocks is seen in Figure 26. Armbruster and Seeber (1985) observed that these aftershocks created a zone about 3 km long and N-NNE in strike. The length of the zone is significantly larger than the location error of - 0.5 km. Therefore, the N-S fracture suggested by the aftershocks appears to be real (Armbruster and Seeber (1985). The epicenter of these aftershocks is near Marticville the area of the maximum intensities observed for the April 23, mainshock (Figure 25).

Furthermore, Armbruster and Seeber (1985) report that all the aftershock hypocenters fall in an insignificantly wide range (- 0.5 km) about the 4.5 km depth. They state that "this depth does not correspond to a discontinuity in the assumed velocity structure and the narrow depth range cannot be solely an artifact of the location procedure".

A double couple fault plane solution based on 37 first motions from the mainshock and the aftershocks indicates a seismogenic fault with a NNE strike of about N 10°E, dipping about 60°E, with reverse and right-lateral displacement (Figure 27) (Armbruster and Seeber, 1985). This solution is generally supported by 20 first motions for the April 23, mainshock recorded by the NE U.S. Seismic Network obtained in this investigation (Figure 27). The fault plane solution of Figure 27 has a P axis which is nearly horizontal and strikes ENE. This is consistent with the ENE maximum compressional stress for this part of the U.S., based on other earthquake generated focal mechanisms, on geological data, and on in situ crustal stress measurements (Zoback and Zoback, 1980; Zoback, 1986).

The surface projection of the seismogenic fault (dashed line in Figure 26), based on the aftershock data and the fault plane solution, falls near the town of Conestoga, about 2 km east of the aftershock epicenters. This inferred fault is in direct line, along strike, with the Fruitville fault zone, which outcrops about 15 km to the north. The two features have about the same strike, approximately N-S, which is also the approximate strike of the preferred plane on the focal mechanism solution (Figure 20 & Figure 26, insert). Thus, the mainshock and its aftershocks indicate a seimogenic fault several kilometers south but on-strike with the youngest of the geologically mapped faults in the area. The faults strike between N 0°E and N 12°E (Figure 20).

Furthermore, 2 km west of the projected outcrop of the aftershock-inferred fault is a Triassic-Jurassic diabase dike, of the same strike (Figure 26). This dike, the Rockhill dike, and the many other N-S striking dikes in the Lancaster area (Figure 4) may be indications of a N-S trending, historically persistent, zone of weakness, which is favorably oriented to be activated in the present stress regime.

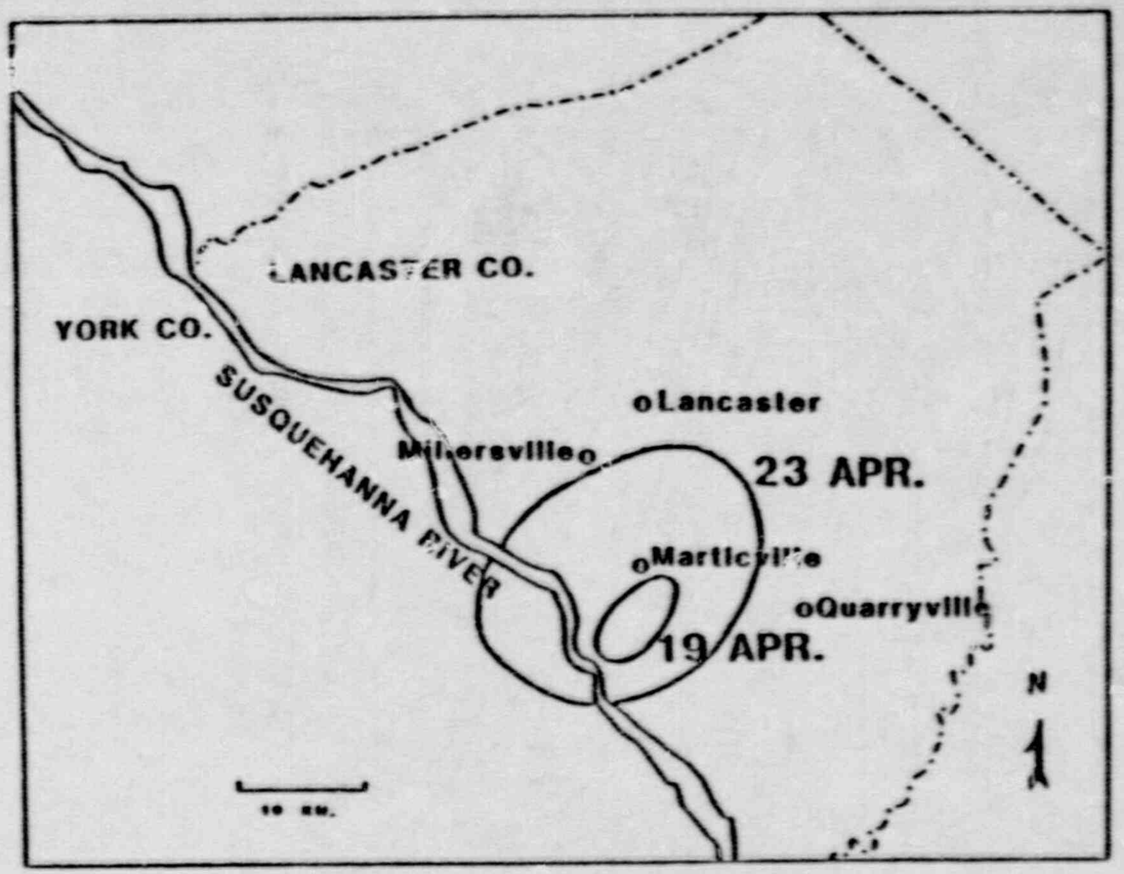

AREAS OF MAX. INTENSITY

FIGURE 25 Areas of maximum intensity for the April 23, 1984 mainshock (MM = V-VI) and the April 19, 1984 foreshock (MM = IV). (after Scharnberger & Howell, 1985)

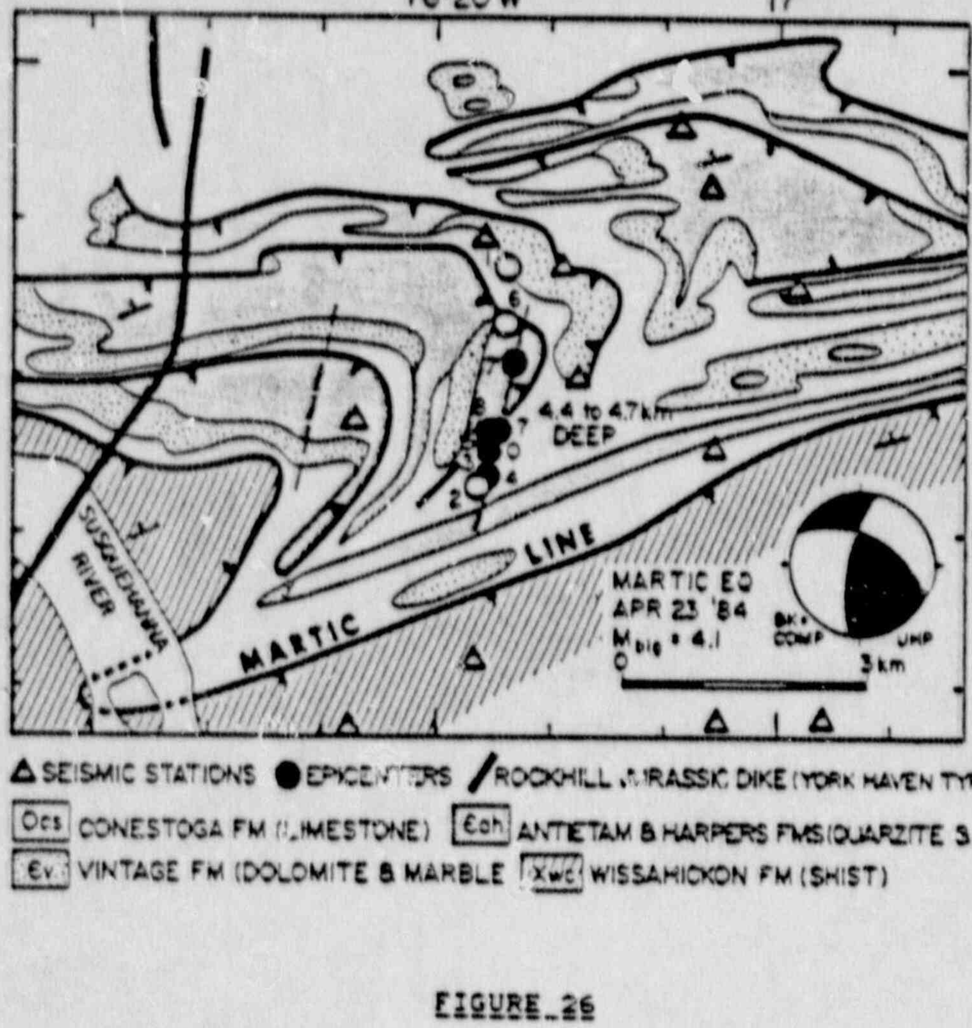

FIGURE 26

Map of the location of the aftershocks for the April 23, 1984 earthquake, and their relation to the geological structures within the area. Inserted is the fault plane solution with the preferred plane striking NNE, parallel to the line of aftershocks The dashed line is the surface trace of this plane. (modified after Armbruster & Seeber, 1985).

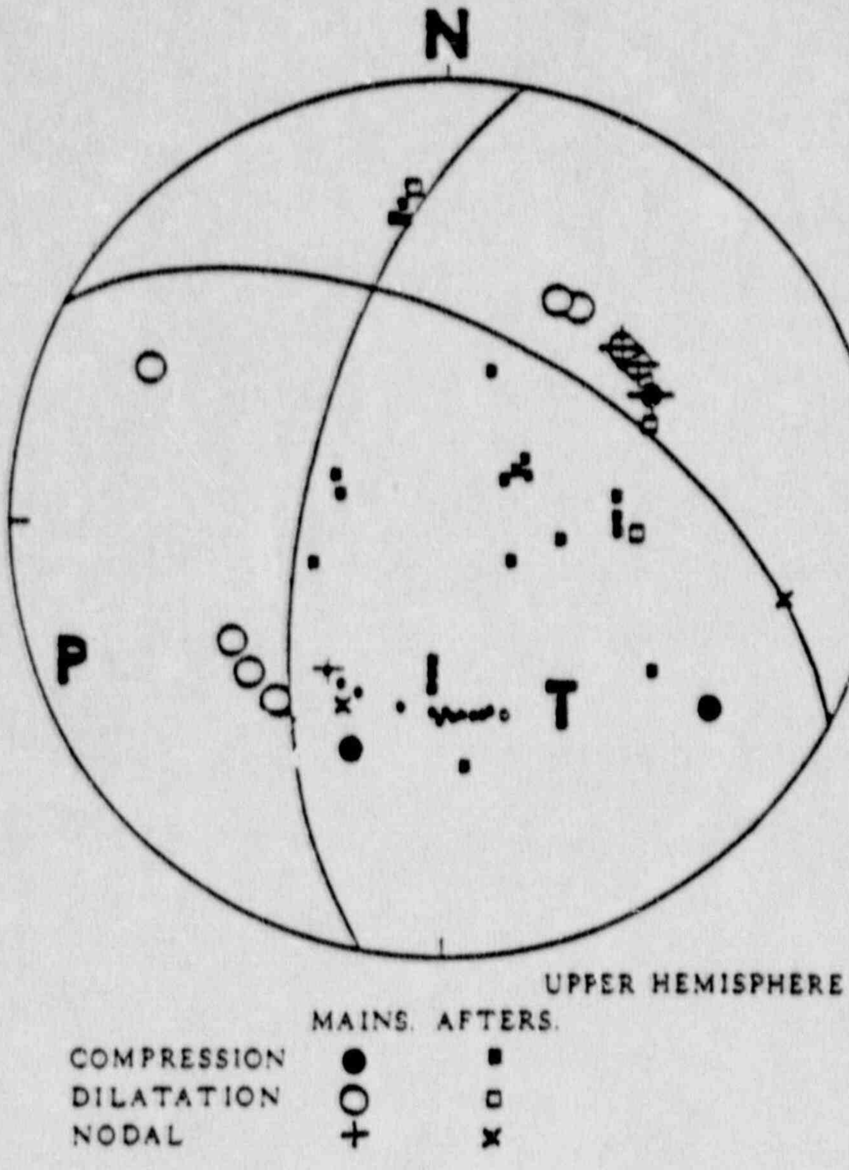

FIGURE 27 Fault plane solution based on the first motion data from the April 23, 1984 earthquake and its aftershocks. The smaller circles represent 20 first motions for the mainshock, as recorded by the N.E. U.S. Seismic Network.

LOCATION OF THE APRIL, 1984 FORESHOCK AND MAINSHOCK

As the intensity data suggest (Figure 25), the foreshock of April 19, 1984 was centered several kilometers south of the mainshock of April 23 (Scharnberger and Howell, 1984). Furthermore, the epicenter, obtained from the intensity data for the mainshock, fell 2 km SE of the aftershock zone (Armbruster and Seeber, 1985).

In order to verify the locations of the foreshock and the mainshock, the hypocenter location program, HYPOINVERSE (Klein, 1978; Lahr, 1980) was used. The travel time data for various stations in New York, New Jersey, Delaware, and Virginia were used for the mainshock locations and data from Pennsylvania and New Jersey stations were used for the foreshock location.

To reinforce the validity of the results obtained by HYPOINVERSE, a relative location algorithm (Baumgardt, D.R., 1977 & 1985) was applied. The HYPOINVERSE mainshock location was used to predict the foreshock location. The location error for the HYPOINVERSE program is given by a 95% confidence ellipse. The location error of the relative location program is about -2 km or less, which is based on the use of this program in the location of the two 1978 Lancaster earthquakes (see Historical Seismicity) (Alexander, personal communication).

In order to utilize the HYPOINVERSE and the relative location algorithms, one needs a body wave, regional, crustal velocity model. Several velocity models for the Pennsylvania area and for the Piedmont geological province have been published, among them: Katz, 1955; Birch, 1961; Abriel, 1978; Isaacs, 1979; Sienko, 1982; and Bollinger and Sibol, 1985. Of these various velocity models, the ones which best located the Lancaster, April 23, 1984 mainshock, in relation to the felt area shown by the intensity maps (Figure 25), were the following:

Lancaster Model I (Alexander, 1984)	V_p(km/s)	V_s(km/s)	thick.(km)
	6.1	3.55	18
	6.75	3.92	22
	8.1	4.71	

Lancaster Model II (Sienko, 1982)	V_p(km/s)	V_s(km/s)	thick.(km)
	6.1	3.55	28
	6.75	3.92	12
	8.1	4.71	

Bollinger Model (Bollinger & Sibol, 1985)	V_p(km/s)	V_s(km/s)	thick.(km)
	6.09	3.53	15
	6.50	3.79	16
	8.18	4.71	

The Lancaster I and Lancaster II velocity models vary only in the thickness of the two crustal layers. The Lancaster I model uses a thinner upper layer relative to the lower layer, and the Lancaster II model has a thicker top layer.

The results of the HYPOINVERSE algorithm and the relative location algorithm are seen in Figure 28 and listed in Table 6.

The absolute locations (HYPOINVERSE) for the mainshock indicate that it was located in the same area as the aftershocks of Figure 28. The velocity model of Bollinger and Sibol (1985) for the Piedmont and the Lancaster I velocity model (Alexander, 1984) located the mainshock in the center of the maximum intensity area of Scharnberger and Howell (1984) (Figure 28). The Lancaster II velocity model (Sienko, 1982) located the event too far north relative to the intensity data (Figure 28). The 95% confidence ellipse for these locations had a N-S axial length of less than 3 km and an E-W axial length of less than 2 km (Figure 28; Table 6).

The absolute location (HYPOINVERSE) for the foreshock is approximately 10 km south of the mainshock and the aftershocks (Figure 28). This more southern location of the foreshock is also indicated by the intensity data (Figure 25). Based on these intensities, Scharnberger and Howell (1984) concluded that the foreshock is "centered several kilometers south of the mainshock". The Lancaster I and the Lancaster II velocity models used in the HYPOINVERSE algorithm result in foreshock locations on the southern part of the maximum intensity area (Figure 28) near Holtwood, Pennsylvania. The error ellipses for these two locations had a N-S axis less than 11 km in length and an E-W axis of less than 6 km in length. The increased size of these 95% confidence ellipses relative to those of the mainshock, is primarily due to the fact that a smaller number of stations was used in the foreshock location than in the mainshock location. The Bollinger velocity model failed to predict a satisfactory solution relative to the intensity data.

The relative location algorithm, which located the foreshock relative to the HYPOINVERSE mainshock location for each velocity model, also indicates that the foreshock was located several kilometers south of the mainshock and aftershock zone. Like the absolute location (HYPOINVERSE) for the foreshock, the relative locations also fell in the Holtwood area. The two solutions for the two methods, and their error bars, overlap (Figure 28). Thus, within the error margins, the solutions are nearly identical. The Lancaster II model gave a foreshock solution which was too far south relative to the intensity data.

Therefore, in summary, the location of the April 1984 seismicity is as follows. The absolute locations (HYPOINVERSE) indicate that the mainshock is centered near Marticville (in the area of the aftershocks), and that the foreshock is centered 10 km south. The results of the relative location algorithm for the two events confirm this as do the maximum intensity locations of Scharnberger and

Howell, (1984). All the events, the foreshock of April 19, the mainshock of April 23, and the aftershocks recorded by Armbruster and Seeber (1985), fall along the projected continuation of the N-S striking Fruitville fault zone, which outcrops near the city of Lancaster. The closest geologically mapped outcrops of this fault are approximately 10 km north of the Marticville, mainshock location (Figure 28).

Finally, of the three crustal velocity models used, the ones with the thinner upper velocity layer, the Lancaster I and the Bollinger models, performed better in establishing locations which agreed with the intensity data, than did the Lancaster II model with the thicker upper velocity layer (Figure 28, Table 6)

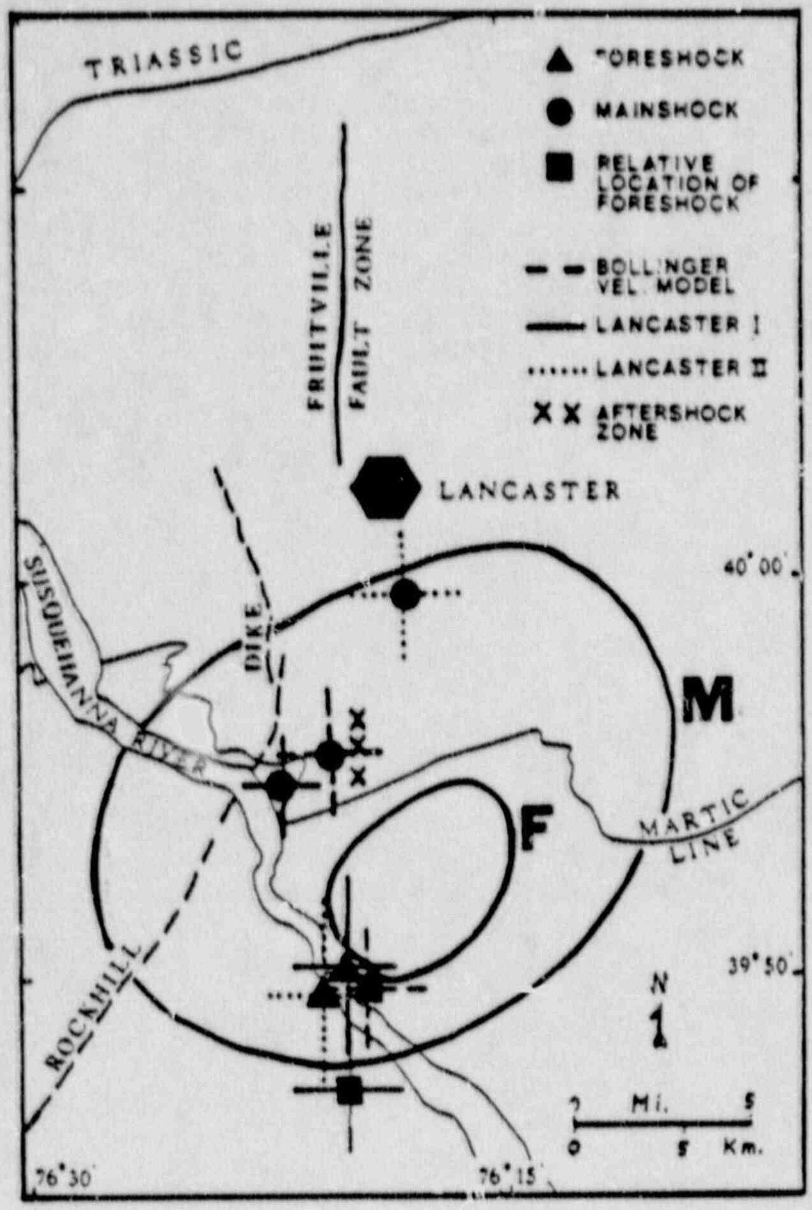

FIGURE 28 Map of the absolute and Relative locations for the April 23, 1984 mainshock and the April 19, 1984 foreshock, using three different velocity models. Error bars are included (see Table 6). he two large circles indicate the maximum intensity rees of the two events ('M' is for the mainshock & F' is for the foreshock) as obtained by Schernberger and Howell (1985), see Figure 25.

TABLE 6

ABSOLUTE (HYPOINVERSE) AND RELATIVE LOCATIONS FOR THE APRIL 23, 1984 MAINSHOCK AND THE APRIL 19, 1984 FORESHOCK

Velocity Model	Location Lat. Long. (Deg.)	Depth (km.)	Error Ellipse Axes (95% certainty) Length of Axis (km.) Azimuth (Deg.) Dip (Deg.)		
ABSOLUTE LOCATION OF MAINSHOCK					
Lancaster I	39 54.56' 76 23.92'	7.12	1.94 0 0	1.54 275 30	5.22 103 74
Lancaster II	39 59.76' 76 18.11'	7.09	2.71 0 0	0.70 275 20	4.49 244 65
Bollinger	39 56.48' 76 20.53'	5.49	2.42 0 0	1.66 268 32	6.38 124 65
ABSOLUTE LOCATION OF FORESHOCK					
Lancaster I	39 50.29' 76 20.74'	4.93	10.32 0 0	3.37 256 7	16.42 57 70
Lancaster II	39 43.36' 76 21.39'	4.94	6.98 0 0	2.98 270 19	31.06 292 85
Bollinger	-- NO GOOD --				
RELATIVE LOCATION OF FORESHOCK					
Lancaster I	39 47.4' 76 32.2'	4.8	error approx. ~ 2 km in the epicentral location (Alexander, personal communication)		
Bollinger	39 49.2' 76 19.2'	4.7			
Lancaster II	-- NO GOOD --				

DE... F THE APRIL 23, 1984 MAINSHOCK THROUGH CEPSTRAL ANALYSIS

The April 23, 1984 earthquake offered an ideal opportunity to test the use of cepstra in identifying P-pP and P-sP arrival time delays, and, thus, predicting a depth for the event, using previously established body-wave, crustal velocity models. The aftershocks of the April 23, 1984 event, which occurred in the same location as the mainshock and predicted the same fault plane solution (Armbruster and Seeber, 1985) as the mainshock, indicated a depth of 4.4-4.7 km. As shown above and in Table 6, the absolute location algorithm, HYPOINVERSE (Klein, 1978; Lahr, 1980), and the relative location algorithm (Baumgardt, D.R., 1977 & 1985) for the mainshock, also indicated a shallow event. Therefore, the mainshock's hypocenter is well-constrained to a depth of 4-5 km. The cepstral analysis of 17 seismograms for the April 23, 1984 mainshock, received at 13 stations operated by Woodward-Clyde Consultants in the New York State area (Figure 29, Table 7), was conducted in order to try to obtain an independent depth estimate for the event.

Theory of Depth Determination through Cepstral Analysis

The following is an overview of the cepstral theory, and its use for depth estimation. It is especially useful for shallow earthquakes where the pP and sP phases are not obvious by inspection of the seismogram (Bogert, 1963).

Let $z(t)$ be a time signal composed of the direct P-wave arrival $f(t)$ plus a pP and a sP phase, delayed by Tp and Ts, respectively.

$$z(t) = f(t) + A\,f(t-T_p) + B\,f(t-T_s) \qquad \text{C-1}$$

where $T_p = t_{pp} - t_p$ or the difference in the arrival times of the pP and P phases,
and where $T_s = t_{sp} - t_p$ or the difference in the arrival times of the sP and P phases,
and where A and B are scaling constants ($-1 \leq A, B \leq 1$).
Take the Fourier Transform of the time series to obtain:

$$F.T.(z(t)) = Z(w) = \int_{-\infty}^{\infty} z(t)e^{-iwt}\,dt$$

$$= F(w)\{1 + Ae^{-iwT_p} + Be^{-iwT_s}\} \qquad \text{C-2}$$

where $F(w)$ is the spectrum of $f(t)$.

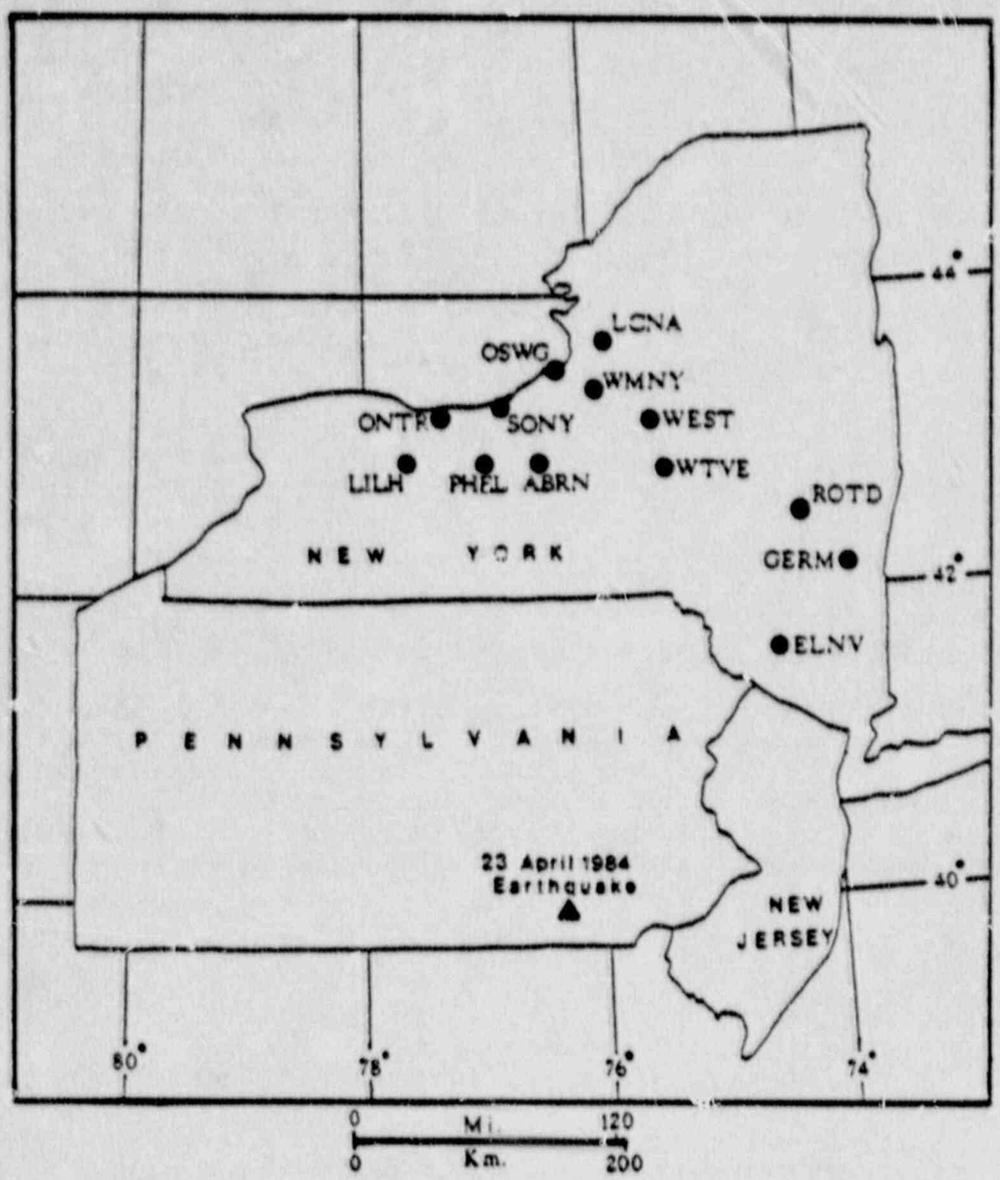

FIGURE 29 Location of the N.E. U.S. Seismic Network stations used in the cepstral analysis of the April 23, 1984 earthquake. These stations are operated by Woodward-Clyde Consultants, of Wayne, N.J. (modified after Woodward-Clyde Consultants, 1985)

TABLE 7

COORDINATES OF THE SEISMIC STATIONS USED IN THE CEPSTRAL ANALYSIS

Station ID	Latitude (Deg.)	Longitude (Deg.)	Elevation (meters)	Location
ABRN	42.9963 N	76.4853 W	224	AUBURN, NY
ELNV	41.5000 N	74.4398 W	323	ELLENVILLE, NY
GERM	42.1570 N	73.8113 W	88	GERMANTOWN, NY
LCNA	43.6442 N	75.9260 W	396	LACONA, NY
LILH	42.9213 N	77.6172 W	122	LIMA, NY
ONTR	43.2738 N	77.3067 W	84	ONTARIO, NY
OSWG	43.5170 N	76.4162 W	84	OSWEGO, NY
PHEL	42.9542 N	77.0950 W	188	PHELPS, NY
ROTD	42.9620 N	74.0872 W	283	ROTTERDAM, NY
SONY	43.1922 N	76.9647 W	122	SODUS, NY
WEST	43.1635 N	75.4800 W	167	WESTMORELAND, NY
WMNY	43.3560 N	76.0313 W	158	WEST MONROE, NY
WTVE	42.9460 N	75.3272 W	426	WATERVILLE, NY

(after Foley, et al., 1984)

The power spectrum is:

$$P(w) = Z(w)\, Z(w)^* = |Z(w)|^2 \qquad \text{C-3}$$

$$= |F(w)|^2 \{1 + A^2 + B^2 + Ae^{+iwTp} + Ae^{-iwTp}$$

$$+ Be^{+iwTs} + Be^{-iwTs} + ABe^{-iw(Ts-Tp)}$$

$$+ ABe^{+iw(Ts-Tp)}\}$$

where $Z(w)^*$ is the complex conjugate of $Z(w)$.

From equation C-3, it is apparent that if Tp, for example, equals 2 sec., the power spectrum peaks for the Tp delay times will have a periodicity of 0.5 Hz.

The logarithm of the power spectrum is not taken in the cepstral analysis applied here. This whitening of the spectrum ideally should increase the number of 'cycles' of the sought-after modulation pattern in the cepstrum by converting the multiplicative terms of equation C-3 to additive terms. However, for a practical case of a 'noisy' spectrum, it increases the number of weaker periodicities (Cohen, 1970). Thus, it has the negative aspect of creating additional harmonics that are introduced by the sharpening of the spectral nulls (Kemerait and Sutton, 1982). The cepstrum of the logarithmic power spectrum was tried for several seismograms of the April 23, 1984 event, but as in the case of Kemerait and Sutton (1982), the additional harmonics created obscured the results. Thus, best results were obtained when the simple power spectrum was used in the cepstral analysis.

The cepstrum was obtained by taking the Fourier Transform of the simple power spectrum:

$$\text{F.T.}(P(w)) = C(u) = \int_{-\infty}^{\infty} P(w)\, e^{-iwu}\, dw \qquad \text{C-4}$$

$$= (1 + A^2 + B^2)h(u) + Ah(u + Tp)$$

$$+ Ah(u - Tp) + Bh(u + Ts) + Bh(u - Ts)$$

$$+ ABh(u + (Tp - Ts))$$

$$+ ABh(u - (Tp - Ts))$$

where $\quad \text{F.T.}(|F(w)|^2) = h(u) \qquad \text{C-5}$

where u is the quefrency domain which is in seconds.

For only the positive values of quefrency (seconds), one gets the following equation for the cepstrum:

$$C(u) = (1 + A^2 + B^2)h(u) + Ah(u - Tp)$$
$$+ Bh(u - Ts) + ABh(u - (Ts - Tp)) \quad \text{C-6}$$

Thus, the cepstrum is a set of values in the quefrency (seconds) domain corresponding to the P-pP and P-sP delay times as well as their differences.

The cepstral theory was tested on a time series which consisted of a simple cosine and a 2 second delayed smaller scaled cosine (see TEST in Figure 30), and on a time series which was composed of a repeating set of cosines (see TEST-R in Figure 30). When the cepstrum of the 2 sec delayed cosine of the 'TEST' signal was taken, the resultant cepstrum had a peak at 2.0 sec in quefrency (see TEST in Figure 31). This peak was equivalent to the 2.0 sec delay in the cosines of the time series (see TEST of Figure 30). When the cepstrum was obtained for the repeated cosines 'TEST-R', it revealed peaks at all four combinations of the delay times ie. 2 sec, 5 sec, 7 sec, and 9 sec (see TEST-R of Figure 31) between the cosine peaks of the original time series (see TEST-R of Figure 30).

In order to enhance the delay time peaks on the cepstrum relative to other information, or noise, the cepstra for all the stations were added together, and multiplied together. However, because the largest peak, which occurs at zero seconds of quefrency in each station's cepstrum, has no information on the delay times, it was removed from each case. This was done by setting the first 0.5 seconds of each cepstrum equal to zero. Then, each cepstrum was normalized so that the highest remaining peak was equal to one. After this, the cepstra for all the stations were summed along quefrency in one case, and multiplied along quefrency in the second case. The resultant peaks should occur at quefrency seconds equal to the pP-P and the sP-P delay times and/or their sums and differences.

These delay times can be used to estimate the depth of the earthquake given a crustal velocity model for the area. The above steps are performed on each seismogram. If all the stations are at regional distances, say within 500 km of the earthquake epicenter, the pP-P and the sP-P delay times can be assumed to be the same for each station, since the distance the ray travels is about the same for each station.

Application and Results

The theory and procedures, mentioned in the previous section, were used in order to determine the depth of the

April 23, 1984 earthquake in Lancaster, Pennsylvania. A set of seismograms from 13 stations of the N.E. United States Seismic Network's Mid Hudson Area Network and North Central Area Network were used for the cepstral analysis of the event. All these stations are located in New York State (Figure 29, Table 7), and operated by Woodward Clyde Consultants (Woodward Clyde Consultants, 1985). They are all within 500 km of the Lancaster earthquake.

The first 40 seconds of the seismograms for the April 23, 1984 event are shown for each station in Appendix 2. The ONTR station of Ontario, N.Y. and the OSWG station of Oswego, N.Y. have all three components of the seismogram (ONTR & OSWG = radial, ONTR2 & OSWG2 = tangential, ONTR3 & OSWG3 = vertical). The remaining stations have only the vertical component of the data (Appendix 2).

The power spectrum of each seismogram was taken at three different time windows. The first time window was only in the noise interval of the time series, before the first P arrival. The noise energy spectrum was smoothed over a 5 sec interval and normalized through division by the time domain window length to obtain the power spectral density (PSD). The resulting PSD's were plotted as the dashed lines in the plots of Appendix 3. Furthermore, the signal from each station was windowed at a 10 sec and a 20 sec time window (listed in Appendix 3). The energy spectra, thus obtained, were normalized through division by the 10 sec and the 20 sec time windows, respectively, in order to produce the PSD. The resulting PSD's for each seismogram are shown in the top and bottom plots of Appendix 3. All the plots for a given station are normalized relative to the largest value present within both the pure noise, and the two windowed signal and noise PSD's. It is worth noting that the amplitude of the noise PSD is low relative to that of the windowed signal and noise PSD in all cases (Appendix 3). Although for some stations (ABRN, GERM, & LCNA) the magnitude of the noise spectrum is significant in frequency band less than 1.0 Hz, it is worth noting that the PSD of most of the windowed signals have a clear periodicity of 0.5 Hz. This is due to the periodicity of the cosine components of equation C-3 in the previous section. This suggests a dominant P-pP or P-sP delay time of about 2 sec within most of the time series used.

After the two windowed PSD's are obtained for each of the seismograms, they are windowed in the frequency band where the magnitude of the PSD of the noise relative to that of the signal is minimal. These frequency windows are listed in Appendix 4. As in the case of windowing in the time domain, above, all the frequency windows are padded with zeros to an equal length, which is a power of 2 and is larger than the widest sampling window used, before they are Fourier transformed. Furthermore, a 10% taper is applied to both ends of each sampling window, in time and in frequency, before Fourier transforming. After Fourier transforming from the frequency domain, one obtains the cepstra in the quefrency domain (seconds) for each station. They are plotted in Appendix 4. The top plot in Appendix 4, for each station, is the cepstrum of the 10 sec time windowed signal and noise, and the bottom plot is the cepstrum of the 20 sec time windowed signal and noise.

After analyzing the cepstral plots of Appendix 4, it is difficult to pick out dominant peaks that are common to all the stations. In order to get a better idea of these peaks, the sum and the product of the cepstra of all the 20 sec time windowed signals are computed. The cepstra of the larger windowed signals are chosen since they include substantial cepstral peaks beyond the quefrency of 2 sec. Therefore, they contain information on longer delay times than the cepstra of the 10 sec time windowed signals. In fact, the 10 sec time window appears to be too small for obtaining cepstral peaks above 1.5-2.0 sec in quefrency, and, thus, delay times longer than 1.5-2.0 sec.

Because the largest peak in each station's cepstrum, which occurs at zero seconds in quefrency (Appendix 4), has no information on the delay times, it is removed in each case. This is done by setting the first 0.5 sec of each cepstrum equal to zero. Then, in order to equally weight the input of each station, the remaining maximum peak of each station's cepstrum is normalized to 1.0. Following this, the cepstra of all 17 seismograms are summed (top plot of Figure 34) and multiplied (bottom plot of Figure 34). The same is done for the cepstra of the "Best Six" original seismograms (ABRN, ELNV, ONTR3, PHEL, ROTD, SONY). The "Best Six" seismograms were chosen based on the clarity of the two P phase arrivals on the trace. They all appear to have a time lag of approximately 2.0 sec (Appendix 2). They act as a check of the cepstrally defined time lags for the two P phases. The sum and the product of the cepstra of these "Best Six" seismograms are shown in Figure 32. Both plots indicate a peak centered at 1.9 sec in the quefrency domain.

The same approach used for the "Best Six" cepstra, above, was applied to the "Best Twelve" cepstra ("Best Six" plus GERM, LILH, ONTR, ONTR2, OSWG, OSWG3). The "Best Twelve" cepstra were chosen because they are dominated by a few large, low frequency peaks, rather than many small, high frequency ones. The sum and the product of the "Best Twelve" cepstra are plotted in Figure 33. The sum, and especially the product, show one dominant peak. This time it is centered at about 1.95 sec, or 0.05 sec higher in the quefrency domain than the peak for the "Best Six" cepstra.

Finally, when the sum and product of all the stations' normalized cepstra is taken, one obtains the results of

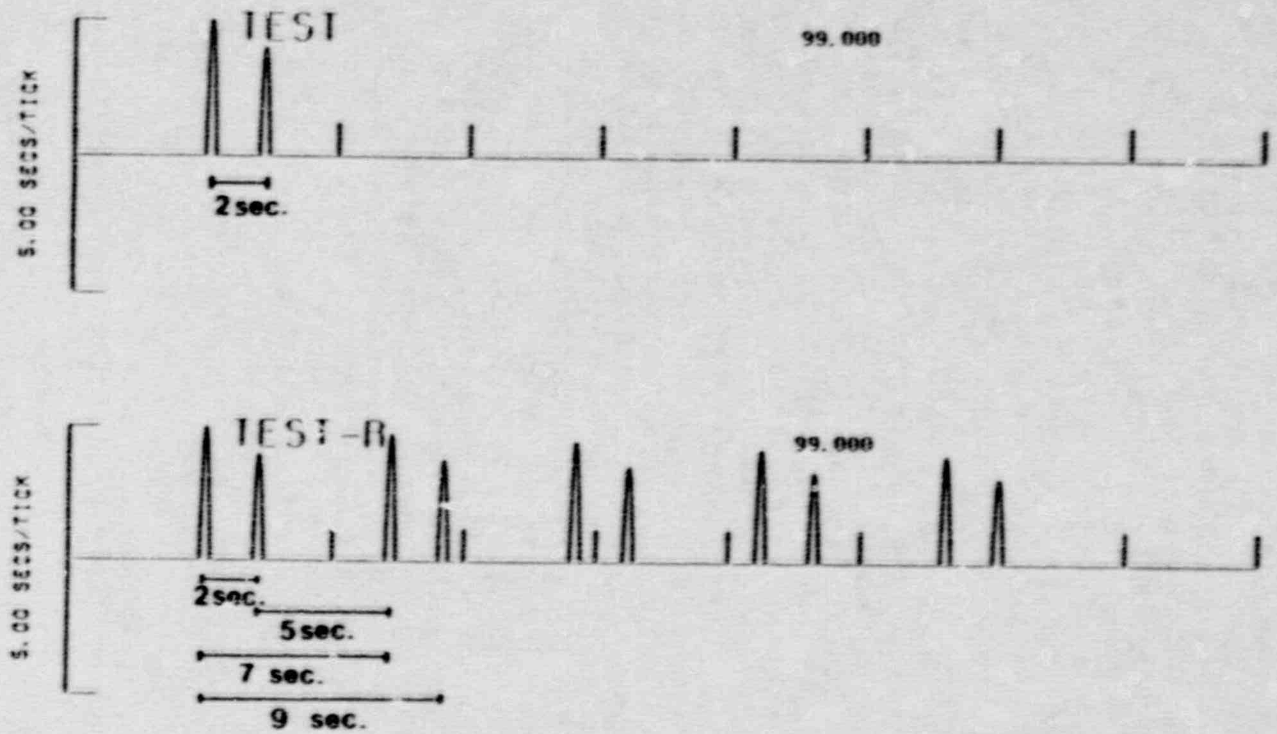

FIGURE 30 Test signal TEST and repeated test signal TEST-R.

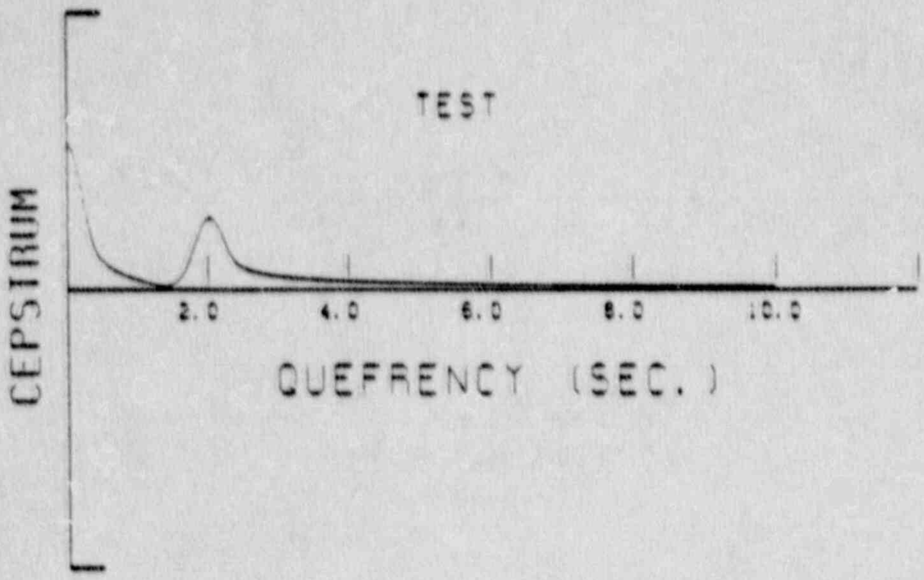

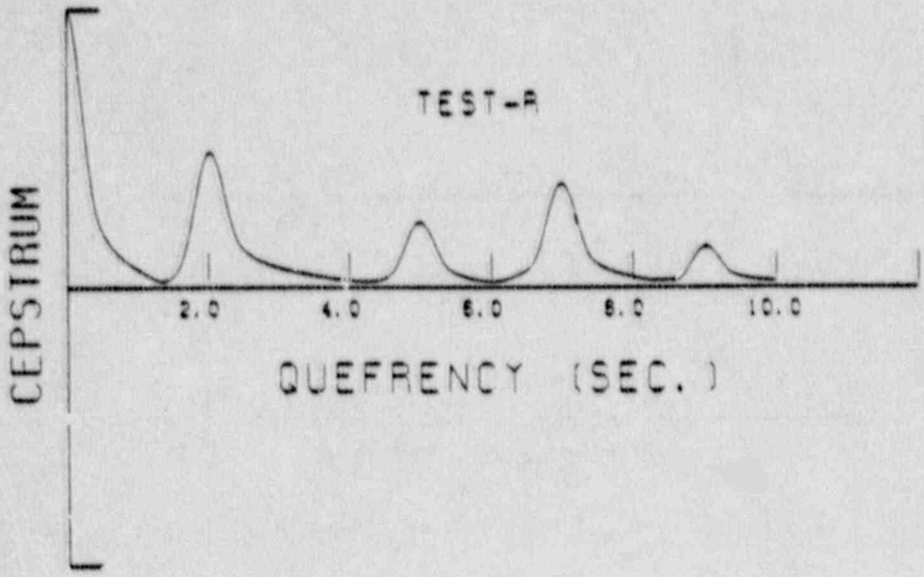

FIGURE 31 Cepstra of test signal TEST and repeated test signal TEST-R.

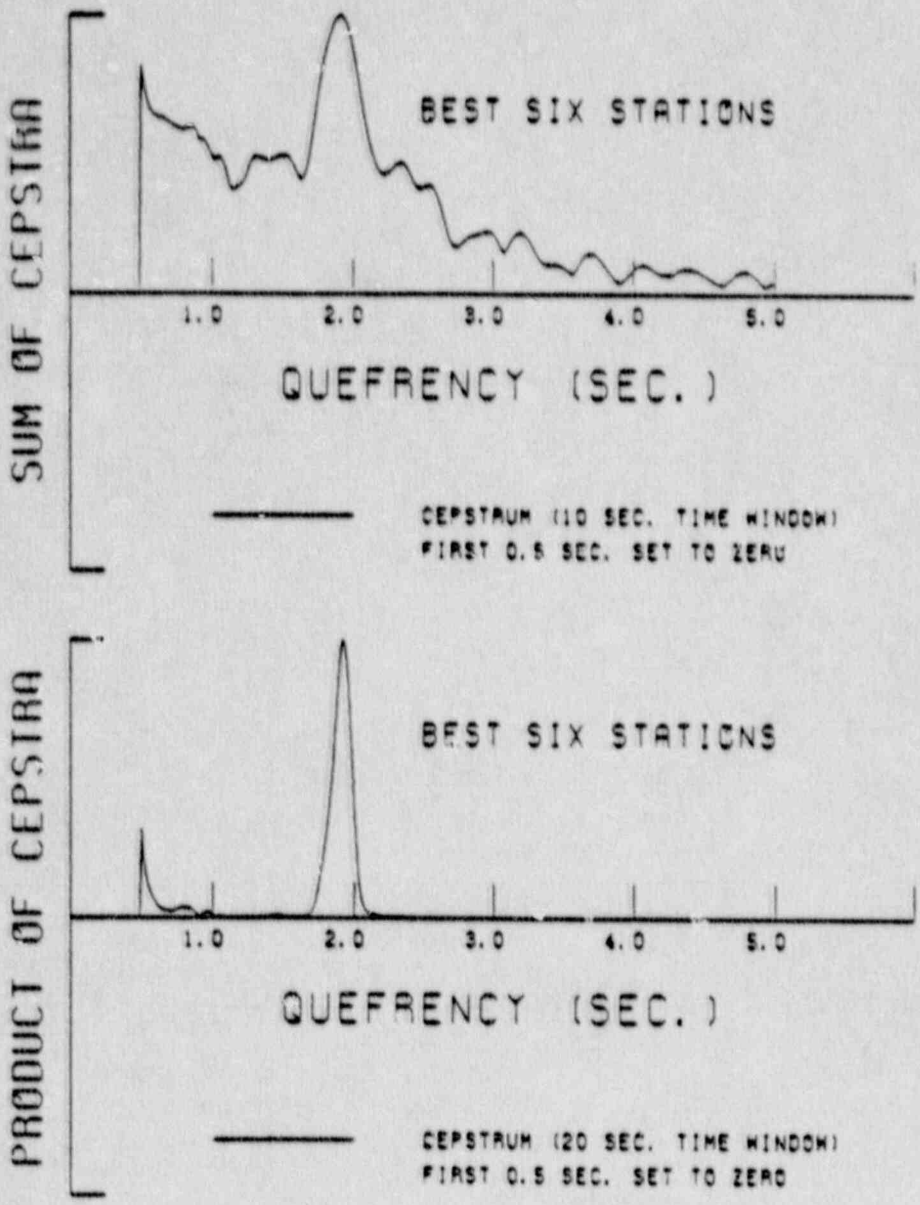

FIGURE 32 The sum and the product of the cepstra for the "Best Six" stations which recorded the April 23, 1984 event.

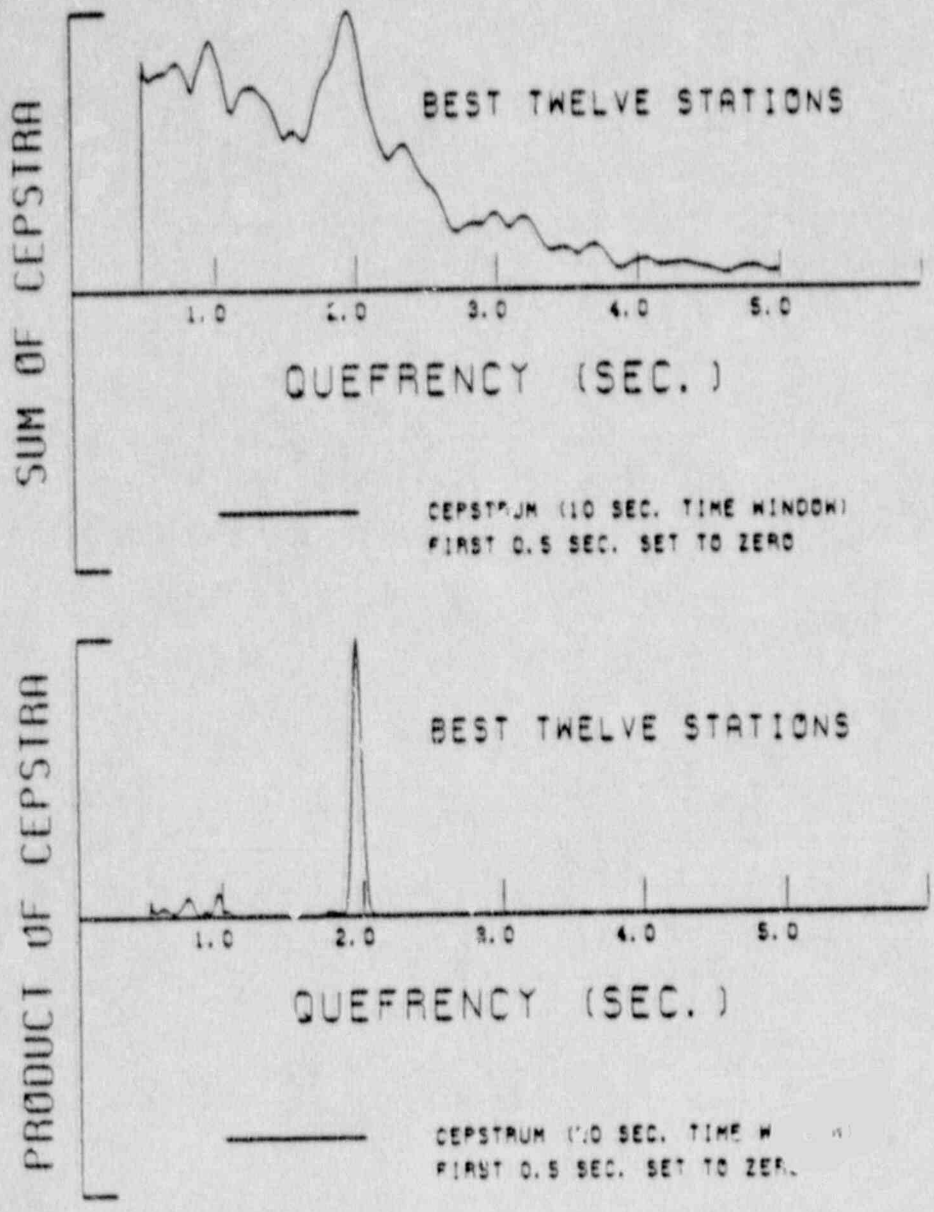

FIGURE 33 The sum and the product of the cepstra for the "Best Twelve" stations which recorded the April 23, 1984 earthquake.

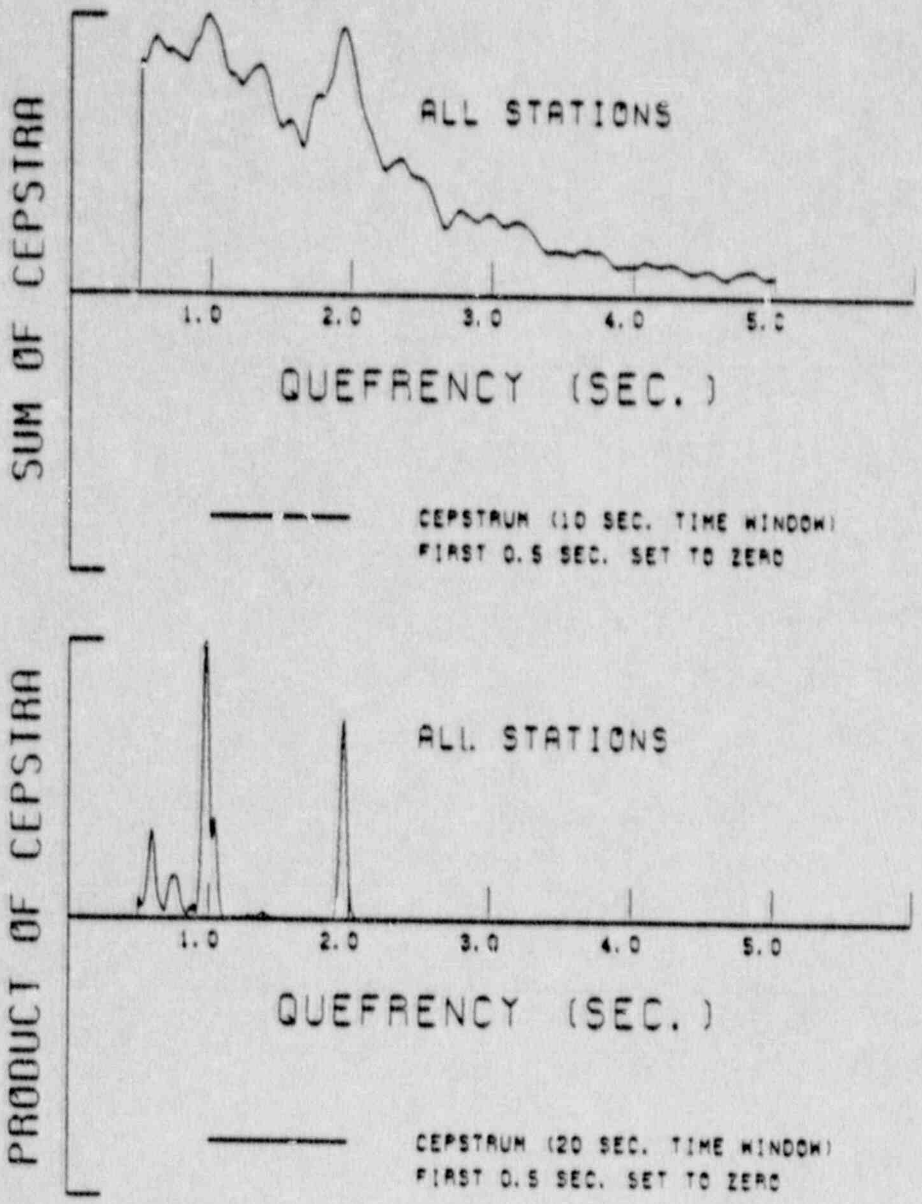

FIGURE 34 The sum and the product for all the stations used in the cepstral analysis of the April 23, 1984 earthquake.

Figure 34. It is clear that the plots of Figure 34 are double peaked. The peak at 1.95 sec remains, and a second peak appears at approximately 1.0 seconds in the quefrency domain.

In order to evaluate these cepstral peaks, and the lag times they may represent, we must determine the presence and the relative significance of the pP and the sP arrivals at the stations used in the cepstral analysis (Figure 29). Thus, we must calculate the relative displacements and the lag times for the P, pP, and sP arrivals at each station.

The distance of the stations, in Figure 29, from the epicenter of the April 23, 1984 earthquake is between 250 km (2.25 degrees) and 450 km (4.05 degrees), and the event is at a depth of 4.0 - 5.0 km, based on aftershock data (Armbruster and Seeber, 1985). This is well within the top, 8 km, Paleozoic layer. Thus, we may apply the equations for cylindrical displacements at teleseismic distances for a point source dislocation arbitrarily oriented in a halfspace, as given by Langston and Helmberger (1975). The total vertical displacement of the P-wave is:

$$W = Rpz\ \{U_p(t)+Rpp*U_p(t-dt_1)+(Rsp*(n_p/n_s)) * U_s(t-dt_2)\} * S(t) * I(t) * Q(t) \qquad \text{R-1}$$

where S(t), I(t), and Q(t) represent the far field source time function, instrumental response, and attenuation operator, respectively.

Since only the relative magnitudes of the displacement for the P, pP, and sP -waves are of interest at each station, the above equation (R-1) may be broken down into the P, pP, and sP far-field displacement components. Thus, the S(t), I(t), Q(t), and Rpz (receiver function) are not considered, and the relative displacement for the direct P-wave (Wp) is given by the following equation:

$$Wp = U_p \quad , \qquad \text{R-2}$$

where U_p is the P-wave displacement potential:

$$U_p = M_o/(4\pi\rho) * \sum_{i=1}^{3} A_i(s,r,d) * C_i * \{H(t-R/V_p)/R\} \qquad \text{R-3}$$

where V_p is the P-wave velocity.
The relative displacement for the pP-wave is:

$$Wpp = Rpp * U_p(t - dt_1) \quad , \qquad \text{R-4}$$

where U_p is the same as above, and dt_1 is the time lag of the pP arrival relative to the direct P arrival. This time lag is given by:

$$dt_1 = 2*h*n_p \quad , \qquad R\text{-}5$$

where h is the depth of the event and n_p is the slowness for the P-wave, as defined below. Finally, the relative displacement for the sP-wave is:

$$Wsp = Rsp * (n_p/n_s) * U_s(t - dt_2) \quad , \qquad R\text{-}6$$

where U_s is the SV-wave displacement potential:

$$U_s = M_0/(4\pi\rho) * \sum_{i=1}^{3} A_i(s,r,d)*SV_i*\{H(t-R/V_s)/R\}, \qquad R\text{-}7$$

and V_s is the S-wave velocity and dt_2 is the time lag of the sP arrival relative to the direct P arrival. It is given by:

$$dt_2 = h*(n_p + n_s) \qquad R\text{-}8$$

where h is the depth and n_p and n_s are the slowness for the P and S -waves, respectively.

Since we are concerned with only the magnitudes of the relative displacements, the displacement potentials of equations R-3 and R-7 become:

$$U_p = \sum_{i=1}^{3} A_i(s,r,d)*C_i \qquad R\text{-}9$$

and

$$U_s = \sum_{i=1}^{3} A_i(s,r,d)*SV_i \qquad R\text{-}10$$

respectively. The three terms in the summation i = 1,2,3 represent the fundamental dislocation terms, vertical strike-slip, vertical dip-slip, and a 45 degree dipping dip-slip. The $A_i(s,r,d)$ describe the horizontal radiation pattern, and they are given by:

$$A_1(s,r,d) = \sin(2s) * \cos(r) * \sin(d) + 0.5 * \cos(2s) * \sin(r) * \sin(2d) \qquad R\text{-}11$$

$$A_2(s,r,d) = \cos(s) * \cos(r) * \cos(d) - \sin(s) * \sin(r) * \cos(2d) \qquad R\text{-}12$$

$$A_3(s,r,d) = 0.5 * \sin(r) * \sin(2d) \qquad R\text{-}13$$

where,

s = strike from the end of the fault plane
r = rake angle measured from the horizontal upward
d = dip angle of the fault.

The C_i and SV_i describe the vertical radiation pattern for the P and SV-wave potentials, respectively.

$C_1 = -p^2$ $\qquad$ $SV_1 = -E*p*n_s$

$C_2 = 2*E*p*n_p$ $\qquad$ $SV_2 = (n_p^2 - p^2)$

$C_3 = (p^2 - 2*n_p^2)$ $\qquad$ $SV_3 = 3*E*p*n_s$

where,

$$E = \begin{cases} +1 & z > h \quad \text{(down-going ray)} \\ -1 & z < h \quad \text{(up-going ray)} \end{cases}$$

V_p = compressional velocity at the source
V_s = shear velocity at the source
p = $\sin(i)/V_p$ = ray parameter
i = incidence angle
$n_v = \{(1/v^2) - p^2\}^{1/2}$

M_o is the seismic moment, ρ is the density, and 1/R is the geometric spreading factor. In the relative magnitude calculations for the displacements, these three factors are left out of the potential equations R-9 and R-10.

Rpp and Rsp are the P -> P and S -> P free surface reflection coefficients, respectively. The two dimensional Cartesian reflection coefficients are given as:

$$Rpp = \frac{4*n_p*n_s*p^2 - (n_s^2 - p^2)^2}{4*n_p*n_s*p^2 + (n_s^2 - p^2)^2} \qquad \text{R-14}$$

and

$$Rsp = \frac{-4*n_s*p*\,(n_s^2 - p^2)}{4*n_p*n_s*p^2 + (n_s^2 - p^2)^2} \qquad \text{R-15}$$

The study assumes a homogeneous source structure, and is only concerned with the far-field medium response for the P-wave.

In order to determine the P, pP, and sP displacements at the various stations used in the cepstral analysis, we must obtain the incidence angle for the P, pP, and sP -waves, the velocity structure, the fault plane orientation, the station locations, and estimate the depth. Let us first look at the incidence angles and the velocity structure.

The distance of the stations from the epicenter of the April 23, 1984 earthquake is between 250 km (2.25 degrees) and 450 km (4.05 degrees) north. At this distance, the Pn-wave, refracted from the Mohorovicic discontinuity, is the first arrival according to the Herrin tables of P-wave travel times (Herrin, et al., 1968).

The best fitting velocity model, based on the location results above, is the Lancaster I velocity model. This model predicts a depth of 40 km to the Mohorovicic discontinuity, and an average P-wave velocity of 8.1km/sec below it. In the top crustal layer, the source layer, this model predicts an S-wave velocity of 3.5 km/sec. Furthermore, Abriel (1978) and Sienko (1982), both assign a P-wave velocity of 5.0 km/sec to the top 8 km of Paleozoic rocks in the Lancaster, Pennsylvania region.

Using these velocities, and Snell's Law, we can find the ray parameter and the incidence angle of the ray which critically refracts at the Mohorovicic discontinuity.

$$p = 1/V_m = \sin(i_1)/V_p \qquad \text{R-16}$$

where p is the ray parameter, and is constant for all the velocity layers. V_m is the P-wave velocity below the Moho, and V_p is the P-wave velocity at the source. Using the above expression and the above values for the velocities, we obtain the following incidence angle for the Pn-wave:

$$i_1 = \sin^{-1}(V_p/V_m) = \sin^{-1}(5.0/8.1)$$

$$= 38.1^\circ \qquad \text{R-17}$$

This incidence angle is the same for the pP ray, which originates in the upper hemisphere of the focal sphere.

Likewise, the incidence angle for the sP ray can be derived through Snell's Law using the P-wave velocity (V_p) and the S-wave velocity (V_s) for the Paleozoic source layer, as given above.

$$p = \sin(i_1)/V_p = \sin(i_2)/V_s \quad , \qquad \text{R-18}$$

where p is the ray parameter, and i_1 and i_2 are the incidence angles for the P and S-wave, respectively. Solving for i_2:

$$i_2 = \sin^{-1}(V_s * p) = 25.6^\circ \quad , \qquad \text{R-19}$$

one obtains an incidence angle of 25.6° for the sP ray.

Having obtained the incidence angles and the velocity structure, we must determine the fault plane orientation, the depth of the event, and the azimuth between this fault plane and each station.

The fault plane solution derived for the April 23, 1984 event by Armbruster and Seeber (1985) (Figure 27) indicates that the preferred fault plane strikes approximately N 10° E, dips about 60° E, and has a rake of 140°. The location of the earthquake is 39.94° N and 76.32° W, and the location of the seismic stations used in the cepstral analysis is given in Table 7. Using the N 10° E strike of the fault plane and the station locations, we calculate the azimuth between the fault plane and each station. These azimuths are shown in Table 8 for the New York State stations of Figure 29. They are measured from N 10° E in a clockwise direction. Finally, the depth of the April 23, event is estimated to be between 4.4-4.7 km based on aftershock data (Armbruster and Seeber, 1985). The depth of 4.5 km was used as a rough estimate of depth for the calculations.

The above strike and depth information, combined with the incidence angles, the velocity structure, and the fault plane orientation data, was applied to the equations of displacement listed above in order to predict the relative displacement magnitudes, and the time lags for the direct P, pP, and sP-waves on each station's vertical seismic record. These relative amplitudes and time lags are listed for each station in Table 9.

In Table 9, the 'RpP' column is the relative amplitude of the pP arrival with respect to the direct P arrival. The very small values of the relative pP amplitudes indicate that looking at the seismic records for the stations, we would not expect to pick out the pP phase for the April 23, 1984 earthquake. Plotting the azimuth and incidence angles for the pP rays, received at the 13 stations of Figure 29, on the fault plane solution, reveals that the pP rays originate on or very near a nodal plane (see the small squares in Figure 35). Therefore, again, we would not expect to see the pP phase on the seismic records. The direct P phase is expected to be apparent since most of the stations plot away from the nodal planes, and within the compressional quadrant (see the small circles in Figure 35). Comparing the values of the direct P-wave amplitudes ('AMP' column in Table 9) with their incidence locations on the fault plane solution (small circles in Figure 35), we can see that the stations closer to the nodal planes, such as GERM, ELNV, and ROTD have the smallest direct P-wave amplitudes, as expected if the fault plane solution is correct.

Although the pP phase does not appear to be very

TABLE 6

AZIMUTHS BETWEEN THE FAULT PLANE
OF THE APRIL 23, 1984 EARTHQUAKE AND THE
STATIONS USED IN THE CEPSTRAL ANALYSIS

Station ID.	Angle in degrees
ABRN	348
ELNV	23
GERM	25
LCNA	354
LILH	334
ONTR	339
OSWG	349
PHEL	341
ROTD	18
SONY	343
WEST	348
WMNY	354
WTVE	3

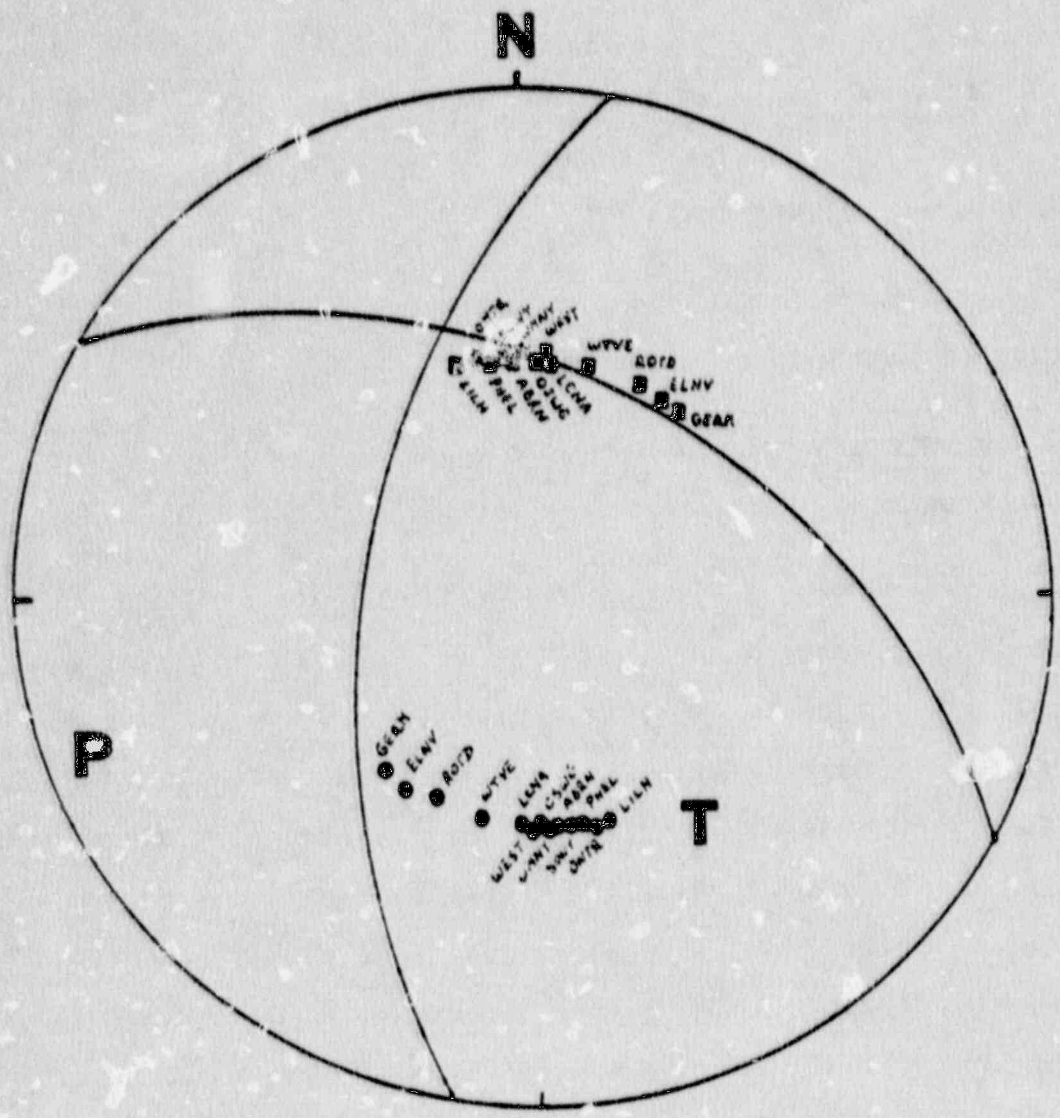

FIGURE 35 A plot of the incidence of the direct P rays (small circles) and the pP rays (small squares) received at the 13 stations used in the cepstral analysis, and superimposed on to the upper hemisphere fault plane solution for the April 23, 1984 mainshock.

TABLE 9

RELATIVE P, pP, & sP AMPLITUDE RESPONSES AND LAG TIMES
PREDICTED FOR THE THIRTEEN STATIONS OF TABLE 7
GIVEN THE FOLLOWING PARAMETERS:

FAULT PLANE ORIENTATION:
STRIKE = N 10° E   DIP = 60° E   RAKE = 140°

ESTIMATED DEPTH OF EVENT = 4.5 km.

INCIDENCE ANGLE OF P-WAVE = 38.12°

CRUSTAL VELOCITY MODEL:
P-WAVE VELOCITY (TOP LAYER) = 5.0 km/sec
S-WAVE VELOCITY (TOP LAYER) = 3.5 km/sec
P-WAVE VELOCITY (BELOW MOHO) = 8.1 km/sec

Station	RpP	RsP	dt1	dt2	AMP
ABRN	0.308E-03	1.48	1.42	1.87	-.347E-01
ELNV	-.730E-02	1.62	1.42	1.87	-.140E-01
GERM	-.823E-02	1.65	1.42	1.87	-.127E-01
LCNA	-.278E-0[illegible]	1.49	1.42	1.87	-.319E-01
LILH	0.926E-03	1 [illegible]	1.42	1.87	-.390E-01
ONTR	0.819E-03	1.46	1.42	1.87	-.378E-01
OSWG	0.225E-0[illegible]	1.46	1.42	1.87	-.343E-01
PHEL	0.742E-03	1.48	1.42	1.87	-.372E-01
ROTD	-.535E-02	1.57	1.42	1.87	-.173E-01
SONY	0.344E-03	1.48	1.42	1.87	-.366E-01
WEF[illegible]	0.308E-03	1.48	1.42	1.87	-.347E-01
WMNY	-.278E-03	1.49	1.42	1.87	-.319E-01
WTVE	-.159E-02	1.51	1.42	1.87	-.269E-01

significant on the seismic records, the relative amplitudes of the sP arrivals, column 'RsP' of Table 9, with values of 1.5 $\pm$ 0.2 observed for all the stations, indicate that the sP phase should be clearly present in all the seismic records. In fact, they should be approximately 1.5 times the amplitudes of the direct P-waves, whose values are listed in the column labeled 'AMP' in Table 9. Thus, the sP phase should dominate the seismic record in comparison with the pP phase, which is indistinguishable from the noise level at each station.

Furthermore, the time lags for the pP-P and sP-P phases have been predicted using equations R-5 and R-8 above, and are listed in Table 9 in columns 'dt1' and 'dt2', respectively. One should note that the P-sP lag time is 1.87 in Table 9. This is close to the value of 1.95 sec of the cepstral peak given by the sum and product of the cepstra in Figures 32, 33, and 34. Thus, the 1.95 sec cepstral peak appears to represent the sP-P lag time for the April 23, 1984 event. Assuming the same ray parameter for the P, pP, and sP waves, the sP-P time lag can be given by:

$$dt_2 = h * (n_p + n_s) \quad . \qquad \text{R-20}$$

The depth (h) of the earthquake based on the 1.95 sec sP-P lag time obtained through the cepstral analysis can be estimated by:

$$h = dt_2 / (n_p + n_s) \quad . \qquad \text{R-21}$$

where n_p and n_s are the slowness for the P and S waves, respectively. They are defined, as above, by:

$$n_v = (1/v^2 - p^2)^{1/2} \quad , \qquad \text{R-22}$$

where v is either the P or S-wave velocity in the source layer, and p is the ray parameter. Using a P-wave velocity of 5.0 km/sec, an S-wave velocity of 3.5 km/sec, a ray parameter of:

$$p = 1/(8.1 \text{ km./sec.}) \quad , \qquad \text{R-23}$$

and the cepstrally derived sP-P time lag of dt_2 = 1.95 sec, as above, equation R-21 gives a cepstrally predicted depth (h) of:

$$h = 4.7 \text{ km} \qquad \text{R-24}$$

for the April 23, 1984, Lancaster earthquake. This depth is in agreement with the 4.4-4.7 km depth obtained through the aftershock data by Armbruster and Seeber (1985). Thus, the mainshock appears to have occurred at the base of the aftershock activity.

Finally, the significance of the first peak at 1.0 sec in the product of all the station's cepstra (Figure 34) is unclear. This peak is unlikely to be the pP-P lag time, since the pP phase is negligible on the seismic records for our set of stations, and has a predicted lag time of 1.42 sec, as obtained by the direct P, pP, and sP response calculations performed above. This is reinforced by the fact that the pP incidence rays from the earthquake to our stations all fall on, or very near, one or both of the nodal planes of the P-wave focal mechanism (Figure 35). Nor is this peak likely to be the sum or difference between the pP-P and the sP-P delay times, since the amplitude of the pP arrival is so small. This peak does not seem to dominate the cepstral product plots of the 'Best Six' and 'Best Twelve' stations (Figure 32 and 33, respectively). Not until the LCNA, WMNY, WEST, and WTVE stations are added to the data set, does this peak become apparent in the cepstral product. Since all four of the stations are within the same region, this peak may be due to reverberations along a local crustal anomaly, or some other local phenomenon.

Discussion

The use of cepstra as a means of obtaining the depth of an earthquake appeared to work in the case of the April 23, 1984 Lancaster, Pennsylvania event. The sP-P delay time obtained was about 1.9 - 1.95 sec. The cepstral peak corresponding to this sP-P delay time was most clearly visible when the cepstra of all the seismograms were normalized to a maximum value of 1.0, and multiplied together over each second in the quefrency domain. The resultant composite cepstrum (bottom plot of Figure 34) produced two main peaks. The peak at 1.9 - 1.95 sec appears to correspond to the sP-P arrival time delay. This was verified by a comparison to calculated amplitude responses and time lags using ray theory, for the P, pP, sP arrivals, given the fault plane orientation, station locations, velocity model, and a rough estimate of the depth of the earthquake, based on the aftershock data. A P-wave velocity of 5.0 km/sec and an S-wave velocity of 3.5 km/sec were used for the source layer. The second peak appears at 1.0 seconds of quefrency in the cepstrum product (bottom plot of Figure 34), when stations LCNA, WMNY, WEST, and WTVE are added. This peak does not appear to be due to the pP-P lag time, or the sum or difference of the pP-P and sP-P delay times. Rather, since all four of these stations are in the same region of New York State (Figure 29), this peak may be due to reverberations along a local crustal anomaly.

The 4.7 km depth for the April 23, 1984 mainshock obtained by the cepstral analysis indicates that it occurred at about the same depth as the aftershocks which were located at a depth of 4.4 - 4.7 km based on local aftershock monitoring.

SUMMARY AND CONCLUSIONS

Although the Lancaster, Pennsylvania area is dominated by an E-W striking structural trend associated with Paleozoic deformation, there is evidence that the less obvious N-S striking structural features have been the dominant zones of tectonic activity from the Mesozoic into the present.

A closer look at the geology of the Lancaster, Pennsylvania region results in the observation that the youngest structural features are the N-S striking ones, and not the E-W striking ones, such as the Martic Line (Figure 1). Based on cross-cutting relationships, the youngest rocks of the area are the N-S striking Late Triassic - Early Jurassic diabase dikes. Likewise, the youngest faults in the region are sets of N-S trending cross faults. The dominant of these sets of faults is the Fruitville Fault Zone, which outcrops just north of the city of Lancaster, and continues north, almost up to the Triassic basin (Figures 1 & 2). These cross-faults offset all the other structural features and lithologies in the area. Historical seismicity and relocated instrumentally recorded events appear to cluster around this main set of cross faults the Fruitville Fault Zone of Lancaster County (Figure 20).

The April 23, 1984 earthquake, which was a magnitude 4.2 and a maximum intensity of MM=VI event, fell along the southern extension of this Fruitville Fault Zone at 39.94°N and 76.325°W. The April 19, 1984, magnitude 3.0, intensity MM=IV foreshock also was located at the southern extension of this fault zone (39.84°N, 76.35°W) (Figure 20), as were the 10 aftershocks (Figure 26). This N-S trending, seismically defined zone, the Lancaster Seismic Zone, is approximately 50-60 km in length and 10-20 km in width. The April 23, 1984 earthquake was among the largest events along this zone, which is characterized by events of maximum intensity MM=VI (Figure 20).

The drainage pattern of the major streams is N-S trending in the Lancaster area (Figures 2 & 10). In addition, there is evidence that along the southern extension of the Fruitville Fault Zone, there had been a pre-glacial falls on the Susquehanna River, called the Great Falls by Thompson (1985). These falls may have been due to a fault scarp and/or an anticlinal uplift in the area.

There is some geophysical evidence that the Fruitville Fault Zone extends to the basement. There are some N-S trending gravity and magnetic anomalies in the area of the fault zone (Figures 11 & 12). However, due to the similarity of the carbonates on either side of the fault, a more precise ground survey may be necessary to clearly define the fault.

Various remote sensing methods, including topographical studies (Wise, 1967), and LANDSAT-1 and LANDSAT-4 images, have revealed major N-S striking lineaments through the Lancaster region. The satellite detected lineaments and the potential field data, also, suggests one of several large scale basement features, possibly faults, striking NW through the region (Lavin, et al., 1982).

As mentioned, the April 23, 1984 mainshock and the April 19, 1984 foreshock, both fell along the Lancaster Seismic Zone. These locations were based on maximum intensity areas (Scharnberger and Howell, 1985), on absolute location using HYPOINVERSE (Klein, 1978; Lahr, 1980), and on the results from a relative location algorithm (Baumgardt, 1977 & 1985). The mainshock and the aftershocks were located near Marticville, approximately 10 km south of the city of Lancaster. The foreshock was located some 5-10 km south of the mainshock, along strike of the Lancaster Seismic Zone, near McCalls Ferry and Holtwood (Figure 28).

The aftershocks of the April 23, 1984 event were observed to be at a depth of 4.4-4.7 km determined from the records of 10 such events. These were recorded by a temporarily assembled local network of 9 stations (3 from Penn State and 6 from Lamont-Doherty) located directly over the location of the mainshock near Marticville (Armbruster and Seeber, 1985).

A cepstral analysis of 17 seismograms from 13 stations of the N.E.U.S. Seismic Network (Figure 29, Table 7), revealed a depth of approximately 4.7 km for the April 23, 1984 mainshock. Therefore, the source of the mainshock appears to be located at about the same depth as the 4.4-4.7 km deep source of the aftershocks. These results were based on a 5.0 km/sec, P-wave velocity, and a 3.5 km/sec, S-wave velocity for the top 8 km Paleozoic layer (Abriel, 1978; Sienko, 1982; Alexander, 1984).

The fault plane solution (Figure 27) based on the first arrivals from the mainshock and the aftershocks, predicts a preferred fault plane which strikes approximately N 10°E and dips 60°E. This fault plane solution indicates that the motion along this fault was right-lateral reverse for the April 23, 1984 event and its aftershocks. The strike of this seismogenic fault is analogous to that of the cross faults within the Fruitville Fault Zone, and its overall N-S trend (Figure 20). Furthermore, these cross-faults, like the fault plane solution for the April, 1984 mainshock and aftershocks, reveal a right-lateral component of motion, based on their offsets of all the other structural features in the region. The P-axis of the fault plane solution (Figure 27) is in the ENE direction. This is the same direction as the strike of the maximum compressional stress axis for the N.E. United States, as obtained from other fault plane solutions, from in situ stress measurements, and from geological data (Zoback and Zoback, 1980; Zoback, 1986). In situ stress measurements in the Kent Cliffs research well of southeastern New York also indicate a maximum compressional stress direction of N 50°E (Zoback, 1986). Data from fault plane solutions for several events nearby Annsville, New York, also, suggest ENE maximum compression (Seborowski, et al., 1982).

Therefore, this suggests that the Lancaster area of S.E. Pennsylvania is in a ubiquitous ENE maximum compressional stress regime, with the youngest N-S trending faults, seemingly of Mesozoic age, being reactivated in a predominantly reverse sense with a right-lateral component. This conclusion is supported by the previously-mentioned fact that the historical seismicity within Lancaster County, Pennsylvania appears to be confined to a N-S trending zone, approximately 50-60 km long and 10-20 km wide zone, which we have named the Lancaster Seismic Zone. At the center of this zone is found the highest concentration of the youngest faults which form the N-S trending Fruitville Fault Zone (Figure 20).

BIBLIOGRAPHY

Abdypoor, G., and Bischke, R. E., 1982, Earthquakes felt in the state of Pennsylvania: with emphasis on earthquakes felt in Philadelphia, Pa. and surrounding areas.: Temple Univ., Dept. of Geology, Philadelphia, 354pp.

Abriel, W. L., 1978, A ground-based study of the Everett-Bedford lineament of Pennsylvania: M.S. thesis, The Pennsylvania State University, University Park, Pennsylvania.

Aggarwall, Y. P., 1978, Earthquakes, faults, and nuclear power plants in southern New York and northern New Jersey: Science, v. 200, p. 425-429.

Alexander, S.S., 1984, Personal communication.

Alexander, S. S., and Stockar, D. V., 1984, The earthquake of April 23, 1984 near Lancaster, Pa. and its associated seismo-tectonic setting: Paper presented at Eastern Section Meeting, Seismological Society of America, October 11, 1984: Earthquake Notes, Oct. 11, 1984 meeting.

Anderson, T. H., Drake, D. E., and Wise, D. U., 1965, Megapetrofabric of the Coatsville - Doe Run area, Pennsylvania: Pa. Acad. Sc. Proceed., v. 38, no. 2, p. 174-182.

Armbruster, J. G., and Seeber, L., 1985, Martic April 23, 1984 earthquake and the Lancaster seismic zone in eastern Pennsylvania: (unpubl.).

Bahat, D., and Engelder, T., 1984, Surface morphology on cross-fold joints of the Appalachian Plateau, New York and Pennsylvania: Tectonophys., v. 104, p. 299-313.

Barstow, N., Schlesinger-Miller, E., and Kafka, A., 1981, Earthquakes in New York state and adlacent areas, 1981: U.S. Earthquakes, 1981, U.S. Geol. Soc. Spec. Publ., p. 108-109

Bascom, F., and Stose, G. W., 1938, Geology and mineral resources of the Honeybrook and Phoenixville quads., Pa.: U.S. Geol. Soc. Bull., v. 891, p. 76-78.

Baumgardt, D. R., 1977, The application of differential travel-time residuals for the study of mantle heterogeneities (abstr.): Earthquake Notes, v. 48, p. 9-10.

Baumgardt, D. R., 1985, Personal communication.

Beck, M. E., Jr., 1965, Paleomagnetic and geological implications of the magnetic properties of the Triassic diabase of S.E. Pennsylvania: Jour. Geophy. Res., v. 70, p. 2845-2856.

Beck, M. E., Jr., 1972, Paleomagnetism of the upper Triassic diabase from S.E. Pennsylvania: further results: Jour.Geophys.Res., v. 77, p. 5673-5687.

Bell, H. III, and others, 1978, Comparison of anomalies detected by airborne and truck-mounted magnetometers in the Haile-Brewer area,S. Carolina: in Geological investigations of the eastern Piedmont, southern Appalachians; Carolina Geol. Soc. Guidebook; ed. A. W. Snoke;p. 21-27

Berg, T., and others, 1930, Geologic map of Pa.: Pa. Geol. Surv., 1:250,000.

Black, R. F., 1964, Paleomagnetic support of the theory of rotarion of the western part of the island of Newfoundland: Nature, v. 202, p. 945-948.

Bogert, B.P., Healy, M.J., and Tukey,J.W., 1963, The quefrency analysis of time series for echoes: cepstrum, psuedo-autocovariance, cross-cepstrum, and saphe cracking, in Symposium on Time Series Analysis, Brown Univ., ed. Rosenblatt, M., 1963, p. 206-243.

Bollinger, G. A., Teague, A.G., Munsey, J.W., and Johnston, A.C., 1985, Focal mechanism analysis for Virginia and eastern Tennessee earthquakes (1978-1984): Prepared for U.S. Nuclear Regulatory Commission, NUREG/CR-4288.

Bott, M. H. P., 1976, Formation of sedimentary basins of graben type by extention of the continental crust: Tectonophys., v. 36, p. 77-86.

Bria, J. J., 1978, Tectonic setting for the emplacement of dikes in the Millersville Area, Lancaster County, Pa.: M.S. thesis, Millersville State College, Millersville, Pa.

Bromery, R. W. and Zandle, G.L., 1959, Aeromagnetic map of the Quarryville quadrangle, Lancaster County, Pa.: U.S.Geol.Survey, Geophys.Invest.Map GP-219.

Bromery, R. W. and Zandle, G.L., 1959, Aeromagnetic map of the Conestoga quadrangle, Lancaster County, Pa.: U.S.Geol Survey, Geophys.Invest.Map GP-218.

Bromery, R. W. and Zandle, G.L., 1961, Aeromagnetic map of the Lititz quadrangle, Lancaster County, Pa.: U.S.Geol.Survey, Geophys.Invest.Map GP-257.

Bromery, R. W. and Zandle, G.L., 1961, Aeromagnetic map of the Lancaster quadrangle, Lancaster County, Pa.: U.S.Geol.Survey, Geophys.Invest.Map GP-259.

Bromery, R. W., and Griscom, A., 1967, Aeromagnetic and generalized geologic map of S.E. Pennsylvania: U.S. Geol. Survey, Geophys. Inv. Map GP-577.

Burch, C. I., Jr., 1985, Enhancement and determination of linear features with application to the Appalachian region: M.S. thesis, The Pennsylvania State University, University Park, Pa.

Campbell, D. L., 1978, Investigation of the stress - concentration mechanism for intraplate earthquakes: Geophys.Res.Lett. 5, p. 477-479.

Carts, D. A., and Bollinger, G. A., 1981, A regional crustal velocity model for the southeastern U. S.: Seis.Soc.Am.Bull., v. 71, p. 1829-1847.

Cloos, E., and Heitanen, A., 1941, Geology of the "Martic overthrust" and the Glenarm series in Pennsylvania and Maryland: Geol.Soc.Am.Sp.Paper # 35, 207pp.

Cloos, E., 1971, The south border of the Triassic graben in Pennsylvania: Fault or graben? (abs.): Geol.Soc.Am. Abst. with Prog., v. 3, # 7, p. 526.

Cloos, E., and Pettijohn, F. J., 1973, Southern border of the Triassic basin, West York, Pa.: Fault or overlap?: Geol.Soc.Am.Bull., v. 84, p. 523-536.

Cohen, T.J., 1970, Source-depth determination using spectral, psuedo-autocorrelation, and cepstral analysis: Geophys. Jour. Royal Astr. Soc., v. 20, p. 223-231.

Cook, F. A., Albaugh, D.S., Brown, L.D., Kaufman, S., Oliver, J.E., and Hatcher, R.D., Jr., 1979, Thin-skinned tectonics in the crystalline southern Appalachians; COCORP seismic-reflection profiling of the Blue Ridge and the Piedmont: Geology, v. 7, p. 563-567.

Daniels, D. L., Zietz, I., and Popenoe,P., 1983, Distribution of subsurface lower Mesozoic rocks in the S.E. U.S., as interpreted from regional aeromagnetic and gravity maps:U.S.Geol.Surv.Prof.Paper 1313-k,24pp.

DeBoer, J., 1967, Paleomagnetic - tectonic study of Mesozoic dike swarms in the Appalachians: Jour.Geophy.Res., v. 72, p 2237-2250.

DeBoer, J., 1968, Paleomagnetic differentiation and corrolation of late Triassic volcanic rocks in the central Appalachians: Geol.Soc.Am.Bull., v. 79, p. 609-626.

Dewey, J. W., and Gordon, D. W., 1984, Map showing recomputed hypocenters of earthquakes in the eastern and central U. S. and adjacent Canada: U.S.Geol.Surv. Map MF-1699.

Dietz, R. S., and Holden, J. C., 1970, Reconstruction of Pangea: breakup and dispersion of continents, Permian to present: Jour.Geophy.Res., v. 75, p. 4939-4955.

Diment, W. H., Urban, T.C., and Revetta, F.A., 1972, Some geophysical anomalies in the eastern U.S.: in Nature of the solid earth; McGraw-Hill, New York, ed. E. Robertson, p. 544-572.

Diment, W. H., Muller, O.H., and Lavin, P.M., 1980, Basement tectonics of New York and Pennsylvania as revealed by gravity and magnetic studies: Virg. Polytech.Inst.Geol.Memoirs #2, The Caledonides in the USA, ed. D. R. Wones, p. 221-227.

Diment, W. H., McKeown, F.A., and Thenhaus, P.C., 1983, Northeastern U.S. seismic source zone: U.S.Geol.Surv. Circular #898, p. 24-31.

Dooley, R. E. and Wampler, J. M., 1983, K-Ar relations in the diabase dikes of Georgia: U.S.Geol.Surv. Prof. Papers 1313-M, 24 pp.

Drake, A. A. Jr., 1980, The taconides, acadides, and alleghenides in the central Appalachians: Virg.Polytech.Inst.Geol.Memoirs #2, The Caledonides in the USA, ed. D. R. Wones, p. 179-187.

Drake, C. L., 1963, Appalachian curvature, wrench faulting, and offshore structures: N.Y.Acad.Sc.Trans., v. 26, p. 48-63.

Ebel, J. E., Vudler, V., and Celata, M., 1982, The microearthquake swarm near Moodus,Conn.: Jour.Geophys. Res., v. 9, p. 397-400.

Engelder, T. and Geiser, P., 1980, On the use of regional joint sets as trajectories of paleostress fields during the development of the Appalachian plateau, N.Y.: Jour.Geophys.Res., v. 85, p 6319-6341.

Epstein, J. B., 1966, Structural control of wind gaps and of stream capture in the Stroudsburg area, Pa. and New Jersey: U.S.Geol.Surv.Prof.Paper 550 D, p. B80-D86.

Erickson, G. P. and Kulp, J. L., 1961, K-Ar measurements on the Palisades Sills, New Jersey: Geol.Soc.Am.Bull., v. 72, p 649-652.

Faill, R. T.,1973, Tectonic developement of the Triassic Newark-Gettysburg basin in Pennsylvania: Geol. Soc. Am. Bull., v. 84, p 725-740.

Fanale, F. P. and Kulp, J. L., 1962, Helium method and age of the Cornwall, Pa. magnetite ore: Econ.Geology, v. 57, p. 735-746.

Fleming, R. S. and Sumner, J. R., 1975, Interpretation of geophysical anomalies over the arcuate Appalachians: Geol.Soc.Am. Abst. with Prog., v. 7, # 1, p. 58.

Fox, F. L., 1970, Seismic Geology of the Eastern U.S.: Bull.Assoc.Eng.Geol., v. 7, p 21-44.

Freedman, J., Wise, D.U., and Bentley, R.D., 1964, Patterns of folded folds in the Appalachian Piedmont along the Susquehanna River:Geol.Soc.Am.Bull., v. 75, p 621-638.

Fullagar, P. D. and Bottino, M. L., 1969, Tertiary felsite intrusions in the Valley and Ridge province, Virg.: Geol.Soc.Am.Bull., v. 80, # 9, p 1853-1858.

Geyer, A. R., Gray, C., Mclaughlin, D.B., and Mosely, J.R. 1958. Geologic atlas of Pa.: Geology of the Lebanon quad., S.E. Pa.: Pa.Geol.Soc., Atlas 167C.

Gir, R, Subhash, S.M.G., and Choudhury, M.A. 1978, Investigation of crustal structure by the analysis of reverberation periodicities: S.S.A. Bull., v.68, p. 1387-1397.

Gold, D. P., Parizek, R.R., and Alexander, S.A., 1973, Analysis and Application of ERTS-1 data for regional geological mapping: Technical presentations of symposium on significant results obtained from the earth resources techn. satellite-1, v. 1, p. 231-246.

Gold, D. P., Alexander, S.A., Parizek, R.R., 1974, Application of remote sensing to nature resources and environmental problems in Pa.: Earth and Mineral Sc., Penn. State Univ., v. 43, # 7.

Gray, C., Geyer, A.R., and McLaughlin, D.B. 1958, Geology of the Richland quad., S.E. Pa.: Pa. Geol. Soc., Atlas 167D.

Gray, C. and Shepps, V. C., 1960, Geologic Map of Pa.: Pa. Geol. Surv., 1:250,000.

Griscom, A., 1963, Tectonic significance of the Bouger gravity field of the Appalachian system : (abs.) Geol.Soc.Am. Sp. Paper # 73, p. 163-164.

Gwinn, V. E., 1964 Thin-skinned tectonics in the plateau and N.W. Valley and Ridge province of the central Appalachians: Geol.Soc.Am.Bull., v. 75, p 863-900.

Hadley, J. B. and Devine, J. F., 1974, Seismotectonic map of the eastren U.S.: U.S.Geol.Surv. Misc. Field Studies Map, MF-620

Harder, E. C., 1910. Structure and origin of magnetite deposits near Dillsburg, York Co., Pa.: Econ. Geology, v. 5, # 7, p. 599-622.

Herrin, E., and others, 1968, 1968 Seismological tables for P phases: Seis.Soc.Am.Bull., v. 58, # 4.

Herrmann, R.B., 1976, Focal depth determination from the signal character of long-period P waves: S.S.A. Bull., v. 66, p. 1221-1232.

Hersey, J. B., 1944, Gravity investigation of central - eastern Pa.: Geol.Soc.Am.Bull., v. 55, p. 417-444.

Hobbs, W. H., 1904, Lineaments of the Atlantic border region: Geol.Soc.Am.Bull., v. 15, p. 483-506.

Hodgson, R. A., 1974, Review of significant early studies in lineament tectonics: Proc. of First International Conference on New Basement Tectonics: Utah Geol. Assoc. Publ. # 5, p. 1-10.

Holt, R. J., 1972, Seismicity analysis, Three Mile Island, Susquehanna River, Pa.: Weston Geophysical Research for Gilbert Assoc. Inc.

Hotz, P. E., 1952, Form of diabase sheets in S.E. Pa.: Am.Jour Sc., v. 250, p. 735-788.

Howell, B. F. Jr. and Schultz, T. R., 1975, Attenuation of modified Mercalli intensity with distance from the epicenter: Seis. Soc. Am. Bull., v. 65, p. 651-665.

Howell, B. F. Jr., Earthquake expectancy in Pa.: Proc. Pa. Acad. Sci., v. 53, p. 205-208.

Isaacs, C. H., 1979, State College, Pennsylvania crustal structure: by modeling of long-period P wave-forms from teleseismic earthquakes: M.S. paper, Pennsylvania State University, University Park, Pa., 82 pp.

Isachsen, Y. W., 1974, Fracture analysis of New York state using multi-stage remote sensor data and ground study: possible application to plate tectonic modeling: Proc. 1st. Int. Conf. on New Basement Tectonics; Utah Geol. Assoc. Publ. #5, p. 200-217.

Jacobeen, F. H. Jr., 1972, Seismic evidence for high angle reverse faulting in the coastal plane of Prince Georges and Charles counties, Maryland: Maryland Geol. Surv. Inf. Circ. # 13, 21 p.

Jeffreys, H. and Bullen, K. E., 1940, Seismological tables: Brit. Assoc. for the Advancement of Sc., London.

Johnston, H. E., 1966, Hydrology of the New Oxford formation in Lancaster county, Pa.: Pa. Geol. Soc., Ground Water Report W23.

Jonas, A. I. and Stose, G. W., 1930, Topographic and geologic atlas of Pa.: Lancaster quadrangle: Pa. Geol. Surv., Atlas # 168

Kane, M. F., 1977, Correlation of major eastern earthquake centers with mafic/ultramafic masses: U.S. Geol. Surv. Prof. Paper 1028-O.

Katz, S., 1955, Seismic study of the crustal structure in Pa. and N.Y.: Seis. Soc. Am. Bull., v. 45, p. 303-325.

Kauffman, M. E., 1967. Geological investigation of Three Mile Island and vicinity: Jan. 14, 1967 Report to Gilbert Assoc. Inc.

Keith, A., 1923, Outline of Appalachian structure: Geol.Soc.Am.Bull., v. 34, p. 309-380.

Kemerait R.C., and Sutton, A.F., 1982, A multidimentional approach to seismic event depth estimation: Geoexploration, v. 20, p. 113-130.

Kerr, R. A., 1985, Signs of an eastern quake?: Science, Nov. 1, 1985.

King, E. R. and Zietz, I., 1978, N.Y.-Alabama lineament: Geophysical evidence for a major crustal break in the basement beneath the Appalachian Basin: Geology, v. 6, p. 312-318.

King, P. B., 1951, The tectonics of middle North America: Princeton University Press, Princeton, N.J., 203 p.

King, P. B., 1961, Systematic pattern of Triassic dikes in the Appalachian region: U.S. Geol. Surv. Prof. Paper 424-B, P. B93-B95.

King, P. B., 1971, Systematic pattern of Triassic dikes in the Appalachian region -second report: U.S. Geol. Surv. Prof. Paper 750-D, p. D84-D88.

Klein, F. W., 1978, Hypocenter location program, HYPOINVERSE: U.S. Geol. Surv. Open-file Report 78-697.

Klitgord, K. D., Dillon, W.P., and Popenoe, P., 1983, Mesozoic tectonics of the southeastern U.S. coastal plain and continental margin: U.S. Geol. Surv. Prof. Paper 1313-P, 15 pp.

Knopf, E. B. and Jonas, A. I., 1929, Geology of the McCalls Ferry - Quarryville district, Pa.: U.S. Geol. Surv. Bull. # 799.

Kowalik, W. S. and Gold, D. P., 1974, Use of Landsat-1 imagery in mapping lineaments in Pa.: 1st. Internat. Conf. on the New Basement Tectonics; Utah Geol. Assoc. Publ. # 5, ed. R. A. Hodgson, et al. p. 236-249.

Kowalik, W. S., 1975, Use of Landsat-1 imagery in the analysis of lineaments in Pa.: M.S. thesis, Penn. State Univ., University Park, Pa.

Kowalik, W. S. and Gold, D. P., 1975, Lineaments and mineral occurrences in Pa.: NASA Tech. Rept., ORSER/SSEL Rept. 14-75 in M.S. thesis, Kowalik, W. S., Penn. State Univ., University Park, Pa.

Lahr, J.C., 1980, Hypoellipse/multics: A computer program for determining local earthquake hypocentral parameters, magnitude, and first motion pattern: U.S.G.S. Open File Rept. 80-159, revised April 1980 for version II, 59p.

Langston, C.A., and Helmberger, D.V., 1975, A procedure for modeling shallow dislocation sources: Geophys. Jour. Royal Astron. Soc. # 42, p. 117-130.

Lanning, R.M., 1973 An olivine tholeiite dike swarm in Lancaster, county Pennsylvania: M.S. thesis, Pennsylvania State Univ.

Lapham, D.M. and Gray, C., 1972, Geology and origin of the Triassic magnetite deposits and diabase at Cornwall, Pennsylvania: U.S.G.S. Bull. M56

Lavin, P.M., and Alexander, S.S., 1981, Evidence for block tectonic structural elements in the eastern U. S. and their present tectonic significance; Earthquake Notes, v. 53, # 3, p. 19.

Lavin, P.M., Chaffin, D.L., and Davis, W.F., 1982, Major lineaments and the Lake Erie - Maryland crustal block: Tectonics, v. 1, p. 431-440.

Le Pichon, X., and Fox, P.J., 1971, Marginal offsets, fracture zones, and the early opening of the North Atlantic: Jour. Geophys. Res. v. 76, p. 6294-6308

Liaw, Z.S., 1984, A modified cepstral method and its application to DWWSSN broadband data: M.S. thesis, Pennsylvania State Univ.

Lloyd, O.B., and Growitz, D.J., 1977, Ground-water resources of central and southern York county, Pennsylvania: Pa. Geol. Surv., Water Resource Report # 42.

Mackin, J.H., 1962, Structure of the Glenarm Series in Chester County, Pennsylvania: G. S. A. Bull., v. 73, p. 403-410.

May, P.R., 1971, Pattern of the Triassic-Jurassic diabase dikes around the North Atlantic in the context of predrift positions of the continents: G. S. A. Bull., v. 82, p. 1285-1292.

McKeown, F.A., 1978, Hypothesis: Many earthquakes in the central and southeastern United States are causally related to mafic intrusive bodies: Jour. Res. U. S. Geol. Survey 6, p. 41-50.

McKinstry H., 1961, Structure of the Glenarm Series in Chester County, Pennsylvania: G. S. A. Bull., v.72, p. 557-578.

McLaughlin, D.B., 1941, The distribution of minor faults in the Triassic of Pennsylvania: Papers of Mich. Acad. of Sc. Arts & Lit., v. 27, p. 465-479.

McLaughlin, D B., 1961, Some features of the Triassic north border in Pennsylvania: Pa. Acad. of Sc. Proceed., v. 35, p. 124-128.

McLaughlin, D.B., 1963, Newly recognized folding in the Triassic of Pennsylvania: Pa. Acad. of Sc. Proceed., v. 37, P. 156-159.

Meisler, H., and Becher, A.E., 1971, Hydrology of the carbonate rocks of the Lancaster 15-min. quad., Pennsylvania: Pa. Geol. Soc. Progress Report 171.

Metcalf, T., and Deboer, J.Z., 1981, Post-Triassic stress patterns along the Appalachians: 207-8 m.y. B.P. (abstr.): G. S. A. Abst. w/ Prog. # 13, p. 510.

Minster, JB., and Jordan, T.H., 1978, Present-day plate motion: J. G. R., v. 83, p. 5331-5354.

Moore, T.P., 1979, Upper crustal velocity structure in southwestern Virginia: M.S. Thesis, Virg. Polytech. Inst.

Mudge, M.R., 1968, Depth control of some concordant intrusions: G. S. A. Bull., v. 79, p. 417-428.

Muller, O.H., and others, 1979, A preliminary gravity map of Pennsylvania: G. S. A. Abst. w/ Prog., v. 11, # 1, p. 46.

Muller, O.H., Diment, W.H., and Lavin, P.M., 1980, Transverse gravity features and seismicity in New York and Pennsylvania: G. S. A. Abst. w/ Prog., v. 12, # 2, p. 74.

Muller, O.H., Diment, W.H., and Lavin, P.M., 1980, The nature and geological implications of three lineaments which terminate or offset geophysical anomalies in New York, Pennsylvania, Michigan, and Ontario: G.S.A. w/ Prog., v. 12, # 7, p. 488.

Muller, O.H., Diment, W.H., and Lavin, P.M., 1980, Major N.W. trending Precambrian strike-slip fault in Pennsylvania: EOS. A.G.U. Trans., v. 61, # 17, P. 360.

Muller, O.H., and Diment, W.H., 1981, Persistent zones of weakness in North America: EOS, A.G.U. Trans., v. 62, # 45, p. 1032.

Muller, O.H., and Diment, W.H., 1981, Is the Scranton Gravity High part of the central North American rift system? (abstr): G.S.A. Abst. w/ Prog., v. 13, # 7, p. 516.

Nettleton, L.L., 1941, Relation of gravity to structure in the northern Appalachian area: Geophys., v. 6, p. 270-286.

Newell, W.L., and Wise, D.U., 1965, Independent joint system superimposed on the metamorphic fabric of the Glenarm Series near Coatsville, Pennsylvania: Pa. Acad. of Sc. Proceed., v. 38, # 2, p. 150-153.

Newmark, N.M., and Hall, W.J., 1971, Final safety analysis report for the Three Mile Island nuclear station: Consulting Eng. Ser., Urbana, Ill.

Nottis, H.N., 1983, Epicenters of N.E.U.S. and S.E. Canada, onshore and offshore, time period: 1534-1980: Map and Chart Series # 38, N.Y. State Museum.

Oliver, J.R., Kovach, R., and Dorman, J., 1961, Crustal structure of the New York - Pennsylvania area: J.G.R., v. 66, p. 215-225.

Oliver, J.R., Johnson, T., and Dorman, J., 1970, Postglacial faulting and seismicity in New York and Quebec, in Symposium on Recent Crustal Movements, Ottawa, Canada., 1969, Papers: Canadian Jour. Earth Sc., v. 7, # 2, pt.2, p. 579-590.

Olsen, P.E., 1980, Triassic and Jurassic formations of the Newark Basin, in Field Studies of New Jersey Geology and Guide to Field Trips: 52nd Meeting of the New York State Geol. Assoc., ed. Man eizer, W.

O'Neill, B.J. Jr., 1975, Potential high-calcium limestone resources in the Mount Joy area, Lancaster County, Pennsylvania: Pa. Geol. Soc. Info. Cir. # 76.

O'Neill, D.C., 1983, Determining crustal structure in parts of eastern North America: M.S. Thesis, Pennsylvania State Univ.

Owens, J.P., 1970, Post-Triassic tectonic movements in the central and southern Appalachians, in Studies in Appalachian Geology: Central and Southern, 1970, ed. Fisher, G.W., p. 417-427.

Page, R.A., Molnar, P.H., and Oliver, J., 1968, Seismicity in the vicinity of the Ramapo fault, New Jersey and New York: S.S.A. Bull., v. 58, p. 681-687.

Parrish, J.B., 1978, Relationship of geophysical and remote sensing lineaments to regional structure and kimberlite intrusions in the Appalachian Plateau of Pennsylvania: M.S. Thesis, Pennsylvania State Univ.

Parrish, J.B., and Lavin, P.M., 1982, Tectonic model for kimberlite emplacement in the Appalachian Plateau of Pennsylvania: Geology, v. 10, p. 344-347.

Phemister, T.D., 1924, A note on the Lancaster Gap Mine: Jour. Geology, v. 32, p. 498-10.

Phillips, J.D., and Forsyth, D., 1972, Plate tectonics, paleomagnetics, and the opening of the Atlantic: G.S.A. Bull., v. 83, p. 1579-1600.

Poth, C.W., 1977, Summary: Ground-water resources of Lancaster County, Pennsylvania: Pa. Geol. Soc. Water Resource Report # 43.

Rios, J.H., 1966, Geology of the Quarryville-Octoraro area, Lancaster Couny, Pennsylvania: M.S. Thesis, Franklin and Marshall College.

Rogers, J., 1964, Basement and no-basement hypothesis in the Jura and the Appalachian Valley and Ridge, in Tectonics of the Southern Appalachians, ed. King, P., p. 71-80.

Root, S.I., 1970, Structure of the northern terminus of the Blue Ridge in Pennsylvania: G.S.A. Bull., v. 81, p. 815-830.

Root, S.I., 1973, Structure, basin development, and tectogenesis in the Pennsylvania portion of the folded Appalachians, in Gravity and Tectonics, 1973, eds. Dejong and Scholten, p. 343-359.

Root, S.I., 1973, Sequence of faulting, southern Great Valley of Pennsylvania: Am. Jour. Sc., v. 273, p. 97-112.

Root, S.I., and Hoskins, D., 1977, Major cross structures in Pennsylvania (Parts I & II): Pa. Geology, v. 8, # 2, p. 8-11, & # 3, p. 4-7.

Root, S.I., and Hoskins, D.M., 1977, Latitude 40°fault zone, Pennsylvania, a new interpretation: Geology, v. 5, p. 719-723.

Root, S.I., and MacLachlan, D.B., 1978, Western limit of Teconic allochthons in Pennsylvania: G.S.A. Bull., v. 89, p. 1515-1528.

Sanders, J.E., 1960, Structural history of the Triassic rocks of the Connecticut Valley belt and its regional implications: N.Y. Acad. of Sc. Trans., v. 23, p. 119-132.

Sanders, J.E., 1962, Strike-slip displacement on faults in the Triassic rocks of New Jersey: Science, v. 136, p. 40-42.

Sanders, J.E., 1963, Late Triassic tectonic history of the northern United States: Am. Jour. Sc., v. 261, p. 501-524.

Sbar, M.L., and Sykes, L.R., 1973, Contemporary compressive stress and seismicity in eastern North America: G.S.A. Bull., v. 84, p. 1861-1882.

Scharnberger, C.K., 1978, Lancaster County earthquake, July 16, 1976; and Another Lancaster County earthquake: Pennsylvania Geology, v. 9, # 5 & # 6.

Scharnberger, C.K., and Howell, B.F., 1985, Intensities and structural setting of the earthquake of 19 April and 23 April, 1984 in Lancaster County, Pennsylvania: Earthquake Notes, 56(2), p. 43-46.

Seborowski, K.D., Williams, G., Kelleher, J.A., and Statton, C.T., 1982, Tectonic implications of recent earthquakes near Annsville, N.Y.: S.S.A Bull., v. 72, p. 1601-1609.

Shaub, F.J., 1975, Interpretation of a gravity profile across the Gettysburg Triassic basin: M.S. Paper, Pennsylvania State Univ.

Siedner, G. and Miller, J.A., 1968, K-Ar age determination on basaltic rocks from S.W. Africa and their bearing on continental drift: Earth & Planetary Sc. Letters, Northland Pub. Co., Amsterdam, p. 451-458.

Sienko, D.A., 1982, Crustal structure of south-central Pennsylvania determined from wide-angle reflections and refractions: M.S. Thesis, Pennsylvania State Univ.

Sinha, A.K., Hanon, B.B., Sans, J.R., and Hall, S.T., 1980, Igneous rocks of the Maryland Piedmont: Indicators of crustal evolution: Va. Polytech. Inst. Dept. Geol. Sc. Mem., # 2, "The Caledonides in the USA", ed. Wones, D.R., p. 131-135.

Smith, L.L., 1931, Magnetite deposits of French Creek, Pennsylvania: Pa. Geol. Surv., 4th ser., M-14.

Smith, R.C., 1973, Geochemistry of the Triassic diabase from southeastern Pennsylvania: PhD. Thesis, Pennsylvania State Univ.

Smith, R.C., Rose, A.W., and Lanning, R.M., 1975, Geology and Geochemistry of the Triassic diabase in Pennsylvania: G.S.A. Bull., v. 86, p. 943-955.

Socolow, A.A., 1974, Geologic interpretation of the aeromagnetic maps of southeastern Pennsylvania: Pa. Geol. Survey Infor. Circ. # 77.

Socolow, A.A., and others, 1980, Geologic map of Pa: Pa. Topog. & Geol. Surv., Map # 1., 1:250,000.

Southwick, D.L., 1970, Structure and petrology of the Harford County part of Baltimore-State Line gabbro-peridotite complex, in Studies of Appalachian Geology: Central and Southern, ed. Fisher, G.W., 1970, p. 397-415.

Stose, G.W., and Lewis, J.V., 1916, Triassic igneous rocks in the vicinity of Gettysburg, Pennsylvania: G.S.A. Bull., v. 27, p. 623-643.

Stose, G.W., 1927, Possible Post-cretaceous faulting in the Appalachians: G.S.A. Bull., v. 38, p. 493-504.

Stose, G.W. and Jonas, A.I., 1930, Lancaster quadrangle atlas: Pa. Geol. Surv., Atlas # 168.

Stose, G.W., and Jonas, A.I., 1932, Geologic map of southeastern Pennsylvania: Pa. Geol. Surv., Bull. W-2.

Stose, G.W., and Jonas, A.I., 1933, Geology and mineral resources of the Middletown quadrangle, Pennsylvania: U.S. G.S. Bull. # 840.

Stose, G.W. and Jonas, A.I., 1939, Geology and mineral resources of York County, Pennsylvania: Pa. Geol. Surv. Bull. C-67.

Stose, G.W., 1949, Fault at the western edge of the Triassic in southern Pennsylvania: Am. Jour. Sc., v. 247, p. 531-536.

Stover, C.W., Reagor, B.G., and Algermissen, S.T., 1981, Seismicity map of the state of Pennsylvania: U.S. G.S., Map MF-1280.

Sumner, J.R., 1975, Geophysical interpretation of the structural configuration of the Newark-Gettysburg Triassic basin: Report Geol.Surv.Grant 14-080001-G150, Dept. of Geol. Sc., Lehigh Univ., Pa.

Sumner, J.R., 1976, Residual gravity anomaly map of the Newark-Gettysburg Triassic basin, G.S.A. Abst. w/ Prog., v. 8, p. 280.

Sumner, J.R., 1977, Geophysical investigation of the structural framework of the Newark-Gettysburg Triassic basin, Pennsylvania: G.S.A. Bull., v. 88, p. 935-942.

Sykes, L.R., 1978, Interplate seismicity, reactivation of preexisting zones of weakness, alkaline magmatism, and other tectonism postdating continental fragmentation: Rev. Geophy. Space Phys., # 16, p. 621-688.

Taylor, P.T., Zietz, I., and Dennis, L.S., 1968, Geologic implications of aero-magnetic data for the eastern continental margin of the United States: Geophysics, v. 33, p. 755-780.

Taylor, S.R., and Toksoz, M.N., 1979, Three dimensional crust and upper mantle structure of the N.E. U.S.: J.G.R., v. 84, p. 7627-7638.

Thompson, A.M., 1978, Lineaments and brittle structural evolution of a portion of the middle Atlantic seaboard region, Del. and Pa.: Proc. of 3rd. Inter. Conf. of Basement Tectonics.

Thompson, G.H., 1985, The preglacial Great Falls of the Susquehanna River (Abstr.), G.S.A. Abstr. w/ Prog., G.S.A. Meeting in Orlando, Fla., Oct. 28, 1985.

Van Houten, F.B., 1965, Composition of the Triassic Lockatong and associated formations of the Newark group, central N. J., and adjacent Pa.: Am. Jour. Sc., v. 263, Dec. 1965, p. 825-863.

Van Houten, F.B., 1969, Late Triassic Newark Group, north-central N.J. and adjacent Pa. and N.Y., in Geology of Selected Areas in N.J. and Eastern Pa. and Guidebook of Excursions: G.S.A. Annual Meeting, Rutgers Univ. Press, p. 314-330.

Van Houten, F.B., 1977, Triassic-Liassic deposits: A.A.P.G., v. 61, # 1, p. 79-99.

Vogfjord, K.S., 1984, P-wave medium response for a shallow dislocation source in a half-space: unpubl.

Voight, B., 1969, Evolution of the North Atlantic Ocean: Relevance of rock-pressure measurements in the North Atlantic geology and continental drift: Am. Assoc. Petroleum Geologists Mem., # 12, p. 955-962.

Volk, K.W., 1977, Paleomagn. of Mesozoic diabase and the deformational history of southeastern Pennsylvania: PhD. Thesis, Pennsylvania State Univ.

1

IMAGE EVALUATION TEST TARGET (MT-3)

150mm

6"

1

IMAGE EVALUATION TEST TARGET (MT-3)

150mm

6"

1

IMAGE EVALUATION TEST TARGET (MT-3)

150mm

6"

Von Hake, C.A., 1976, Earthquake history of Pennsylvania: Earthquake Inform. Bull., v. 8. # 4, p. 28-31.

Watson, E.H., 1955, Triassic faulting near Gwynedd, Pa.: Pa. Acad. of Sc. Proceed., v. 29, p. 122-127.

Wentworth, C.M., and Keefer, M.M., 1983, Regenerated faults of small cenezoic offset - Probable earthquake sources in the southeastern U.S.: U.S.G.S. Prof. Paper 1313-S, 18 pp.

Weston Geophysical Research Inc., 1967, Seismicity and response spectra analysis; proposed nuclear power plant, Three Mile Island, Susquehanna River, Pa.: Report for Gilbert Assoc. - purchase order # 154720 Dated Dec. 29, 1966.

Wheeler, G., 1939, Triassic Fault-line deflections and associated warping: Jour. of Geol., v. 47, p.337-370.

Wheeler, R.L., Mullennex, R.H., Henderson, C.D., and Wilson, T.H., 1974, Major cross strike structures of the central sedimentary Appalachians: Progress Report, Proc. W. Va. Acad. Sc.: v. 46.

Wheeler, R.L., and others, 1978, Cross-strike structural discontinuities in the thrust belts, with special reference to the Appalachians: Proc. of 3rd. Inter. Conf. of Basement Tectonics.

White, W.A., 1952, Post-Cretacous faults in Virg. and N.C., G.S.A. Bull., v. 63, p. 745-748.

Wise, D.U. and Kauffman, M.E., 1960, Some tectonic and structural problems of the Appalachian Piedmont along the Susquehanna River, Pa.: Guidebook. 25th Annual Field Conference of Pa. Geologists.

Wise, D.U., 1967, Radar geology and psuedo-geology on an Appalachian Piedmont cross-section: Photogrammetic Eng., July, 1967, p. 752-761.

Wise, D.U., and Grauch, R.I., 1967, Regional Joint pattern superimposed on the metamorphic rocks of Southern Pa.: Pa. Acad. of Sc. Proceed., v. 40, p. 104-110.

Wise, D.U., 1968, Regional and sub-continental sized fracture systems detected by topographic shadow techniques: Geol. Surv. Canada Paper 68-52, p.175-199.

Wise, D.U., and Werner, M.L., 1969, Tectonic transport domains and the Pa. elbow of the Appalachians: A.G.U. Trans., v. 50, # 4, p. 313.

Wise, D.U., 1970, Multiple deformation, geosynclinal transitions and the Martic problem in Pennsylvania, in Studies of Appalachian Geology: Central and Southern, ed. Fisher, G.W., 1970, p. 317-333.

Wise, D.U., 1974, Sub-continental sized fracture systems etched into the topography of New England: Proc. First Int. Conf. on the New Basement Tectonics, 1974, Utah Geol. Assoc. Publ. # 5, p. 416-422.

Withington, C.F., 1974, Basement tectonics of the Atlantic Coastal Plain as seen from ERTS-1 imagery (Abstr.), in Proc. 1st Int. Conf. on New Basement Tectonics, Utah Geol. Assoc. Publ. # 5, p. 423.

Wood, G.H., Arndt, H.H., and Carter, M.D., 1969, Systematic jointing in the western part of the anthracite region of eastern Pennsylvania: U.S. G.S. Bull. 1271-D.

Woodward, H.P., 1957, Structural elements of the north-eastern Appalachians: A.A.P.G. Bull., v. 41, p. 1429-1440.

Woodward-Clyde Consultants Inc., 1985, Aug. 1985, Report on the North Central Area Network and the Mid-Hudson Area Network: Aug 1985, 80c4086 Monthly Report (ESEERC).

Woollard, G.P., 1943, Geologic correlation of aerial gravitational and magnetic studies in N.J. and vicinity: G.S.A. Bull., v. 54, p. 791-818.

Zartman, R.E., Brock, M.R., Heyl, A.V., and Thomas, H.H., 1967, K-Ar and Rb-Sr ages of some alkalic intrusive rocks from central and eastern U.S.:Am.Jour.Sc., v. 265, p. 848-870.

Zoback, M.L., and Zoback, M.D., 1980, State of stress in the continental U.S.: J.G.R., v. 85, p. 6113-6156.

Zoback, M.D., 1983, State of stress in the lithosphere: Rev. of Geophys. and Space Phys., v. 21, p. 1503-1511.

Zoback, M.D., 1986, In-situ stress measurements in the Kent Cliff research well: prepared for the Empire State Electric Energy Corp., N.Y., N.Y.

APPENDIX 1

PIEDMONT STRATIGRAPHY NEAR
THE SUSQUEHANNA RIVER

(after Wise and Kauffman, 1960)

PIEDMONT STRATIGRAPHY NEAR THE SUSQUEHANNA RIVER

Marvin E. Kauffman
Franklin and Marshall College

TRIASSIC

Upper Triassic

Gettysburg formation

Shale member - soft red shale with interbedded coarse red sandstone and conglomerate tongues which become the Robeson conglomerate in Chester County.

Elizabeth Furnace conglomerate member - basal pebbly sandstone and conglomerate up to 2500 feet thick.

New Oxford formation (= Stockton formation of eastern areas)

Arkoses, ranging from very coarse to fine-grained, with some quartz pebble conglomerates, minor amounts of shale, siltstone, and some impure nodular limestone and limestone conglomerates.

ORDOVICIAN

Upper Ordovocian

Conestoga limestone (exact age uncertain, possibly equivalent in part to Martinsburg-Cocalico)

Blue limestone, closely folded, thin-bedded, argillaceous, with dark graphitic shale or slate and coarse conglomerate and breccia of limestone fragments in dark argillaceous and calcareous matrix (more than [illegible] feet thick). Contains <u>Strophomena</u> st[illegible] [illegible]sts unconformably on formations as [illegible] Beekmantown and as old as Antietam.

Martinsburg formation

Gray to black shale, argillaceous sandstone, with purple and red shale near base; contains volcanic contributions in Jonestown area; Cocalico shale of Lancaster County is probably equivalent to the Martinsburg; it also contains bluish-black and dark gray fissile shale with some purple, green, and red shale near the base, possibly derived from volcanic ash (?). Contains some graptolites.

Middle Ordovician

Hershey limestone

Dark gray-black, thin bedded limestone; weathers to brownish-gray surface and shows well developed cleavage (200-350 feet thick in Lebanon area).

Myerstown limestone

Gray-tan, thin bedded limestone, graphitic at base, usually medium to finely crystalline (250 feet thick in Lebanon area).

Annville limestone

Light gray, high calcium limestone, massive or thick-bedded, weathers to white sugary-appearing surface (450 feet thick in Lebanon area).

Lower Ordovician

Beekmantown group

Ontelaunee, Epler, Rickenbach, and Stonehenge formations comprise this group in the Lebanon area. Light to dark gray limestone and dolomite with crystalline and fossiliferous beds; some dark gray chert and edgewise conglomerate (2000-2500 feet thick). Contains *Isochilina seelyi* (Whitfield), *Turritoma* sp., *Ophileta* sp., *Lophospira* sp., *Eccyliopterus* sp., *Orospira* sp., *Maclurites oceanus*, *Cryptozoon steeli*.

CAMBRIAN

Upper Cambrian

Conococheague limestone

Impure, dark-blue limestone, with bands of black chert, oolites, edgewise conglomerates, and cryptozoocan reefs; contains several dolomite beds. (Subdivided into following members in northern Lancaster and adjacent counties: Richland, Millbach, Schaefferstown, Snitz Creek, and Buffalo Springs members.) Contains *Cryptozoon proliferum* and *C. undulatum* (1000-1500 feet thick).

Middle Cambrian

Elbrook limestone

Thin-bedded, shaly, laminated, fine-grained argillaceous limestone and dolomite; weathers to buff surface (approximately 1000 feet thick).

Lower Cambrian

Ledger dolomite

Light gray to white coarsely crystalline dolomite; weathers to rough sugary surface (approximately 1000 feet thick).

Kinzers formation

Dark banded argillaceous dolomite, spotted marble, and dark calcareous shale; contains many Lower Cambrian fossils including Bonnia, Olenellus, Wanneria, and Paedumias (0-500 feet thick).

Vintage dolomite

Gray thick bedded, knotty dolomite with argillaceous partings and marble at base. Contains Salterella conica (up to 600 feet thick).

Antietam quartzite

Gray-tan quartzite and quartz or mica schist with a calcareous, ferruginous, vitreous, granular quartzite at the top (200-800 feet thick). Contains Olenellus, Camerella, Obolella, Hyolithes, Scolithus.

Harpers phyllite

Fine-grained albite schist, gray-green, quartzose phyllite, dark shale and slate (approximately 1000 feet thick).

Chickies quartzite

Thick-bedded, light colored, vitreous quartzite; locally schistose with sericite partings and interbedded black slate. Contains Scolithus linearis. (500-600 feet thick)

Hellam conglomerate (not well developed in Lancaster County)

Milky-quartz pebbles up to six inches long in finer quartz-sericite matrix; some pebbles and cobbles of red and black jasper and quartzite and some bluish-green quartz.

PRECAMBRIAN

Crystalline basement complex

Baltimore gneiss, Byrum gneiss, Pickering gneiss, Pochuck gneiss, metadiabase, gabbro, graphitic gneiss, anorthosite, granodiorite, quartz monzonite, and serpentine.

ROCKS OF QUESTIONABLE AGE (Probably Lower Paleozoic)

Glenarm Series

Peach Bottom Slate

Dark bluish-gray to bluish black slate, consisting of muscovite, quartz, andalusite, and graphite with some magnetite and pyrite.

Cardiff Conglomerate

Quartz pebbles in schistose fine quartz, sericite, and chlorite matrix.

Peters Creek Schist

Chlorite and sericite quartz schists with schistose quartzites and conglomerates.

Wissahickon formation

Light gray to bluish gray mica schist with abundant biotite, muscovite, quartz, epidote, oligoclase, albite, hornblende, and chlorite.

Cockeysville Marble

White to light bluish gray marble.

Setters Formation

White feldspathic quartzite with gray mica gneiss and schist.

APPENDIX 2

SEISMOGRAMS FOR THE APRIL 23, 1984 EARTHQUAKE

SEISMOGRAMS FOR THE APRIL 23, 1984 EARTHQUAKE

The following plots are the first 40 seconds of the seismic signal used in the cepstral analysis of the April 23, 1984 earthquake of Lancaster County, Pennsylvania . The seismograms are from stations in the Mid-Hudson Area Network and the North Central Area Network of New York State. They are operated by Woodward-Clyde Consultants of Wayne, New Jersey. The four letter identification code for a particular station appears in the upper left-hand corner of each seismic trace. The location of each station is given in Figure 29 and Table 7. The maximum value for the first 40 seconds of each seismogram appears above the center of each trace. The signals are plotted on a scale of 5 seconds per tick mark.

NOTE: Stations ONTR and OSWG have all three components plotted. The identification is as follows:

ONTR = RADIAL component from station ONTR
ONTR2 = TANGENTIAL component
ONTR3 = VERTICAL component

OSWG = RADIAL component from station OSWG
OSWG2 = TANGENTIAL component
OSWG3 = VERTICAL component

The remaining stations have only the VERTICAL component plotted, and only this component was used in the cepstral analysis.

LIST OF FIGURES FOR APPENDIX 2

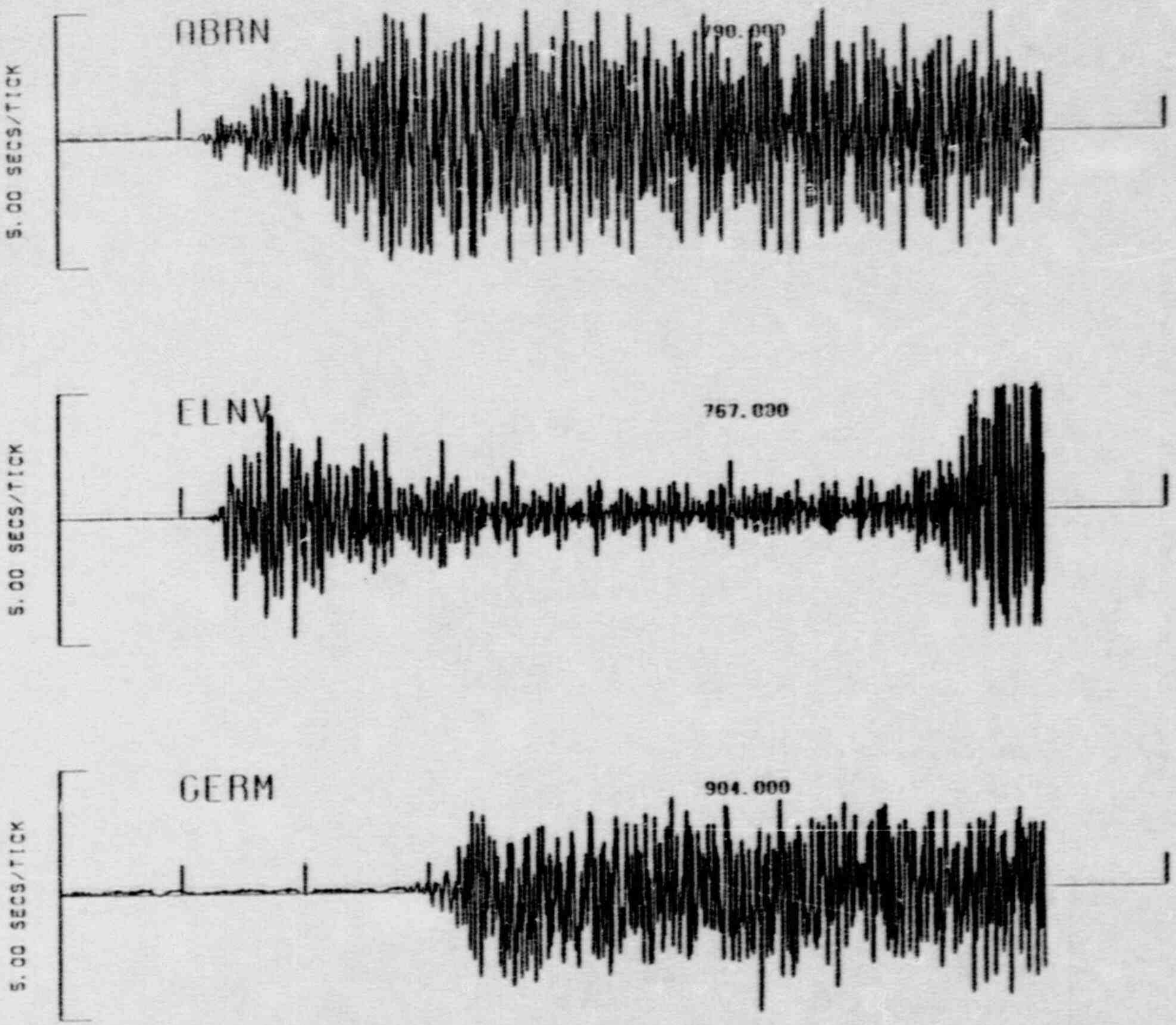

FIGURE 2-1 First 40 sec of the seismograms (vertical components) for stations ABRN, ELNV, and GERM.

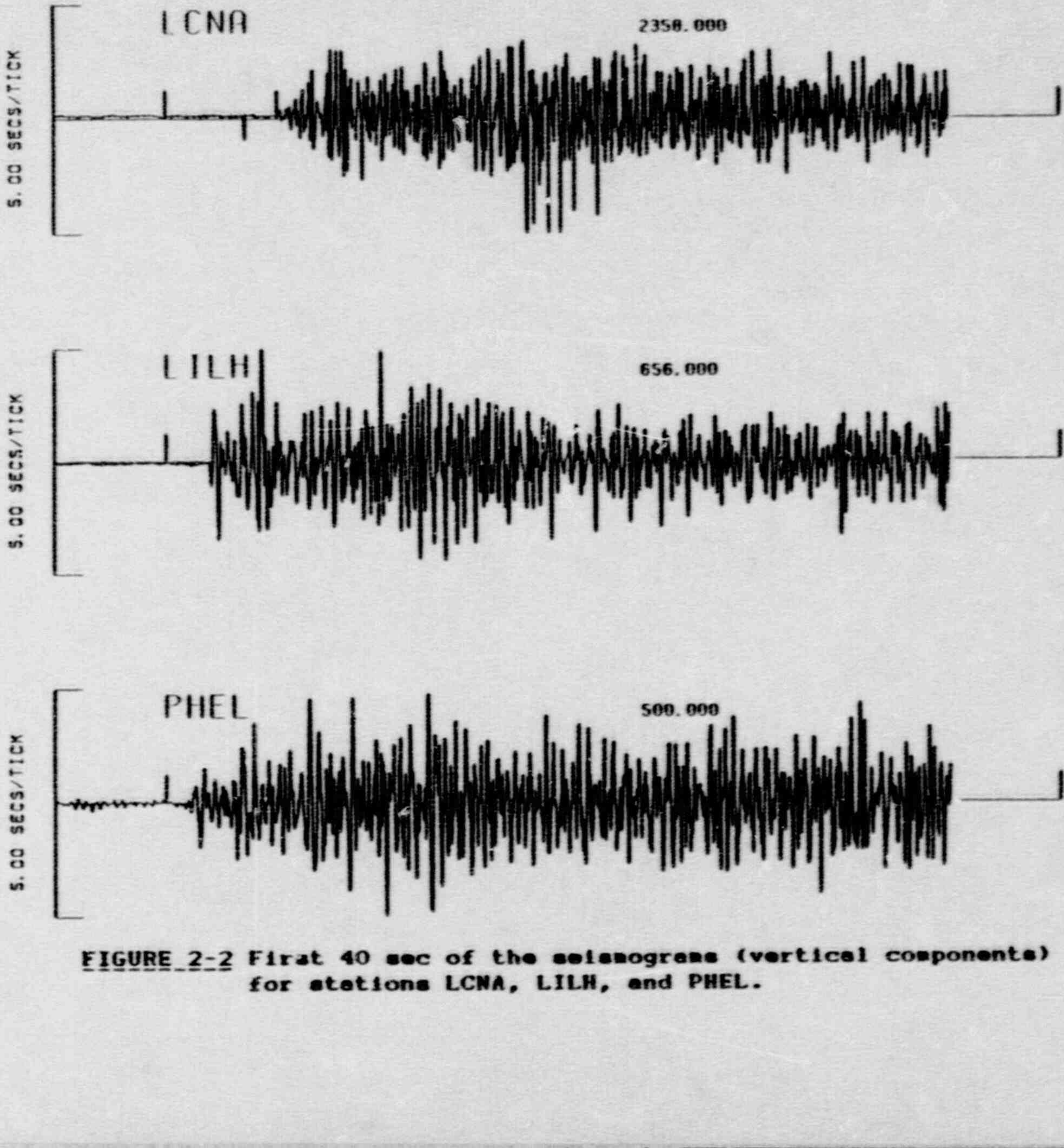

FIGURE 2-2 First 40 sec of the seismograms (vertical components) for stations LCNA, LILH, and PHEL.

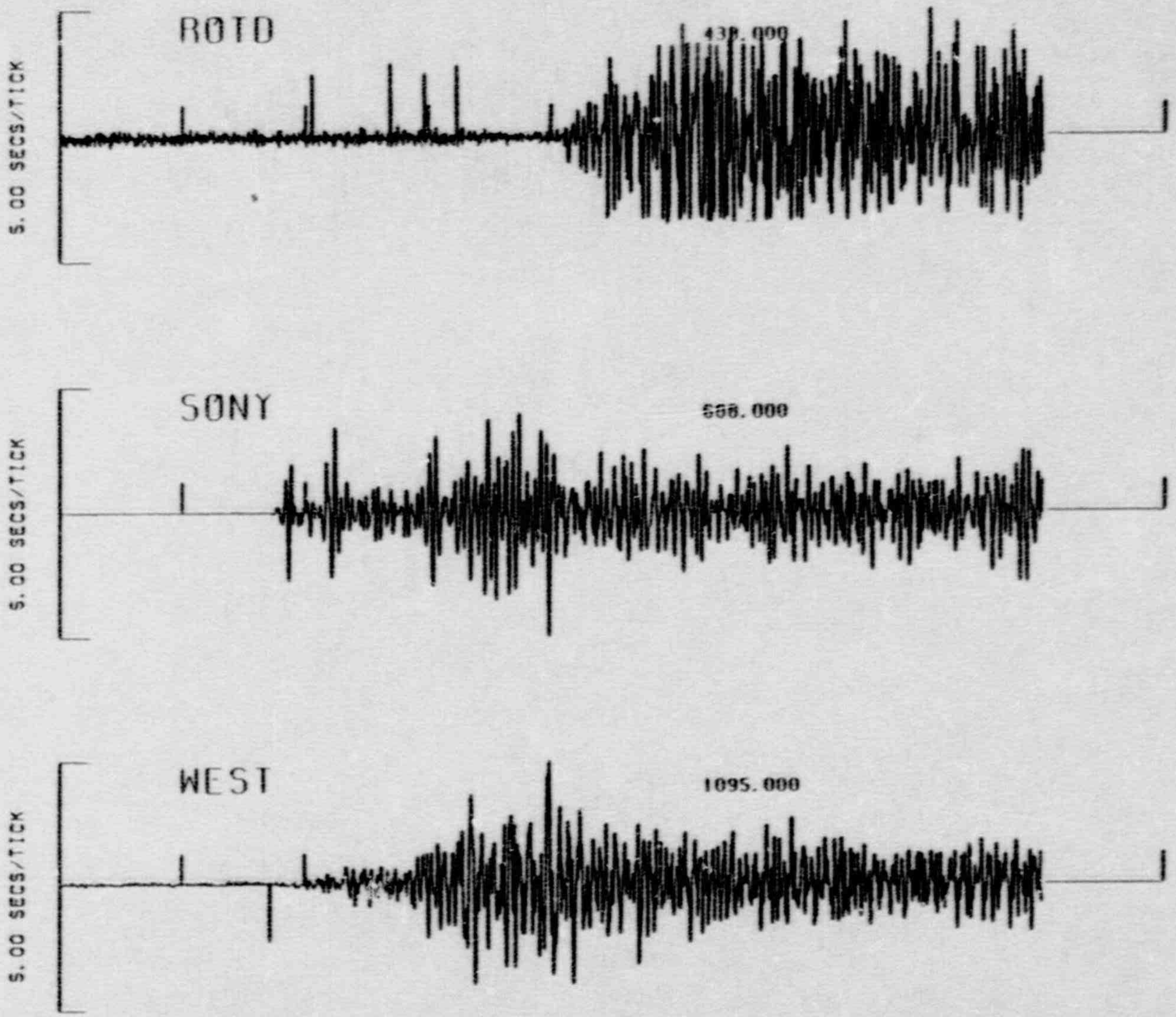

FIGURE 2-3 First 40 sec of the seismograms (vertical components) for stations ROTD, SONY, and WEST.

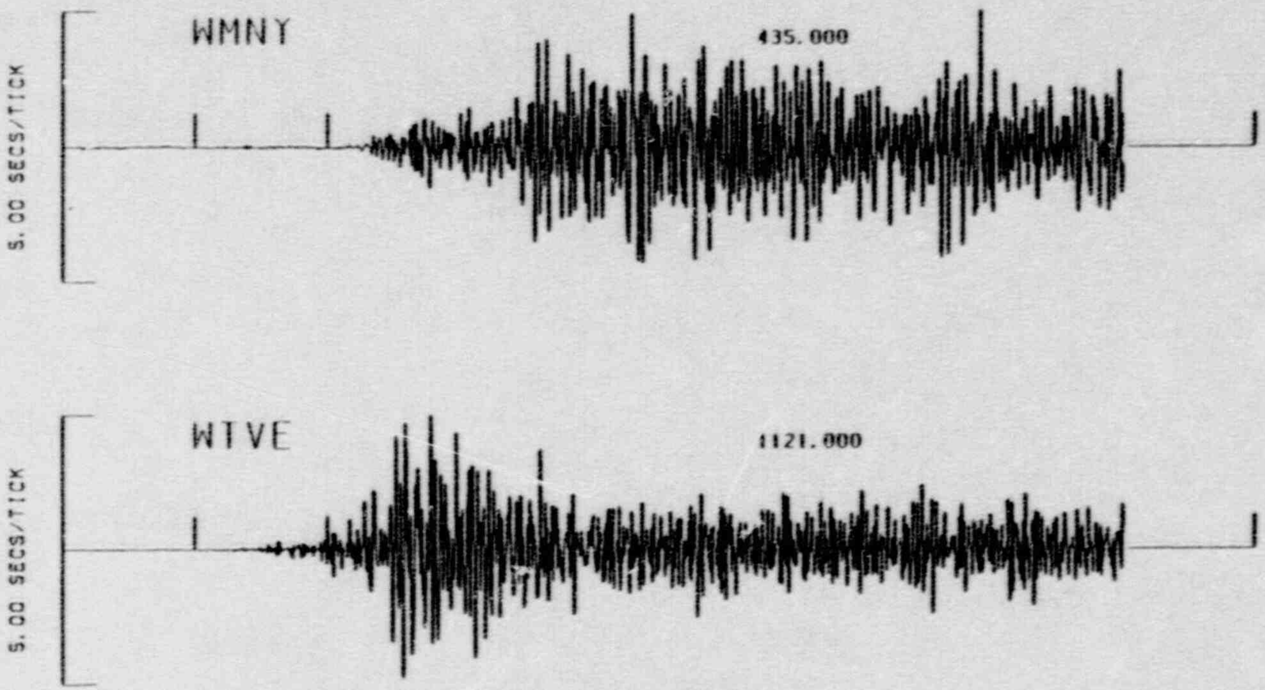

FIGURE 2-4 First 40 sec of the seismograms (vertical components) for stations WMNY and WTVE.

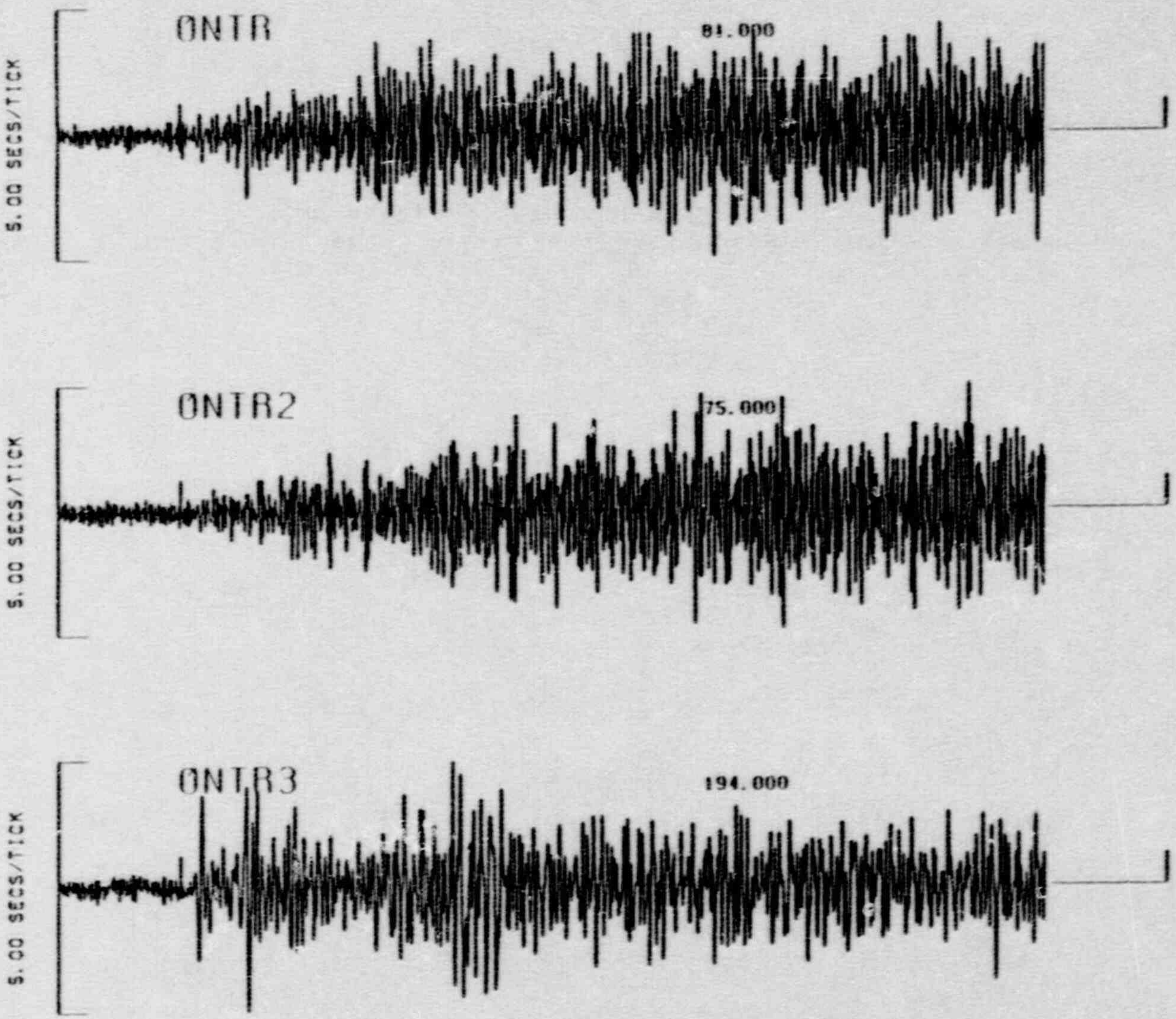

FIGURE 2-5 First 40 sec of the radial (ONTR), tangential (ONTR2), and vertical (ONTR3) components for station ONTR.

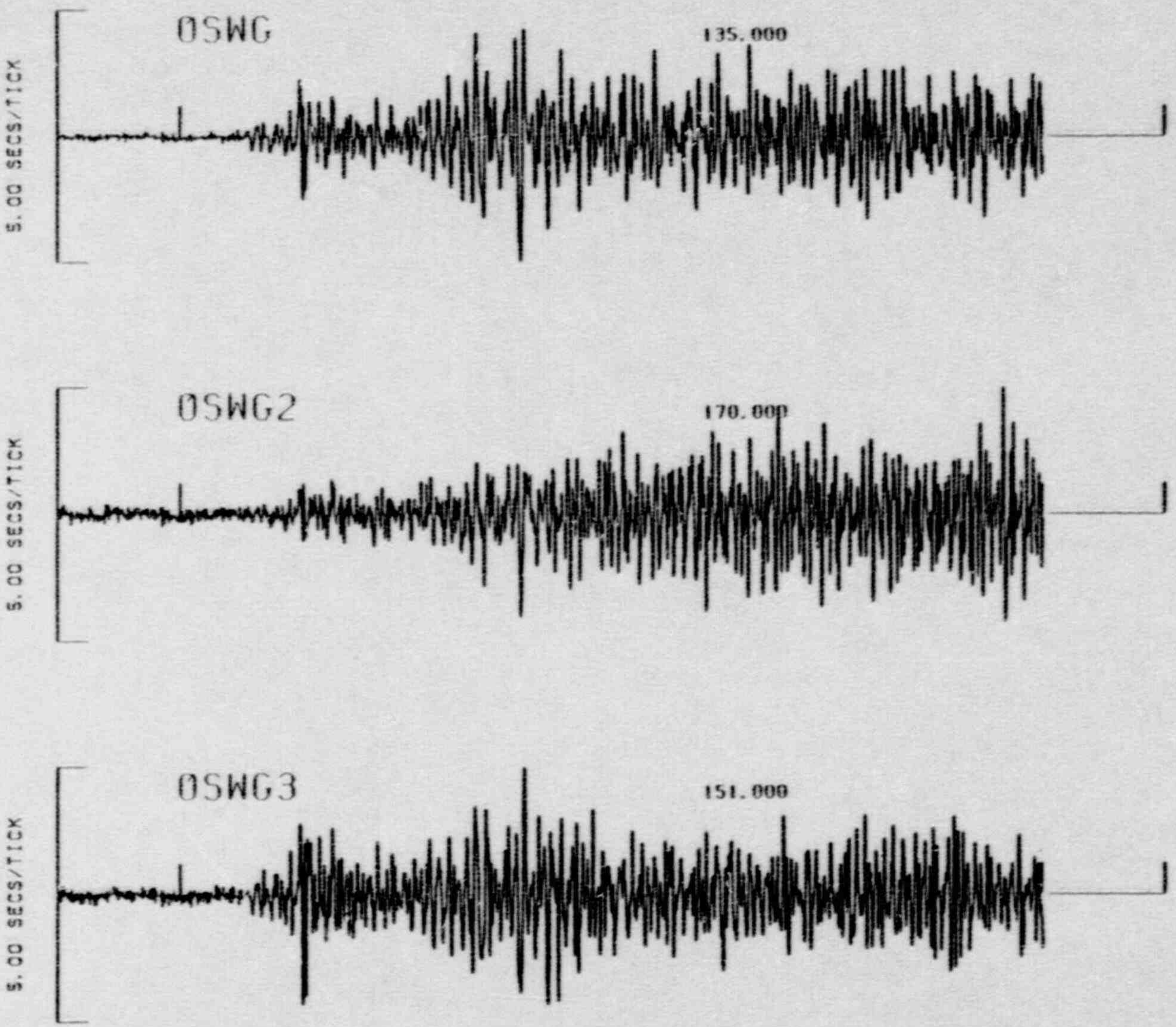

FIGURE 2-6 First 40 sec of the radial (OSWG), tangential (OSWG2), and vertical (OSWG3) components for station OSWG.

APPENDIX 3

POWER SPECTRA FOR THE APRIL 23, 1984 EARTHQUAKE

POWER SPECTRA FOR THE APRIL 23, 1984 EARTHQUAKE

The following plots are the first 10 Hertz of the power spectra for the stations used in the cepstral analysis of the April 23, 1984 earthquake of Lancaster County, Pennsylvania. Two plots are given for each station. The top plot shows the smoothed noise power spectrum (dashed line) superimposed onto the signal and noise power spectrum for a 10 second time window. The lower plot shows the smoothed noise power spectrum (dashed line) superimposed onto the signal and noise power spectrum for a 20 second time window. The maximum values for the 10 second and the 20 second windowed power spectra are listed in the upper right-hand corner of the top and bottom plot respectively. The three power spectra for each station are plotted on the same vertical scale which is determined by the maximum value of all of them. The time windows used for each station is listed on the following page.

LIST OF FIGURES FOR APPENDIX 3

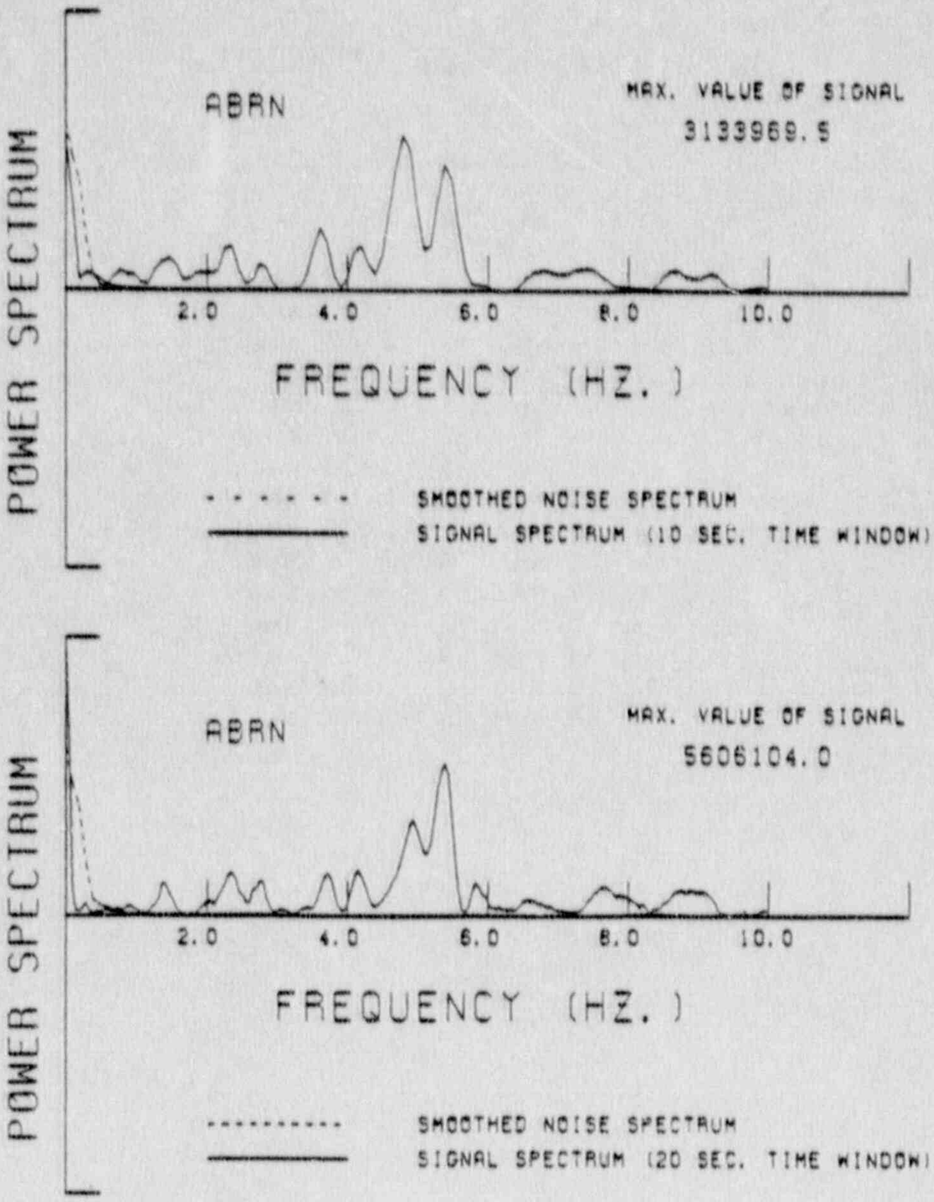

FIGURE 3-1 Power spectral density for a 10 sec window (top) and a 20 sec window (bottom) of station ABRN.

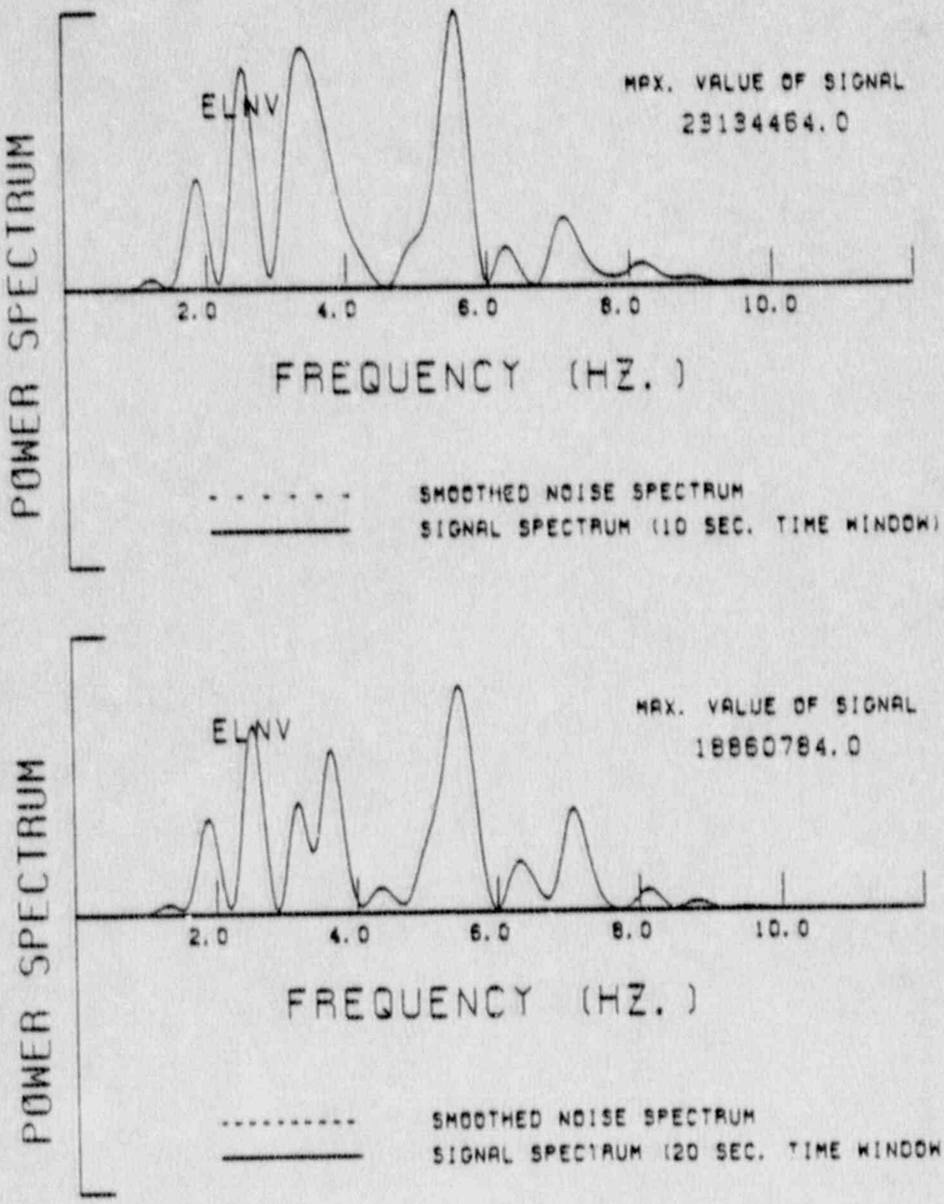

FIGURE 3-2 Power spectral density for a 10 sec window (top) and a 20 sec window (bottom) of station ELNV.

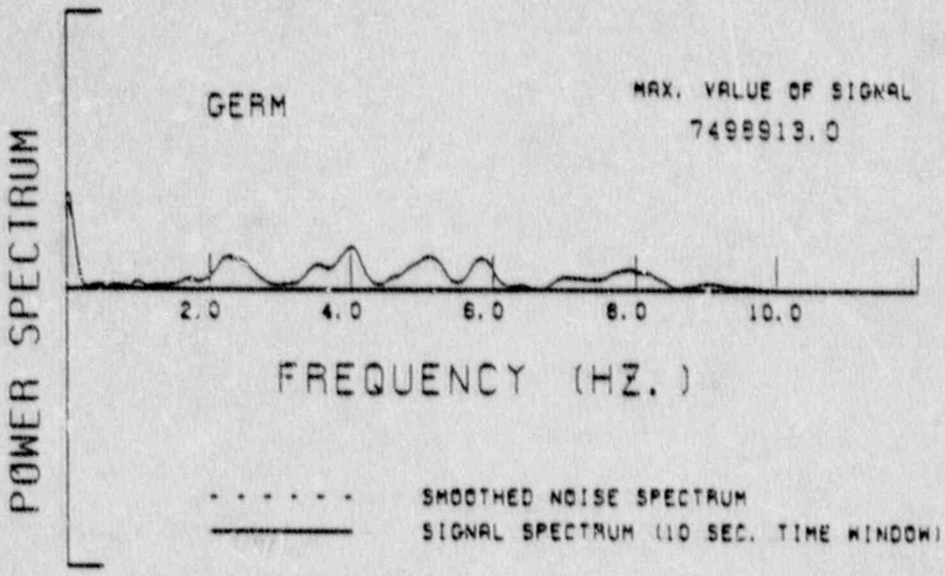

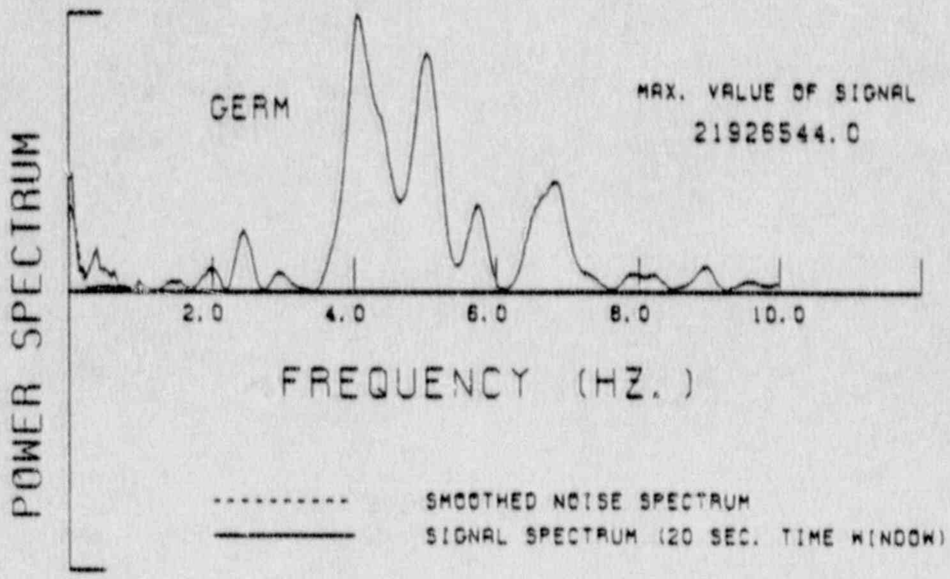

FIGURE 3-3 Power spectral density for a 10 sec window (top) and a 20 sec window (bottom) of station GERM.

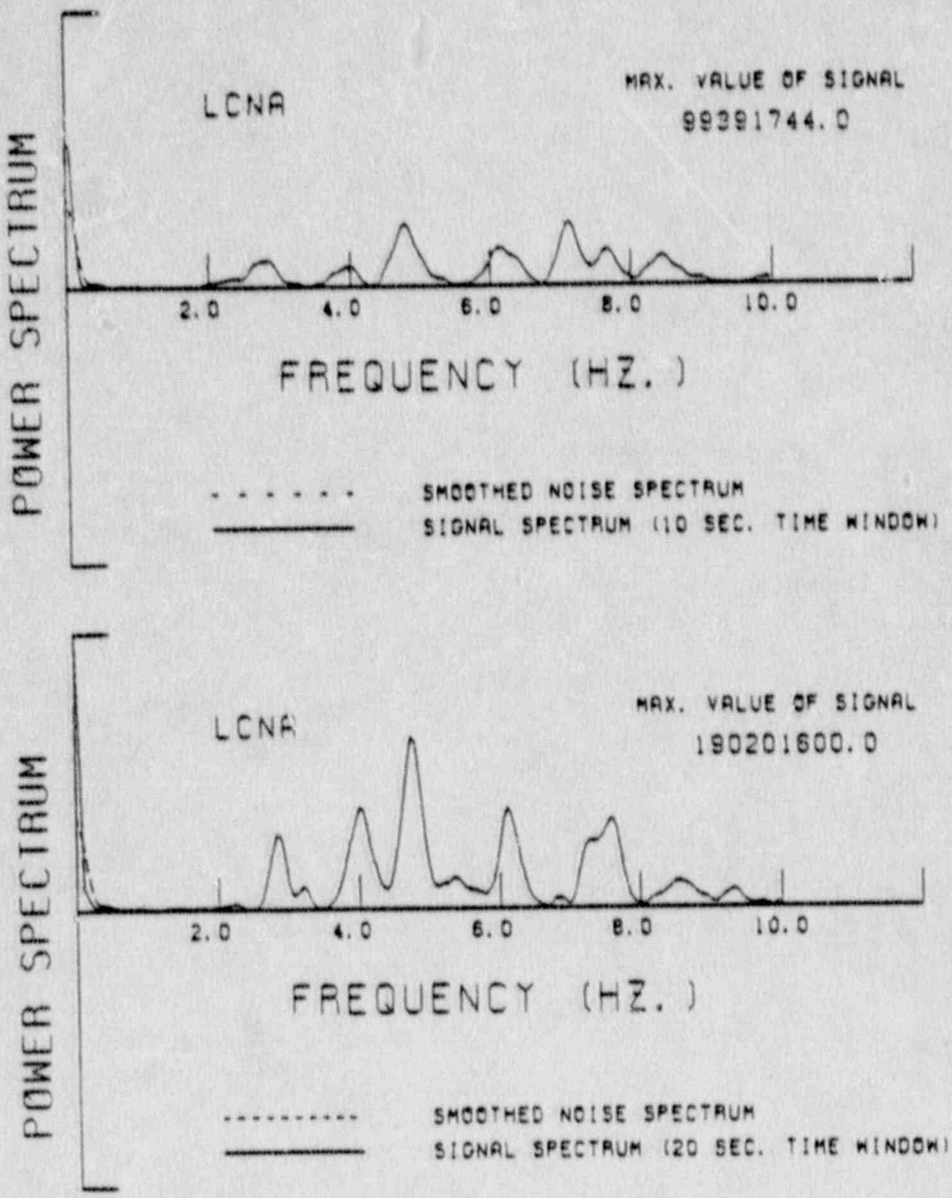

FIGURE 3-4 Power spectral density for a 10 sec window (top) and a 20 sec window (bottom) of station LCNA.

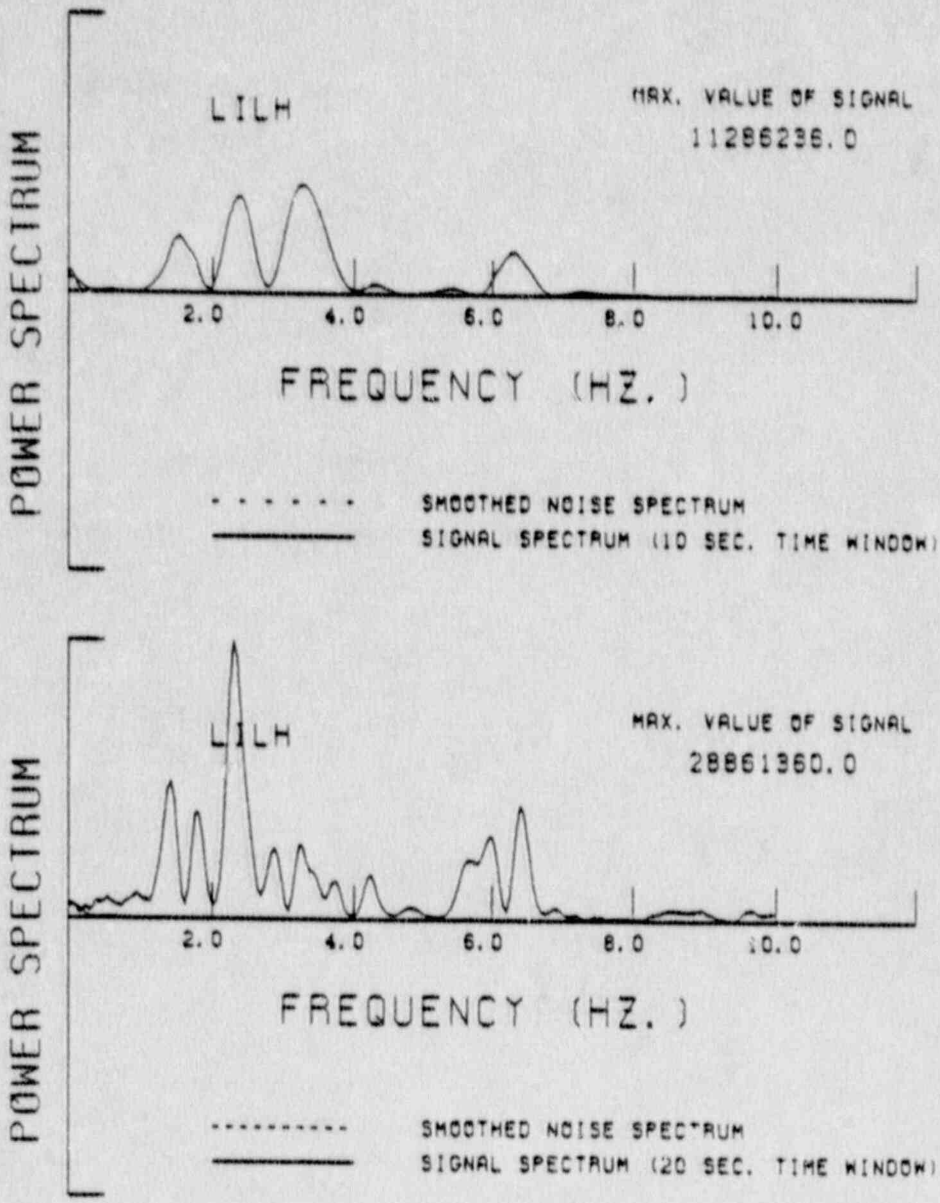

FIGURE 3-5 Power spectral density for a 10 sec window (top) and a 20 sec window (bottom) of station LILH.

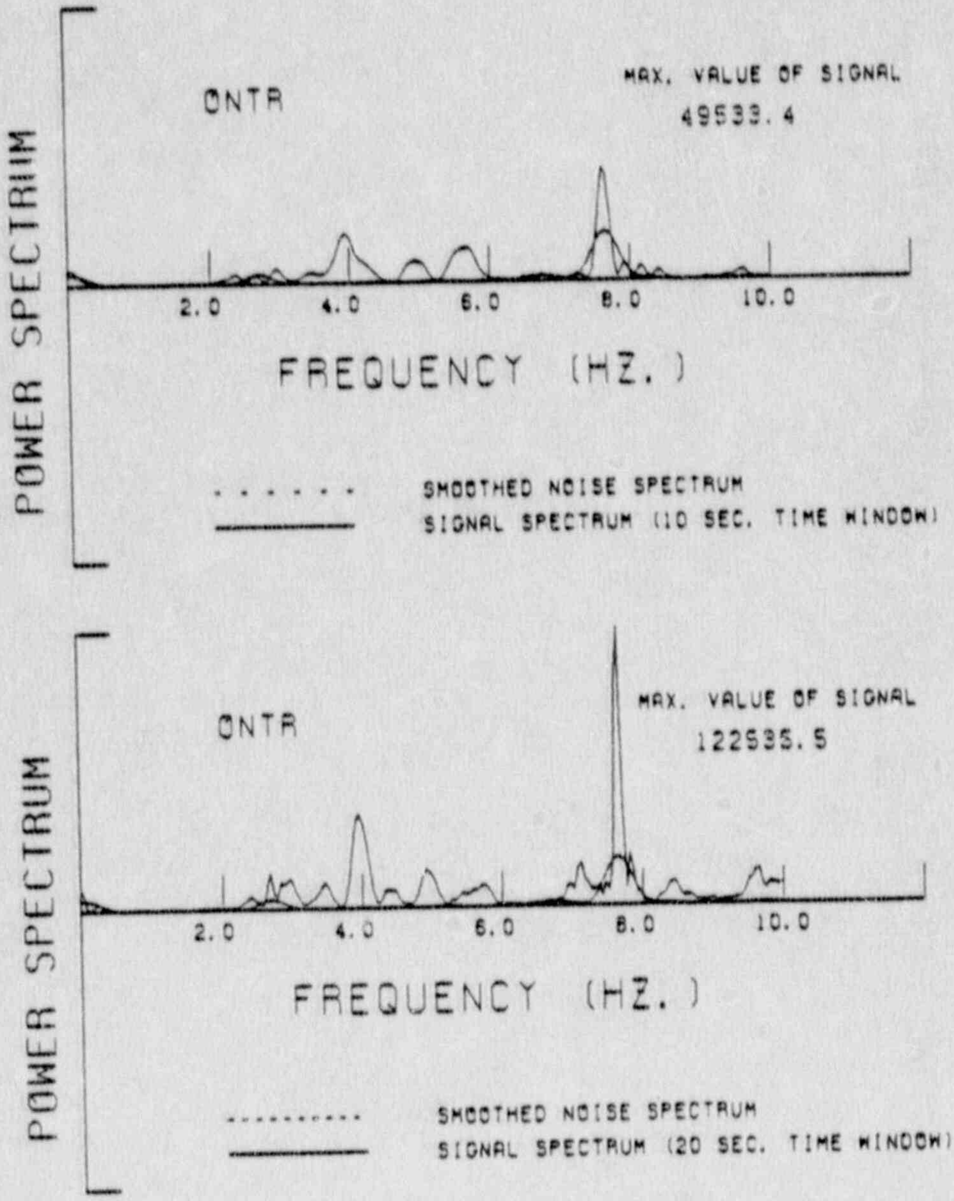

FIGURE 3-6 Power spectral density for a 10 sec window (top) and a 20 sec window (bottom) of station ONTR (radial).

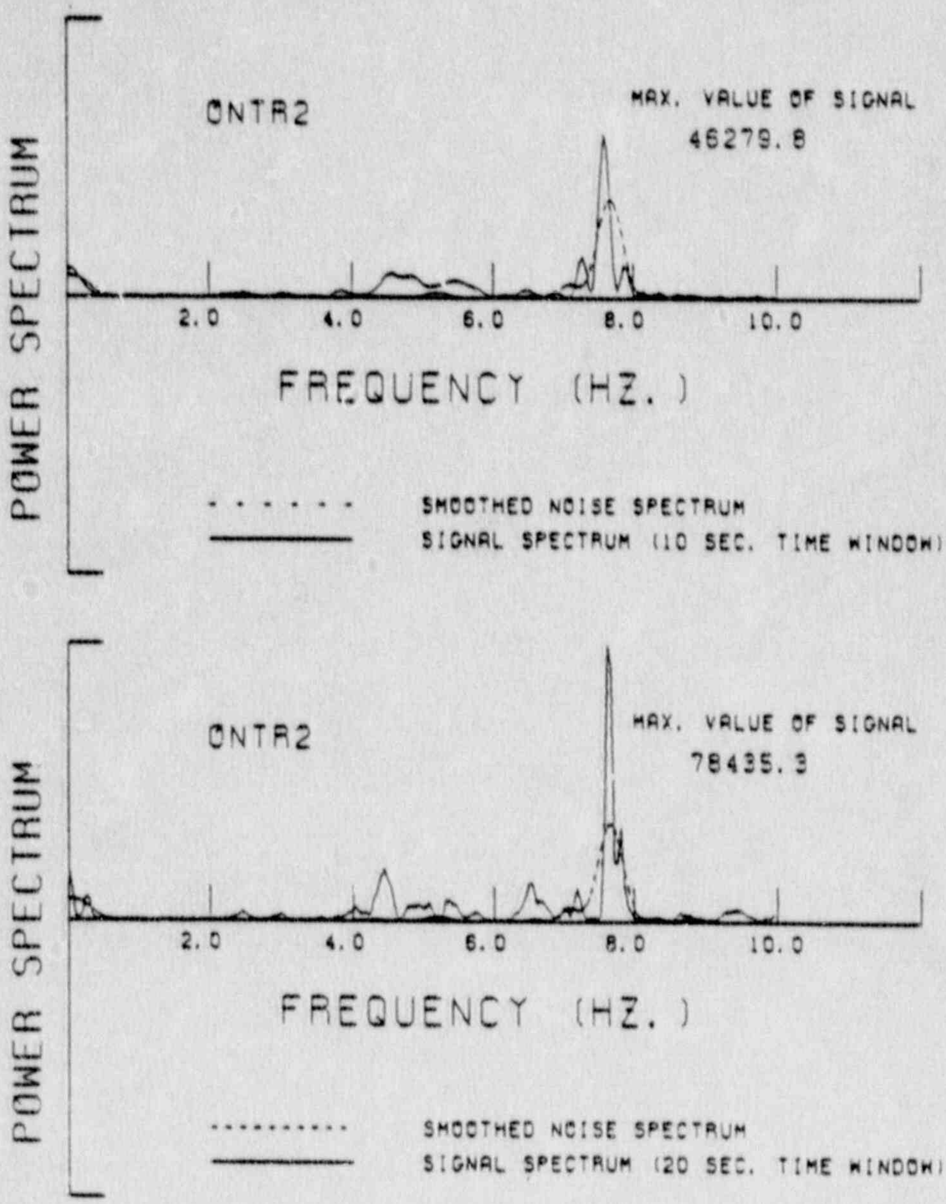

FIGURE 3-7 Power spectral density for a 10 sec window (top) and a 20 sec window (bottom) of station ONTR (tangential).

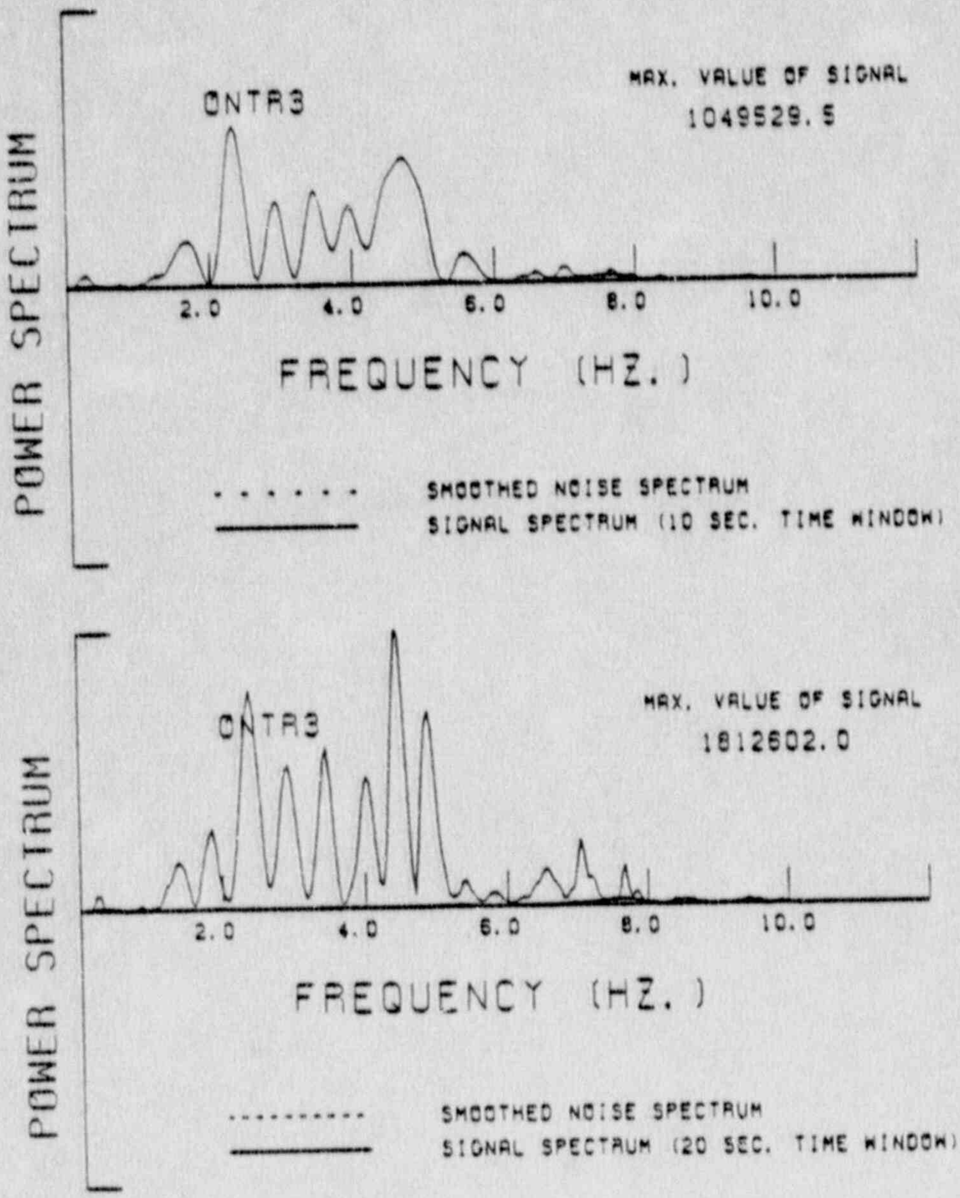

FIGURE 3-8 Power spectral density for a 10 sec window (top) and a 20 sec window (bottom) of station ONTR (vertical).

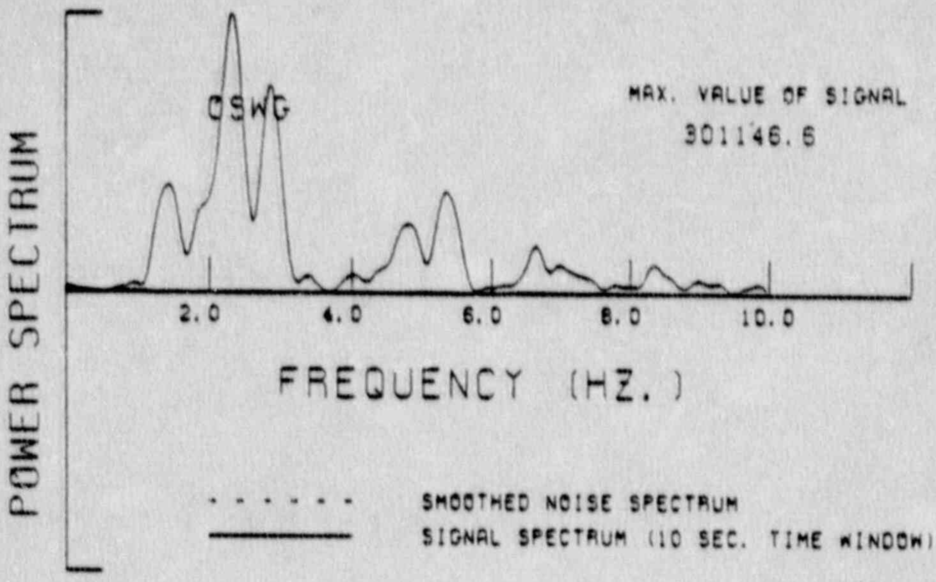

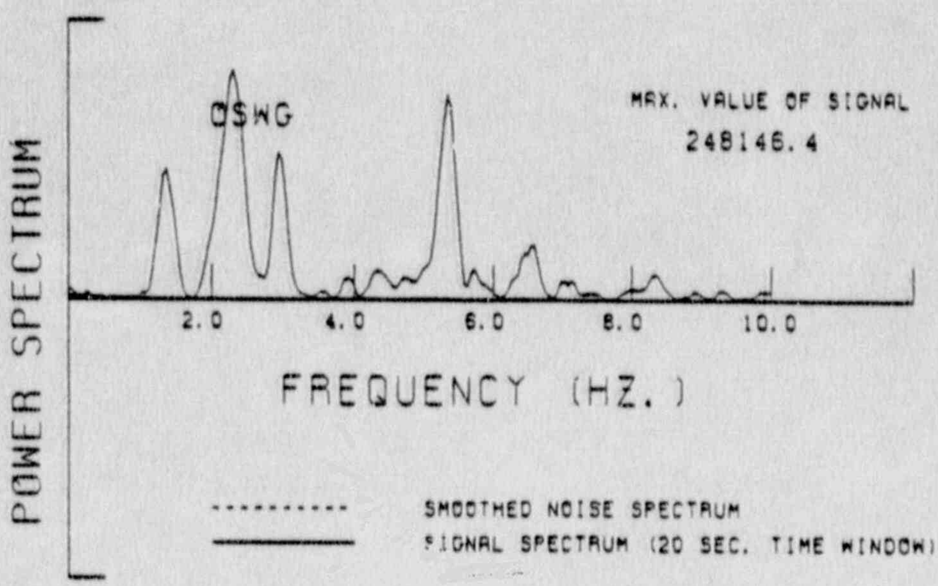

FIGURE 3-9 Power spectral density for a 10 sec window (top) and a 20 sec window (bottom) of station OSWG (radial).

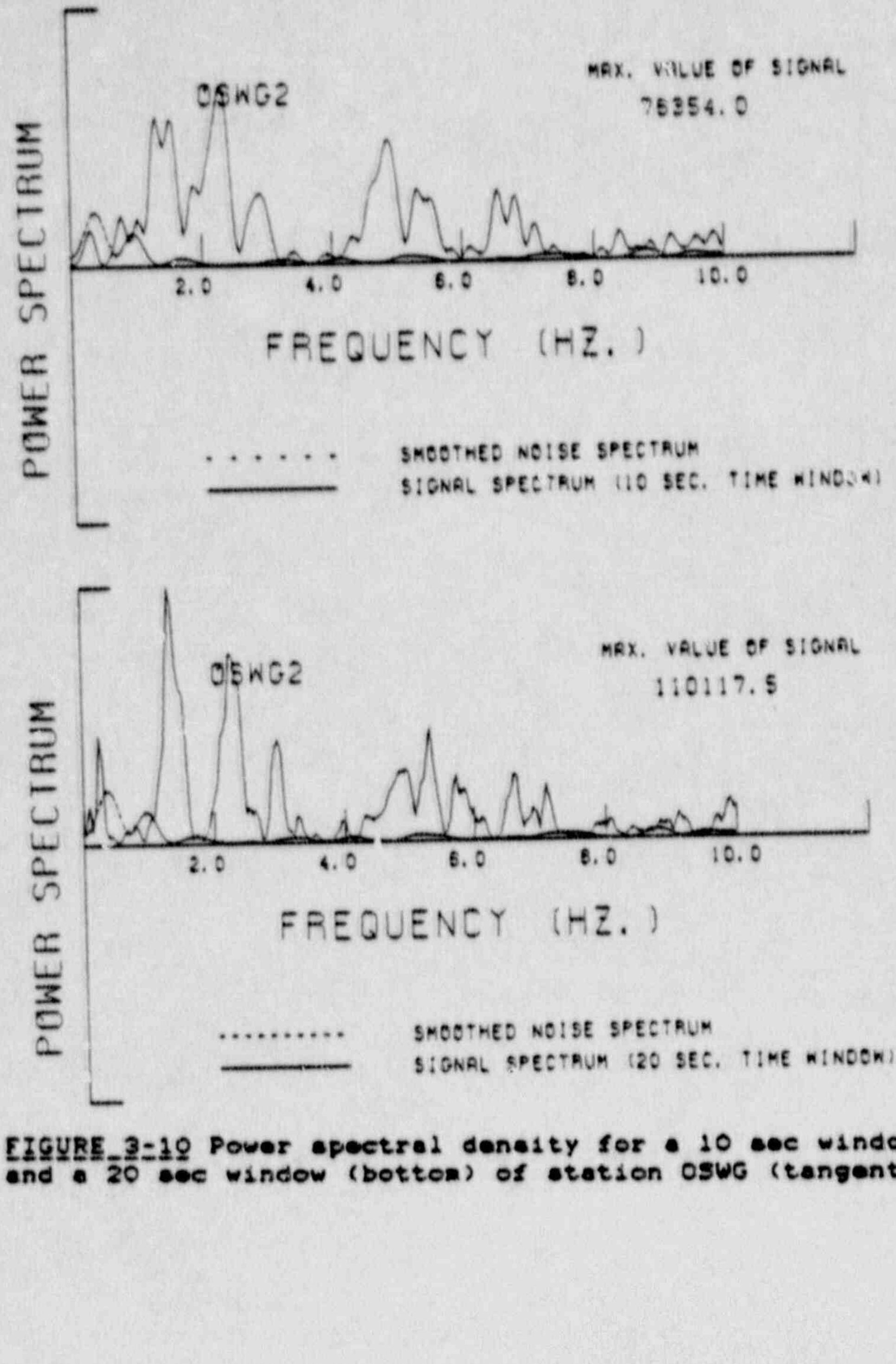

FIGURE 3-10 Power spectral density for a 10 sec window (top) and a 20 sec window (bottom) of station OSWG (tangential).

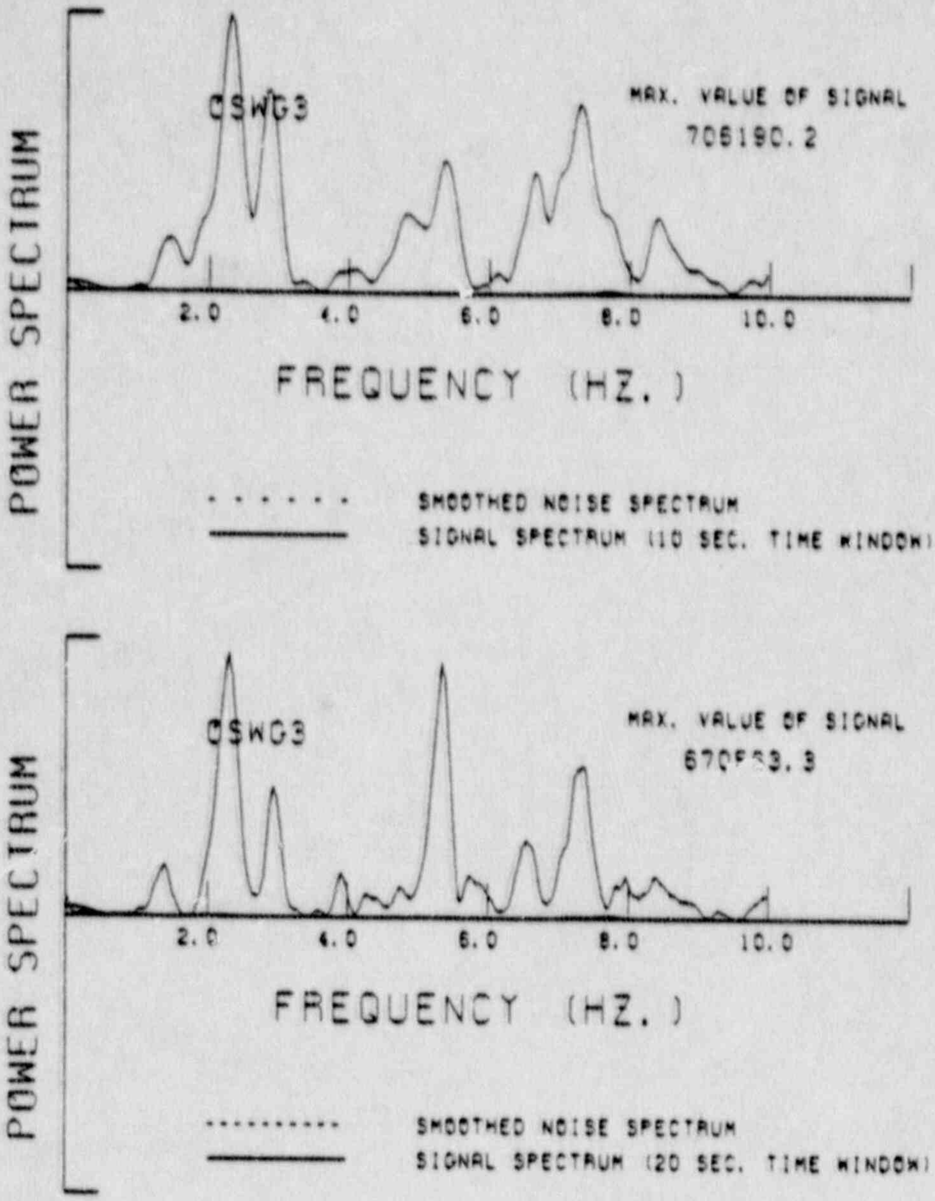

FIGURE 3-11 Power spectral density for a 10 sec window (top) and a 20 sec window (bottom) of station OSWG (vertical).

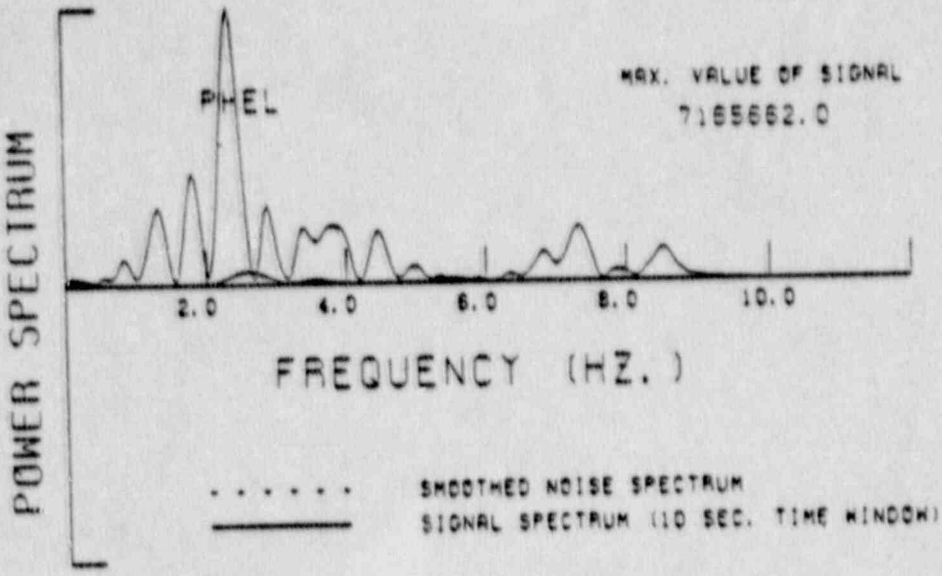

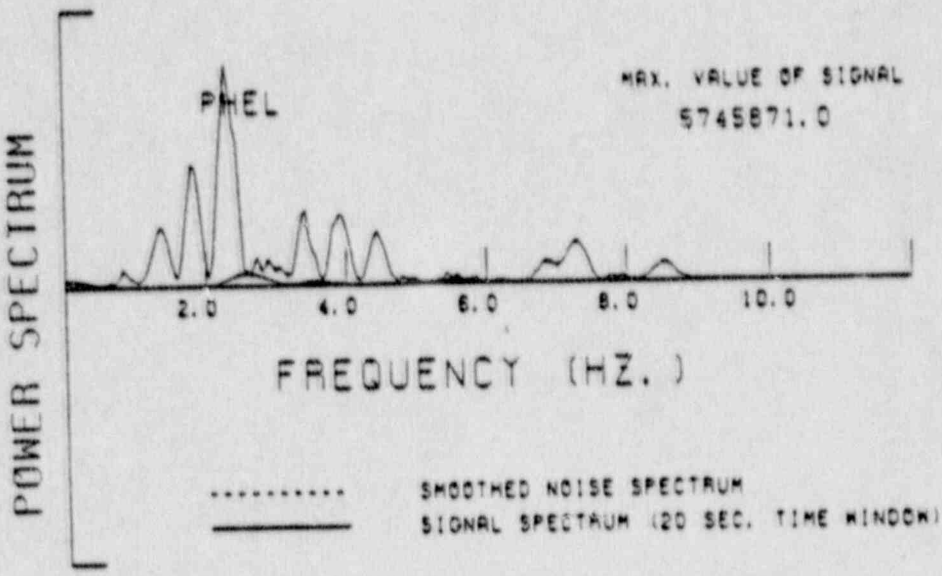

FIGURE 3-12 Power spectral density for a 10 sec window (top) and a 20 sec window (bottom) of station PHEL.

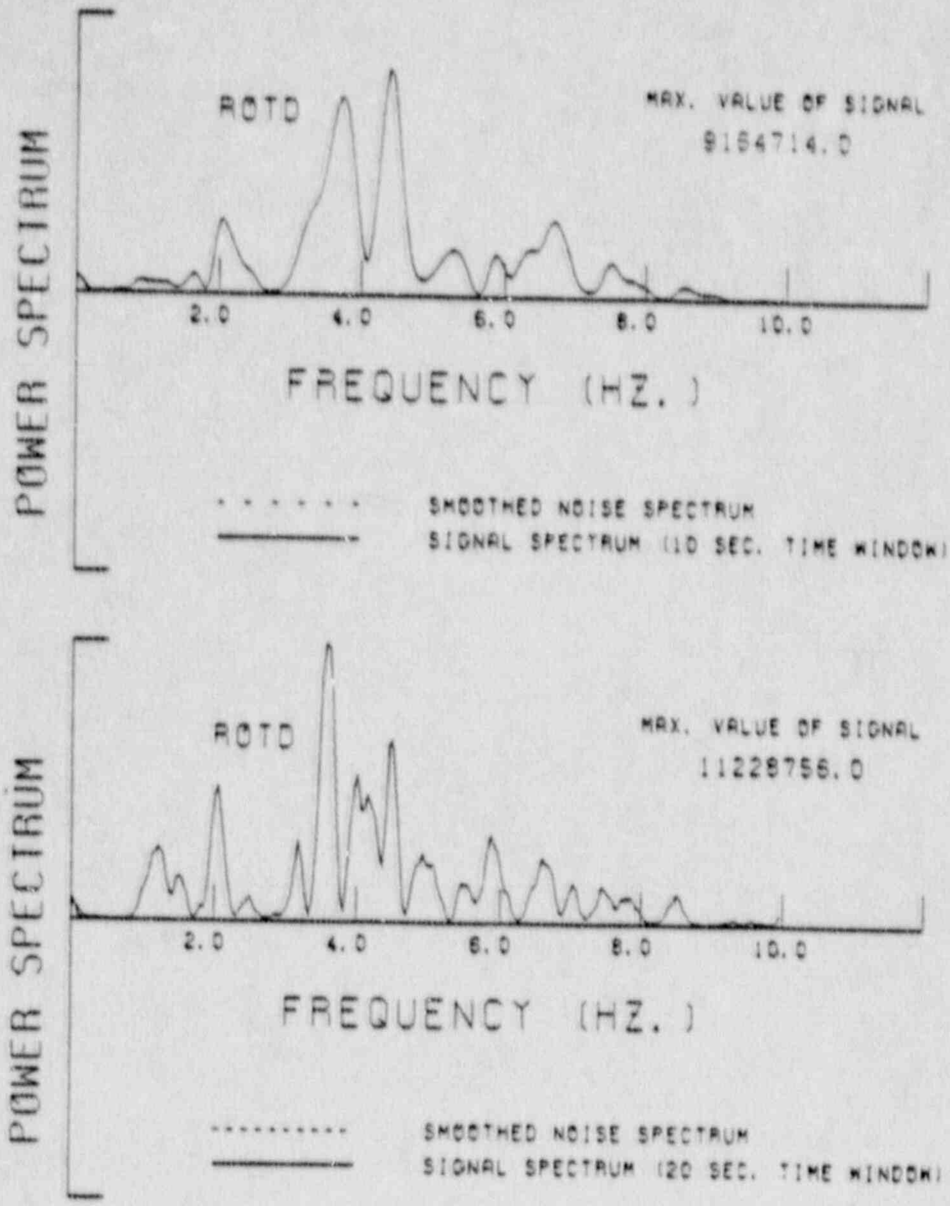

FIGURE 3-13 Power spectral density for a 10 sec window (top) and a 20 sec window (bottom) of station ROTD.

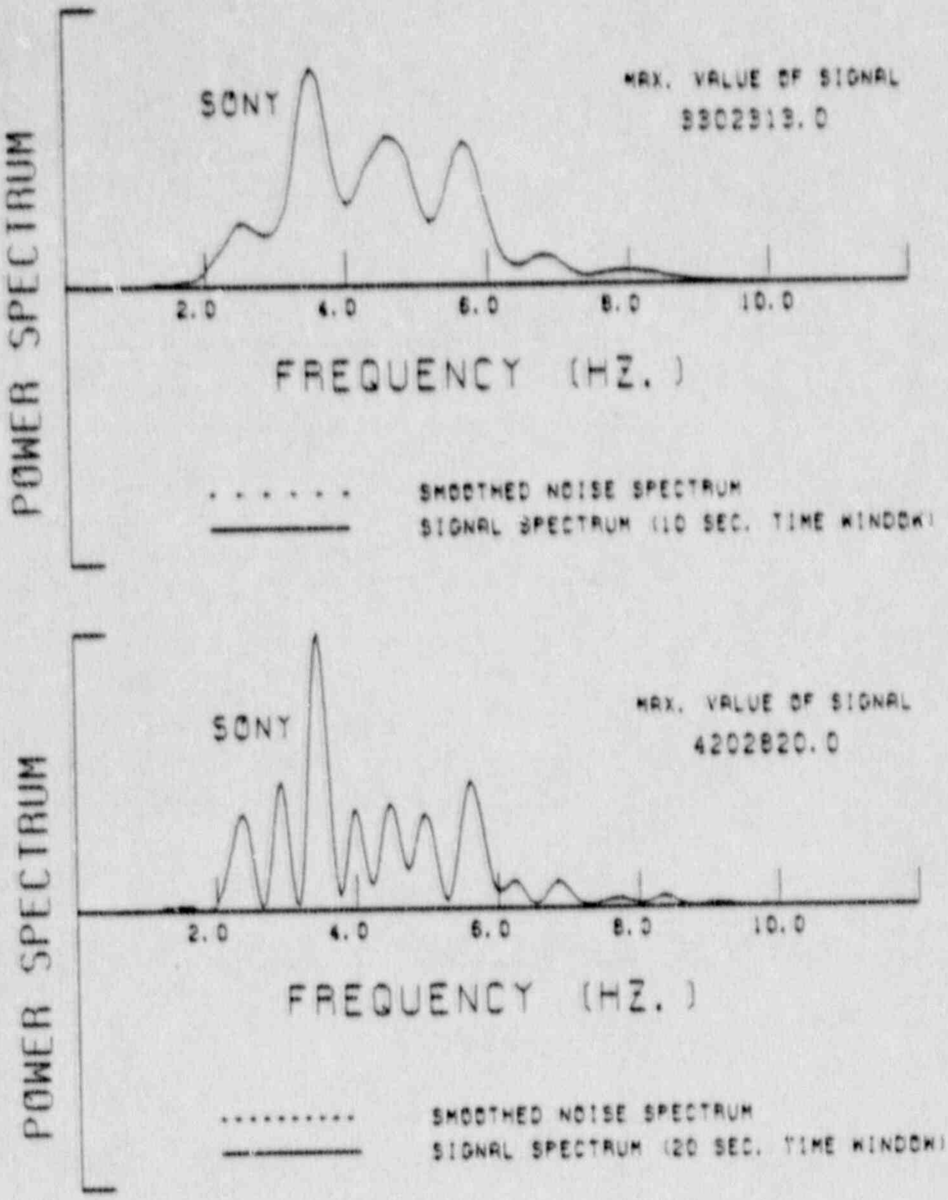

FIGURE 3-14 Power spectral density for a 10 sec window (top) and a 20 sec window (bottom) of station SONY.

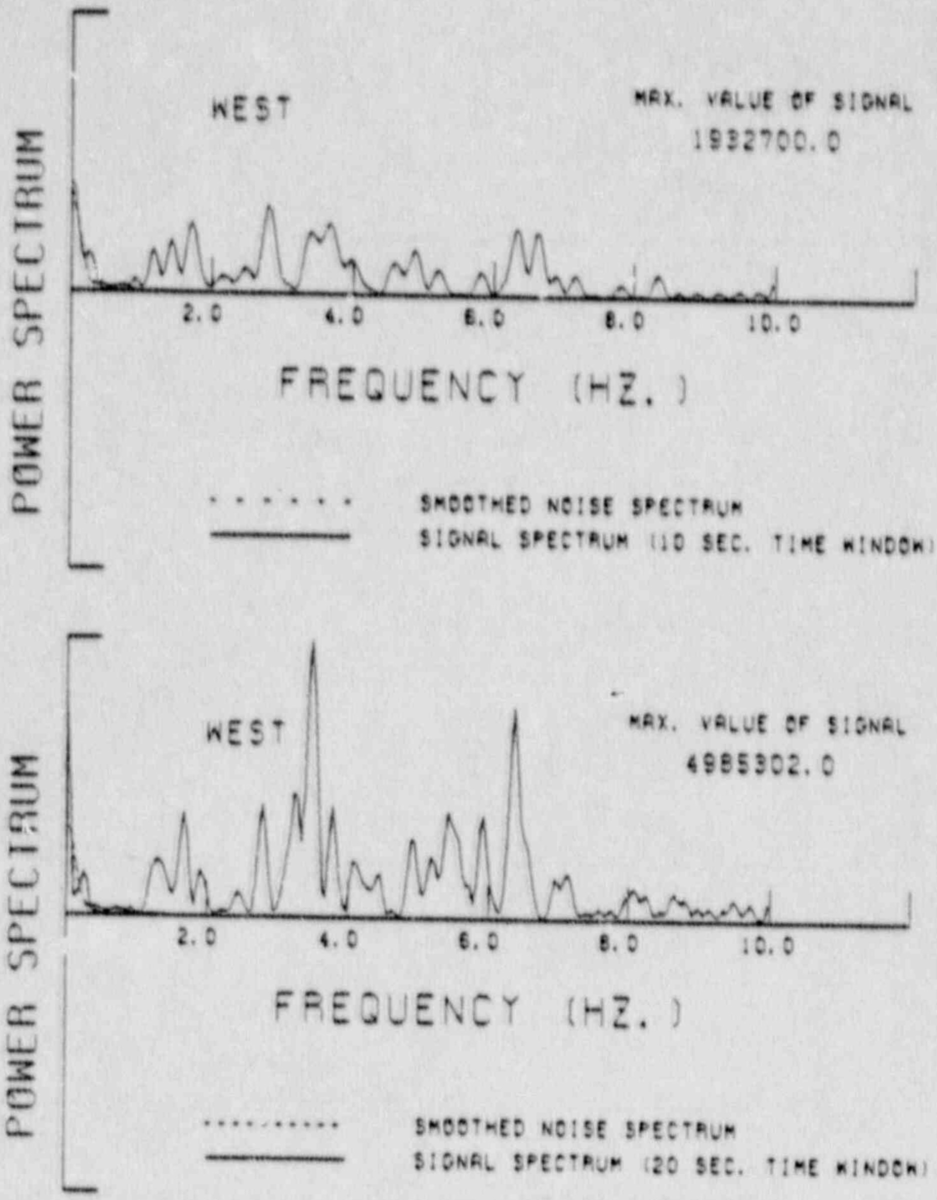

FIGURE 3-15 Power spectral density for a 10 sec window (top) and a 20 sec window (bottom) of station WEST.

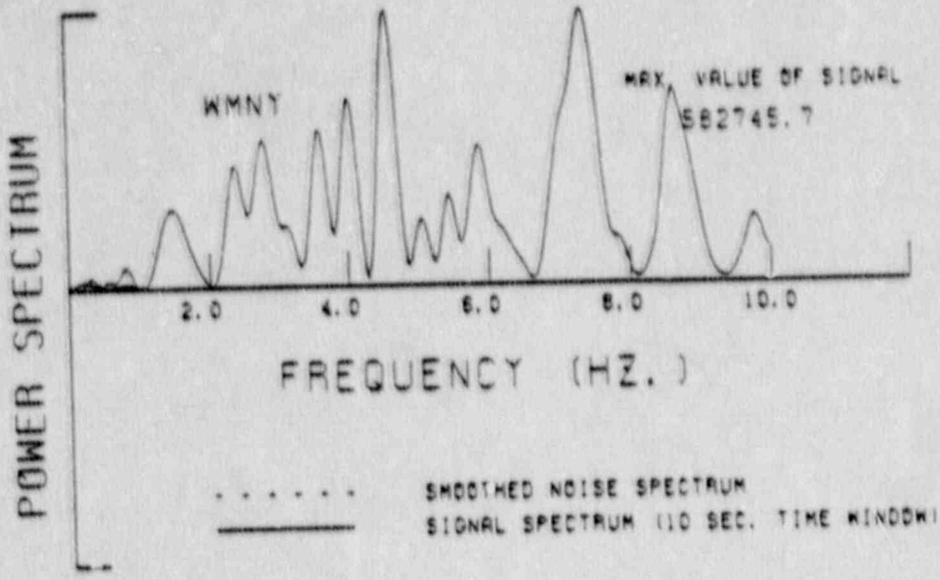

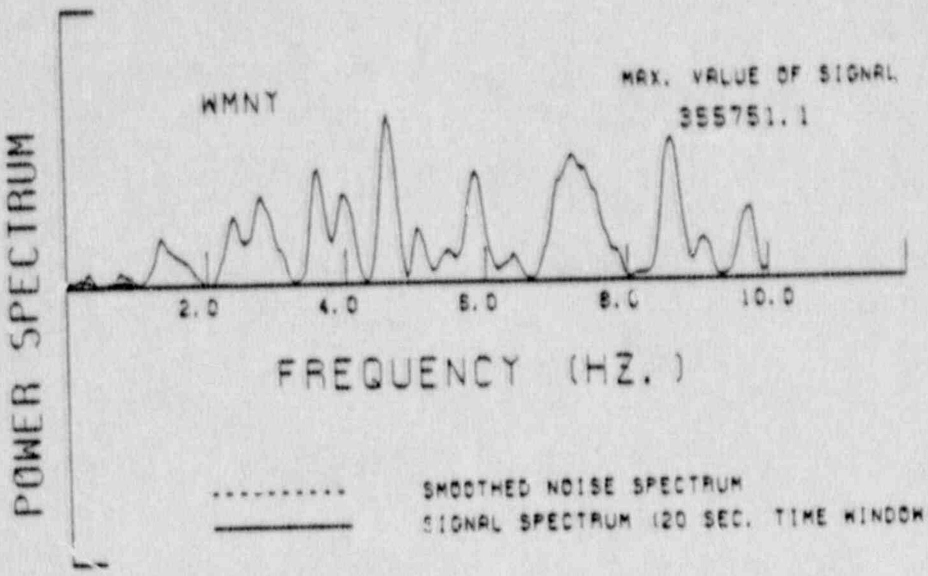

FIGURE 3-16 Power spectral density for a 10 sec window (top) and a 20 sec window (bottom) of station WMNY.

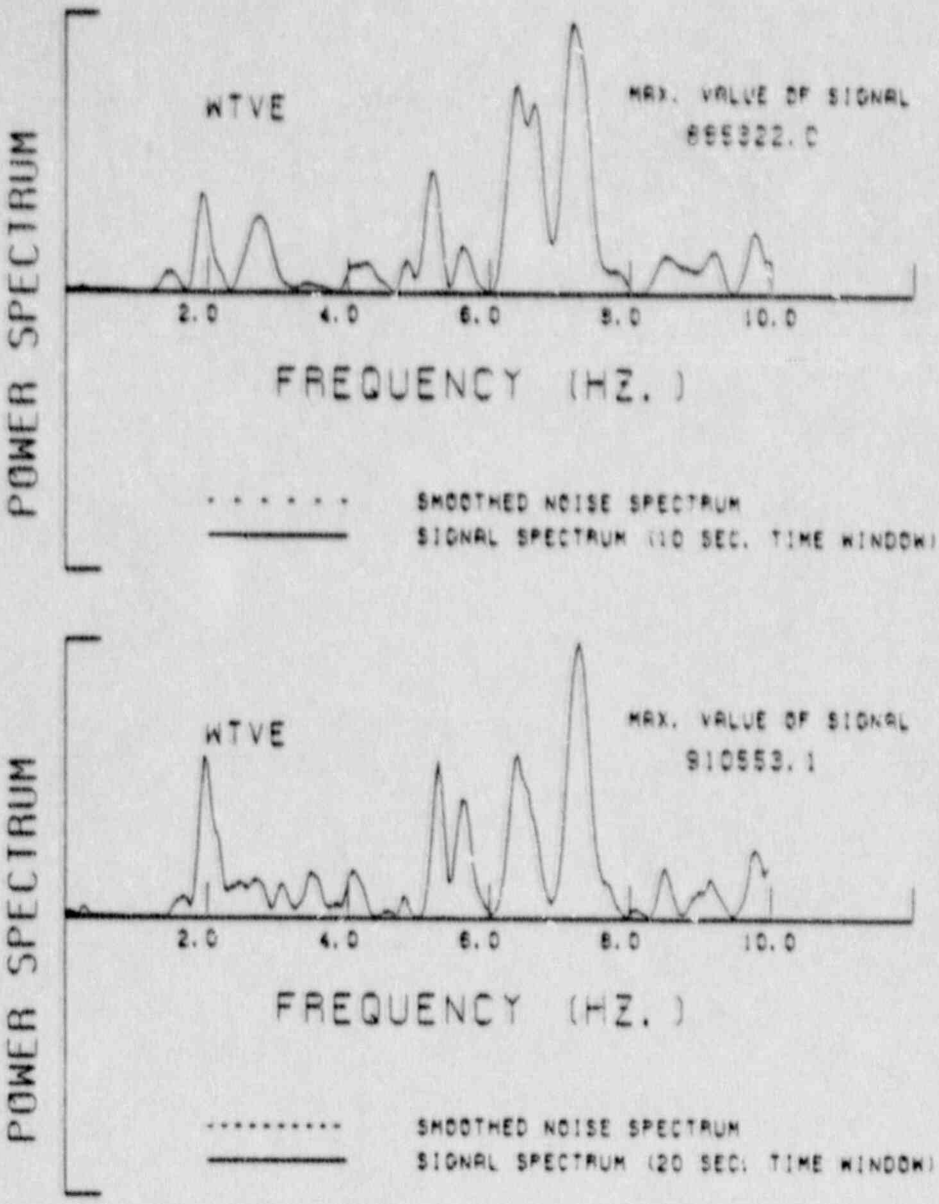

FIGURE 3-17 Power spectral density for a 10 sec window (top) and a 20 sec window (bottom) of station WTVE.

APPENDIX 4

CEPSTRA FOR THE APRIL 23, 1984 EARTHQUAKE

CEPSTRA FOR THE APRIL 23, 1984 EARTHQUAKE

The following plots are the first 10 quefrency seconds of the cepstra for the windowed power spectra from the stations used in the cepstral analysis of the April 23, 1984 earthquake in Lancaster County, Pennsylvania. Two plots are shown for each station. The top plot is the cepstrum of the 10 second windowed signal, and the bottom plot is the cepstrum for the 20 second windowed signal. The power spectrum was windowed in the region were the noise to signal ratio is minimal. Each frequency window was padded to the same number of points. The frequency window used for each station is listed at the bottom of each plot, and in the table on the following page.

LIST OF FIGURES FOR APPENDIX 4

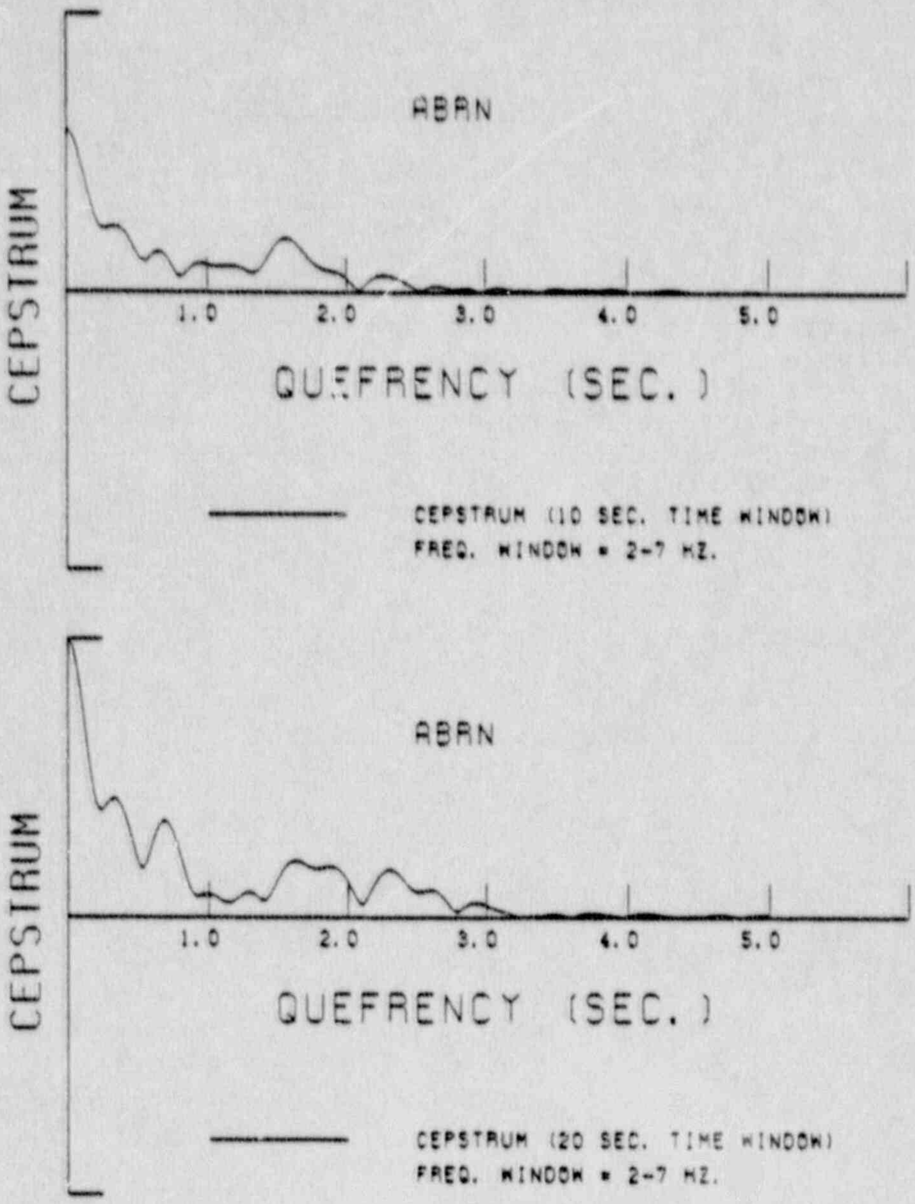

FIGURE 4-1 The cepstrum for a 10 sec window (top) and a 20 sec window (bottom) of station ABRN.

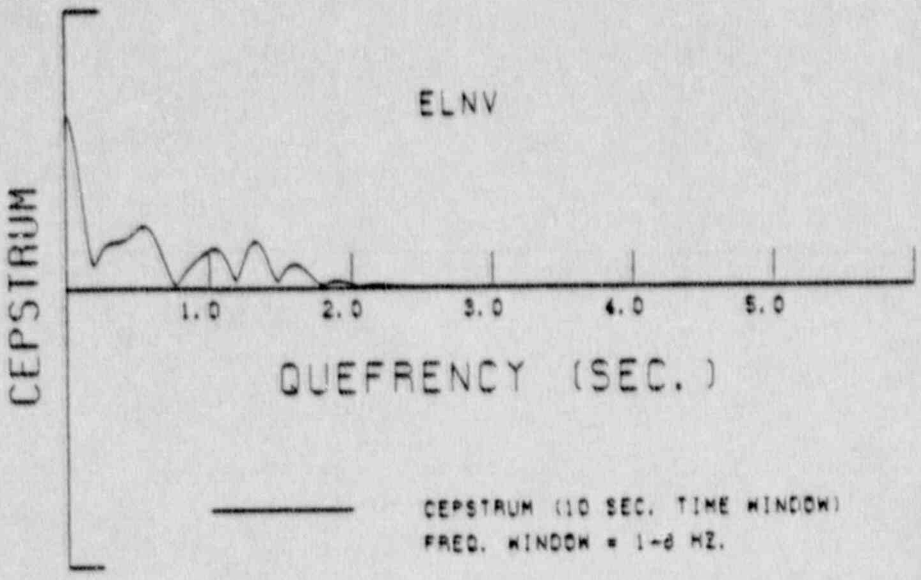

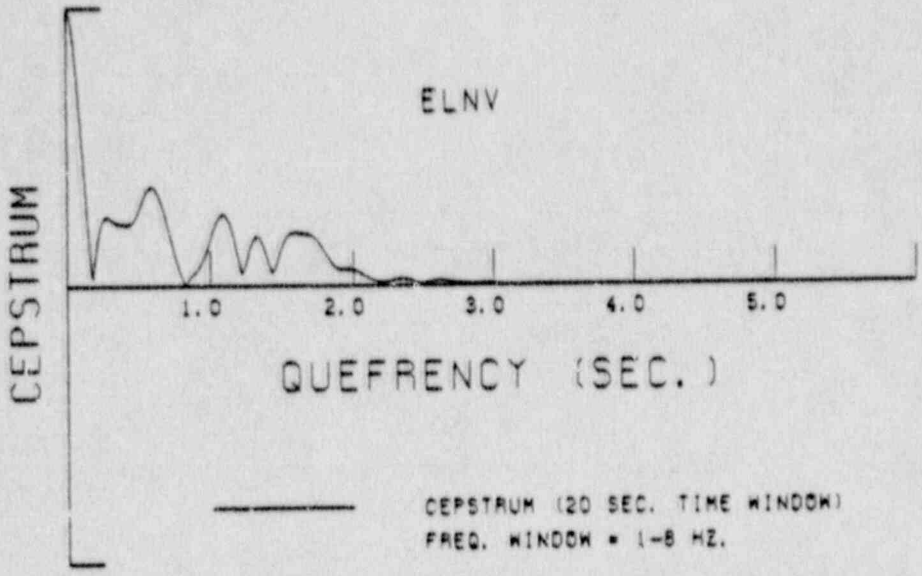

FIGURE 4-2 The cepstrum for a 10 sec window (top) and a 20 sec window (bottom) of station ELNV.

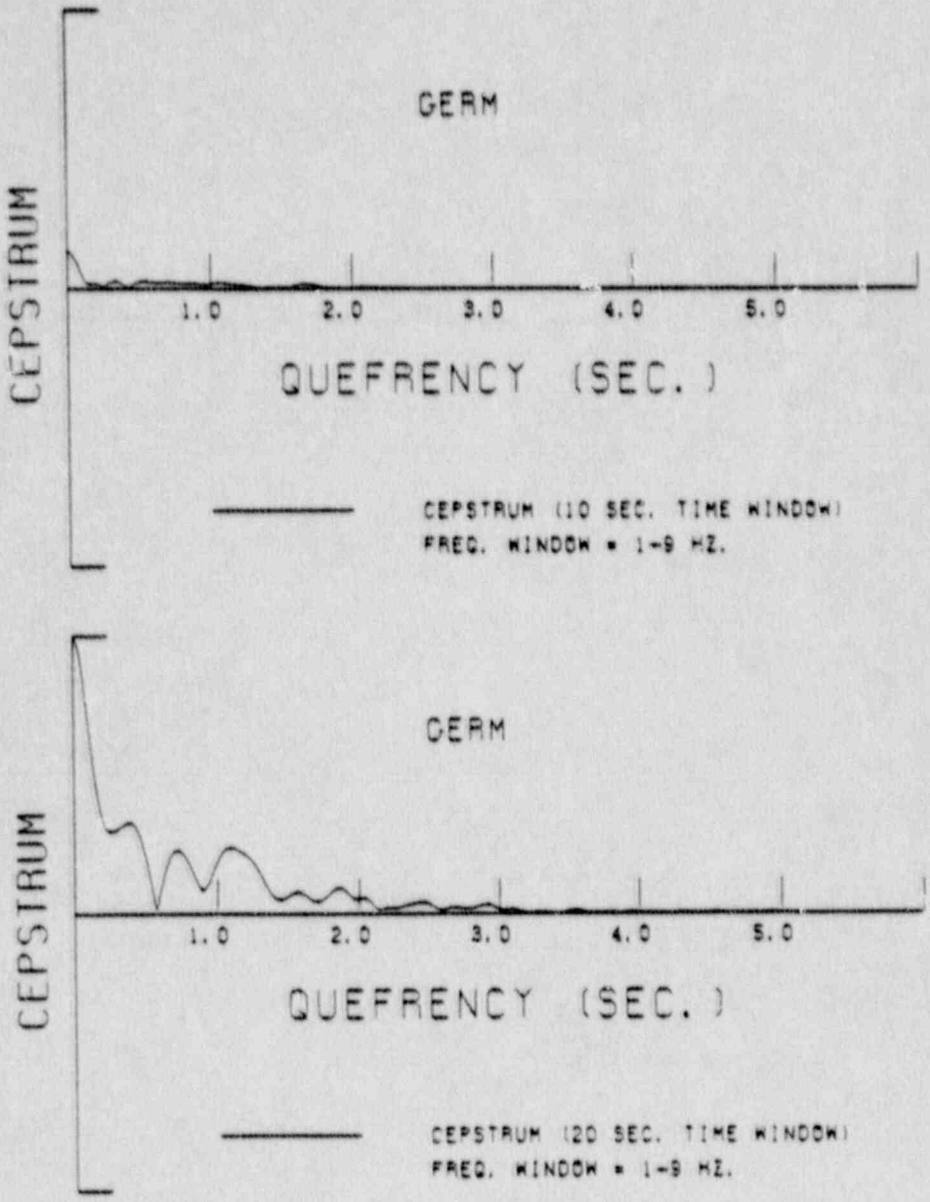

FIGURE_4-3 The cepstrum for a 10 sec window (top) and a 20 sec window (bottom) of station GERM.

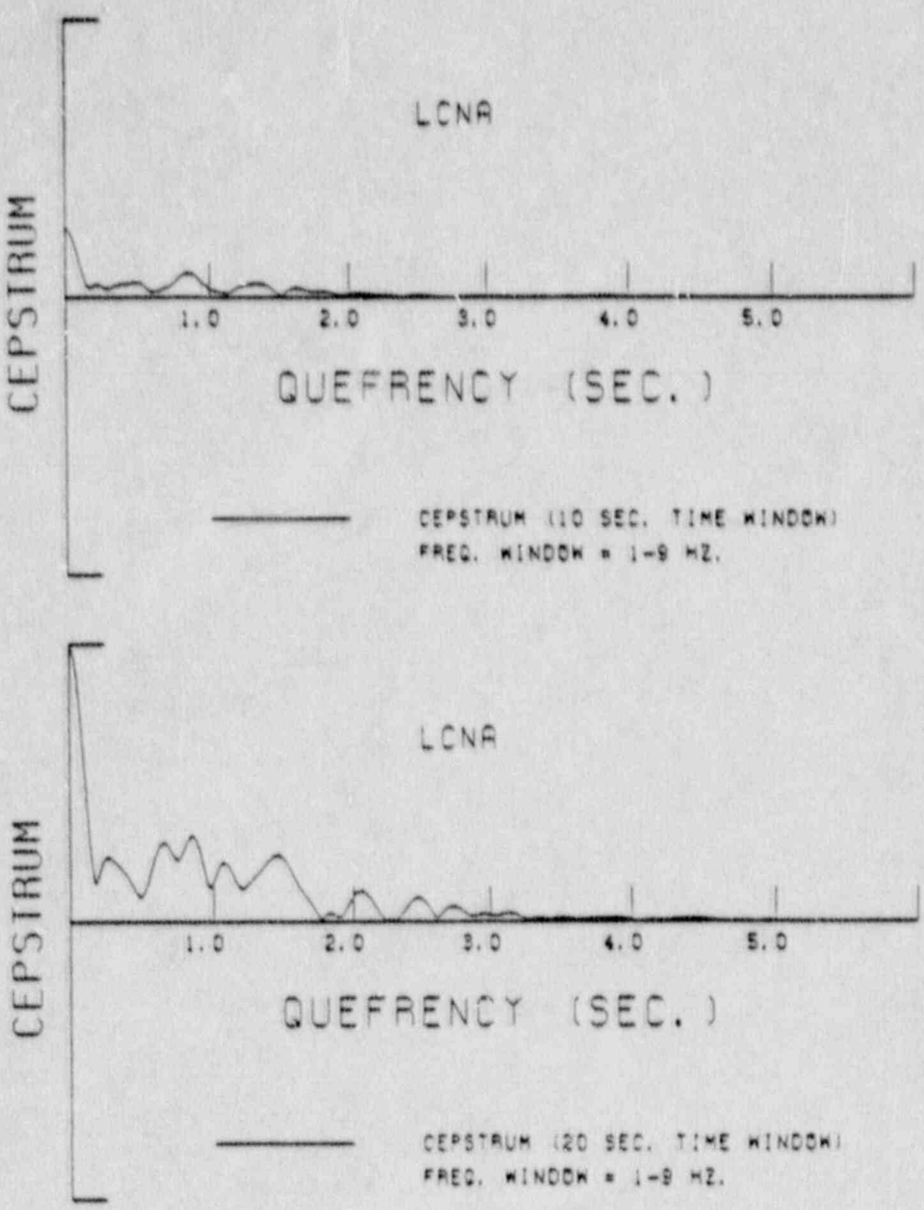

FIGURE 4-4 The cepstrum for a 10 sec window (top) and a 20 sec window (bottom) of station LCNA.

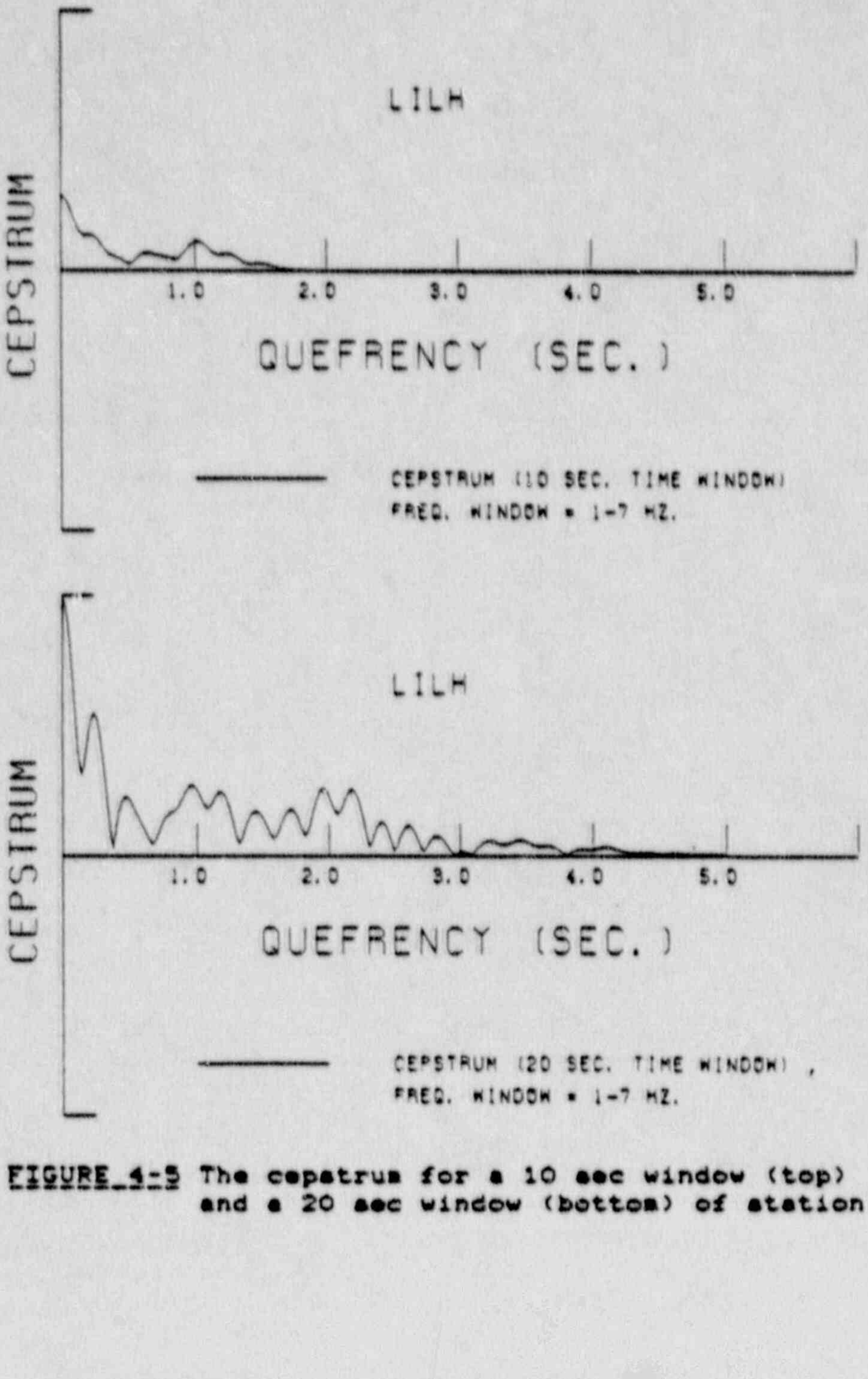

FIGURE 4-5 The cepstrum for a 10 sec window (top) and a 20 sec window (bottom) of station LILH.

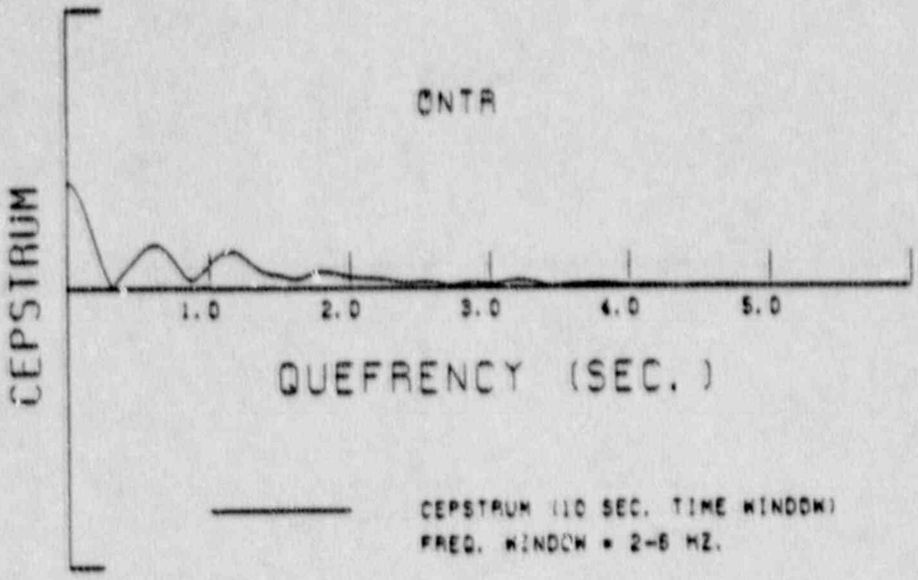

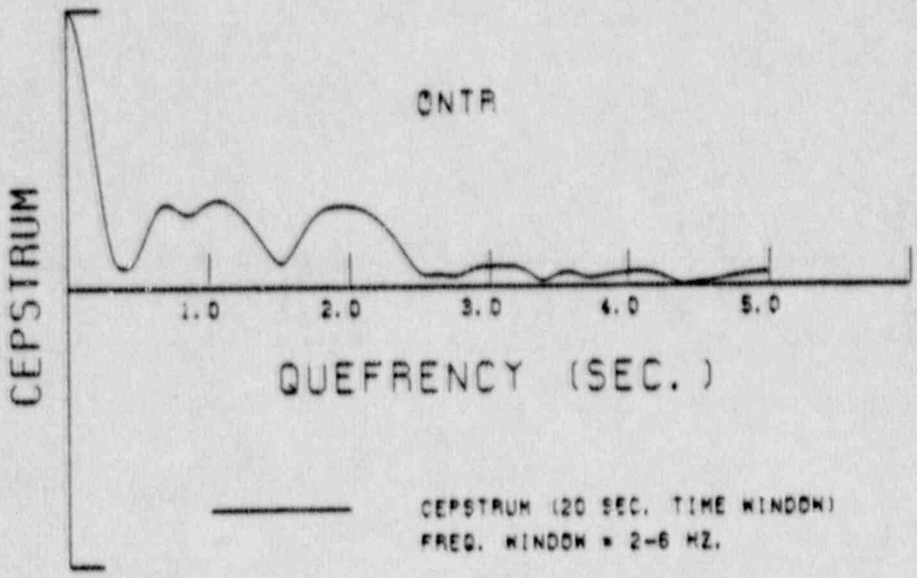

FIGURE 4-6 The cepstrum for a 10 sec window (top) and a 20 sec window (bottom) of station ONTR (radial).

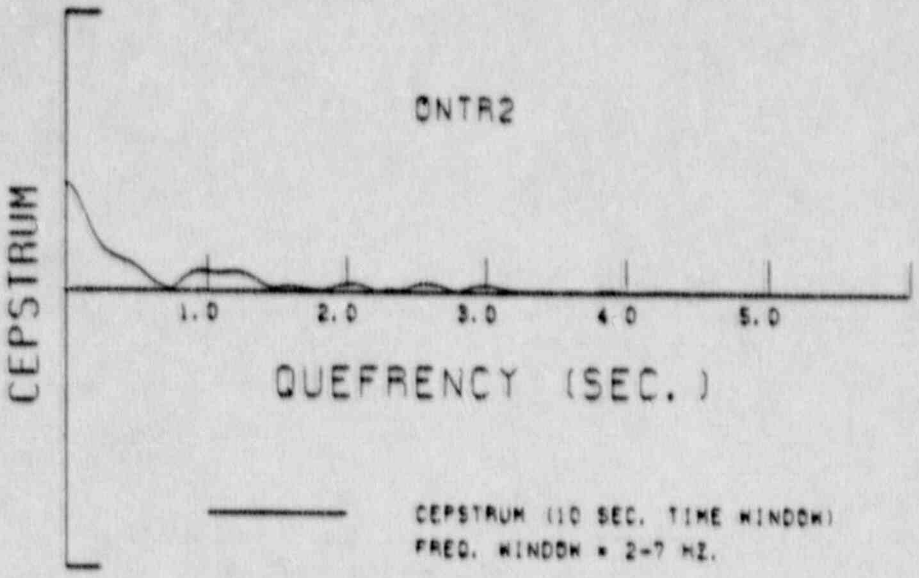

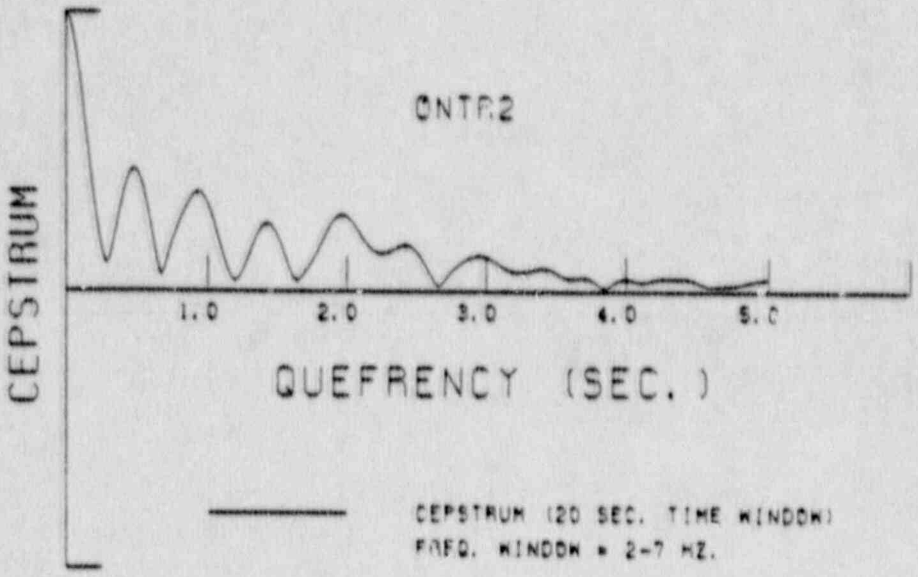

FIGURE 4-7 The cepstrum for a 10 sec window (top) and a 20 sec window (bottom) of station ONTR (tangential).

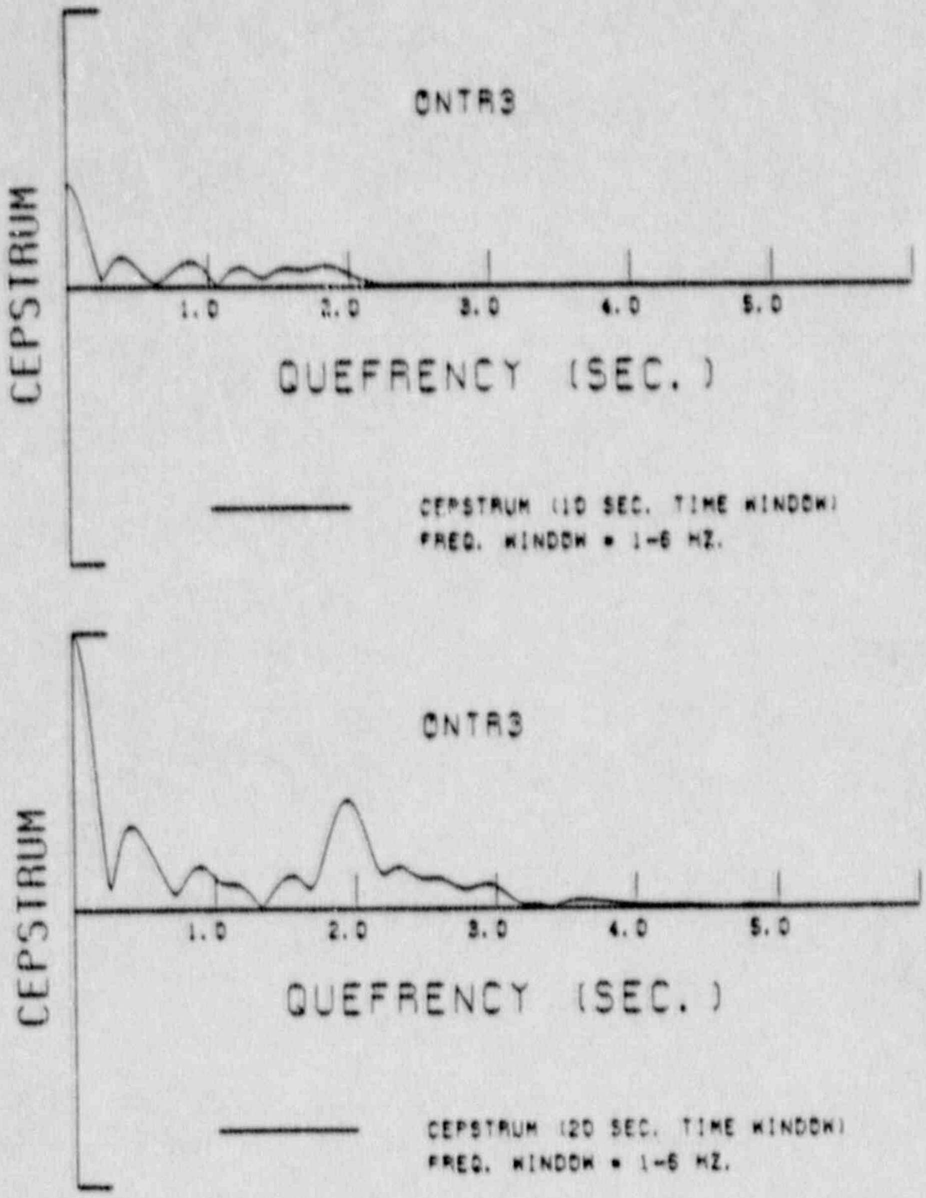

FIGURE 4-8 The cepstrum for a 10 sec window (top) and a 20 sec window (bottom) of station ONTR (vertical).

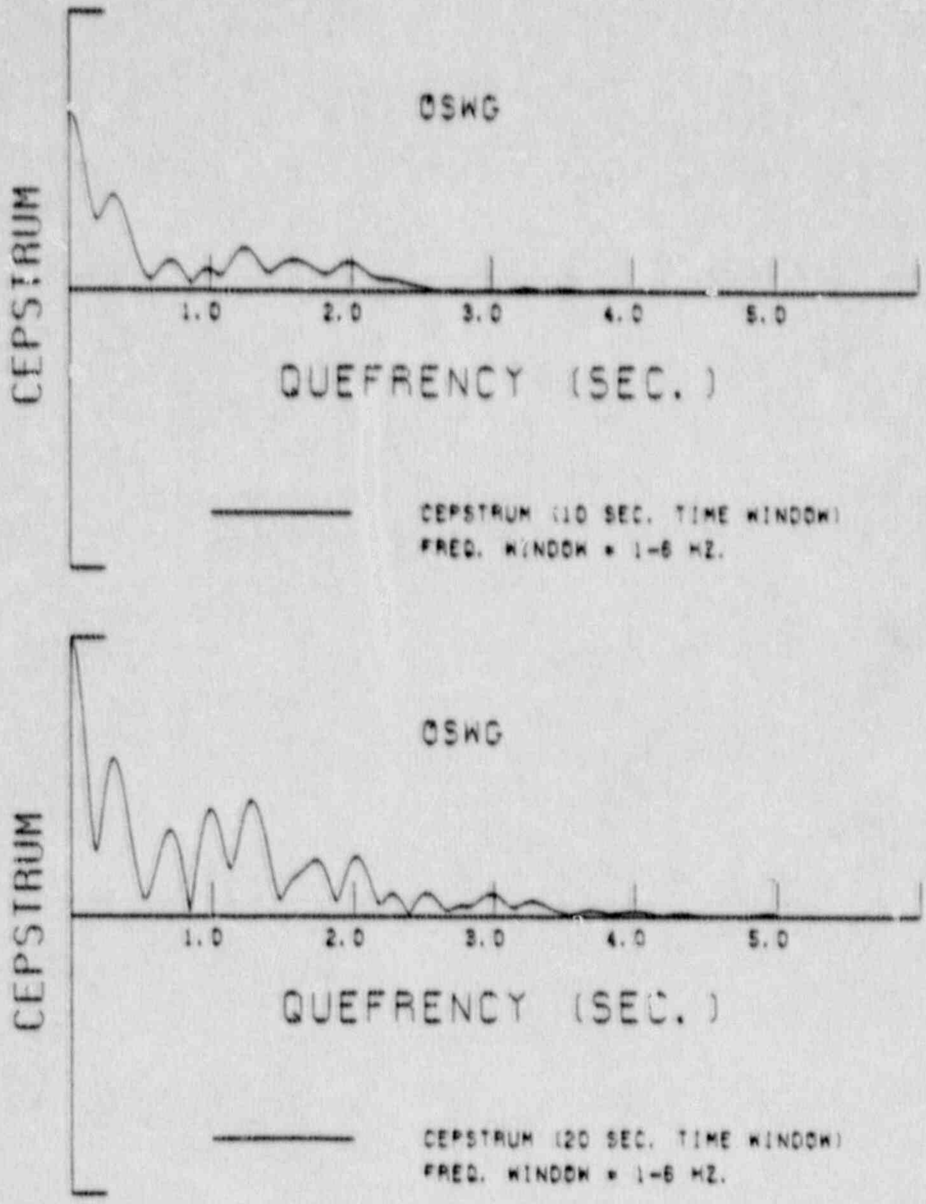

FIGURE 4-9 The cepstrum for a 10 sec window (top) and a 20 sec window (bottom) of station OSWG (radial).

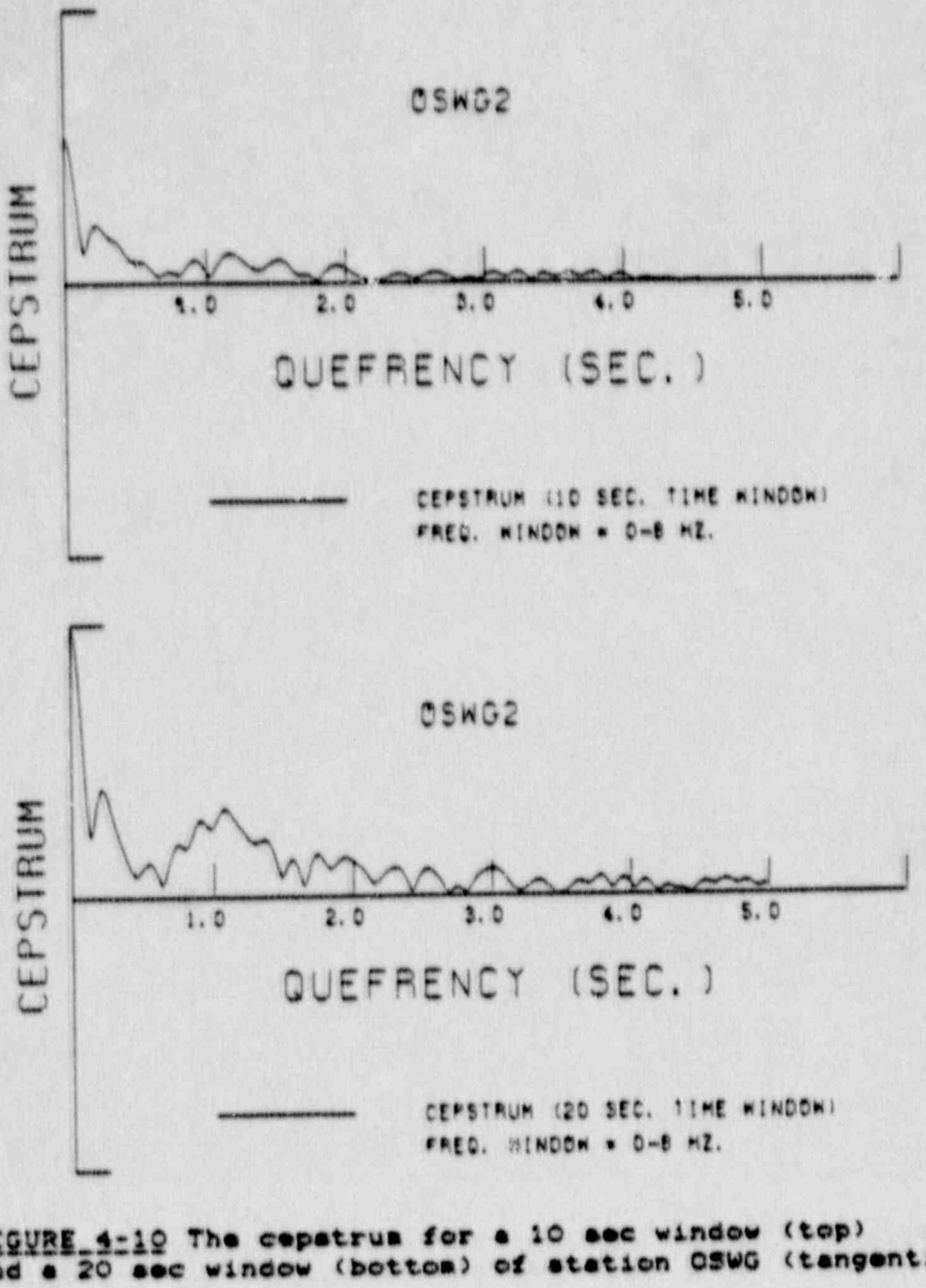

FIGURE 4-10 The cepstrum for a 10 sec window (top) and a 20 sec window (bottom) of station OSWG (tangential).

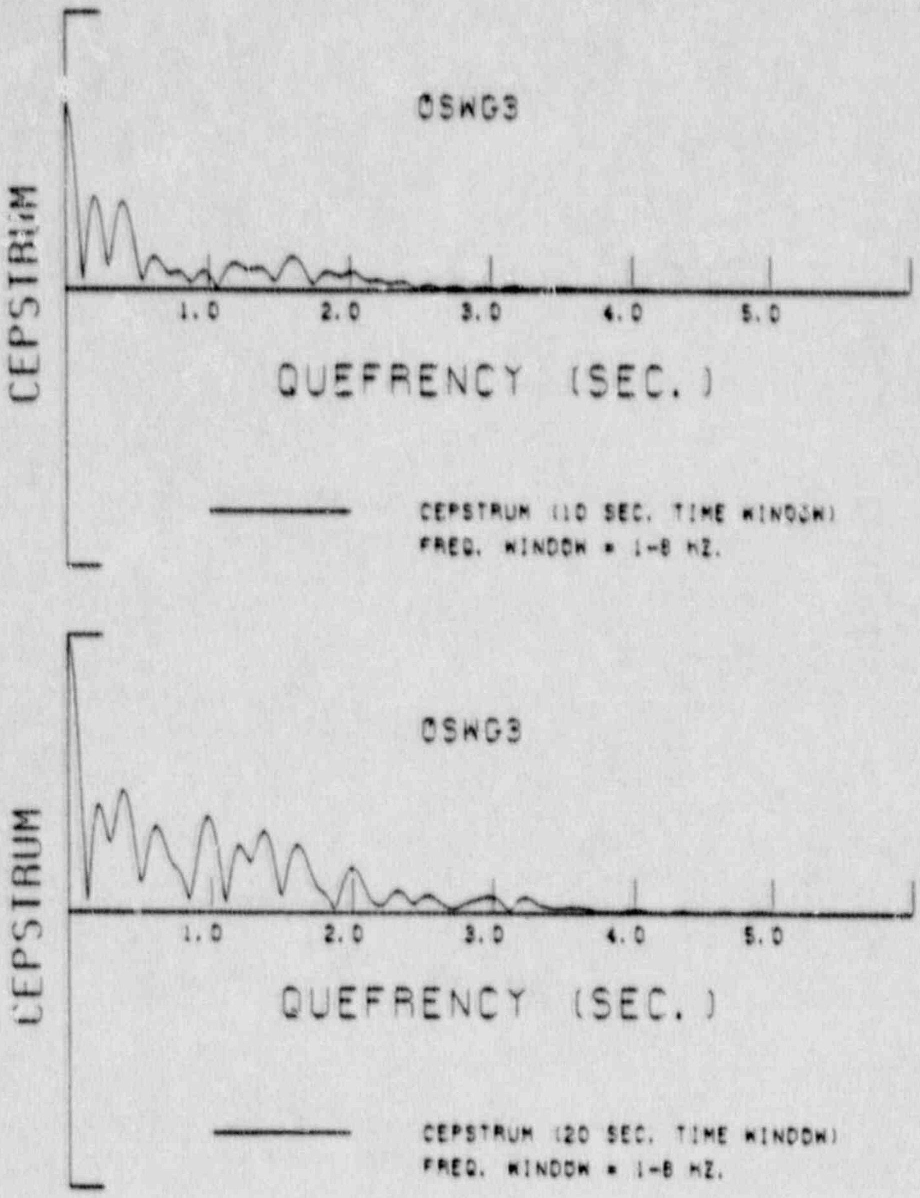

FIGURE 4-11 The cepstrum for a 10 sec window (top) and a 20 sec window (bottom) of station OSWG (vertical).

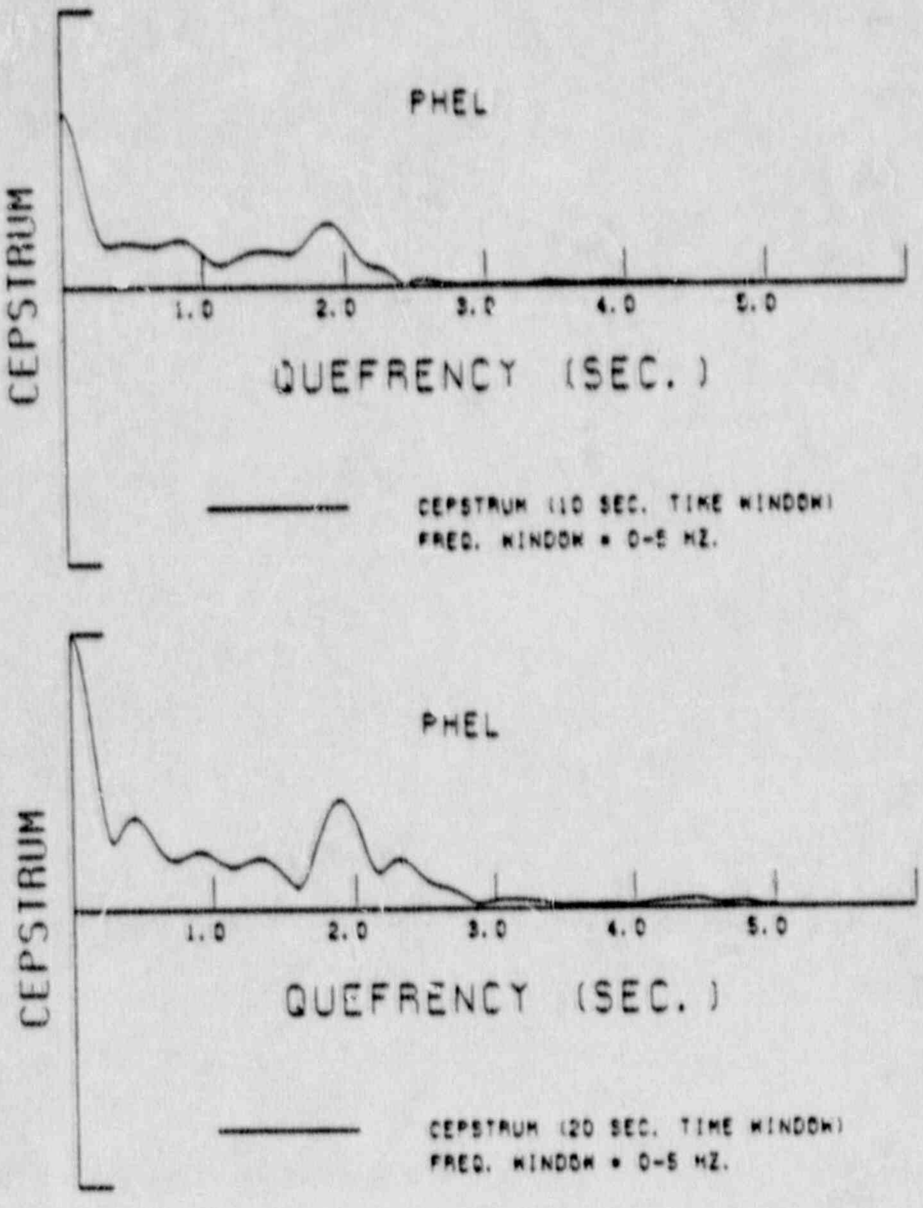

FIGURE 4-12 The cepstrum for a 10 sec window (top) and a 20 sec window (bottom) of station PHEL.

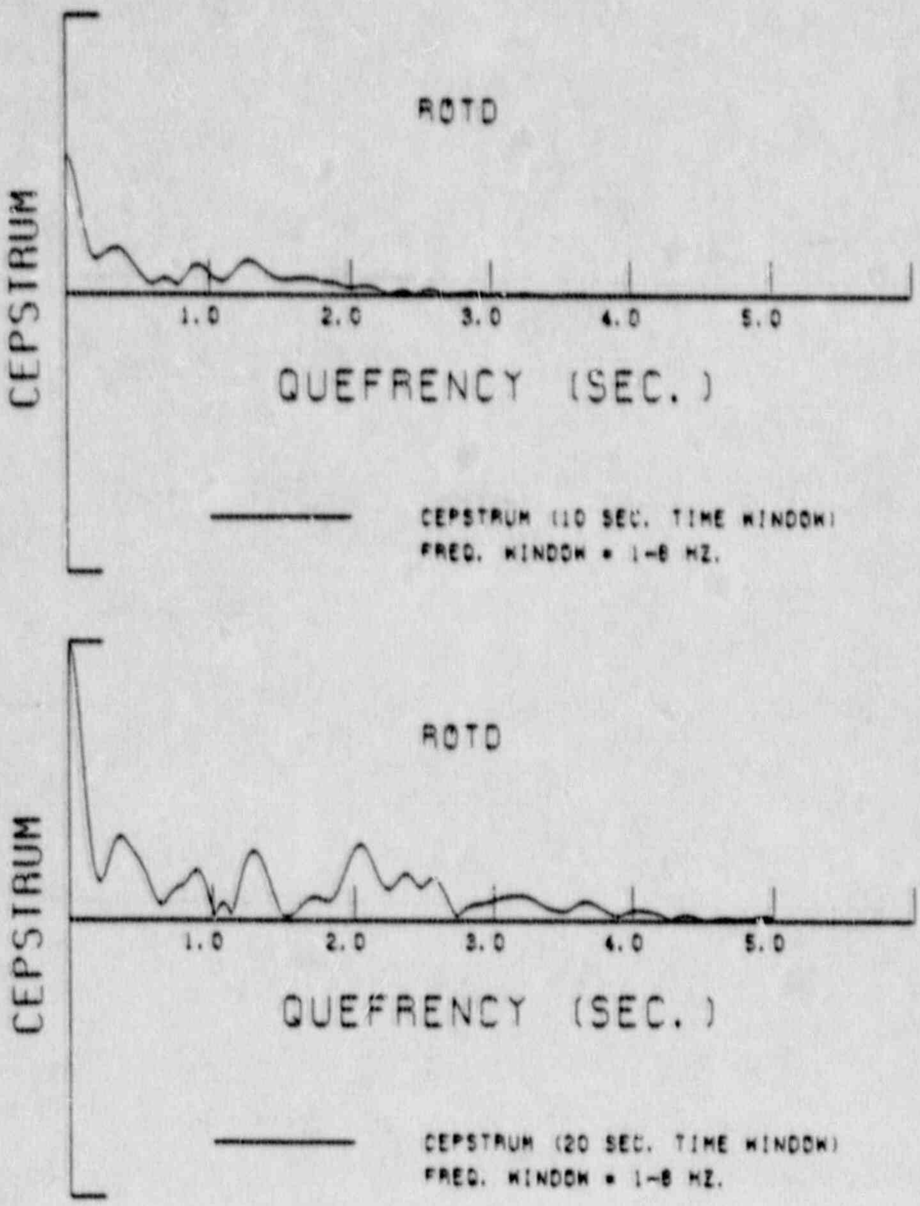

FIGURE 4-13 The cepstrum for a 10 sec window (top) and a 20 sec window (bottom) of station ROTD.

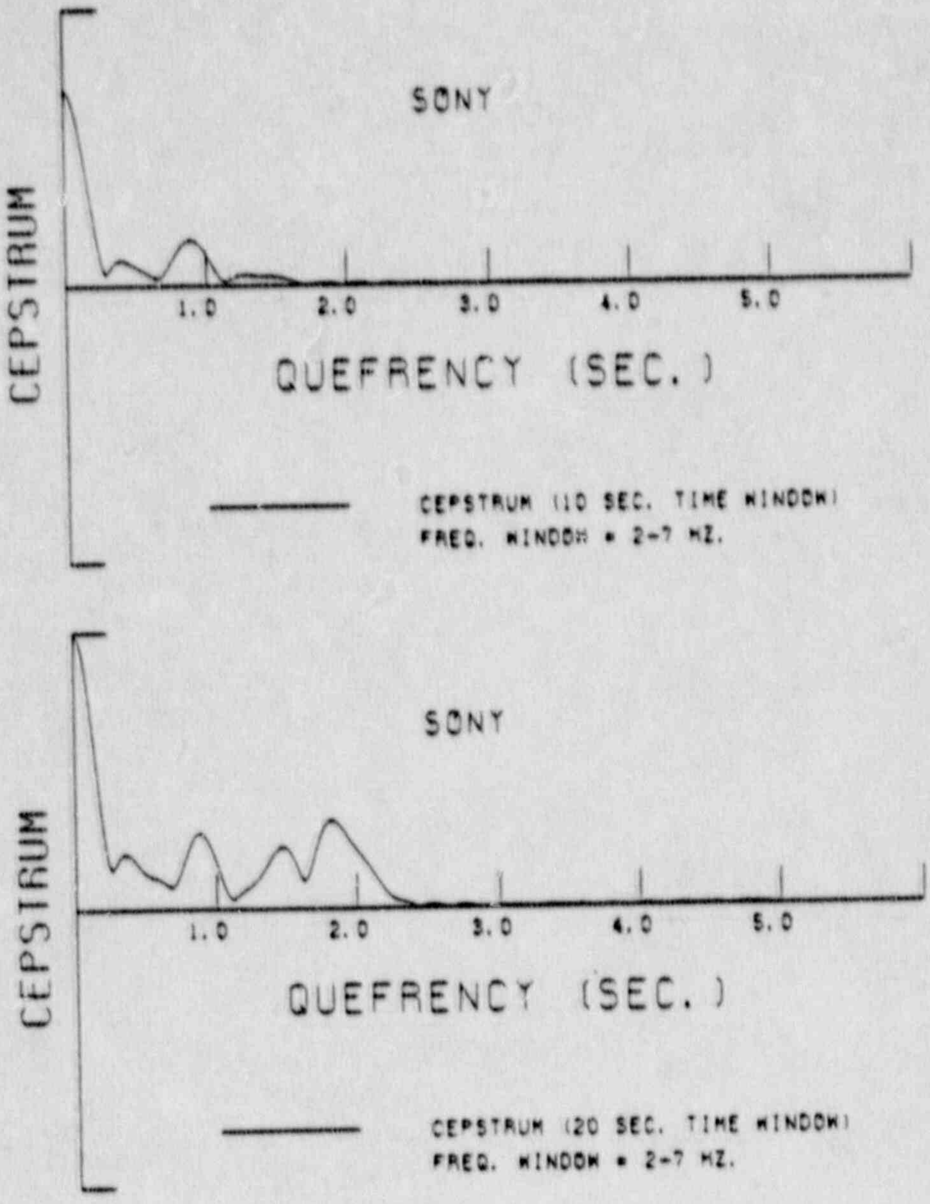

FIGURE 4-14 The cepstrum for a 10 sec window (top) and a 20 sec window (bottom) of station SONY.

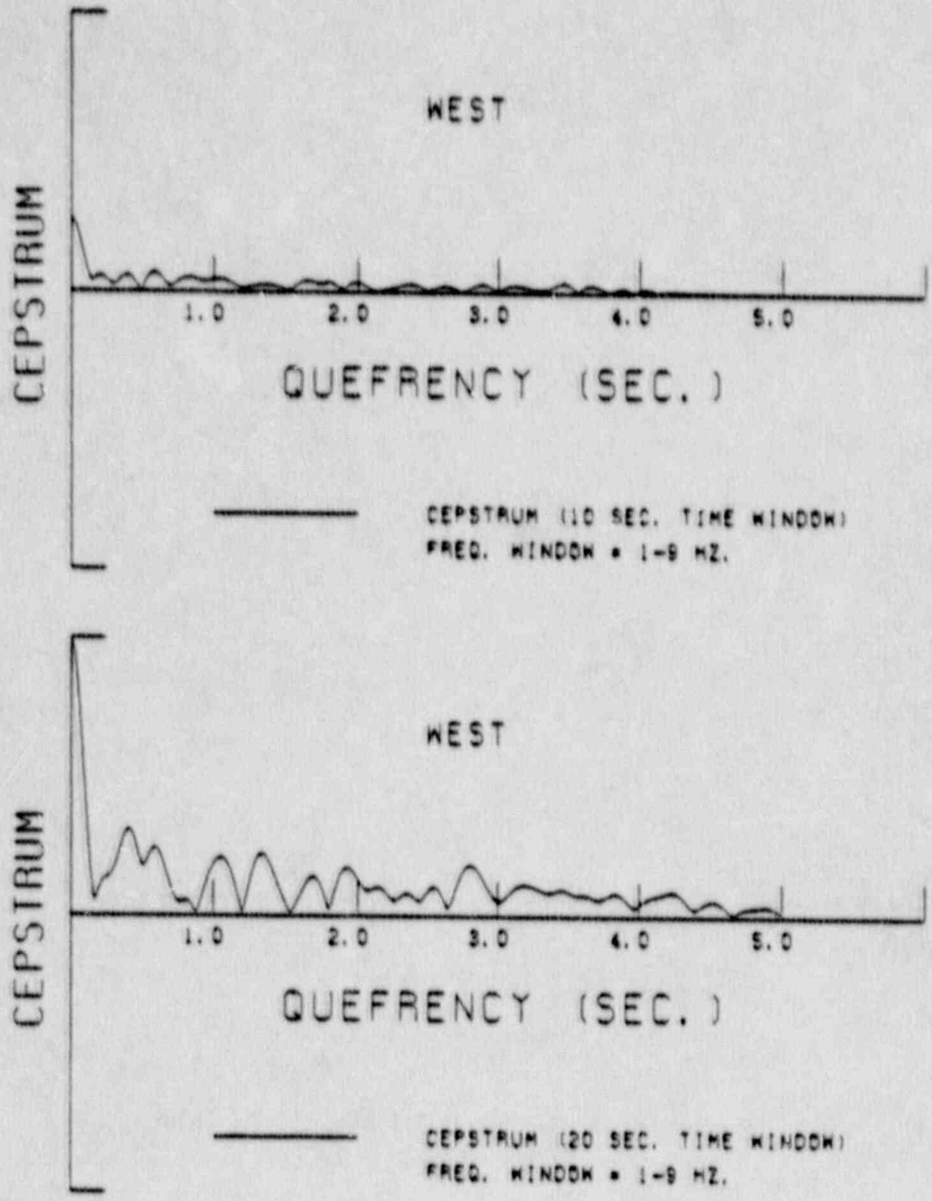

FIGURE 4-15 The cepstrum for a 10 sec window (top) and a 20 sec window (bottom) of station WEST.

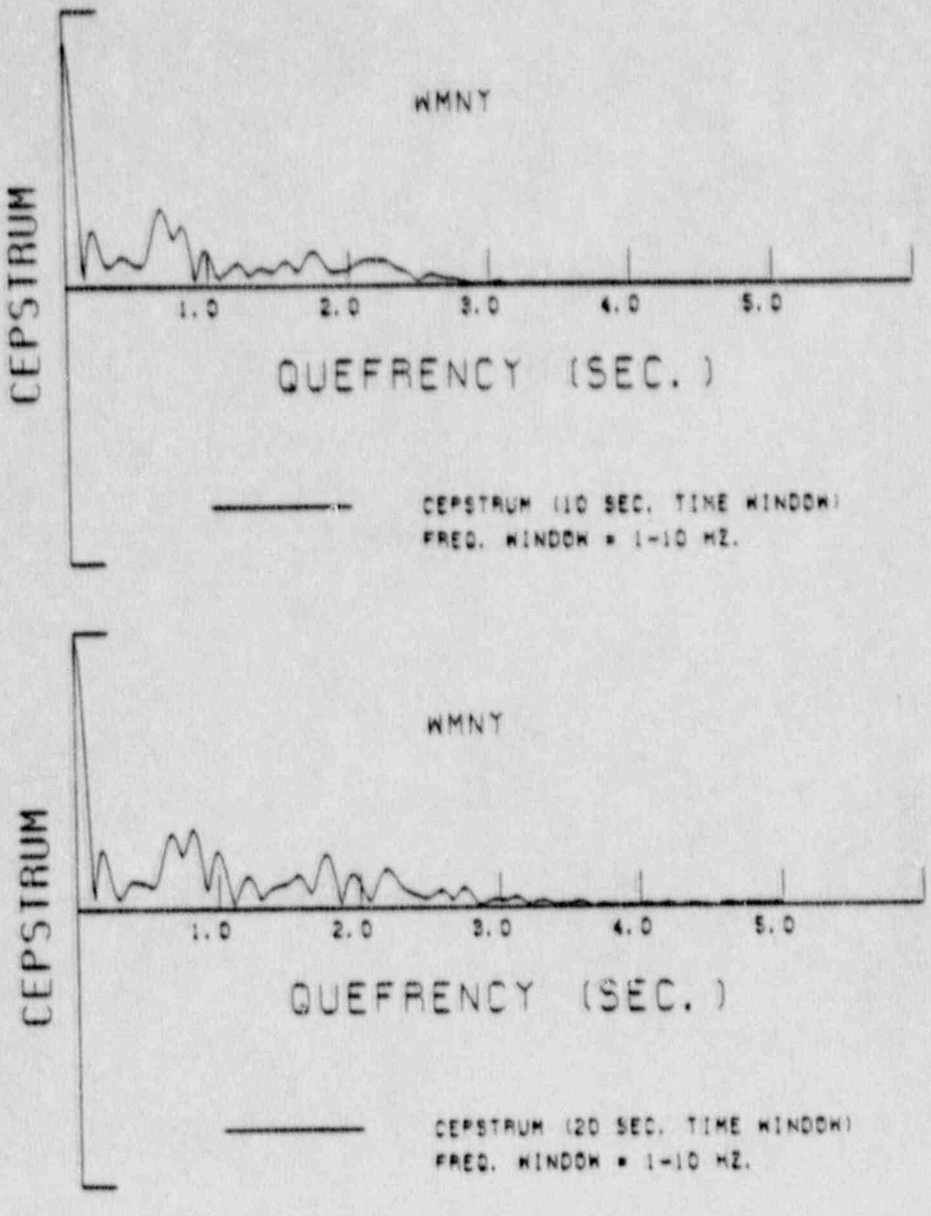

FIGURE 4-16 The cepstrum for a 10 sec window (top) and a 20 sec window (bottom) of station WMNY.

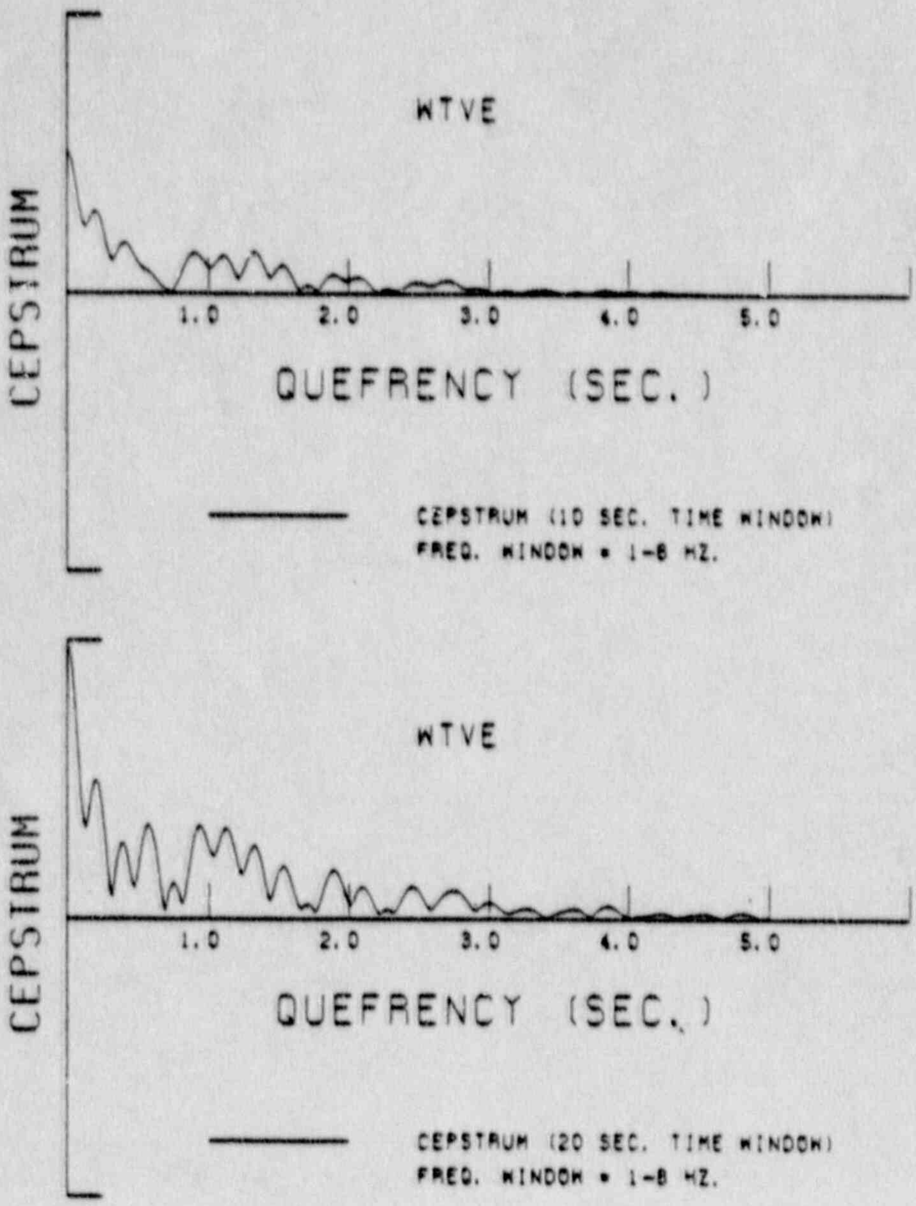

FIGURE 4-17 The cepstrum for a 10 sec window (top) and a 20 sec window (bottom) of station WTVE.

APPENDIX 5

THE RELATIVE LOCATION ALGORITHM THEORY

THE RELATIVE LOCATION ALGORITHM THEORY

The relative location algorithm works in the following manner:

if

θ, λ, z, τ = unknown parameters

$\theta_R, \lambda_R, z_R, \tau_R$ = reference event parameters

where θ is the latitude, λ is the longitude, Z is the depth, and τ is the origin time, and if

t_i = N travel times observed for the unknown event

t_{R_i} = N travel times observed for the reference event

then

$$\overline{\Delta t} = \begin{bmatrix} t_1 - t_{R_1} \\ t_2 - t_{R_2} \\ \vdots \\ t_N - t_{R_N} \end{bmatrix} \qquad (5\text{-}1)$$

where $\overline{\Delta t}$ is the relative time difference vector, and

$$\overline{\Delta P} = \begin{bmatrix} \theta - \theta_R \\ \lambda - \lambda_R \\ z - z_R \\ \tau - \tau_R \end{bmatrix} \quad (5\text{-}2)$$

where $\overline{\Delta P}$ is the perturbation vector, and where

$$\bar{P} = \begin{bmatrix} \theta \\ \lambda \\ z \\ \tau \end{bmatrix} \quad (5\text{-}3) \qquad \bar{P}_R = \begin{bmatrix} \theta_R \\ \lambda_R \\ z_R \\ \tau_R \end{bmatrix} \quad (5\text{-}4)$$

are the parameter vectors for the unknown and the reference events, respectively. Thus,

$$\underset{\approx}{A} = \begin{bmatrix} \left.\frac{\partial t_1}{\partial \theta}\right|_R^1 & \left.\frac{\partial t_1}{\partial \lambda}\right|_R^1 & \left.\frac{\partial t_1}{\partial z}\right|_R^1 & \left.\frac{\partial t_1}{\partial \tau}\right|_R^1 \\ \vdots & \vdots & \vdots & \vdots \\ \left.\frac{\partial t_i}{\partial \theta}\right|_R^i & \left.\frac{\partial t_i}{\partial \lambda}\right|_R^i & \left.\frac{\partial t_i}{\partial z}\right|_R^i & \left.\frac{\partial t_i}{\partial \tau}\right|_R^i \end{bmatrix} \quad (5\text{-}5)$$

where $\underset{\approx}{A}$ is the condition matrix, and

$$\bar{e} = \left[e_R^1 , e_R^2 \ldots\ldots e_R^i \right] \quad (5\text{-}6)$$

where $\bar{\epsilon}$ is the error vector. The relative time difference vector $\overline{\Delta t}$, thus equals:

$$\overline{\Delta t} = \underset{\approx}{A} \cdot \overline{\Delta P} + \bar{\epsilon} \quad . \quad (5\text{-}7)$$

The least squares solution is obtained by minimizing the norm (X) with respect to the perturbation $\overline{\Delta P}$:

$$\overline{\Delta P} = (\underset{=}{A}^T \cdot \underset{=}{A})^{-1} \cdot \underset{=}{A}^T \cdot \overline{\Delta t} \quad , \quad (5\text{-}8)$$

and the norm is given by:

$$X = \overline{\Delta t}^T \cdot \overline{\Delta t} \quad . \quad (5\text{-}9)$$

The estimated location of the unknown event is:

$$\bar{P}_E = (\underset{=}{A}^T \cdot \underset{=}{A})^{-1} \cdot \underset{\approx}{A} \cdot \overline{\Delta t} + \bar{P}_R \quad , \quad (5\text{-}10)$$

and the estimated travel time difference vector is:

$$\overline{\Delta t}_E = \underset{\approx}{A} \cdot (\bar{P}_E - \bar{P}_R) \quad . \quad (5\text{-}11)$$

The estimated travel time difference standard deviation is:

$$\tilde{\sigma}_E^2 = 1/(N-2) \cdot [\overline{\Delta t}_E - \overline{\Delta t}]^T \cdot [\overline{\Delta t}_E - \overline{\Delta t}]$$
$$= 1/(N-2) \cdot \sum_{i=1}^{N} (\Delta t_E^i - \Delta t^i)^2 \quad . \quad (5\text{-}12)$$

The variance - covariance matrix of the estimated perturbation ($\overline{\Delta P}$) is:

$$S = \bar{\sigma}_t^2 \cdot [A^T \cdot E^{-1} \cdot A]^{-1} \quad , (5\text{-}13)$$

where E is the error matrix:

$$E = \begin{bmatrix} \sigma_1^2 & & & \\ & \sigma_2^2 & & \\ & & \ddots & \\ & & & \sigma_i^2 \end{bmatrix} \quad (5\text{-}14)$$

and σ_i is the estimated travel time variance at station i. The equation of the confidence ellipse is:

$$\overline{\Delta P}^T \cdot S^{-1} \cdot \overline{\Delta P} = C_2^2 \quad (5\text{-}15)$$

where C_2^2 is the suitable statistic:

for the F-distribution:

$$C_2^2 = 2/(N-2) \cdot F [100 \cdot (1-\alpha): \bar{\sigma}_E, N-2] \quad (5\text{-}16)$$

using two degrees of freedom, and for the chi-squared factor:

$$C_2^2 = \chi^2 [100 \cdot (1-\alpha): 2] \quad (5\text{-}16)$$

using two degrees of freedom.

For this relative location algorithm, one needs two events which are located within approximately 1 degree of each of each other. Otherwise, the two events may have drastic dissimilarities in their travel paths.

The relative location algorithm removes earth model and travel time path errors from the calculation since the same travel path is assumed for both of the events.

APPENDIX B

EXCERPT FROM PROFESSOR C.P. THORNTON'S PH.D. THESIS DESCRIBING FAULT-ASSOCIATED TRAVERTINE DEPOSITS IN VIRGINIA

Tufa Deposits

Tufa, according to Pettijohn (1949, p. 308), is a spongy porous limestone that forms a thin surficial deposit about springs and seeps and exceptionally in rivers. It is to be distinguished from travertine, which is more dense and banded. The deposits found in the Valley of Virginia are commonly called travertine by workers there, but are actually tufa according to the definition given above. The tufa occurs in two different ways, although in both cases it is a stream deposit. Large amounts of the material are deposited as dams across some of the smaller streams at points where the stream channel widens abruptly; such dams are rather spectacular features, reaching heights of up to four feet. Tufa is also deposited in concretionary masses, generally formed around small pebbles or pieces of wood, so that the floor of the stream channel appears to be covered with white pebbles of rather uniform size.

Within the Mount Jackson quadrangle, tufa dams are found along Smith Creek and Holman Creek west of the Massanutten Range; tufa pellets occur along a small tributary to Passage Creek in the northern Massanutten Range.

Holman Creek tufa. The first tufa dam crosses the stream at the east side of Forestville just below the abandoned mill on State Road 767. The dam appears to be still growing. It is composed of soft, porous limestone, apparently of algal origin, which forms the rounded structures of which the dam is built. In some cases imprints of leaves and other apparently organic structures such as root molds are found. The surface of the dam has a greenish-yellow color due to the presence of a thin film of algae over the damp parts of the rock. Pockets and basins along the front of the dam contain dark-green filimentous algae of undetermined identity. The occurrence of this first tufa dam appears to be controlled by an outcrop of Edinburg limestone that crosses the stream just above the dam.

The second dam occurs about half a mile downstream from the first one. It is about one foot high, i.e., water flowing over it falls a distance of about one foot, and in other respects it is quite similar to the first one.

No tufa occurs through the next two miles of the stream's course. The next dam is found a few hundred feet downstream from the point where State Road 698 crosses the creek, and from this point to the Southern Railway bridge over the creek a series of tufa dams can be seen. The first dam in the series is four to five feet high and apparently lacks any stratigraphic control. It is composed of soft brown or yellow porous limestone, locally containing impressions of leaves of sycamore trees such as are still growing along the banks of the stream. At places parts of this dam are overlain by as much as four feet of alluvial clay, but other parts of the dam seem to be still growing. About eighty feet downstream is a second dam, this one only about one foot high. At the edge of the stream channel it is overlain by seven feet of alluvium. At places the tufa is conglomeratic, consisting of stream gravels cemented by travertine. This dam does not appear to be actively growing at present. Other dams, with approximately the same features, occur downstream all the way to the railroad bridge.

In the case of these dams near Quicksburg the situation is somewhat unique. Just below the first dam in this group, the dam east of State Road 698, Holman Creek turns abruptly to the south, cutting its channel through a fill terrace, then turning slowly northward until it again flows to the east. Further investigation shows that the former stream channel is a rather straight east-west extension of its course above the first tufa dam. At some time in the historic past a dam was built across the creek just below the first tufa dam and the water of the stream was diverted into a millrace northeast of the stream to operate a small mill that lay downstream from the artificial dam. From this mill, now represented only by its stone foundations, the water was returned to the stream. The stream has since succeeded in bypassing the dam, however, by overflowing onto the fill terrace to the southwest and cutting a new channel down through this fill. In the process of cutting its new channel, however, the stream has uncovered a series of tufa dams which were formerly buried beneath the alluvium in the fill terrace. It would thus appear that most of the tufa dams now exposed along the creek near Quicksburg are ancient ones, the building of which was followed by a period of alluviation. No such alluviation is indicated in the case of the tufa dams farther upstream, however, and deposition would appear to be limited to the mouthward parts of the stream.

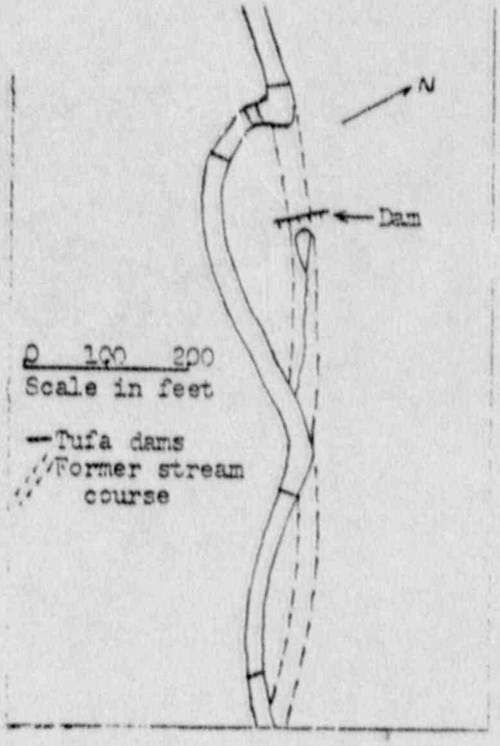

Smith Creek tufa. The tufa dams along Smith Creek are not so numerous as those along Holman Creek; they are, however, more impressive in both height and width. The dams occur along the creek from a point just south of State Road 608 to a point about half a mile south of State Road 698. Thus tufa formation here is restricted to a smaller part of the stream's course than along Holman Creek.

The terraces here are much like those along Holman Creek in the character of the material of which they are constructed. Like the Holman Creek dams, they are in some cases overlain by alluvium along the banks of the stream, although this alluvial cover is generally only about one foot thick. The creek here is wider and the dams are thus longer. The trace of the dams

a. Tufa dam on Smith Creek near the northern end of Lincoln Hill, Rockingham County.

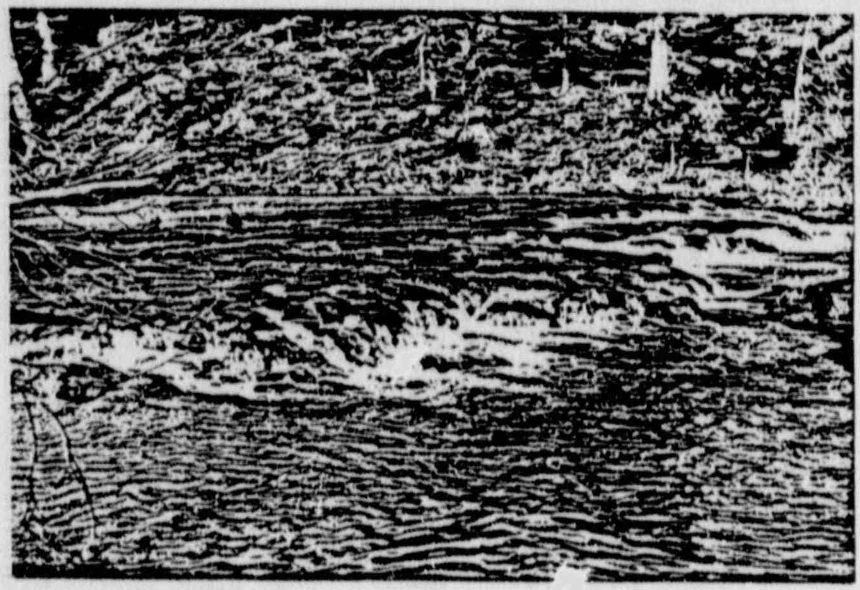

b. Tufa dam several hundred yards downstream from the one shown above.

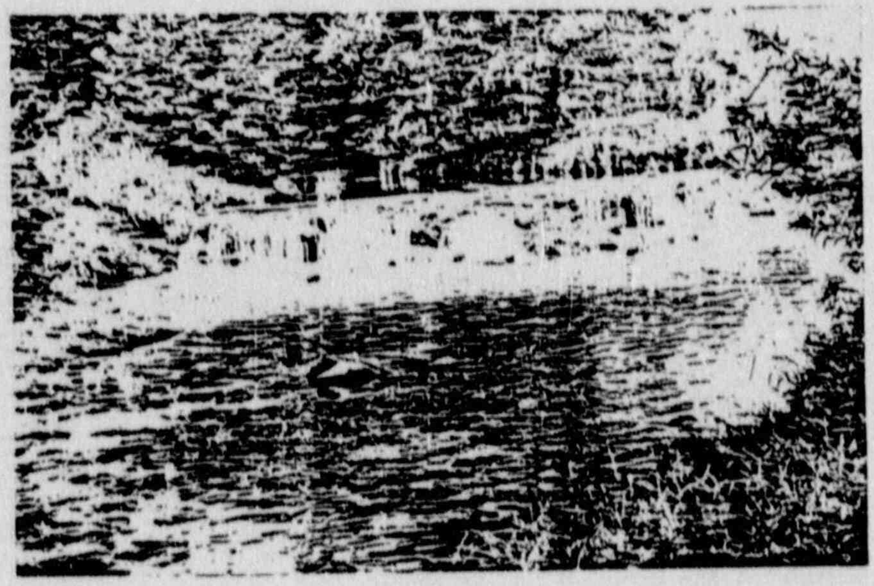

Tufa dam on Holman Creek west of Quicksburg, Shenandoah County.

across the stream is often quite sinuous and the dams are generally formed just a few feet upstream from especially wide parts of the stream's channel. The height of these dams is generally about four feet; they were visited during a period of high water, however, and they may be larger than this.

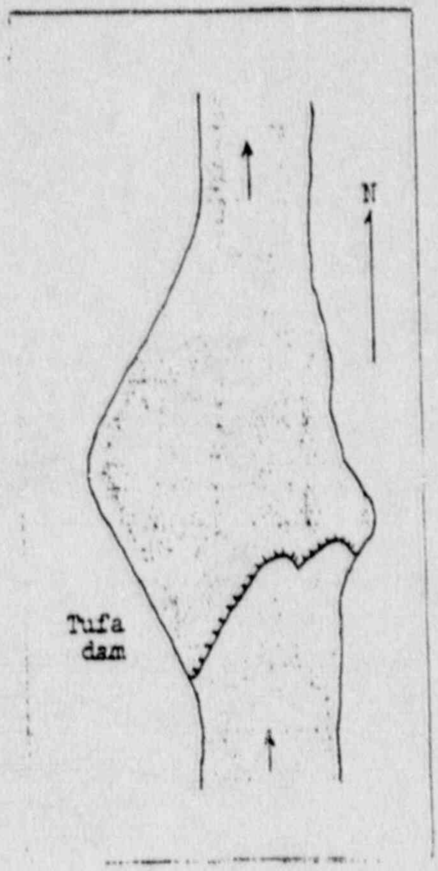

The first of these dams, that is, the one farthest upstream, is located just south of the bridge on State Road 608, from which it is clearly visible. The second tufa dam, apparently the largest of the group, is located about 400 yards upstream from the bridge on State Road 698. Its form is shown in the diagram produced above. Downstream from this bridge three more tufa dams are found, only the last one being of any appreciable size.

Fort Valley tufa. A much smaller, but somewhat different deposit of tufa was found along an east-flowing tributary to Passage Creek about a half-mile northeast of Camp Roosevelt. The stream is small and intermittent, but the deposit is of some interest. Small tufa dams have been formed at various points along the stream and are apparently still active; they are controlled in occurrence by outcrops of the Romney shales. In addition the floor of the stream is covered by vast members of small white pellets ranging in size from two to fifteen millimeters. These pellets show a rather poorly developed concentric structure and have at their centers grains of sand or, sometimes, pieces of wood. The deposition of tufa is brought about by even the slightest irregularity in the stream channel; roots, leaves, sticks, pebbles, etc., all have at least a thin covering of the material.

Source of the tufa. In all three areas of tufa deposition the material is deposited from a stream at points downstream from where the stream crosses a fault. In two of the cases (Holman and Smith Creeks) the fault actually cuts through limestone layers where it outcrops; in the third case, it is probable that the fault cuts or at least shatters limestone formations below the surface. The calcium carbonate is brought to the surface by underground waters circulating in the fault plane or fault zone; the crushed condition of the limestone makes their solution easy. Travertine terraces have not been found in this quadrangle along streams which cross these same formations where they are not affected by faulting and they have not been found along these same streams headward from the fault zones.

The cause of deposition of the tufa is another problem. Along Holman Creek in many cases the dams were found to be covered with algae, which may or may not be responsible for the formation of the tufa. The algae may be present because of the abundance of dissolved calcium carbonate. Some of the dams appear to be controlled by bedrock outcrops. Water saturated in calcium carbonate would lose some of its dissolved carbon dioxide on flowing over irregularities in the channel, and this in turn would reduce the solubility of the calcium carbonate, causing some of it to be deposited. The process would be self-accelerating; the higher the dam is built, the more tufa will be precipitated. In other cases the tufa dams are associated with wide spots in the stream channel. Sudden widening of the stream would expose more of the water to the air and to the sun; this increase in heated surface would cause some reduction in the dissolved carbon dioxide and perhaps bring about deposition of tufa.

APPENDIX C

NEOTECTONIC, GEOCHEMICAL, AND LINEAMENT STUDIES OF THE MOODUS SEISMIC AREA

NEOTECTONIC, GEOCHEMICAL, AND LINEAMENT STUDIES

OF THE MOODUS SEISMIC AREA

A Report to the Nuclear Regulatory Commission

Contract Number: NRC-04-85-111-01

Christopher A. Shuman, M.S.

TABLE OF CONTENTS

ABSTRACT

In an attempt to identify neotectonic, geochemical, and lineament characteristics of a seismically active area in the northeastern United States, studies were conducted during the late summer and fall of 1987 in and around the Moodus, Connecticut, area. This project focused on a six quadrangle region centered on the "Moodus seismic area", an area of anomalously high seismic activity in recent and historic times.

This study included a review of the literature, particularly for mention of features that might be related to the seismic activity, and field work to locate and examine those neotectonic features. Also, the local drainage network was examined and water samples were taken to assess their degree of saturation by chemical species which might indicate deep fluid movement along faults or fractures. Finally, remote sensing imagery at four scales (1:250,000 SLAR imagery, 1:100,000 SPOT satellite image, 1:80,000 high-altitude photography, and 1:18,000 low-altitude photography) were examined for the presence of lineaments that may reveal bedrock fracturing and tectonic stress orientations.

The results of this study are limited, but the techniques involved do offer an interesting approach which may be applied in future studies of seismically active zones. No distinct, positive evidence of neotectonic features or activity was found during this study. No evidence of tectonically disturbed glacial drift or stream deposits appeared in previous reports covering the area, except possibly in one study where the critical outcrop was regraded and obscured. The geochemical studies revealed no evidence of mineral precipitates or supersaturated species in 33 stream bottom samples and 8 water samples. Lineament analysis of the six quadrangle area at the three smaller scales and the Moodus quadrangle at the 1:18,000 scale produced varying data on lineament orientation, frequency, and length. The lineament orientations are concentrated in the northwest quadrant, although secondary peaks occur in the north-northeast and east directions. The similar distribution of lineament orientations produced from the SPOT and high-altitude images, indicates that these similarly scaled products may be sampling a common set of lineaments. The differences between the distributions may be a result of stereoscopic viewing of the aerial photographs. The overall orientation of lineaments is reasonably compatible with other lineament studies in this region, as well as, the contemporary state of stress in the subsurface. An easterly orientation peak at 080 degrees correlates well with the orientation of the maximum compressive stress (σ_1) determined from recent in situ stress and seismic data analyses.

The variation in the orientation of lineament features appears to be compatible with a first-, second-, and third-order shear couple model. Lineament frequency was observed to increase on the radar, SPOT, and high-altitude photography in the Moodus quadrangle block relative to adjacent quadrangles. This indicates that a higher degree of fracturing may be present in the vicinity of the seismic area. In addition, scale phenomena functions related to the lineament analysis were developed. They show: 1) an exponential decay in lineament frequency per unit area with increasing scale number, and 2) a linear increase in average lineament length with increasing scale number.

LIST OF FIGURES

ACKNOWLEDGMENTS

The author wishes to thank the following individuals and organizations for their support, advice, and assistance during this study: the Nuclear Regulatory Commission, Bob Altamura of the Connecticut Geological and Natural History Survey, and Shelton Alexander, Charlie Thornton, Duff Gold, Mike Machesky, and Laura Karkowski of the Pennsylvania State University.

1.0 INTRODUCTION

This report summarizes a study of an area of anomalous earthquake activity, the Moodus seismic area (Barosh et al, 1982; London, 1987). This region of Connecticut has been the site of numerous, generally low-intensity events in recent years and has a record of seismic activity dating from New England's colonial era. Scientific efforts to investigate the cause of this activity have ranged from detailed geologic mapping of the area (London, 1987) to drilling deep (1000'+) research boreholes (Connecticut Geological and Natural History Survey (CGNHS) 1987). This study complements those projects and provides data and techniques that can be used for analyses of other seismic zones.

1.1 Purpose of Investigations

As part of a larger study on seismically active areas being conducted by the Pennsylvania State University's Department of Geosciences, this investigation of the Moodus seismic area was to: review the literature discussing the area's neotectonic and geologic features; sample local streams for geochemical indicators of deep fluid movement; and examine various scales of remote sensing imagery and aerial photography for lineaments and fracture traces in an effort to identify fractures in the bedrock. Although this project was limited in scope, it does provide a preliminary assessment of the neotectonic activity of the site as well as an approach that may be useful for the study of other seismic areas.

1.2 Scope of Investigations

The study area for this project is not defined by any natural or man-made boundaries but it is roughly centered on the town of Moodus, Connecticut. The study area extends from this point across six 7.5 minute quadrangles covering nearly 1940 square kilometers. The study area quadrangles are (from west to east in two rows): (1) Middle Haddam; (2) Moodus; (3) Colchester; (4) Haddam; (5) Deep River; and (6) Hamburg. Although portions of the project examined larger or smaller areas, this group of quadrangles was always the focal point of this study.

1.3 Review of Literature

Because of the varied nature of this project, a review of selected sources of data is necessary. However, as this report concentrates on lineament and fracture trace analyses, this area will be covered more extensively than will be the review of neotectonic features and geochemical studies.

The primary sources of information used to provide a review of background data for this report are Weston Geophysical Corp. (1982a; 1982b), Barosh et al. (1982), and London (1987). These reports include data on many investigations concerned with neotectonic, geochemical, lineament, and other geologic features in the Moodus area. Other studies have attempted to identify neotectonic features that may be related to active subsurface faults or uplift areas. Of these, LaFleur's (1980) study was concerned specifically with identifying surface features which could be attributed to modern tectonic and seismic activity. Many disturbances of glacial overburden deposits were identified in this study and in the Weston reports, but all were attributed to, or were indistinguishable from, deformation related to ice-marginal melting and sediment slumping or the movement of ice masses over preexisting glacial deposits. In addition, LaFleur notes that glacial terraces (as mapped by Flint (1978) and O'Leary (1975; 1977)) along the Connecticut River and its tributaries are spatially restricted and not sufficiently continuous laterally to allow identification of offsets caused by motion on bedrock structures. Where they were observed, LaFleur notes that undeformed glacial deposits overlie deformed bedrock. This conclusion is compatible with our assessment from the available information on glacial deposits in this area.

London (1987) identifies a site to the southwest in the study area (see Plate 1) where stratified sand outwash became unstratified towards its contact with a sheared, granulated, and slickensided bedrock surface of the "Rely Fault". If this site has been characterized accurately, then evidence for post-glacial fault movement probably exists. However, this site may be the result of post-glacial isostatic rebound instead of tectonic stress and fault movement. Unfortunately, the exposure has been found in a field inspection to be regraded and covered, making it unavailable for assessments of other potential causes of the feature. As other studies have indicated, the lack of distinctly positive evidence for fault movement and disturbance of overlying recent deposits related to earthquake and neotectonic activity does not mean that such evidence does not exist. It does mean that exposures capable of providing this evidence are not currently available. This may be the result of few exposures and the relative instability of glacial deposits in this setting.

Although London's detailed study of the Moodus area gathered a great deal of information on the geochemistry of the local bedrock units and structures, it did not gather data on stream water chemistry. While this type of data is more likely to be affected by seasonal variables and sampling factors (Drever, 1982), the chemistry of surface waters has proven to aid investigations of subsurface structural conditions in other areas (Hubbard et al., 1985). In addition, a recently published work by Costain et al. (1987) ascribes some seismic activity to deep fluid movement and transient hydrologic surface loading. This indicates the importance of studying hydrologic variables in the future as they may provide clues to subsurface structures and seismic activity.

Hubbard et al. (1985) and Thornton (1953) detail the presence of travertine-marl deposits downstream from major faults in the Ridge and Valley province of Virginia. Other workers also have documented such deposits in other areas of similar litho-structural setting (Thornton, pers. comm. 1987). These deposits apparently result from the influx, along permeable fractures or faults, of carbonate-saturated ground water into the surface streams. The dissolved carbonate then precipitates on stream bottom materials whenever turbulent flow and or aeration occur. Because of these studies and the presence of a carbonate-bearing schist within the Hebron Formation (London, 1987), a search for travertine-marl deposits was initiated in the Moodus area. Due to the relatively minor amounts of carbonate in the subsurface, it was expected that these deposits would not be as significant as in areas with abundant carbonate bedrock. Therefore, water samples were taken across the study area in addition to examining the stream sediments for the presence of carbonate deposits. Due to the limited scope of this project, other hydrologic variables were not examined for their possible relationship to faults and fractures, or to recorded seismic events.

Because of the controversial nature of the lineament analysis, it is appropriate to review the technique and how it was applied to the different types of imagery available to this study of the Moodus area. The purpose of lineament analysis is usually the identification of linear features which may characterize tectonic fractures, faults and joints, and provide clues to the present and past structural setting of an area. This technique is also used for more practical geotechnical purposes. It should be noted that the results of lineament analyses must be investigated by field techniques in order for these features to be positively distinguished from non-fracture related geologic or man-made linear features.

The importance of linear features observed on maps or photographs of the earth's surface was only alluded to in the earliest studies of these features (Hobbs, 1905; 1911; Rich, 1928; Blanchet, 1957; Lattman, 1958; Lattman and Matzke, 1961). These authors discussed the occurrence of joints, faults, and weathering zones associated with linear features, as well as the relationship of these features to regional stresses. Generally, linear traces up to a mile in length (1.6 kilometers) are termed fracture traces, while longer structures are called lineaments (Lattman, 1958). (For the purpose of convenience, all features mapped in this study will be referred to as lineaments.) Although these workers did establish some of the general subsurface structural characteristics of these features, other studies investigated more specific aspects, such as their relationship to increased hydrogen, helium, and radon gas movement from the subsurface (Banwell, 1986; Rodgers and Anderson, 1984). Lavin et al. (1982) notes the offset of geophysical anomalies along one major feature. In addition, lineaments have been related to major and minor ore body emplacement in a variety of terranes (Keim, 1962; Krohn, 1976). Other studies have related fracture traces and lineaments to zones of vertical to near-vertical zones of fracture concentration and to increased well yield (Lattman and Parizek, 1963; 1964; Siddiqui, 1969; Siddiqui and Parizek, 1971). Although some authors (Wise, 1982; Taylor, 1980) are critical of the lineament analysis and believe that non-fracture-related geologic structures and human errors in interpretation create unacceptable difficulties, the technique is still generally considered to be useful for regional fracture analysis, structural studies, and water resource assessments. For details on how the technique is applied in water resource studies, see Meiser and Earl (1982) and Parizek (1976).

With regard to lineaments mapped in the Moodus area, Barosh et al. (1982) records the presence of numerous lineaments with a dominant northwesterly trend as well as other orientations. They also identified the Salmon River as a major, probably fault controlled, lineament that connects with the possibly fault controlled Connecticut River valley. The Weston Geophysical Corp. studies (1982a; 1982b) also document northerly trending lineaments in this area and relate them to current and relict stress conditions in the crust. Further discussions of lineament relationships will be included in a later section of this report.

2.0 SETTING OF STUDY AREA

The physiographic and geologic setting of the six study quadrangles discussed in the first part of this report will be described briefly in order to provide a suitable basis for subsequent discussion. Where they are appropriate, references to important physiographic and geologic study area features will be made.

2.1 Physiographic Setting

The Moodus area lies largely within the Eastern Highlands province of Connecticut. This area has a rolling, irregular topography which is characterized by narrow valleys, steeply sloping hillsides, and rare, broad uplands. The region has been extensively modified by glacial activity (from the north-northwest) as is evidenced by the numerous lakes, swamps, and deranged drainages that are visible on maps of the area (Flint, 1978; O'Leary, 1975; 1977). Variations in topography are probably a result of changes in glacial scour direction and till deposition, as well as the composition and structure of the underlying bedrock. The eastern portion of the six-quadrangle study area extends into Connecticut's Central Lowlands province. This topography of this area is generally more subdued in elevation and land surface features are largely obscured by human development, although it does contain some significant ridges.

In the study area where these two provinces contact, the Connecticut River crosses from the Central Valley into the Eastern Highlands in a narrow channel. This major drainage system has two major tributaries in the study area, the Salmon River and the Moodus River, both of which drain to the west. Other minor streams flow in northwest-southeast and north-south directions (see Plate 1). The orientation of these drainage channels may be related to fault and fracture patterns in the subsurface (Weston Geophysical Corp., 1982b).

2.2 Geologic Setting

The study area is underlain by an assemblage of largely metamorphic units in a complex structural pattern (see Figure 1). Structural and stratigraphic relationships between these units have been the subject of a number of studies over the years. Earlier workers, through quadrangle by quadrangle bedrock mapping, have managed to derive a coherent model of the geological evolution of the area.

Lundgren (1963; 1966; 1972; 1979; and et al., 1971) identified the major stratigraphic and structural elements of the Eastern Highlands and had succeeded in connecting them to adjoining areas in New England. Large anticlinal and synclinal structures were identified on the basis of symmetry of mappable units about their fold axes. In sequence, the Monson Gneiss - Middletown (Ammonoosuc) Formation - Collins Hill

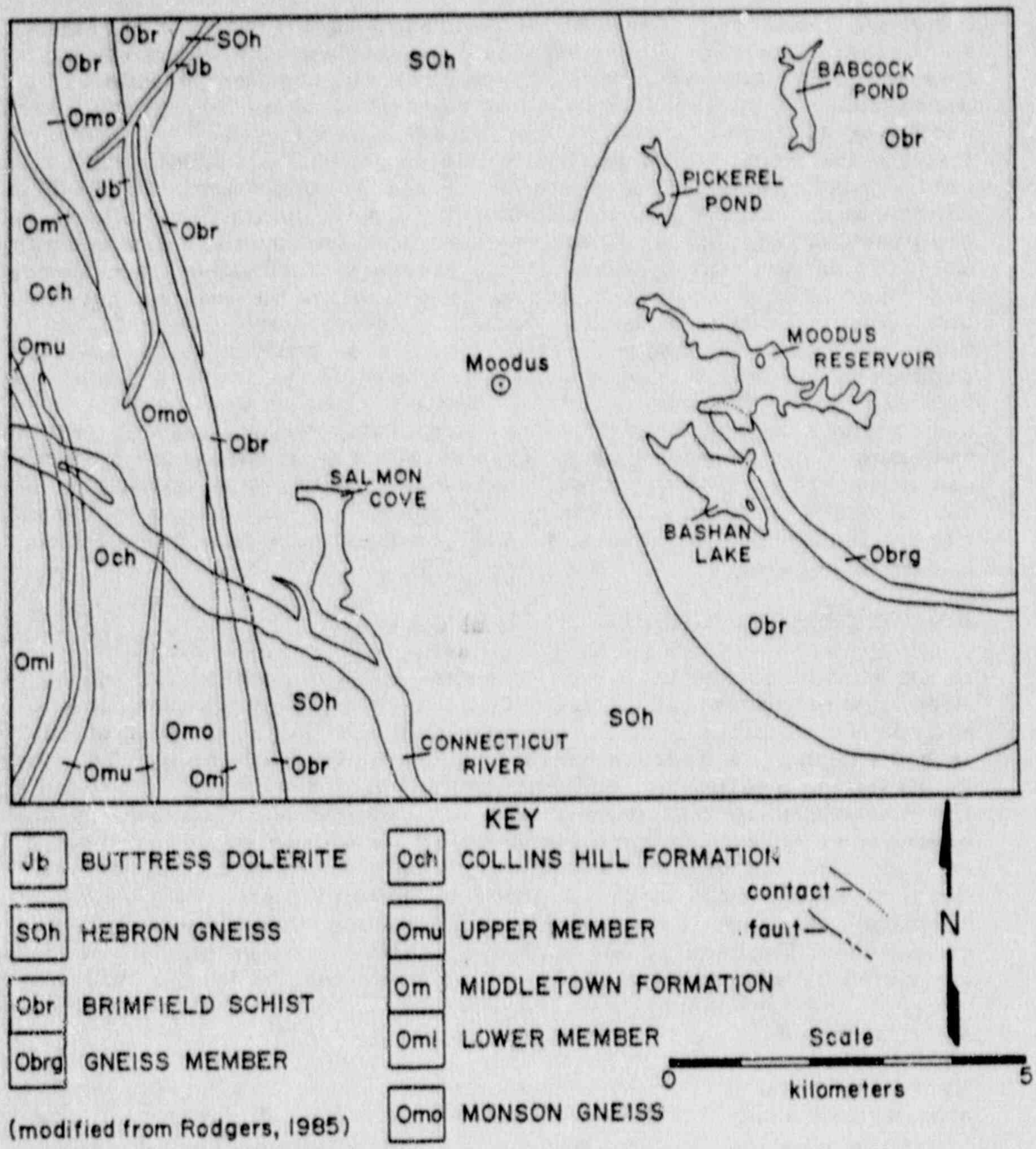

Figure 1, Geologic map of the study area

Formation - Hebron Formation, was regarded as a relatively complete stratigraphic package which recorded the emplacement of probable lower Paleozoic units onto an Avalonian age basement complex (Weston Geophysical Corp., 1982b). This has been challenged by other workers, particularly London (1987), who by detailed mapping at the 1:12,000 scale in the Moodus area has been able to show the discontinuous, chaotic nature and lack of symmetry of the mappable units in the area. London supports the overall tectonic picture of the area but discards the previous mapping units and concentrates on identifying the major metamorphic structures of the area. Previously identified major thrust and other fault systems still appear to define the boundaries between tectonically emplaced Paleozoic rocks and the probable Precambrian basement rocks. Evidence for the presence of a major fault boundary was supported by data derived from drilling logs of the Moodus Deep Hole (CGNHS, 1987). In addition to the complex Paleozoic and earlier deformations, superimposed Mesozoic structural features are present in the area. This overprinting is largely brittle in nature and therefore can commonly be distinguished from earlier ductile deformations (London, 1987). The most obvious Mesozoic feature in the study area is the major border fault which separates the Eastern Highlands from the Central Lowlands region.

3.0 GEOCHEMICAL STUDIES OF STREAM WATERS

In an attempt to identify areas of anomalous water chemistry in the Moodus area that might be related to recent and historic seismic activity, local tributary streams were examined during August of 1987. In some carbonate bedrock areas (such as central Virginia or Lancaster, Pennsylvania), saturated, effluent ground waters, possibly produced by the dissolution of fault gouge, have been identified in streams by the presence of travertine-marl deposits and anomalous concentrations of related dissolved species downstream from some fault traces. These deposits are thought to be produced by precipitation of saturated chemical species in turbulent, aerated stream riffles (Thornton, pers. comm., 1987; Hubbard et al., 1985). Because stream sampling was restricted in scope, the significance of these results is also limited.

3.1 Methodology

By visual inspection, 33 stream points throughout the Moodus seismic area were examined for the presence of carbonate deposition during the course of this study (see Plate 1). Stream bottom sediments were examined during late summer, low flow conditions, when it was thought that the presence of saturated ground waters discharging to the surface streams might be more easily detected. In addition, stream water samples from 8 selected sites were collected in order to provide some background data on stream water chemistry (see Plate 1 and Table A). These samples were analyzed and concentrations of specific anions and cations common to stream waters were determined. The concentration values were then used to calculate the ionic balance of each sample as a check on laboratory accuracy. These and other field data were then used to calculate the degree of saturation of the calcium carbonate in the stream waters.

3.2 Discussion of Results

The results of the analyses were interesting but they did not show anomalous concentrations of dissolved species. While this is not overly surprising, the degree of undersaturation (100 to 1000 times) of the calcium carbonate and other species was more extreme than expected (Machesky, pers. comm., 1987). The results of the sample analyses, as well as the analysis parameters are shown in Figure 2. Note the one value that was apparently affected by laboratory error. In general, the stream waters had very little mineral content and appeared to be well buffered, perhaps by the glacial overburden deposits. Although these data reflect only one isolated sampling of stream waters, the lack of precipitated minerals on stream bed materials in the area, as well as the highly undersaturated nature of the dissolved species in the water samples, indicates that potentially saturated ground waters are not discharging to surface streams in this area.

This may be the result of several factors that are related to the nature and distribution of geologic materials in this area. If the streams are not receiving any mineralized, deep circulating waters from fractures, faults, or other discharge points, then there may not be any dissolved species in the streams to be precipitated. However, the previously noted glacial deposits which cover this area may prevent saturated chemistries from flowing directly into surface streams. If saturated species are present, they may simply precipitate within some permeable zone of the overburden after being discharged from their bedrock source. An additional possibility is that low-flow and depressed water-table conditions in the summer produced the observed absence of anomalous water chemistries. Heavy precipitation and dilution of the concentration of the available species is another, although less likely, possibility. However, it is likely that if significant amounts of mineralized waters are in this area, then some indication of their presence would have been discovered by this aspect of the study.

To further investigate the possible association of mineralized ground water and seismic activity in the Moodus area, variable depth monitoring boreholes should be installed, sampled, and analyzed for a similar set of parameters on a regular basis. This would allow seasonal factors to be evaluated and the effects of surficial glacial and soil deposits on effluent ground waters to be eliminated. Although such an undertaking was beyond the scope of this project, future researchers might make use of the deep research boreholes that have been drilled in this area to conduct geochemical studies (see Plate 1).

4.0 LINEAMENT ANALYSIS OF STUDY AREA

In order to provide an evaluation of the orientation, "frequency", and length of lineaments present in the six-quadrangle study area, several scales of imagery were examined for the presence of linear topographic, tonal (shadow), vegetative, or combination features. As these mapped linear features have been correlated in other studies with zones of fracture concentration, aligned ore bodies, offset geophysical anomalies, faults, and zones of increased ground-water yield, lineament analysis is a commonly used technique for general, macroscopic scale,

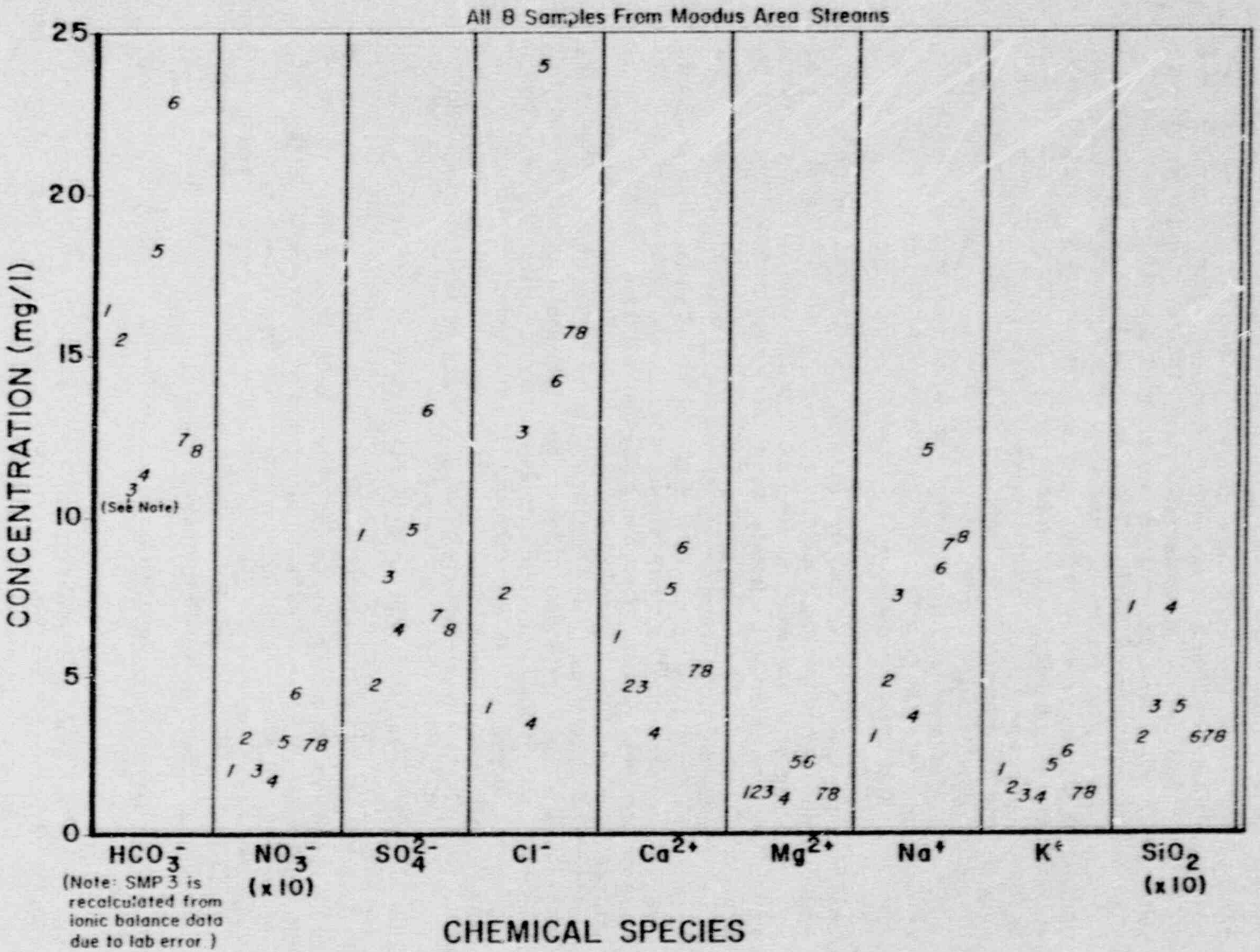

Figure 2, Results of geochemical water analyses site studies. In this study, the analysis was designed to yield data revealing regional fracture directions and other information on subsurface conditions in the Moodus area. It should be noted here that determining the age relationship(s) of the mapped lineament features is critical to their use as indicators of the tectonic history of an area. In addition, as mentioned previously, all linear features mapped in this study will be termed lineaments for the purpose of convenience.

4.1 Methodology

Through the use of techniques adapted from Lattman (1958) and Meiser and Earl (1982), the 1:250,000 scale SLAR side-looking aerial radar imagery, 1:100,000 scale SPOT satellite image, 1:80,000 scale high-altitude and 1:18,000 scale low-altitude aerial photographs were examined for the presence of lineaments (see Figure 3). These products, single images for the SLAR and SPOT, and multiple stereo pairs for the aerial photographs, were covered by clear acetate overlays to provide a permanent base for the analysis. Soft-tipped pens were then used to mark the ends and to number each observed linear feature. By making pairs of elongate marks on the overlays, the entire feature can be identified without obscuring or biasing the observation of subsequent features. The acetate overlays are also marked for identification and to allow accurate repositioning over the study area.

Identifying the lineaments of interest to the study is somewhat subjective and accounts for the general variability in the results. However, through careful analysis of individual and stereo pairs of images, linear alignments of topographic, tonal, vegetative, and combination features can be readily identified. Varying the angle of the incident lighting of the imagery and the use of magnifying lenses is also beneficial to the analysis. In the opinion of the author, extremely subtle features should be avoided as should features even possibly related to the works of man. Cultural features such as abandoned farm fields, pipelines, right-of-ways, drainage ditches, and old fence lines are not of interest to a study of this sort. The orientation and length of each feature mapped on the overlays is then determined. This is done by determining the direction of true north and the scale of the photograph and then measuring the bearing and length of the features on the overlay acetate. (Unless the imagery has been orthographically rectified, the orientation data may be subject to some distortion (see Lillesand and Kiefer, 1979).) A base map may be used to determine the scale and north direction of each photograph.

The preceding discussion describes the general technique used to produce the lineament analyses presented in the following sections. Probably the most important aspect of any analysis is maintaining objectivity about what constitutes a lineament feature. By examining the imagery for short intervals during a longer period of time, objectivity can be best maintained. This is critical because of the subjective nature of lineament analysis and the potential, at any scale, for confusing cultural features with geological lineaments. Again, it should be noted that results of imagery-based lineament analyses should be field checked for accuracy and to eliminate cultural features from the data.

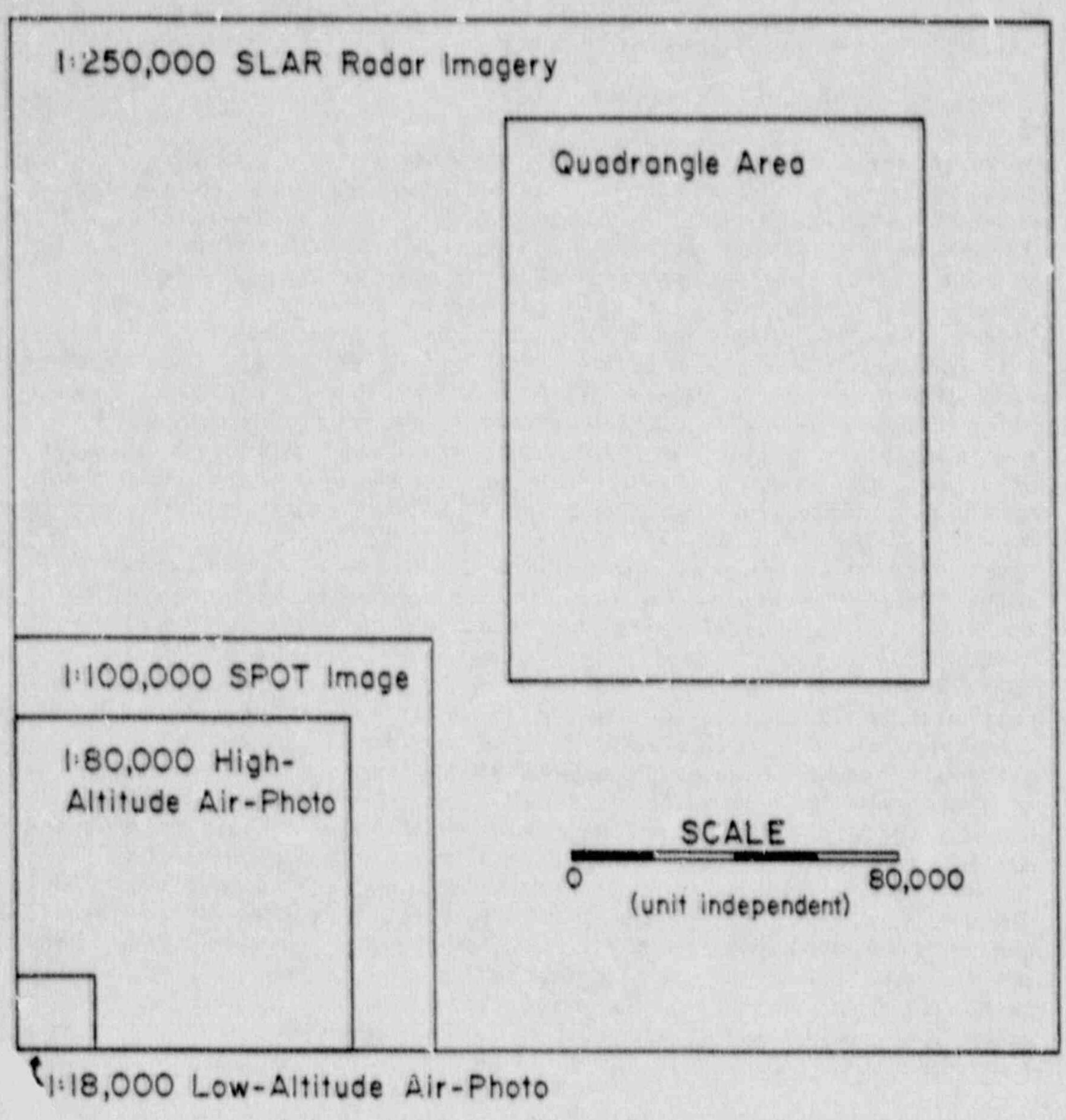

Figure 3, Comparison of imagery scales used in lineament analyses

4.2 Side-Looking Aerial Radar Imagery

The radar imagery used in this portion of the study was produced by the U.S. Geological Survey (USGS) for the CGNHS in May 1984. The look direction for this product is to the east and its small scale allowed the entire state of Connecticut to be viewed on one sheet. Radar is especially suited to analyses of this sort because the emitted radar beam can penetrate atmospheric phenomena and some vegetative cover before being reflected to the receiver. This provides an extremely detailed representation of the land surface that is sensitive to morphological features. However, the radar image can bias lineament analysis because the radar signal will reflect relatively poorly from linear features that are oriented parallel to the look direction and strongly from those features oriented perpendicular to the look direction (Lillesand and Kiefer, 1979).

In all, 48 lineaments were identified within or intersecting the six-quadrangle study area.* These features, ranging in length from 6 to 27 kilometers, may identify first-order tectonic fractures largely in the Eastern Highlands province. Interestingly, the Salmon River "fault" and the Moodus River both appear as lineaments and intersect in the vicinity of the Haddam Neck Station (see Plate 1). Another feature marks the border fault at the edge of the Central Valley area. Other features may identify stratigraphic or other linear non-fracture, geologic features. However, the results of this study compare well to an analysis prepared by the CGNHS on a radar image at 1:125,000 scale (Altamura, 1985). In the area covered by this study, there was about 70% spatial coincidence with this earlier work.

The azimuthal half-rose orientation diagram of the radar lineaments is shown in Figure 4. This diagram reveals that lineaments observed in the six-quadrangle study area have a primary orientation maximum to the northwest between 340 and 350 degrees. A secondary orientation maximum is also in the northwest quadrant, between 300 and 320 degrees. Other peaks are present but are not as dominant. This compares generally to lineament analysis results included in the Weston Corp. documents (1982a; 1982b). They also note the potential for look-direction bias in the radar imagery, which may explain the overall lack of east-west trending lineament structures.

4.3 SPOT Satellite Imagery

This imagery was selected for this study because of its ability to provide extremely detailed images of the ground surface from space. It has only recently become available and has approximately a 10 meter ground resolution in the black and white panchromatic band. The study area was examined from a cloud-free portion of an image at the 1:100,000 scale taken in March of 1986. However, as a result of the spacing of the satellite's scenes, only the three upper quadrangles were covered by the available product. While the SPOT image provides a superior image of the actual land surface (roads, fields, streams, urban areas, and other features are recognizable), the penetrating nature of the radar is lost.

* Table B.

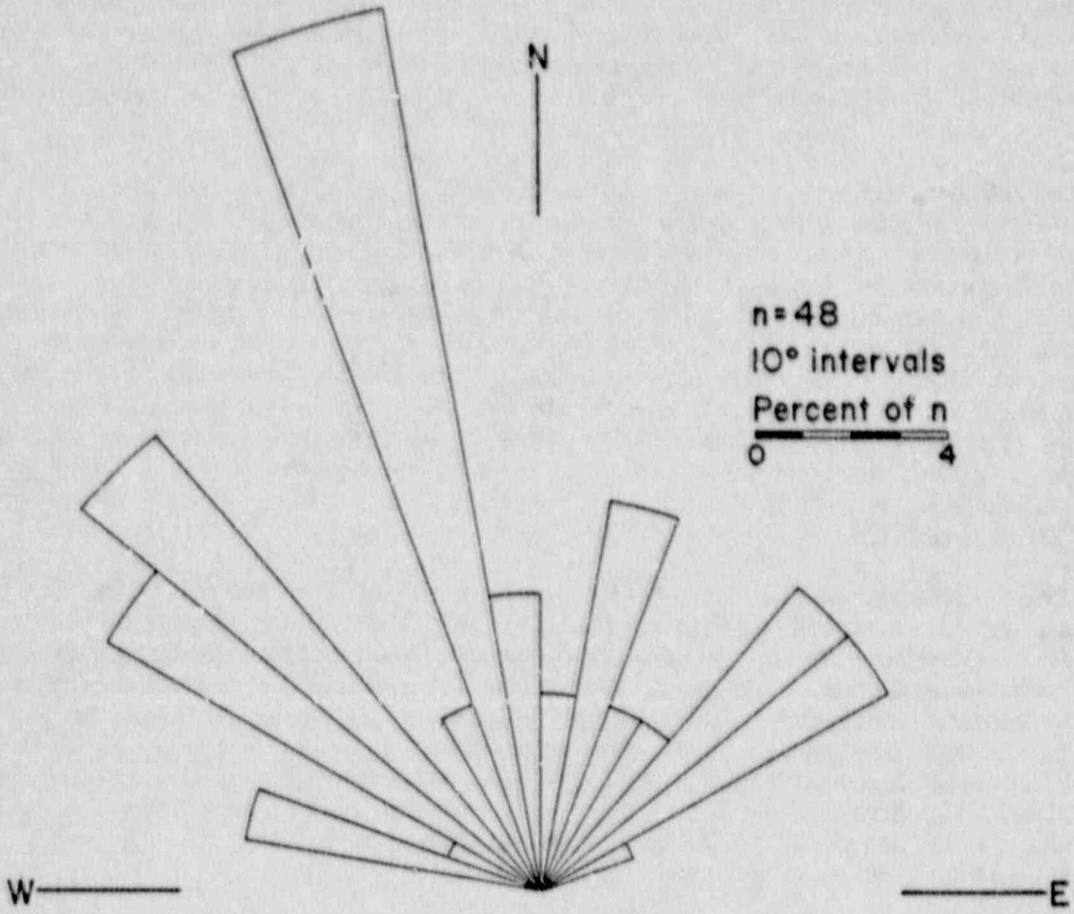

Figure 4, Orientation of lineaments observed on 1:250,000 scale SLAR radar imagery

Over the three quadrangles covered, a total of 37 lineaments were mapped.* These features ranged from about 4 to 10 kilometers in length, and included some possible lithologic strike lines as well as probable fracture features. As with the radar imagery, most of the lineaments were mapped in the metamorphic rocks of the Eastern Highlands, with only a few being mapped in the heavily urbanized Central Valley.

The rose diagram of SPOT lineament orientations (Figure 5) reveals a different distribution of observed features than the radar imagery. This distribution records two primary peaks: a broad one to the northeast between 020 and 040 degrees and a narrow peak to the northwest between 340 and 350 degrees that coincides closely with the maximum found in the analysis of the radar image. Secondary peaks are less distinct and may not be significant.

The 340 to 350 degree peak, common to both the SLAR and SPOT data sets, may be significant due to its orthogonal relationship to the present stress field (maximum compressive stress, σ_1 = 080) (Alexander, pers. comm., 1987). These values, derived from borehole stress measurements and earthquake focal mechanism solutions, indicate that faults and fractures at 90 degrees to σ_1, or 350 degrees, may be under a reverse (thrust) stress regime. Therefore, it is likely that the lineament orientation peak between 340 and 350 degrees may be a function of the contemporary stress field present in the Moodus area. However, the absence of an east-west orientation peak at this scale in support of the field evidence is notable.

The cause of the difference between this data set and the observed radar lineaments is uncertain. It may be due to the theoretical relationship between first- and second-order shear structures discussed in Canich and Gold (1977) or it may be simply a function of the scale of observation and the imagery look direction. The orientation of the northeasterly primary peak may be due solely to the subdivision of the Salmon River lineament into a number of smaller northeast trending lineaments. However, the Weston Geophysical Corp. report (1982b) also notes some north and northeast trending lineaments to the southeast of the Salmon River.

4.4 High-Altitude Aerial Photography

Fourteen 1:80,000 scale, 1980 flight, aerial photographs were required to cover the six-quadrangle study area.+ In all, 113 linear features were observed on the stereo-pairs of aerial photographs used to analyze this area. These features ranged in length from about 2 to 13 kilometers and revealed aspects of the structural nature of the area. The Salmon River lineament, observed on both the SLAR and SPOT imagery, was revealed as a number of discontinuous, shorter features and the Moodus River feature was similarly divided. Other lineaments apparently correlate to the Central Valley border fault and to other lesser structural features. In addition, a number of nearly parallel features were observed near where the Connecticut River crosses into the Eastern Highlands terrane.

---

* Table C.

+ Table D.

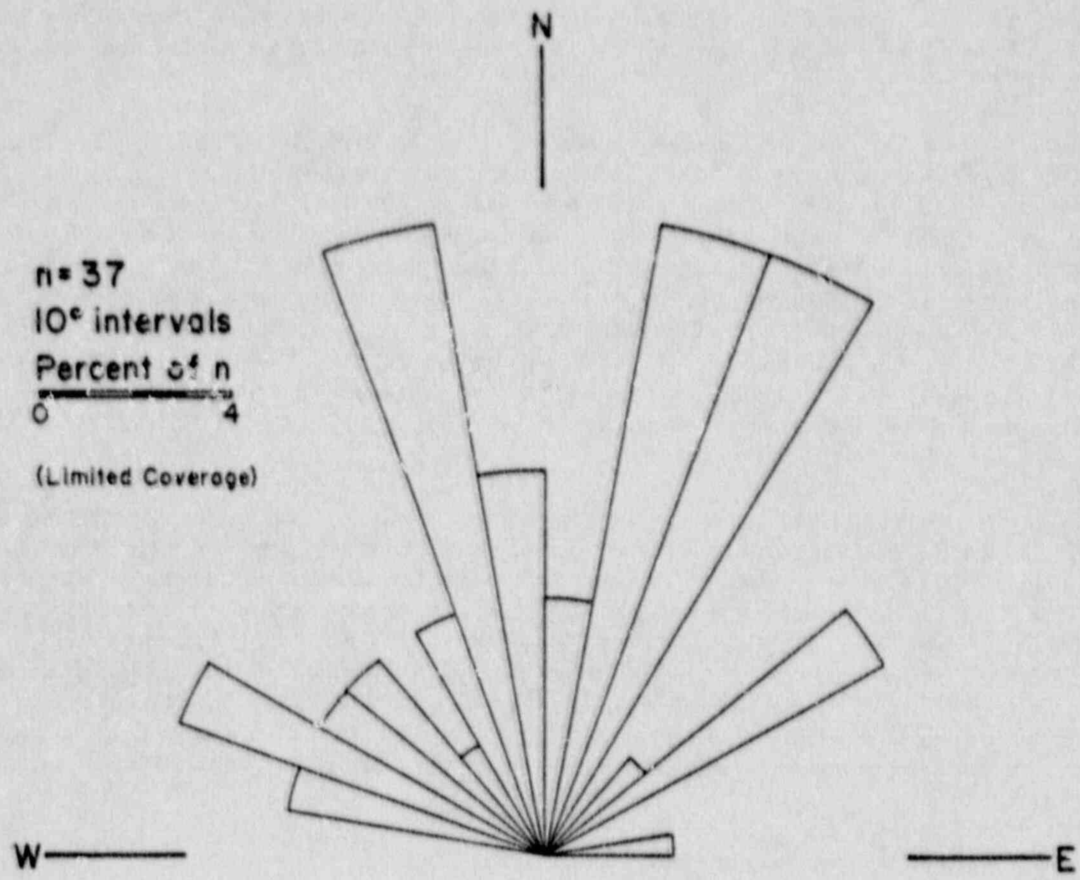

Figure 5, Orientation of lineaments observed on 1:100,000 scale SPOT satellite image

The orientation of the lineaments mapped on the high-altitude aerial photographs (Figure 6) compares closely to the SPOT imagery lineament distribution. The rose diagram reveals a narrow northeast primary peak and a broader northwest peak. The northeast maximum is oriented between 030 and 040 degrees whereas the northwest maximum lies between 330 and 350 degrees. Northerly orientations between these two peaks are represented by secondary maxima. The reasonably close correlation between the SPOT and aerial photograph data is interesting because it suggests that these two scales of imagery are capable of sampling the same set of features, although with differing degrees of sensitivity.

4.5 Low-Altitude Aerial Photography

Because of the time and manpower limitations of this study, only the Moodus Quadrangle was subjected to the 1:18,000 scale lineament analysis. However, as 25 stereo aerial photographs from a 1965 flight were required to provide adequate stereo coverage of the quadrangle, the analysis was still considerable. In all, 159 linear features, ranging in length from 1 to 2 kilometers, were observed in this area.* In some cases these features could be correlated with major lineaments observed at the other, smaller scales. However, some of the features show no distinct relationship to the major lineaments. These short lineaments are thought to be related to joint and fault traces, lithologic variability and strike, and possibly glacial scouring directions (Weston Geophysical Corp., 1982b). In other terranes, foliation directions have also been observed on low-altitude photography.

The orientation diagram for the low-altitude lineaments is quite distinct from the previously observed distributions (Figure 7). These data show a pair of primary maxima; one between 320 and 330 degrees and one between 080 and 090 degrees. The first peak is about 10 degrees off the dominant northwest maxima (340 to 350 degrees) observed on the SLAR and SPOT imagery and close to the high-altitude photography lineament maximum (330 to 350 degrees). However, the easterly peak was a new orientation for lineament features in this study, but one that is compatible with the previously mentioned σ_1 direction of 080. In addition to these two peaks, indistinct maxima (possibly noise in the data) to the northwest, north, and northeast directions are also present. Overall, these features may be indicative of the disturbed nature of the subsurface in this area.

4.6 Discussion of Results

Besides examination of the overall distribution of the lineament data, the features which are present within the Moodus Quadrangle can be investigated specifically. By preparing orientation rose diagrams for each scale of mapping and plotting them adjacent to each other (Figure 8), the variation in orientation maxima can be compared. Again, the overall trend of lineaments is dominantly to the northwest, but only some of the maxima are consistent with the other results. The secondary peaks to the north-northeast and east are distinct, but have not been correlated with known subsurface features. However, the recent data from in situ borehole stress testing at the Moodus Deep Hole (see Plate 1), as well as earthquake focal mechanism solutions for local October

* Table E.

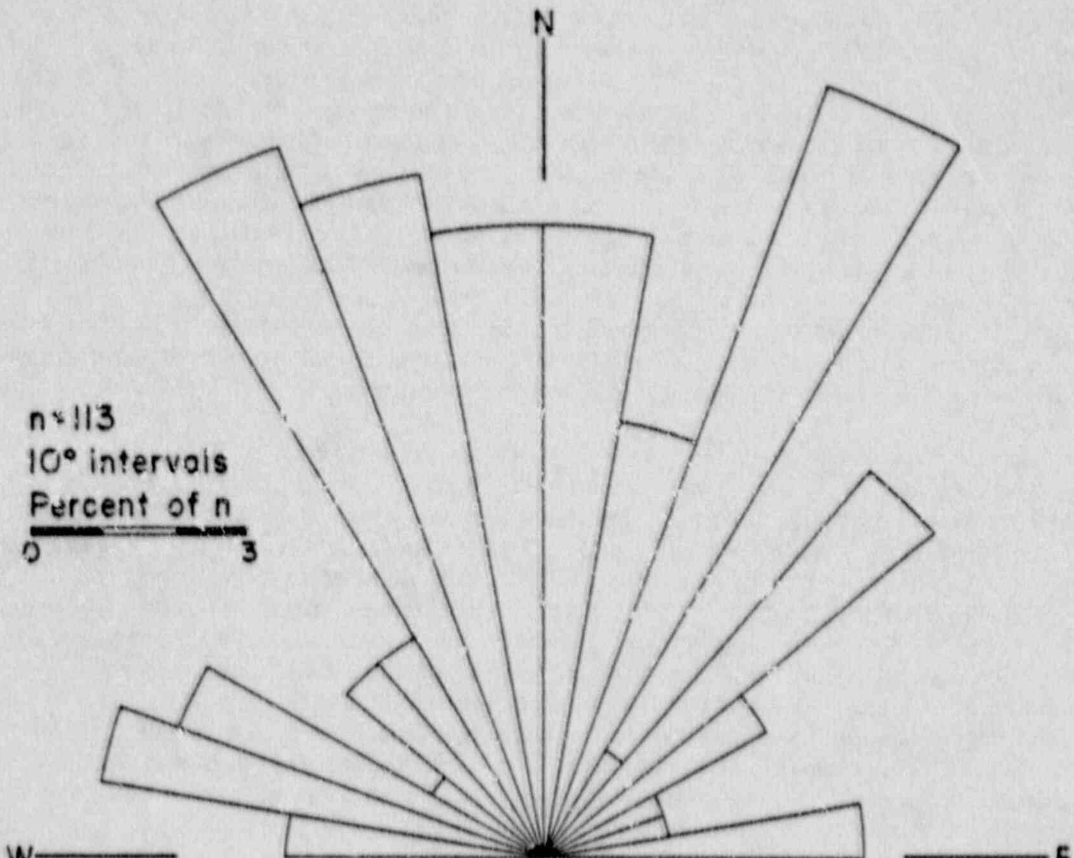

Figure 6, Orientation of lineaments observed on 1:80,000 scale high-altitude aerial photographs

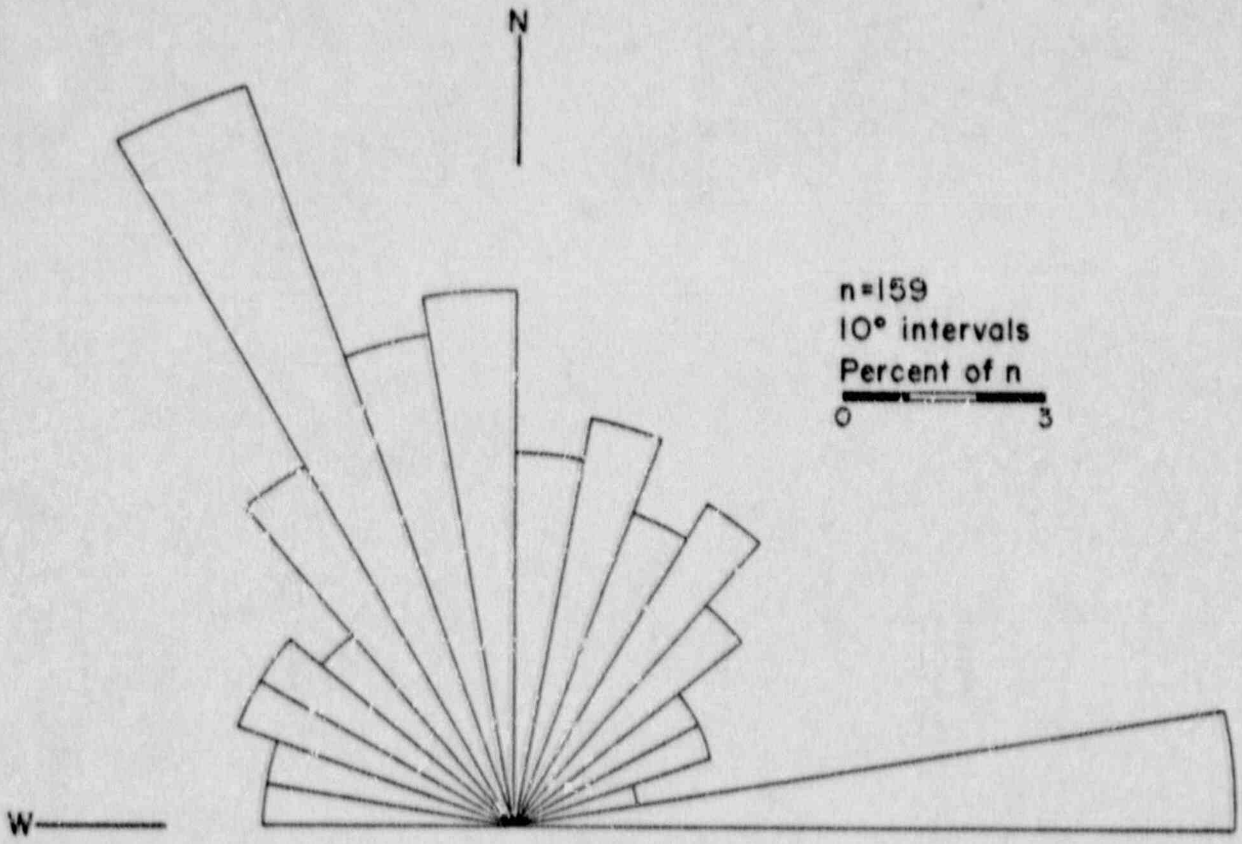

Figure 7, Orientation of lineaments observed on 1:18,000 scale low-altitude aerial photographs (Moodus quadrangle only)

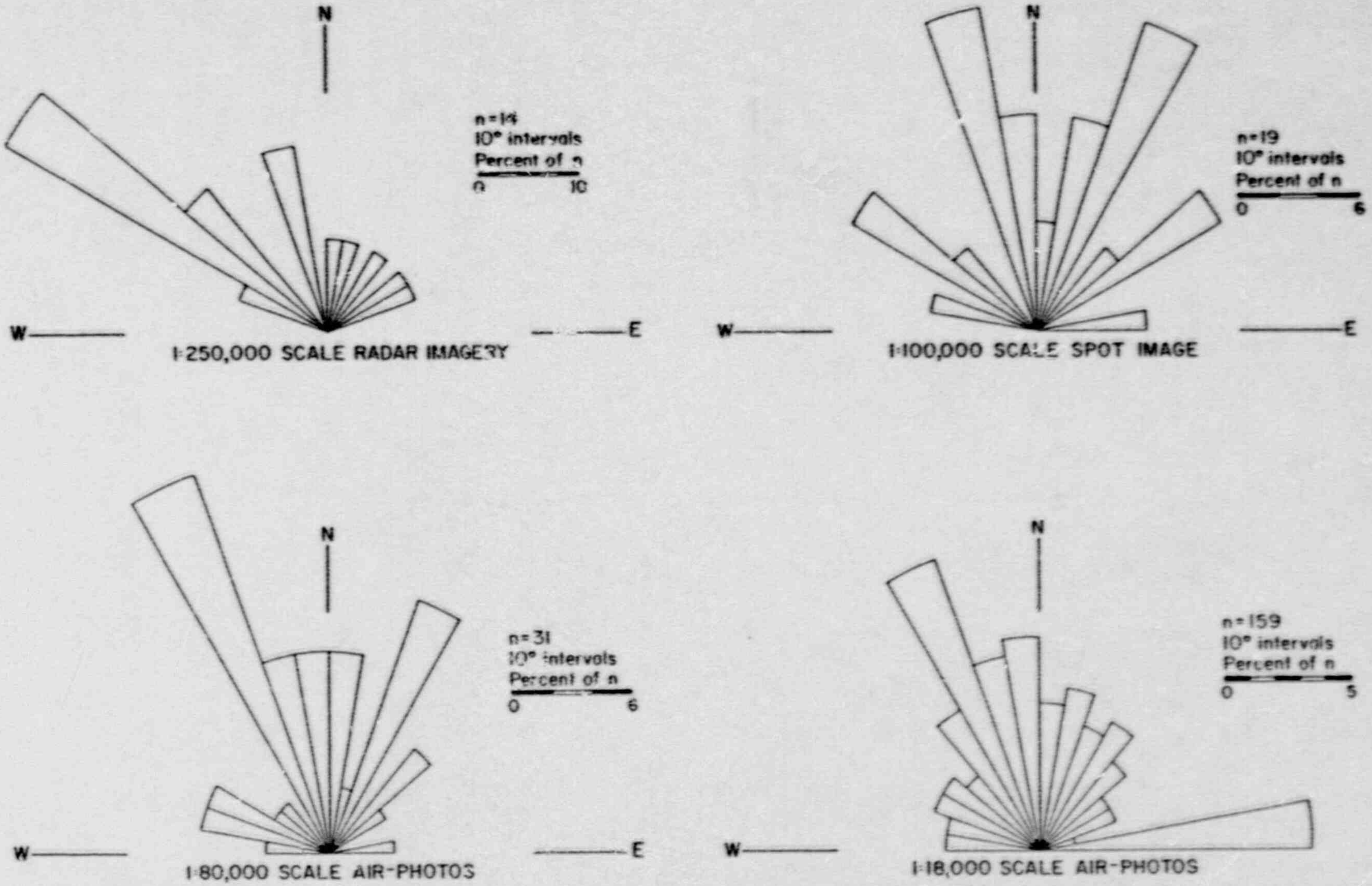

Figure 8, Comparison of lineament orientation data from the Moodus quadrangle

1987 earthquakes, have indicated a 080 degree direction for the σ_1 maximum compressive stresses in this area (Alexander, pers. comm., 1987). This orientation correlates well with the results of the low-altitude survey and indicates that these smaller features may be extensional joints formed or opened parallel to the current maximum stress. The lack of an easterly peak at the other scales indicates that these 080 features may be overprinting an older, northwest oriented stress field. As mentioned, the 340-350 degree maximum may also be related to, or reactivated by, the present tectonic stress regime.

Additional analysis results, produced by subdividing the data for the small-scale imagery on a quadrangle basis (Figure 9), indicate a possible reason for the seismic activity that is endemic to the Moodus area. At all three scales examined in this study, the Moodus quadrangle was observed to have a higher number of lineaments intersecting or within it. This measure of lineament "frequency" indicates that the Moodus area may be more fractured than adjacent areas, possibly contributing to, or as a result of, higher numbers of seismic events. While this frequency value is probably real, it may possibly be the result of operator bias. In either case, it appears to characterize spatial, neotectonic features that may be related to the contemporary stress field and seismic activity in the area.

While lineament analyses are limited in the degree of detail they can provide about an area, they do offer a means of identifying potentially major structural features and indications of the orientation of the contemporary state of stress. This is usually accomplished by examining one, possibly two, scales of imagery. However, this study may have also produced some less specific, but more interesting results by examining and reexamining the same area at four different scales. Across the six quadrangle study area, data on the general frequency and length of lineaments per unit study area were gathered. When those data were examined, some interesting relationships regarding lineaments and scale of observation were revealed.

Figure 10 shows the observed relationship between the average number of lineaments intersecting a quadrangle block and the scale of the imagery used in the analysis. The plot shows the exponential decay of observed lineament frequency with increasing scale number. This indicates that as the size of the lineament feature increases, then fewer features of that size will be observed in a given area. Intuitively, this makes sense because joints, which are observable only at a large scale, are much more numerous than multi-kilometer lineaments, which are observable only at a small scale. Canich (1976) and Canich and Gold (1977) used this as the theoretical basis for a model of the relationship between first-, second-, and third-order shear structures.

An additional relationship for the multi-scale data is illustrated in Figure 11. When the average lineament length observed at each scale is plotted against the scale of the imagery, a distinct, positively sloped, linear trend results. This relationship indicates that there may be an appropriate scale for the observation of particular size features. This may be the result of the imagery resolution or the perception of the observer. In any case, the linear relationship argues for a length

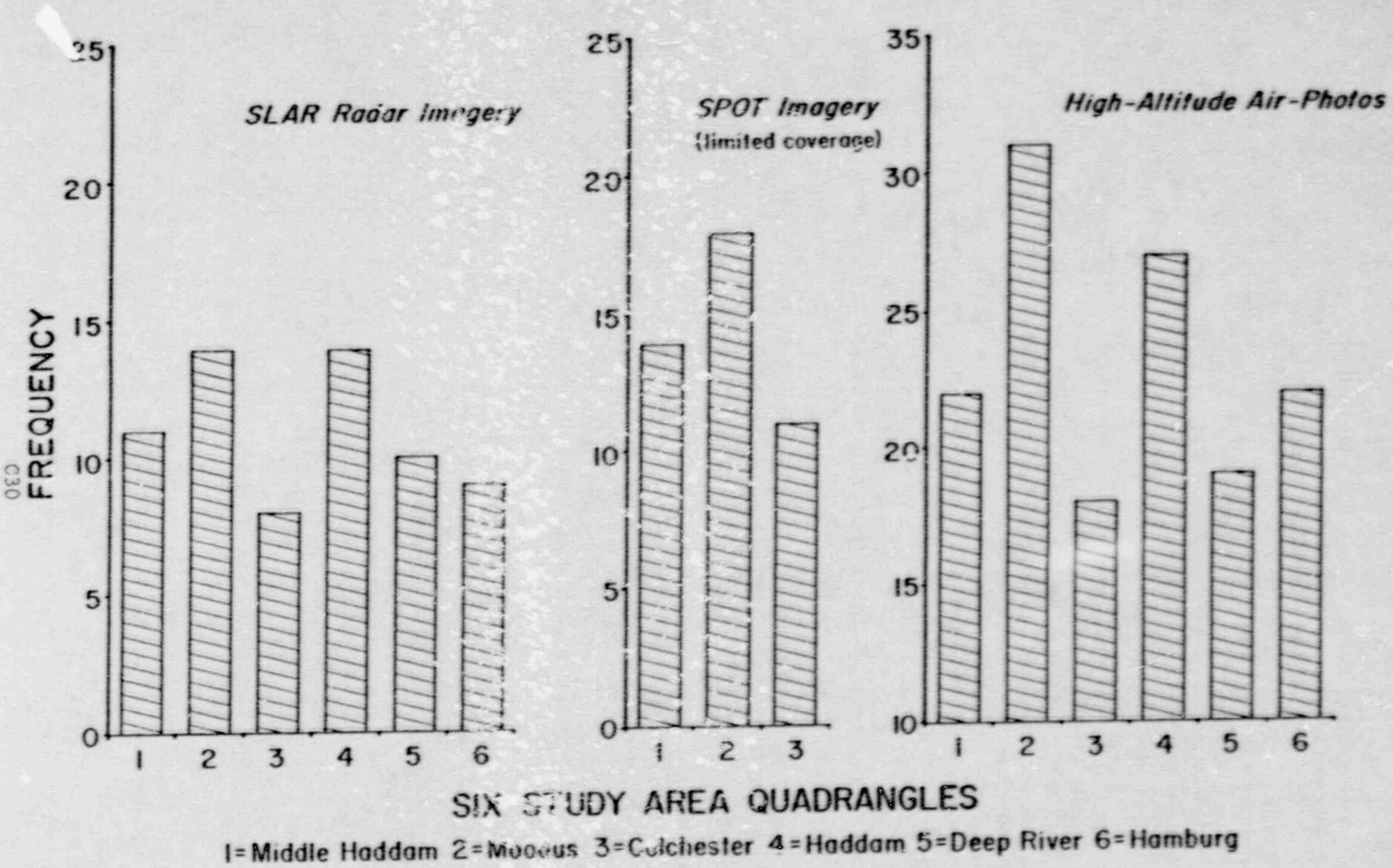

Figure 9, Areal lineament frequency data by quadrangle

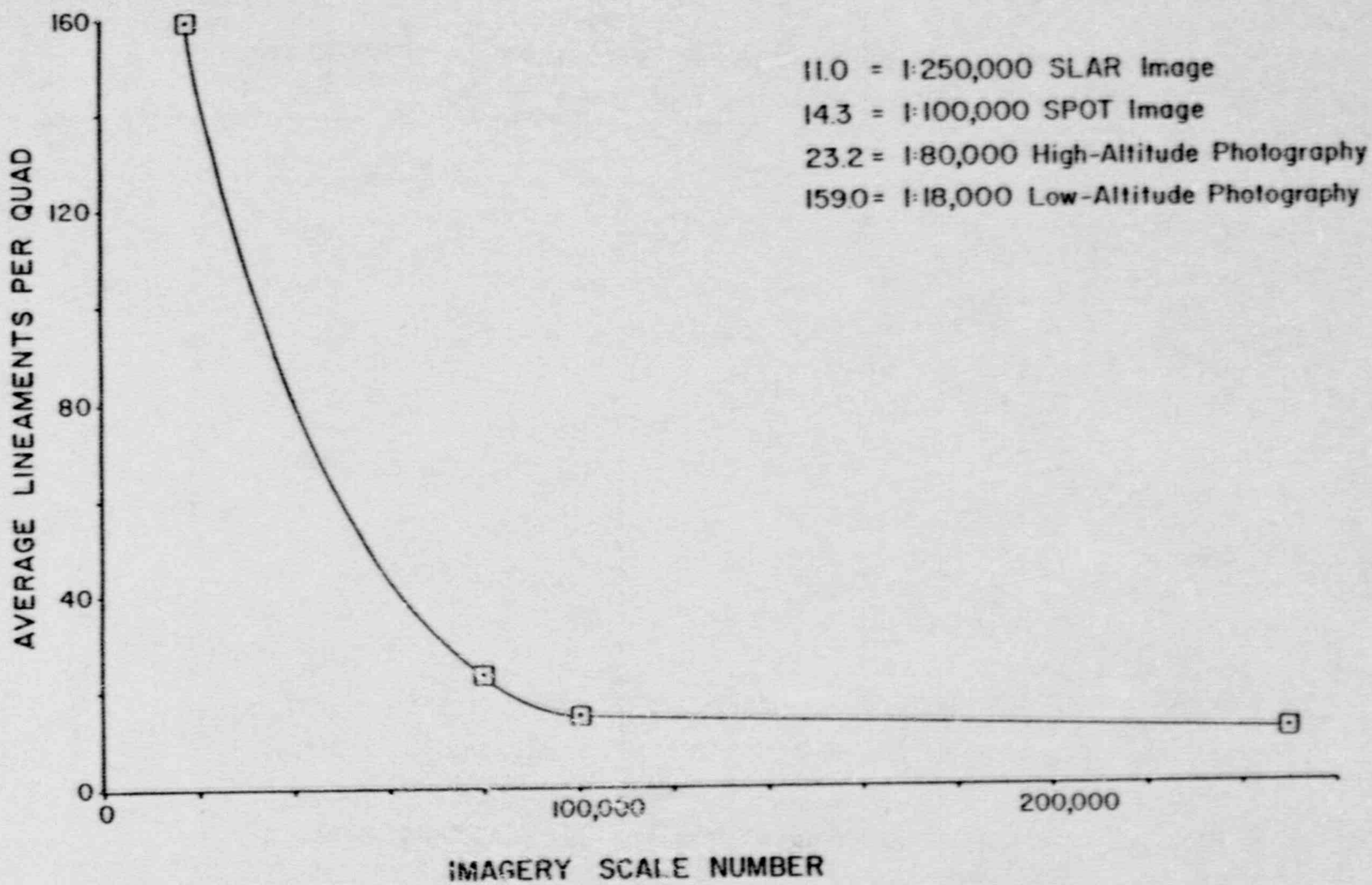

Figure 10, Observed relationship between average lineament frequency per quadrangle and imagery scale number

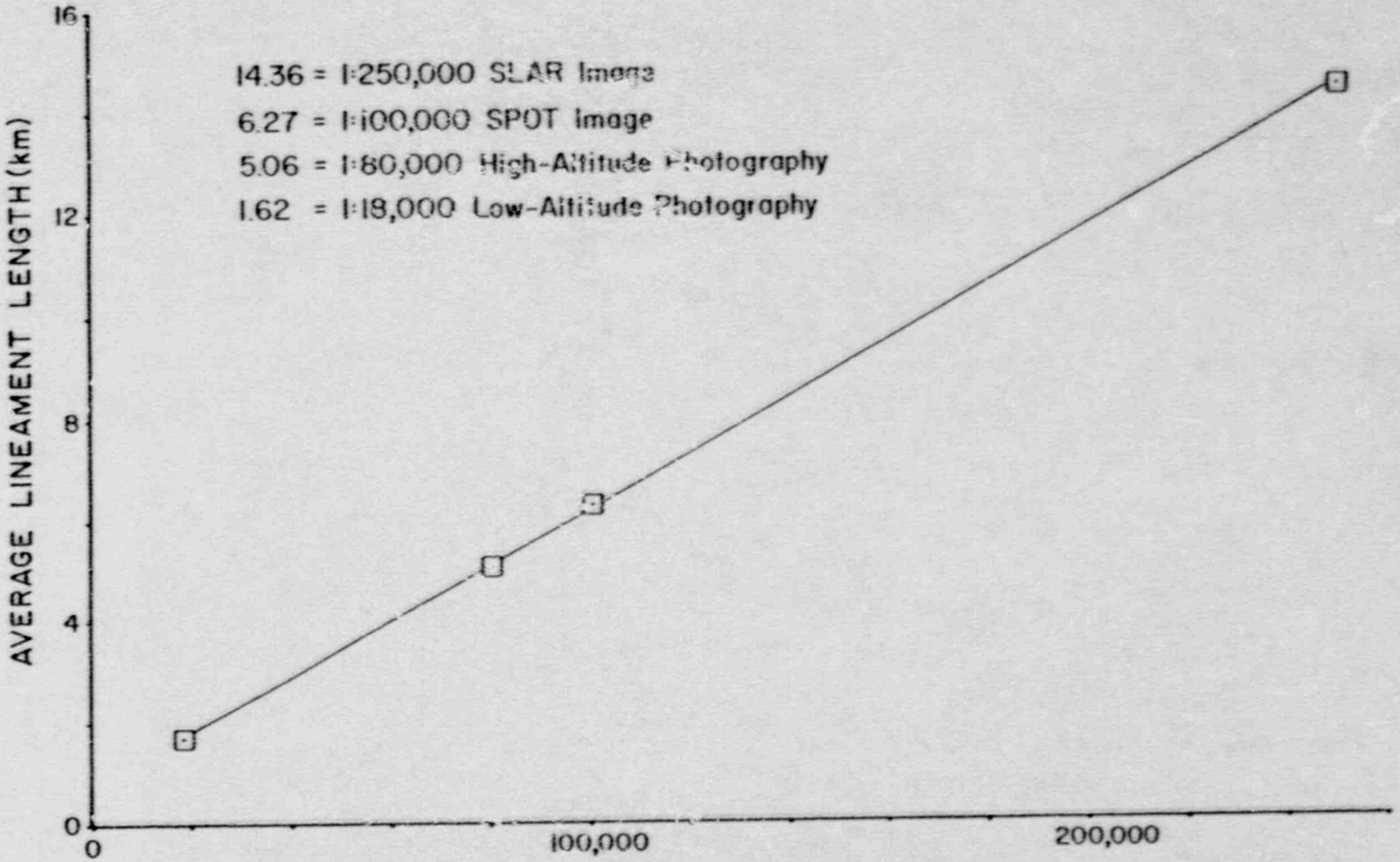

Figure 11, Observed relationship between average lineament length and imagery scale number relationship that is consistent over different scales of geologic phenomena. It should be noted that appropriate observation scales for various geologic phenomena have been investigated (Gold, 1980).

The potential benefit of these relationships may only be revealed after further study on why and how they exist. If these relationships describe the characteristics of lineaments, then they may be used to predict the number or average length of features likely to be observed in a given area for a given scale of imagery. Likewise, they may be able to indicate the appropriate scale imagery to use for examination of particular scale features. Another interesting possibility is the variation of these relationships with changes in age, tectonic, and lithologic setting. As this study focused on an seismically active, highly deformed area, the data obtained in this area may not be representative of other younger and more stable areas. In actuality, there may be comparably systematic, but different, scale relationships that depend on the strain effects of the past and present stress fields.

5.0 CONCLUSIONS AND RECOMMENDATIONS

Although it is obvious that a great deal of additional work will be necessary to fully understand the Moodus seismic area, this study is able to offer specific conclusions and recommendations which may benefit further studies of this area. Those conclusions and recommendations may also benefit research in other seismically active zones, as well as geologic investigations of other regions.

5.1 Conclusions

The principal conclusions that can be drawn from this study of the Moodus seismic area are:

1. No distinctly positive evidence of neotectonic disturbances of the land surface or of glacial deposits was recorded. Both field and literature studies were unable to identify evidence of recent land surface disturbances that could be attributed to tectonic activity.

2. The limited geochemical studies of stream bottom materials and water samples in the Moodus area produced no evidence of saturated ground waters being discharged to surface streams. In other seismic areas, the location of faults and fractures have been identified by the presence of anomalous carbonate deposition on stream bottoms and the presence of associated carbonate-rich water chemistries.

3. Lineament analysis of the study area was conducted through the use of 1:250,000 scale radar imagery, 1:100,000 scale SPOT satellite imagery, and 1:80,000 scale high-altitude aerial photographs. The Moodus quadrangle was also examined with 1:18,000 scale low-altitude aerial photographs. The results of these studies revealed varying distributions of lineament orientation, frequency, and length.

4. Lineament orientations are concentrated in the northwest quadrant, although other distribution peaks occur to the northeast and east. The easterly (080 to 090 degrees of azimuth) peak correlates well with the results of recent in situ stress and earthquake focal mechanism solutions which indicate an 080 degree orientation of the maximum compressive stress, probably σ_1. This regime would favor the formation or opening of fractures oriented parallel to the maximum

stress and high shear (reverse) stresses on faults or fractures at 90 degrees to this orientation. This may account for the orientation of numerous lineaments oriented between 340 and 350 degrees. These lineaments may also be reactivated features, originally formed by a previous principal stress regime oriented to the northwest.

5. The SPOT imagery (1:100,000 scale) and high-altitude aerial photographs (1:80,000 scale) appear to sample a common set of lineament features, although with differing degrees of sensitivity. The aerial photography's higher sensitivity may be the result of their ability to be viewed stereoscopically.

6. An increase in lineament frequency was observed over the Moodus quadrangle on the radar, SPOT, and high-altitude aerial photographs. This indicates the seismic area may be more fractured than surrounding regions in the present stress field, possible as a result of higher seismic activity.

7. Average lineament frequency per quadrangle block and average lineament length vary with imagery scale. The former exhibited an exponential decay in average lineament frequency with increasing scale number, and the latter exhibited a linear increase in average lineament length with increasing scale number.

5.2 Recommendations

In order to refine the analysis conducted during this project, several specific recommendations for additional work can be made:

1. The "Rely Fault" exposure should be reexcavated and examined for its possible neotectonic significance.

2. Regular geochemical sampling of stream and well waters should be conducted to evaluate the hydrogeochemical factors at work in the Moodus area. Thermal data associated with this sampling may also prove of interest.

3. Compilation of all lineament data on a suitable base map is also suggested. This information can then be checked for supporting field evidence (such as increased well yields, subsurface gas migration, aligned ore bodies, or earthquake foci) that will indicate if the mapped linear features are related to subsurface fractures and possibly to seismic activity.

4. The observed lineament data illustrating the relationship between average lineament frequency per unit area and lineament length versus imagery scale should be further investigated.

5. As stream systems appear to be tectonically sensitive, drainage networks could be profiled and monitored for neotectonic changes.

6. Joint studies should be conducted on all available outcrops for evidence of current and previous stress field orientations.

BIBLIOGRAPHY

Abriel, W.L., 1978. A ground-based study of the Everett-Bedford Lineament of Pennsylvania, Unpublished M.S. Paper, The Pennsylvania State University, University Park, Pennsylvania, 90p.

Alexander, S.S., 1987. Personal communication, Professor of Geophysics, The Pennsylvania State University, Department of Geosciences, University Park, PA.

Altamura, R.J., 1985. Preliminary radar (SLAR) lineament map of Connecticut, Open-file map, scale 1:125,000, Connecticut Geological and Natural History Survey project.

Banwell, G.M., 1986. Helium-4 and Radon-222 concentrations in groundwater and soil gas as indicators of the extent and depth of fracture concentration in rock, Unpublished M.S. Thesis, The Pennsylvania State University, University Park, Pennsylvania, 136p.

Barosh, P.J., D. London, and J. de Boer, 1982. The structural geology of the Moodus Seismic Area, south-central Connecticut, in Guidebook for Fieldtrips in Connecticut and South Central Massachusetts, New England Intercollegiate Geological Conference, R. Joesten and S.S. Quarrier, eds., Connecticut Geological and Natural History Survey, Guidebook No. 5, pp. 419-451.

Barosh, P.J. and M.H. Pease, 1981. Geologic structure in the area of the 1981 Moodus earthquakes, south-central Connecticut, Earthquake Notes, vol. 52, no. 3, pp. 8-9.

Blanchet, P.K., 1957. Development of fracture analysis as an exploration method, Bulletin of the American Association of Petroleum Geologists, vol. 41, no. 8, pp. 1748-1759.

Canich, M.R., 1976. A study of the Tyrone - Mt. Union lineament by remote sensing techniques and field methods, Unpublished M.S. Paper, The Pennsylvania State University, University Park, PA, 59p.

Canich, M.R. and D.P. Gold, 1977. A study of the Tyrone-Mt. Union Lineament by remote sensing techniques and field methods, CRSER Technical Report 12-77, The Pennsylvania State University, University Park, Pennsylvania, 59p.

Cline, G.D., 1968. Geologic factors influencing well yields in a folded sandstone-siltstone-shale terrane within the East Mahantango Creek Watershed, Pennsylvania, Unpublished M.S. Thesis, The Pennsylvania State University, University Park, Pennsylvania, 180p.

Connecticut Geological and Natural History Survey, 1987. Moodus Deep Bedrock Drill Hole: News Note #4, May 11, 1987, 4p.

Costain, J.K., G.A. Bollinger, and J.A. Speer, 1987. Hydroseismicity - A hypothesis for the role of water in the generation of intraplate seismicity, Geology, vol. 15, pp. 618-621.

Drever, J.I., 1982. The Geochemistry of Natural Waters, Prentice-Hall, Inc. Englewood Cliffs, NJ, 388p.

Eaton, G.P. and J.L. Rosenfeld, 1972. Preliminary bedrock geologic map of the Middle Haddam Quadrangle, Middlesex County, Connecticut, U.S. Geological Survey, Open-File Report 72-99.

Ebel, J.E., V. Vudler, and M. Celata, 1982. The 1981 microearthquake swarm near Moodus, Connecticut, Geophysical Research Letters, vol. 9, no. 4, pp. 397-400.

Famy, S.M., 1978. Relationship between cross-strike lineaments and the distribution of oil and gas fields in northwestern Pennsylvania, Unpublished M.S. Thesis, The Pennsylvania State University, University Park, Pennsylvania, 95p.

Flint, R.F., 1978. The surficial geology of the Haddam Quadrangle, Connecticut Geological and Natural History Survey, Quadrangle Report No. 36, 27p.

Gold, D.P., 1980. Structural geology, Chapter 14 in: Remote sensing in Geology, B. Siegal and A.R. Gillespie eds., John Wiley, pp. 419-484

Gold, D.P., S.S. Alexander and R.R. Parizek, 1974. Application of remote sensing to natural resource and environmental problems in Pennsylvania, Earth and Mineral Sciences, vol. 43, no. 7, pp. 49-53.

Hobbs, W.H., 1911. Repeating patterns in the relief and in the structure of the land, Bulletin of the Geological Society of America, vol. 22, pp. 123-176.

Hobbs, W.H., 1905. Examples of joint controlled drainage from Wisconsin and New York, Journal of Geology, vol. 13, pp. 363-374.

Hubbard, D.A., W.F. Giannini, and M.M. Lorah, 1985. Travertine-marl deposits of the Valley and Ridge Province of Virginia -A preliminary report, Virginia Minerals, vol. 31, no. 1, pp. 1-12.

Keim, J.W., 1962. A study of photogeologic fracture traces over the Bisbee Quadrangle, Cochise County, Arizona, Unpublished M.S. Thesis, The Pennsylvania State University, University Park, Pennsylvania, 42p.

King, P.B., 1977. The Evolution of North America, Revised Edition, Princeton University Press, 197p.

Kowalik, W.S., 1975. Use of LANDSAT-1 imagery in the analysis of lineaments in Pennsylvania, Unpublished M.S. Thesis, The Pennsylvania State University, University Park, Pennsylvania, 93p.

Krohn, M.D., 1976. Relation of lineaments to sulfide deposits and fracture zones along Bald Eagle Mountain: Centre, Blair, and Huntingdon Counties, Pennsylvania, Unpublished M.S. Thesis, The Pennsylvania State University, University Park, Pennsylvania, 80p.

Krothe, N.C. and M.P. Bergeron, 1981. The relationship between fracture traces and joints in a Tertiary basin, southwest Montana, Ground Water, vol. 19, no. 2, pp. 138-143.

LaFleur, R.G., 1980. Investigation of possible earthquake related deformation of glacial overburden deposits in the Moodus-Haddam area, Connecticut, Report, Ressalear Polytechnic Institute, 14p.

Lattman, L.H., 1958. Technique of mapping geologic fracture traces and lineaments on aerial photographs, Photogrammetric Engineering, vol. 19, no. 4, pp. 568-576.

Lattman, L.H. and R.R. Parizek, 1964. Relationship between fracture traces and the occurrence of ground water in carbonate rocks, Journal of Hydrology, vol. 2, pp. 73-91.

Lattman, L.H. and R.R. Parizek, 1963. Relationship between fracture traces and the occurrence of ground water in carbonate rocks, Annual Meeting of the Geologic Society of America, Paper.

Lattman, L.H. and R.H. Matzke, 1961. Geologic significance of fracture traces, Photogrammetric Engineering, vol. 27, pp. 435-438.

Lattman L.H. and R.P. Nickelsen, 1958. Photogeologic fracture-trace mapping in the Appalachian Plateau, American Association of Petroleum Geologists Bulletin, vol. 42, pp. 2238-2245.

Lattman, L.H. and W.W. Olive, 1955. Solution-widened joints in Trans-Pecos, Texas, Bulletin of the American Association of Petroleum Geologists, vol. 39, pp. 2084-2087.

Lavin, P.M., D.L. Chafin and W.F. Davis. 1982. Major lineaments and the Lake Erie-Maryland crustal block, Tectonics, vol. 1, no. 5, pp. 431-440.

Lillesand, T.M. and R.W. Kiefer, 1979. Remote Sensing and Image Interpretation, John Wiley and Sons, New York, 612p.

London, D., 1987. (in press) Bedrock geology of the Moodus Seismic Area, south-central Connecticut, Connecticut Geological and Natural History Survey, Report of Investigations No. 11, 47p.

Lundgren, L., Jr., 1963. The bedrock geology of the Deep River Quadrangle, Connecticut Geological and Natural History Survey, Quadrangle Report No. 13, 42p.

Lundgren, L., Jr., 1966. The bedrock geology of the Hamburg Quadrangle, Connecticut Geological and Natural History Survey, Quadrangle Report No. 19, 41p.

Lundgren, L., Jr., 1979. The bedrock geology of the Haddam Quadrangle, Connecticut Geological and Natural History Survey, Quadrangle Report No. 37, 44p.

Lundgren, L., Jr., L. Ashmead, and G. Snyder, 1971. The bedrock geology of the Moodus and Colchester Quadrangles, Connecticut Geological and Natural History Survey, Quadrangle Report No. 27, 24p.

Lundgren, L., Jr., 1972. Honey Hill Fault in eastern Connecticut: Regional relations, Geological Society of America Bulletin, vol. 83, no. 9, pp. 2773-2794.

Machesky, M., 1987. Personal communication, Associate Professor of Geochemistry, The Pennsylvania State University, University Park, PA.

Meiser, E. and T. Earl, 1982. Uses of Fracture Traces in Water Well Location: A Handbook, Office of Water Research and Technology, U.S. Department of the Interior, 55p.

Meisler, H., 1963. Hydrogeology of the carbonate rocks of the Lebanon Valley, Pennsylvania Geological Survey, 4th ser., Water Resources Report 18, Harrisburg, Pennsylvania. 81p.

Meisler, H. and A.E. Becher, 1966. Hydrology of the carbonate rocks of the Lancaster-15 minute Quadrangle, Pennsylvania. Pennsylvania Bureau of Topographic and Geologic Survey, Progress Report 171. Harrisburg, Pennsylvania, 36p.

Norman, J.W. and J.F. Huntington, 1974. Possible applications of photo geology to the study of rock mechanics, Quarterly Journal of Engineering Geology, vol. 7, pp. 107-120.

Nutter, L.J., 1973. Hydrogeology of carbonate rocks, Frederick and Hagerstown Valleys, Maryland, Maryland Geological Survey, Report of Investigations, No. 19, 70p.

O'Leary, D.W., 1975. Surficial geology of the Moodus Quadrangle, Connecticut, U.S. Geological Survey, Map GQ-1205.

O'Leary, D.W., 1977. Surficial Geology of the Deep River Quadrangle, Connecticut, U.S. Geological Survey, Map GQ-1370.

O'Leary, D.W., J.D. Friedman, and H.A. Pohn, 1976. Lineament, linear, lineation, some proposed new standards for old terms, Geological Society of America Bulletin, vol. 87, no. 10, pp. 1463-1469.

Parizek, R.R., 1976. On the nature and significance of fracture traces and lineaments in carbonate and other terranes, in: Karst Hydrology and Water Resources, Proceedings of the U.S. - Yugoslavian Symposium, Dubrovnik, Water Resources Publications, Fort Collins, Colorado, pp. 41-100.

Parizek, R.R., W.B. White and D. Langmuir, 1971. Hydrogeology and geochemistry of folded and faulted rocks of the central Appalachian type and related land use problems, Circular 82, Mineral Conservation Series, Earth and Mineral Sciences Experiment Station, The Pennsylvania State University, University Park, Pennsylvania, 182p.

Parizek, R.R. and B. Voight, 1970. On remote sensing in karst terranes, Question 37, Commission Internationale des Grand Barrages, Montreal.

Parizek, R.R. and L.J. Drew, 1966. Random drilling for water in carbonate rocks, Proceedings of the Symposium and Short Courses on Computers and Operations Research in the Mineral Industries, The Pennsylvania State University, University Park, Pennsylvania, pp. 1-22.

Rader, E.K. and T.M. Gathright, II, 1984. Stratigraphy and structure in the Thermal Springs area of the Western Anticlines, Virginia Division of Mineral Resources, Sixteenth Annual Virginia Geologic Field Conference Guidebook, October 13-14, 1984, 55p.

Rich, J.L., 1928. Jointing in limestones as seen from the air, Bulletin of the American Association of Petroleum Geologists, vol. 12, no. 8, pp. 861-862.

Rodgers, J., 1985. Bedrock geological map of Connecticut, Natural Resources Atlas, Connecticut Geological and Natural History Survey.

Rodgers, M.R. and T.H. Anderson, 1984. Tyrone-Mt. Union cross strike lineament of Pennsylvania: A major Paleozoic basement fracture and uplift boundary, The American Association of Petroleum Geologists Bulletin, vol. 68, no. 1, pp. 92-105.

Sharpe, W.F. and R.R. Parizek, 1979. Groundwater sources located by fracture trace technique, Water and Sewage Works, vol. 126, no. 5, pp. 38-40.

Shuman, C.A., 1987. Fracture studies and in situ permeability testing with borehole packers, Unpublished M.S. Thesis, The Pennsylvania State University, University Park, Pennsylvania, 185p.

Siddiqui, S.H., 1969. Hydrogeologic factors influencing well yields and aquifer hydraulic properties of folded and faulted carbonate rocks in central Pennsylvania, Unpublished Ph.D. Dissertation, The Pennsylvania State University, University Park, Pennsylvania, 502p.

Siddiqui, S.H. and R.R. Parizek, 1971. Hydrogeologic factors influencing well yields and hydraulic properties of folded and faulted carbonate rocks in central Pennsylvania, Water Resources Research, vol. 7, no. 5, pp. 1295-1312.

Taylor, L.F., 1980. Fracture traces and water wells, Pennsylvania Geology, vol. 11, no. 3, pp. 2-4.

Thornton, C., 1953. The geology of the Mount Jackson quadrangle, Virginia, Unpublished Ph.D. Thesis, Yale University, 211p.

Thornton, C., 1987. Personal communication, Professor of Geochemistry, The Pennsylvania State University, University Park, PA.

Thorson, R.M., W.S. Clayton, and L. Seeber, 1986. Geologic evidence for a large prehistoric earthquake in eastern Connecticut, Geology, vol. 14, pp. 463-467.

Weston Geophysical Corporation, 1982. Geological and seismological studies, Haddam Neck Nuclear Station, Parts I (a) and II (b), Report for Northeast Utilities Service Company, 104p. and 66p.

Wheeler, R.K., 1980. Cross strike structural discontinuities: Possible exploration tool for natural gas in the Appalachian Overthrust Belt, American Association of Petroleum Geologists Bulletin, vol. 64, no. 12, pp. 2166-2178.

Wintsch, R.P., 1984. A tectonic model for the late Paleozoic of southeastern New England, (abs.) Geological Society of America, Abstracts with Programs, vol. 16, p. 71.

Wise, D.U., 1967. Radar geology and pseudo-geology on an Appalachian Piedmont cross-section, Photogrammetric Engineering, July. pp. 752-761.

Wise, D.U., 1982. Linesmanship and the practice of linear geo-art, The Geological Society of America Bulletin, vol. 93, pp. 886-888.

Zoback, M.L. and M.D. Zoback, 1980. State of stress in the conterminous United States, Journal of Geophysical Research, vol. 85, no. 11, pp. 6113-6156.

TABLE A

RESULTS OF GEOCHEMICAL WATER ANALYSES

PARAMETER KEY - Block 1 - SMP# sample number - DATE sampling date - LAB PH laboratory pH - ALKALI alkalinity in mg CaCO3/l (milligrams per liter) - ACIDTY acidity in mg CaCO3/l - SP CND specific conductance in micromohs - HCO3 bicarbonate in mg/l - NO3 nitrate as N in mg/l - SO4 sulfate in mg/l - Cl chloride in mg/l - Block 2 - SMP# as above - TEMP sample temperature degrees Celsius - FLD PH field pH - Ca calcium in mg/l - Mg magnesium in mg/l - Na sodium in mg/l - K potassium in mg/l - SiO2 silica in mg/l -
CATION cation product and ANION anion product both in milliequiv/l -

SMP#	DATE	LAB PH	ALKALI	ACIDTY	SP CND	HCO3	NO3	SO4	Cl
01	8/30/87	7.39	13.45	2.73	50.1	16.40	0.21	9.53	4.01
02	8/31/87	7.30	12.69	2.51	48.0	15.47	0.31	4.78	7.53
03	8/31/87	7.22	33.70	1.80	62.8	41.09	0.21	8.16	12.73
04	8/31/87	7.15	9.29	1.85	36.1	11.33	0.17	6.44	3.41
05	8/31/87	7.46	15.07	2.60	100.1	18.37	0.30	9.74	24.02
06	8/31/87	7.63	18.85	1.67	91.2	22.98	0.45	13.34	14.23
07	8/31/87	7.19	10.26	1.58	70.7	12.51	0.29	6.87	15.70
08	8/31/87	7.23	9.94	2.20	72.5	12.11	0.30	6.45	15.79

SMP#	TEMP	FLD PH	Ca	Mg	Na	K	SiO2	CATION	ANION
01	17.5	6.82	6.22	1.33	3.01	2.02	0.7	0.60	0.58
02	18.5	6.91	4.75	1.33	4.80	1.49	0.3	0.59	0.57
03	18.5	7.24	4.68	1.35	7.57	1.34	0.4	0.71	1.21
04	17.5	7.28	3.12	1.17	3.61	1.07	0.7	0.44	0.42
05	21.0	7.20	7.76	2.26	12.00	2.20	0.4	1.15	1.19
06	22.0	7.10	9.00	2.22	8.21	2.59	0.3	1.06	1.06
07	19.0	7.29	5.12	1.38	9.15	1.29	0.3	0.80	0.80
08	19.0	7.29	5.15	1.43	9.32	1.39	0.3	0.82	0.78

TABLE B

DATA ON SIDE-LOOKING RADAR IMAGERY LINEAMENTS

PARAMETER KEY - LINE# lineament number - ORIENT lineament orientation (azimuth) - LNGTH lineament length (kilometers) - QUADS quadrangles intersected -

LINE#	ORIENT	LNGTH	QUADS
1	005	24.7	2
2	358	14.2	3
3	018	12.0	3
4	344	14.9	2
5	016	16.1	2
6	018	15.8	1
7	023	19.9	1
8	318	17.4	2
9	311	13.9	2
10	293	11.7	1,2
11	308	9.5	1,2
12	280	9.2	3
13	345	14.9	3
14	059	6.3	3
15	347	8.5	3,6
16	348	12.0	2,5
17	344	17.7	3,6
18	056	10.1	2,5
19	060	14.9	2,4
20	284	12.7	1
21	053	15.2	1
22	339	27.5	4
23	356	16.8	1
24	305	12.0	6
25	343	14.6	6
26	312	19.9	4
27	041	9.2	1,4
28	343	12.3	4
29	341	11.7	4
30	038	25.3	1,2,4
31	357	13.3	5
32	003	12.7	5
33	055	13.0	5,6
34	042	15.5	6
35	019	12.0	5,6
36	317	14.9	5
37	289	9.5	4,5
38	341	17.1	4
39	041	16.8	4
40	310	15.2	4
41	038	13.3	4
42	022	13.6	4
43	306	17.4	2,3
44	302	11.7	1,2
45	305	18.7	2,5,6

TABLE B (continued)

LINE#	ORIENT	LNGTH	QUADS
46	312	11.7	4,5
47	043	12.7	1
48	339	9.5	6

TABLE C

DATA ON SPOT SATELLITE IMAGERY LINEAMENTS

PARAMETER KEY - LINE# lineament number - ORIENT lineament orientation (azimuth) - LNGTH lineament length (kilometers) - QUADS quadrangles intersected -

LINE#	ORIENT	LNGTH	QUADS
1	026	5.5	1
2	354	8.3	2
3	344	9.6	2
4	014	8.6	2
5	025	6.3	2,3
6	341	7.1	3
7	015	5.8	3
8	023	8.3	3
9	310	7.3	3
10	348	10.6	2
11	051	5.5	2,3
12	305	4.5	1,2
13	014	5.3	1
14	293	6.0	1
15	350	5.5	1
16	298	4.8	1
17	306	6.8	1.2
18	029	6.5	1,2
19	021	4.0	2
20	281	3.5	2
21	347	5.0	2
22	283	6.0	3
23	055	6.3	3
24	027	7.8	3,6
25	346	6.5	3
26	006	5.3	2,5
27	058	9.3	1,2
28	352	5.5	2
29	040	5.3	2
30	087	7.3	1,2
31	014	5.0	2,4
32	008	5.3	1
33	292	6.3	1
34	310	4.0	2,4
35	332	5.5	3,6
36	331	5.3	1
37	010	6.5	1

TABLE D

DATA ON HIGH-ALTITUDE AERIAL PHOTOGRAPHY LINEAMENTS

PARAMETER KEY - LINE# lineament number - ORIENT lineament orientation (azimuth) - LNGTH lineament length (kilometers) - QUADS quadrangles intersected -

LINE#	ORIENT	LNGTH	QUADS
1	341	3.4	1
2	074	3.8	1
3	359	2.4	1
4	000	5.1	1
5	024	3.8	1
6	331	7.6	1,2
7	055	5.1	1
8	355	4.3	1
9	016	13.4	1
10	349	8.2	1,4
11	010	4.5	1
12	013	4.0	1
13	344	5.6	1,2,5
14	358	4.7	1
15	289	3.8	1
16	281	3.0	1
17	294	3.4	1
18	314	4.6	1,4
19	359	6.8	1,4
20	276	2.6	1,2
21	334	6.6	2
22	020	7.7	1,2
23	335	5.7	2
24	355	3.1	2
25	346	6.2	2
26	002	4.[illegible]	2
27	331	5.2	2
28	338	4.6	2
29	002	4.1	2
30	282	4.6	2
31	021	2.7	2
32	004	3.7	2
33	308	5.5	2,3
34	346	4.3	2
35	043	3.3	2
36	025	4.3	2
37	310	3.2	2
38	086	7.1	1,2
39	299	4.2	2
40	333	6.8	2,3
41	350	9.9	2,5
42	358	4.0	2
43	290	2.0	2
44	043	3.2	2
45	011	5.0	2,5

TABLE D (continued)

LINE#	ORIENT	LNGTH	QUADS
46	289	8.0	2,3,6
47	054	4.7	2,5
48	029	7.0	2,3
49	008	3.4	3
50	343	5.7	3
51	316	4.7	3
52	319	4.4	3
53	338	2.9	3
54	282	7.2	3
55	346	6.0	3
56	358	3.3	3
57	359	8.1	3,6
58	025	7.9	3,6
59	060	5.6	3
60	340	3.2	3
61	020	7.6	3,6
62	299	3.9	3,6
63	044	6.3	4
64	000	5.1	4
65	001	4.9	4
66	004	4.7	4
67	004	5.1	4
68	057	4.5	4
69	084	7.4	4
70	045	7.9	4
71	051	4.4	4
72	331	3.4	4
73	018	5.5	4
74	021	5.4	4
75	022	5.6	4
76	341	6.2	4
77	089	1.9	4
78	324	3.8	4
79	338	5.2	4
80	029	3.5	4
81	295	3.8	4,5
82	022	3.7	4
83	036	4.8	4
84	330	2.7	4
85	321	2.7	4
86	273	4.5	4,5
87	324	4.3	5
88	309	5.0	5
89	279	4.2	5,6
90	016	5.5	5
91	042	3.4	5
92	342	3.1	5
93	330	8.4	5
94	347	4.5	5
95	005	8.3	5
96	324	2.9	5

TABLE D (continued)

LINE#	ORIENT	LNGTH	QUADS
97	286	4.1	5
98	350	6.4	6
99	045	7.2	6
100	295	5.4	6
101	271	3.8	6
102	013	7.3	6
103	069	3.2	6
104	076	7.9	5,6
105	022	6.3	6
106	043	7.4	6
107	080	5.9	6
108	336	5.2	6
109	285	4.2	6
110	020	5.5	5,6
111	045	4.9	6
112	033	2.9	6
113	087	6.7	6

TABLE E

DATA ON LOW-ALTITUDE AERIAL PHOTOGRAPHY LINEAMENTS

PARAMETER KEY - LINE# lineament number - ORIENT lineament orientation (azimuth) - LNGTH lineament length (kilometers) - QUADS quadrangles intersected - (Moodus Quadrangle Only)

LINE#	ORIENT	LNGTH	QUADS
1	023	1.5	2
2	087	1.7	2
3	336	1.8	2
4	046	1.5	2
5	333	1.1	2
6	355	1.2	2
7	011	1.2	2
8	080	1.5	2
9	053	1.1	2
10	031	1.2	2
11	304	1.3	2
12	287	1.7	2
13	003	1.4	2
14	039	1.2	2
15	089	1.6	2
16	302	1.3	2
17	283	1.2	2
18	345	1.6	2
19	351	1.1	2
20	046	1.9	2
21	011	1.8	2
22	082	1.4	2
23	010	1.6	2
24	088	1.4	2
25	335	1.1	2
26	028	1.3	2
27	292	1.2	2
28	052	1.4	2
29	277	1.8	2
30	012	1.1	2
31	340	1.2	2
32	014	1.8	2
33	294	1.1	2
34	330	1.0	2
35	310	1.2	2
36	325	1.3	2
37	036	1.5	2
38	343	1.0	2
39	331	2.2	2
40	350	1.4	2
41	004	1.5	2
42	087	1.7	2
43	033	1.4	2
44	356	1.6	2
45	065	1.6	2

TABLE E (continued)

LINE#	ORIENT	LNGTH	QUADS
46	016	1.5	2
47	076	1.7	2
48	284	1.7	2
49	009	1.1	2
50	089	2.1	2
51	287	2.0	2
52	333	1.7	2
53	083	2.2	2
54	005	1.9	2
55	009	2.6	2
56	075	1.2	2
57	315	1.2	2
58	290	2.1	2
59	005	1.8	2
60	350	1.3	2
61	006	2.5	2
62	022	1.5	2
63	296	1.4	2
64	316	1.6	2
65	085	1.6	2
66	025	1.6	2
67	346	1.9	2
68	339	1.9	2
69	051	2.9	2
70	321	1.0	2
71	004	1.3	2
72	317	1.4	2
73	309	1.3	2
74	283	1.7	2
75	348	1.6	2
76	270	1.7	2
77	328	1.1	2
78	330	2.1	2
79	036	1.5	2
80	089	1.6	2
81	007	1.9	2
82	083	1.6	2
83	341	1.4	2
84	320	1.6	2
85	082	2.3	2
86	344	1.5	2
87	016	1.1	2
88	309	2.4	2
89	024	1.3	2
90	031	1.6	2
91	049	1.0	2
92	050	1.4	2
93	337	1.6	2
94	089	1.7	2
95	342	1.1	2
96	061	1.8	2

TABLE E (continued)

LINE#	ORIENT	LNGTH	QUADS
97	323	1.5	2
98	027	2.4	2
99	274	1.5	2
100	330	2.1	2
101	048	2.8	2
102	326	1.5	2
103	298	1.9	2
104	011	1.9	2
105	065	0.9	2
106	350	1.5	2
107	325	1.9	2
108	357	1.1	2
109	334	1.5	2
110	335	1.2	2
111	021	1.4	2
112	347	1.5	2
113	294	1.0	2
114	339	1.6	2
115	045	0.7	2
116	345	2.2	2
117	341	1.2	2
118	021	3.4	2
119	035	1.4	2
120	339	1.5	2
121	081	2.3	2
122	339	1.6	2
123	317	1.9	2
124	076	2.0	2
125	334	0.7	2
126	295	1.3	2
127	019	1.4	2
128	273	1.8	2
129	013	1.2	2
130	084	1.1	2
131	326	2.0	2
132	332	2.1	2
133	349	1.3	2
134	326	1.6	2
135	330	1.9	2
136	310	3.4	2
137	276	1.5	2
138	042	2.4	2
139	277	1.9	2
140	306	2.5	2
141	359	1.6	2
142	088	2.5	2
143	359	2.5	2
144	045	2.0	2
145	358	1.9	2
146	304	1.9	2
147	054	2.3	2

TABLE E (continued)

LINE#	ORIENT	LNGTH	QUADS
148	069	1.1	2
149	069	1.5	2
150	083	2.1	2
151	037	1.5	2
152	339	1.6	2
153	301	1.6	2
154	351	1.4	2
155	031	2.3	2
156	350	1.3	2
157	351	1.7	2
158	323	1.1	2
159	287	1.1	2

PLATE 1, Location map of study area features

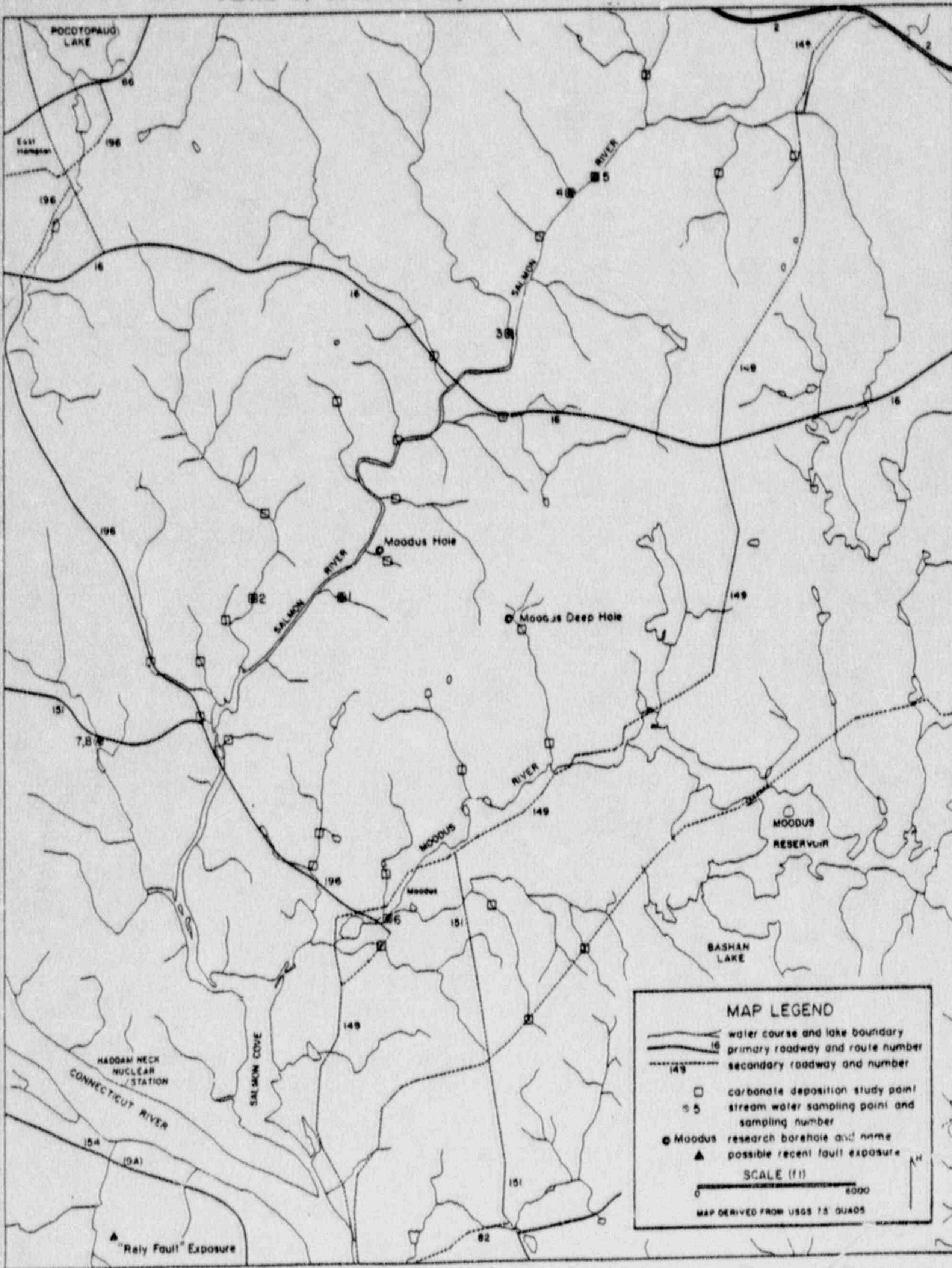

APPENDIX D

PUBLISHED ABSTRACTS OF TECHNICAL PAPERS

geophysical evidence in support of a Late Precambrian or Early Paleozoic rifting event in the Mississippi Embayment.

S41-13 1145h
Frequency dependence of Q for upper crustal rocks of the central Rio Grande rift

P.J. CARPENTER (Dept. of Geology, Northern Illinois University, DeKalb, IL 60115)
A.R. SANFORD and J.P. AKE (Both at: Geoscience Dept., New Mexico Institute of Mining and Technology, Socorro, NM 87801)

Spectra from 38 microearthquakes in four swarms were used to compute Q(f) (1-40 Hz) for a region of disturbed upper crust in the central Rio Grande rift near Socorro, New Mexico. Both stacked and unstacked spectra were fit with a model of the form $Q(f) = Q_0 f^n$. Due to consistency from event to event, fitting the unstacked spectra and averaging n and Q_0 over each swarm produced a more precise Q(f) model than fitting spectra stacked over each swarm.
Using both techniques, n for P waves was found to vary from 0.26 to 0.45 and Q_0 was found to vary from 29 to 66. For S waves, n was found to vary from 0.04 to 0.66 and Q_0 from 17 to 295. In general, as deeper regions are sampled the degree of frequency dependence, n, decreases, while Q_0 increases. n and Q_0 have been observed to vary in a similar fashion with increasing tectonic activity. These observations suggest the incidence of near-surface fracturing may strongly influence the frequency dependence of Q.

Seismicity
Room 319 Thurs PM
Presider, L. T. Long
Georgia Institute of Technology
D. V. Stockar
Pennsylvania State Univ

S42A-01 1330h INVITED
The Charleston Earthquake of 1886: A Centennial View

PRADEEP TALWANI, Department of Geology, University of South Carolina, Columbia, S.C. 29208

Historically, one of the most destructive earthquakes along the U.S. East Coast occurred near Charleston, S.C. on August 31, 1886. It occurred soon after the birth of seismology as a science and provided data to test the ideas and methods of Mallet. It attracted many investigators including in early September McGee (USGS), Mendenhall (U.S. Signal Service) and Hayden (U.S. Navy). [illegible] Sloan studied the epicentral tracts for two months and Manigault and other members of Charleston's Elliot Society reported on the effects of the earthquakes on structures. The nearly 4000 accounts from over 1500 locations (including Hayden's intensity data) were made available to Capt. Dutton (USGS) whose report was published in 1889. After initially suggesting the presence of three epicenters (based on Sloan's work) at Woodstock, Rantowles and Middleton Place, he dropped the latter in his final report. He was thus one of the first to recognize two detached epicenters. Incorporating Mallet's ideas, Dutton calculated the depth of foci at 19 km (W) and 13 km (R) and the velocity of 'earth waves' to be 5.2 km/s. Evaluating the report of an insurance company that examined all the 8000 buildings in Charleston, Freeman (1931) concluded that only one building in 71 was irreparable. Taber (1914) suggested the presence of a NE fault to account for the 1886 event. An apparent NW trend of epicenters of historical earthquakes was noted by Bollinger (1972). A multidisciplinary effort to understand the cause of seismicity began in 1974. The results of it and the discovery of a possible decollement in NE Georgia spawned many hypotheses including association of earthquakes with buried plutons, backslip/reactivation of the decollement, and reactivation of border faults of Mesozoic basins and the presence of steeply dipping intersecting faults. I will discuss these in light of the data and concepts in 1986.

S42A-02 1350h
[illegible]

K.A. MROTEK, C.T. STATTON, J.D. AGNEW, P.G. NAUMOFF, R.C. QUITTMEYER (Woodward-Clyde Consultants, PO Box 290, Wayne, NJ 07470)
G. LEBLANC, G. KLIMKIEWICZ (Weston Geophysical Corp., PO Box 550 Westboro, MA 01581)

A magnitude 4.9 earthquake occurred in northeastern Ohio on 31 January 1986. Analog and digital instruments were deployed in the epicentral area beginning about 12 hours after the mainshock. Eleven stations were initially installed, the final array consisted of 14 stations. As of 25 February 1986, 8 aftershocks have been detected and located. Seven of these events occurred within the first 10 days of monitoring. Signal duration magnitudes for the aftershocks range from near 0.0 to about 2.5. Focal depths calculated using HYPOINVERSE fall between about 2.5 and 8.0 km. A two-layer over a half-space crustal model (4.25 k/s to 2 km, 6.5 to 35 km, and 8.1 in the half-space) was derived to locate the events. The aftershocks form a linear trend striking approximately N20E and with a length of about 3 km. A composite fault plane solution based on 33 first-motions from 7 events indicates either right-lateral strike-slip motion on a NNE striking plane, or left-lateral faulting on a ESE striking plane. The spatial distribution of the aftershocks suggests the NNE oriented nodal plane is the fault plane. The direction of maximum compressive stress inferred from the fault plane solution is east-northeast.

S42A-03 1405h
Source and Propagation Characteristics for Aftershock Sequence Near Painesville, Ohio

G. GLASSMOYER, R. Borcherdt (U.S. Geological Survey, 345 Middlefield Road, Menlo Park, CA 94025)
J. Kind (Electric Power Research Institute), C. Dietel, E. Sembera, E. Roeloffs, C. Valdes, and C. Nicholson (all at U.S. Geological Survey, 345 Middlefield Road, Menlo Park, CA 94025)

Dynamic seismic moments, stress drops, and corner frequencies have been derived for aftershocks of the January 31, 1986 M ≈ 4.9 earthquake near Painesville, Ohio. The aftershock sequence was recorded on a wide dynamic range (96 dB) broad bandwidth (400 sps) array (GEOS) encircling the epicentral region and extending along a linear profile to a distance of 55 km. Eight seismic events were detected as of February 10, 1986 with moments ranging from 2×10^{17} to 4×10^{19} dyne-cm, and inferred stress drops based on Brune model up to more than 100 bars. Determination of peak acceleration amplitudes from the observed high-frequency ground motions vary widely across the array. Accelerations near 1% gravity for both P and S waves were observed for the larger events (M ≈ 1.8, 2.3) during the short (0.06 to 0.16 sec) impulsive arrivals. Possible changes in the crustal state of stress are being investigated in relation to observed seismicity.

S42A-04 1420h
Earthquakes in the Greater New York City Area of the Past 250 Years: Locations, Magnitudes and Recurrence Rates

SYKES, LYNN R. (Lamont-Doherty Geological Observatory and Department of Geological Sciences of Columbia University, Palisades, NY 10964)

A magnitude/felt-area relationship is derived for eastern U.S. earthquakes for which instrumental data are available and is used to calibrate m_{bLg} as measured in the frequency band near 1 Hz for historic shocks in New Jersey, southern New York and eastern Pennsylvania. Cumulative plots of number of events per unit time extending progressively back in time since 1983 are used to calculate time periods for which the historic record is complete. For example, the record of $m_{bLg} \geq 4.0$ is complete for the entire 250-year period studied whereas that for $m_{bLg} = 2.4$ is only complete since 1974. Recurrence relationships are derived using completeness intervals that vary as a function of magnitude and which thus permit the greatest amounts of data to be utilized. Like the instrumental record of the past 12 years, historic earthquakes are concentrated in a "U" shaped zone near the margins of the Newark basin. One arm of the "U" follows the Fall Line from Wilmington, Del. to New York City and thence to Westchester County, N.Y. while the other occupies the southeastern half of the Precambrian Hudson Highlands and Reading Prong. I speculate about the structures responsible for these zones of moderate seismicity and the near-absence of activity within the Newark basin and in the area to the northwest of the Hudson Highlands-Reading Prong.

S42A-05 1435h
The Lancaster Seismic Zone: Geological and Geophysical Evidence for a North-South Trending, Presently Active Zone of Weakness Through Lancaster County, PA

DAVID V. STOCKAR
SHELTON S. ALEXANDER (Both at Department of Geosciences, Pennsylvania State University, University Park, PA)

The hypocenter of the m_{bLg} 4.2, MM VI earthquake that occurred on April 23, 1984 was at a depth of 4.5-5.0 km at 39.94 N, 76.325 W near Marticville, about 10 km south of Lancaster, Pennsylvania, of the mainshock. The mainshock was followed by several aftershocks oriented in a north-south trend over a 2 km zone. The focal mechanism of the mainshock also indicates a NS-striking fault plane. This strike is perpendicular to the dominant EW structural grain of the Appalachians within the Pennsylvania salient and of the Martic Line. However, the youngest structures in the Lancaster region are all NS-trending and not EW-striking like the dominant Paleozoic features. Based on cross-cutting relationships, the youngest rocks present are the NS-striking Triassic-Jurassic diabase dikes, and the youngest faults present are the NS-trending cross-faults which offset all other structural features and lithologies of the area. The April, 1984 event is within the dominant zone of these faults. The historical seismicity and relocated instrumentally recorded events also define a NS-trending zone, the Lancaster Seismic Zone. It is approximately 50 km in length and 10 km in width. The seismic zone is parallel to the fault zone. The drainage pattern of the major streams is also predominantly NS-trending near Lancaster. Potential field (aeromagnetic and gravity) anomalies and prominent remote sensing lineaments provide further evidence of the presence of the cross-structural zone inferred from the geology and seismicity, including evidence for related large scale basement features.

S42A-06 1450h
Earthquakes and faults in central New Hampshire.

José Wilson C. ROSA and Gene SIMMONS (Dept. of Earth, Atmospheric, and Planetary Sciences, M.I.T., Cambridge MA 02139)

Thirty-six shallow earthquakes with magnitudes to 4 have occurred near Laconia, NH since November 1976. We have used the following to search for possible faults associated with the earthquakes: residual gravity map based on 750 stations in 3000km²; aerial photographs; topographic maps; aeromagnetic map. Stream and topographic alignments, gravity anomalies, photograph linears, and the temporal migration of earthquakes -- all features commonly associated with faults -- indicate a fault that strikes N45°W, extends roughly through Gaza and Bristol, and is at least 50 km long.

S42A-07 1520h
Seismicity and Crustal Structure in Southeastern Tennessee

LELAND TIMOTHY LONG, JEIH-SAN LIOW, AN TIE, and KARL-HEINZ ZELT (All at: School of Geophysical Sciences, Georgia Institute of Technology, Atlanta, GA 30332)

Three major features define the crustal structure of southeastern Tennessee. First, the New York-Alabama Lineament (NYAL) probably represents the trace of an ancient strike-slip fault which separates crust of different thickness and seismic velocity. Second, a negative Bouguer anomaly which follows the trend of the NYAL in southeastern Tennessee can be interpreted as an area of sediment thickening in the shallow crust. Third, a north-northeast striking positive gravity anomaly in northern Tennessee represents a Precambrian rift. This relic rift is truncated at the negative gravity anomaly and the NYAL. The area of the negative Bouguer anomaly and the intersection of the Precambrian rift with the NYAL correspond to the area of active seismicity in southeastern Tennessee. In this active zone, all events from [illegible] through [illegible] have been relocated by first using S-P times to obtain origin time and by, second, using a velocity gradient in the velocity model to obtain the epicentral parameters. The velocity model is based on an interpretation of refraction data from earthquakes and explosions. The travel time residuals at individual stations agree with the structural model and confirm a zone of low-velocity sediments. The relocated distribution of events suggests that both northwest and north trending zones of seismicity exist in response to crustal stresses resulting from structural inhomogeneities and topographic loading. The features responsible for these stresses in southeastern Tennessee are the Great Smoky Mountains and the truncation of the Precambrian rift at the NYAL.

S42A-08 1535h
Crustal Structure and Seismicity in the Fiji Platform

IAN B. EVERINGHAM (Mineral Resources Department, Private Mail bag, G.P.O., Suva, Fiji)
MICHAEL W. HAMBURGER (Department of Geology, Indiana University, Bloomington, IN 47405)

Six years of data from a telemetered seismic network in Fiji are used to constrain the crustal structure and crustal deformation within the Fiji Platform. Crustal thickness in Fiji is typical of active island arcs, averaging 15-20 km. Locally the thickness probably approaches 25-30 km beneath the [illegible] islands. [illegible] portion of the main island of Viti Levu. Mantle velocity beneath the platform is low (7.6 km/sec), in the same range as that observed beneath the neighboring marginal basins and island arcs.
Shallow earthquakes are observed both within and along the boundaries of the Fiji Platform. Major deformation is concentrated along the earthquake zones located on the edges of the platform. These zones are continuously active at moderate magnitudes. Earthquakes within the platform occur more sporadically than those along its margins, separated by long periods of quiescence. Despite large rates of relative plate motion, earthquake magnitudes have been less than [illegible]; apparently the thin lithosphere of the Fiji region is

ABSTRACTS OF PAPERS PRESENTED AT THE NORTHEASTERN SECTION (22nd Annual Meeting) of THE GEOLOGICAL SOCIETY OF AMERICA, Pittsburgh, Pennsylvania, March 4-7, 1987

Vol. 19, No. 1, 1987

GEOMORPHIC INDICATORS OF NEOTECTONIC ACTIVITY IN THE LANCASTER AREA, PENNSYLVANIA

№ 115507

WU, Haiyan, CHOU, Hue Chung, and GOLD, David P., Department of Geosciences, The Pennsylvania State Univ., University Park, PA 16802

There are no reports of any permanent surface manifestation of the seismic activity, recorded in recent and historic times, from the epicenter area near Lancaster, Pennsylvania. The lack of any fault-related features such as scarps, stream offsets, and sag ponds in the Lancaster area, suggests that there were no tectonic displacements at the surface, or that if there were any, they were small and rapidly obliterated by agricultural practices. However, the first order streams in modern drainage networks have been shown elsewhere to be sensitive to small lateral and vertical displacements of the ground surface in response to neotectonic events.

A systematic study of the first order drainage pattern and gully density using ASCS low altitude aerial photographs (scale 1:20,000) flown in 1964, was initiated for Lancaster County. Gully density varied 0-60 per each photo-cell of approximately 9 km^2. A density of more than 30/photo-cell was considered anomalous. Three high density cell areas are identified, viz., (1) a dispersed southern area around Wakefield and Quarryville, (2) an arcuate central anomaly to the south and west of Lancaster, and (3) an northern, dumbell-shaped pattern centered on Elizabethtown. NNE trending Triassic diabase dikes are exposed in the anomalous areas, and the N-S trending epicenters of recent earthquakes lie 3.5 to 5 km beneath the central area. A number of Paleozoic thrust faults also are exposed in the central area.

Gullys exhibit two dominant orientations: a sharp spike on N5°E, and a broad peak on N20°W. Although there is a N-S elongation to many of the anomalies, they collectively define a N-W trend, subparallel to the Susquehannan River. We suggest that these anomalies represent the intersection of neotectonic deformation zones with a subtle river terrace.

p. 20

LANCASTER, PENNSYLVANIA SEISMIC ZONE: EVIDENCE FOR A PRESENTLY ACTIVE ZONE OF WEAKNESS

№ 115508

STOCKAR, David V. and ALEXANDER, Shelton S., Dept. of Geosciences, The Pennsylvania State University, University Park, PA 16802

Historical seismicity and relocated instrumentally recorded events define a north-south trending zone of seismic activity. It is approximately 50 km in length and 10 km in width, encompassing the central region of Lancaster County and the city of Lancaster. Recent activity, such as the April 23, 1984 (mbLg 4.2, MM VI) mainshock at a depth of 4.5-5.0 km and associated foreshocks and aftershocks near Marticville, about 10 km south of the city of Lancaster, is attributed to this seismic zone.

Structural cross-cutting relationships indicate that the youngest rocks present are the north-south striking Triassic-Jurassic diabase dikes, and the youngest faults present are the north-south trending cross faults which offset all other structural features and lithologies. The recent and historical seismic activity appears to be concentrated along the most dominant of these cross fault zones, the Fruitville Fault Zone.

Remote sensing lineaments and potential field (gravity and aeromagnetic) anomalies support the structural and seismic evidence for a north-south deformational zone. Likewise, the drainage pattern of the major streams is predominantly north-south trending near the city of Lancaster. Finally, preliminary studies indicate up to 30 m of uplift within the Miocene to recent Susquehanna River terraces of Lancaster County. The maximum uplift appears to be near Safe Harbor, PA.

p. 60

ABSTRACT OF PAPER PRESENTED AT THE SOUTHEASTERN SECTION (36th Annual Meeting) OF THE GEOLOGICAL SOCIETY OF AMERICA, Norfold, Virginia, March 25-27, 1987. Vol. 19, No. 2, p. 133.

TUFA/MARL DEPOSITS AS INDICATORS OF NEOTECTONIC ACTIVITY

Nº 132294

THORNTON, Charles P., Department of Geosciences, The Pennsylvania State University, University Park, PA 16802; GOLD, David P., Department of Geosciences, The Pennsylvania State University, University Park, PA 16802; HERMAN, Janet S., Department of Environmental Sciences, University of Virginia, Charlottesville, VA 22903

Holocene deposits of calcium carbonate (tufa and/or marl) occur along many streams in the Shenandoah Valley of Virginia and in the southern Cumberland Valley of Pennsylvania, in many (and perhaps in all) cases just downstream from points where these streams cross faults or where they cross lineaments that intersect faults at depth. Many of the deposits are forming at the present time, but others are inactive and are being eroded by the streams. Along Holman Creek between Forestville and Quicksburg, Virginia, deposition of tufa was followed by alluviation, and the deposits are overlain marginally by up to 3 m of sands and silts, yet the travertine is still younger than the establishment of the present vally of Holman Creek. Localization of the deposits downstream from fault or lineament traces seems to indicate the source of the $CaCO_3$-saturated waters to be the fault zones, along which crushing of the limestones resulted in their higher-than-normal solubility. However, it seems unlikely that this crushing dates from the time of origin of these faults some 250 m.y. ago: the supply of crushed limestone produced at that time should long since have been exhausted. The more probable alternative is that recent movement along these faults has produced a new supply of crushed limestone for the circulating ground water to act on; the age of a deposit then reflects the time of most recent movement along the fault. In one case, the Saumsville fault in the Shenandoah Valley, this hypothesis is supported by the systematic right-lateral offset of $CaCO_3$-depositing streams crossing the fault, evidence that movement has occurred along this fault since the time of establishment of the present drainage pattern.

Also reprinted in Oklahoma Geology Notes, Oklahoma Geol. Surv., Vol. 47, No. 4, 1987, p. 194-195.

ABSTRACTS (Alphabetical Order)

EARTHQUAKES, INJECTION WELLS AND THE PERRY NUCLEAR POWER PLANT, CLEVELAND, OHIO

AHMAD, Moid U., Professor of Hydrogeology, Ohio University, Athens, OH 45701

On January 31, 1986, an earthquake of magnitude 4.9 occurred about 11.3 km south of the Calhio injection wells. Accelerometers on site at the Perry Nuclear Power Plant (PNPP) recorded accelerations as high as 0.19 to 0.23 g. A large number of instruments tripped due to high amplitude vibrations. There seems to be a possible correlation between abnormally high annulus pressures and the time of earthquakes. This same correlation extends to the two 1983 earthquakes recorded in the area. Micronetworks have recorded 6 earthquakes around the injection well with focal depths ranging from 0.5 to 2.2 km. A hydrological model of an anisotopic reservoir 6.44 km wide and 17.7 km long indicates a pressure build up between 53 bars at the epicenter and 118 bars at the injection well. The simulation matched average yearly pressure data and displayed a good correlation. The assumption of an anisotropic reservoir is consistent with available geophysical and geological data. The indicated pressure buildup is similar in magnitude to that resulting in the Denver earthquake of 1962. This critical value is interpreted as the pressure buildup above which induced earthquakes may occur in this area.

TRAVERTINE AS AN INDICATOR OF NEOTECTONIC DEFORMATION IN THE LANCASTER, PA SEISMIC ZONE AND OTHER AREAS

ALEXANDER, S.S., STOCKAR, D., and THORNTON, C.P., Department of Geosciences, Pennsylvania State University, University Park, PA 16802

The vicinity of Lancaster, Pennsylvania has been a region of persistent recent seismic activity. Earthquakes there, with a maximum magnitude of 4.2 (April 23, 1984), appear to be concentrated within a NS-trending seismic zone which is approximately 20 km wide and 50 km long. This zone, the Lancaster Seismic Zone, contains a reverse fault, the Fruitville Fault, which strikes NNE through central Lancaster County, along which most of the recent earthquake activity is concentrated.

Recent ground-based studies in the area have revealed that the southern trace of the Fruitville Fault Zone is associated with presently active travertine deposition, preferential north-south drainage of the major streams in the area and the occurrence of springs. Travertine deposits have been found at four separate locations in small streams crossing the Lancaster Seismic Zone. Present deposition occurs downstream from the inferred active fault trace which cuts carbonate bedrock. It is postulated that the seismically active fault(s) may be mylonitizing the carbonate country rock at depth and acting as a conduit for the calcium-carbonate-rich groundwater to reach the surface where it super-saturates in nearby streams and precipitates as travertine. This association of travertine with geologically recent fault movements was first suggested by Thornton (1953) based on field studies in Virginia, and there appears to be numerous other such occurrences globally. It is potentially very important in studies of paleoseismicity in relatively aseismic areas such as the eastern United States.

YIELD ESTIMATES OF SOVIET EXPLOSIONS FROM PROPAGATION-CORRECTED Lg SPECTRA

ALEXANDER, S.S., and TANG, L., Department of Geosciences, Pennsylvania State University, University Park, PA 16802

Application of an empirical approach to correct observed Lg spectra for propagation effects gives estimates of source excitation spectra for Soviet explosions. Path attenuation is accounted for by using Q estimates derived from average spectral slopes for a suite of events of different magnitude in a given source area or by a source-path-receiver decomposition when sufficient observing stations are available. Yield estimates are then obtained by comparing attenuation-corrected source spectra with theoretical source spectra for explosions of different yield. Tectonic release effects do not appear to bias these estimates, if frequencies above about .5 Hz are used. Under the partially confirmed assumption of transportability of empirical relationships developed in North America, direct estimates from m_{bLg} provide an alternative means of estimating Soviet yields that agree well with those obtained by this spectral approach and with Nuttli's coda-Q estimates using Lg.

CHARACTERIZATION OF SEISMICALLY-INDUCED LIQUEFACTION SITES ASSOCIATED WITH THE 1886 CHARLESTON, S.C. EARTHQUAKE

AMICK, D.C. and MAURATH, G., Ebasco Services Incorporated, 2211 West Meadowview Rd., Greensboro, NC 27407

Recent studies of paleoliquefaction features in the epicentral area of the 1886 Charleston, SC earthquake suggest that this area has been the site of several large prehistoric Holocene earthquakes (Gohn *et al.*, 1984; Obermeier *et al.*, 1985; Talwani and Cox, 1985; Weems *et al.*, 1986; and Obermeier *et al.*, 1986). The time between successive large events is estimated to be 1200 to 1800 years. In light of this relatively long recurrence interval, the U.S. Nuclear Regulatory Commission is presently funding a systematic search for similar prehistoric paleoliquefaction features in other areas of the Eastern United States. The objective of this study is to determine whether or not seismically induced paleoliquefaction features are present elsewhere in young sediments of the Atlantic Coastal Plain or within late Quaternary or Holocene river deposits. If they are present, the study will attempt to determine the size and frequency of the causative earthquakes.

Initial investigations center on cataloging the characteristics of earthquake induced liquefaction features in the Charleston, SC area and identifying the criteria by which similar features outside the mezoseismal area of the 1886 event could be identified. To date a total of 103 liquefaction sites in the Charleston area have been identified. Of these, 63 sites were identified based on the authors' evaluation of both published and unpublished historical accounts of the 1886 earthquake, 28 have been identified as a result of ongoing field studies by the U.S. Geological Survey, 4 were identified during past field studies carried out by investigators of the University of South Carolina and 8 were identified by the authors during reconnaissance field studies conducted as part of these investigations. Each of these 103 sites have been located on topographic maps, county soil maps, available remote sensing imagery, and available geologic maps. In addition, the authors conducted confirmatory field investigations at 32 of the sites. This information has been used to characterize each site's depositional environment, age of host and liquified materials, hydrogeologic setting,

14:15

INVERSION OF GEODETIC DATA FOR SPATIAL DISTRIBUTION OF FAULT SLIP OF THE 1946 NANKAIDO EARTHQUAKE

YABUKI, T., and MATSU'URA, M., Geophysical Institute, Faculty of Science, The University of Tokyo, Tokyo 113, Japan

We have developed a general method for obtaining tomographic images of seismic sources from surface displacement data, using Akaike's Bayesian Information Criterion (ABIC). In the present study we apply this method to zero-frequency data. Given a slip distribution on a fault surface, we can calculate surface displacements due to an earthquake by integrating solutions to point sources over the source region. We represent the slip distribution by a weighted sum of a finite number of known basis functions. By replacing the order of integration and summation, the surface displacement can be expressed as a weighted sum of the displacements due to the slip distributions prescribed by the basis functions. Then the inverse problem is stated as the problem of determining the weights in superposition of the basis functions from observed surface displacements. The problem is highly nonunique in general. We incorporate prior information about the smoothness of spatial variation of fault slip into observed data, and construct a Bayesian model with hyper-parameters which control the degree of the smoothness. Using ABIC, we can select the best model among the family of parametric models controlled by the hyper-parameters. We demonstrate the applicability of this method to actual observed data through the analysis of geodetic data associated with the 1946 Nankaido earthquake, which is one of the greatest earthquakes that occurred at the boundary between the Eurasian plate and the Philippine Sea plate.

14:30

PRESEISMIC, COSEISMIC, AND POSTSEISMIC SURFACE DEFORMATIONS ASSOCIATED WITH THE LARGE SUBDUCTION EARTHQUAKE IN SOUTHWEST JAPAN

KAORU MIYASHITA
Department of Earth Sciences, Ibaraki University, Japan

The preseismic, coseismic, and postseismic changes in the surface elevation in southwest Japan, which are associated with the 1946 Nankaido earthquake (M8.2), the large subduction earthquake at the plate boundary between the Asian and Philippine Sea plates, are estimated. These estimations are obtained from the first-order leveling data during the period of 1890-1960 on the basis of an epoch reduction and net-adjustment analyses.

The preseismic (1900-1946) surface deformation is characterized by trenchward tilting in the eastern part of Shikoku and the Kii peninsula, which can be interpreted in terms of a steady state subduction of the Philippine Sea plate. The coseismic (1946/1947) surface movement in these regions indicates characteristics of the deformation due to low-angle thrust faulting. On the other hand, the western part of Shikoku differs from these regions in the surface deformation pattern: slight uplift during the preseismic period, and significant subsidence at the time of the earthquake. Such a regional difference is also recognized concerning the postseismic deformation. Moreover, such a type of regional difference has been also reported with respect to the seismicity in the crust. Consequently, it can be said that there are some regional differences in the mechanism of subduction of the Philippine Sea plate.

14:45

DEDUCING SOURCE PROPERTIES OF THE M = 7.8 1931 HAWKES BAY, NEW ZEALAND, EARTHQUAKE FROM THE PATTERN OF UPLIFT AND SUBSIDENCE.

HAINES, A.J., Seismological Observatory, Geophysics Division, DSIR, Wellington, New Zealand.

The 1931 Hawkes Bay earthquake is the second largest that has occurred in New Zealand during the 150 years of European settlement. Because of its proximity to the city of Napier, it was also the most destructive. Marked uplift and subsidence were observed over an area of the order of 10^3 km² surrounding Napier. Though point values of vertical displacement are not known sufficiently accurately to justify full formal inversion for source properties including the areal distribution of fault displacement, the pattern of uplift and subsidence is well enough established for the main properties to be deduced. The maximum fault displacement was close to 10 m, consisting of similar amounts of reverse dip-slip and dextral strike-slip movement on a steeply-dipping crustal fault striking in the same direction as the Pacific-plate lithosphere subducted beneath the North Island. It is also deduced that the fault extends down to near the top surface of the subducted lithosphere 30 km beneath Napier. The dislocation models consistent with the vertical deformation predict horizontal displacements that agree to within errors with coarse geodetic observations. In contrast, to match the geodetic observations more exactly, movement has been postulated on the interface between the Pacific and overlying Australian plates, as well as on the crustal fault. Such additional movement is inconsistent with the pattern of vertical displacement.

15:00

DEFORMATION OF HONSHU DEDUCED FROM OFFSETS ON THE STRIKE-SLIP FAULTS DISTRIBUTED WITHIN THE ISLAND

MARUYAMA, T., Earthquake Research Institute, University of Tokyo, Bunkyo-ku, Tokyo, 113 Japan

The basic assumption of this paper is that if a region has been subject to the deformation large enough during a long but geologically short period of time, it can be traced in the offsets on the faults distributed within the region. Though the formulas on the dislocation are based on the elasticity theory, they can cope with the permanent deformation of solid and seem to be successfully applicable to the case. This is because the non-elastic field can be modelled by the elastic singularity. Not the stress state within the region but only displacements on the boundary, derived also from displacements on the segments within the region, are called in question. In the formulation of the problem the boundary of the region is set free for two reasons, 1) to obtain results independent of the surroundings, 2) to be possibly freed from restraint of elasticity in a certain sense. The deformation in the horizontal plane deduced from the offsets on the strike-slip faults is considered. Thus the problem is to calculate the displacement along the free boundary of a region including many dislocations in it in two-dimensional elasticity theory. Techniques of conformal mapping or integral equations due to D.I.Sherman are utilized.

The theory is applied to the offsets accumulated during the past ca. 2 Ma on the strike-slip faults within the Honshu Island, Japan. The result is compared with those from other sources, such as paleo-magnetic survey.

15:15

PLATE BOUNDARY DEFORMATION IN CALIFORNIA INFERRED FROM GEODETIC DATA

JACKSON, D.D., Department of Earth and Space Science, UCLA, Los Angeles, CA 90024, and Hirata, N., Geophysical Institute, University of Tokyo, Tokyo 113, Japan.

We model tectonic deformation in California in terms of elastic blocks which can translate, rotate, and deform elastically because of stresses imposed at their edges. We then determine the rates of rotation, translation, and boundary displacement from geologically determined fault displacement rates as well as fault creep, trilateration, triangulation, VLBI, and GPS data. Estimating the above quantities becomes a linear inverse problem when the fault geometry is known. Cumulative displacement rates from geodesy agree with plate tectonic theory and with geologically determined rates except in the Transverse Ranges, where the geodetic rates are much lower. Geodetic displacements, even in interseismic periods, are concentrated along major fault zones, except in the Transverse Ranges where the displacement appears roughly uniform. The model can be used to estimate the rate of stress accumulation on faults, and to assess the tectonic significance of faults with incomplete geologic data.

15:30

▶ **NEAR-SURFACE EVIDENCE OF NEOTECTONIC DEFORMATION IN SEISMICALLY ACTIVE AREAS IN THE NORTHEASTERN UNITED STATES.**

ALEXANDER, S.S., STOJKAR, D.V. and SHUMAN, C.A., Department of Geosciences, Penn State University, University Park, PA 16802

Although fault displacements associated with earthquakes in eastern North America apparently never reach the surface there is evidence of surface or near-surface neotectonic deformation in the first two seismically active areas that we have investigated: the Lancaster, PA and Moodus, CT seismic zones. In both areas satellite and aircraft remote sensing imagery together with ground-based geological and geophysical observations were used to look for indications of geologically-recent near-surface deformation. In the Lancaster Seismic Zone lineament density and orientation patterns, stream terrace elevation anomalies, and the occurrence of localized travertine deposits all appear to be causally associated with the elongated (~40x10 km), NS-trending zone of seismicity. In the Moodus Seismic Zone distinctive lineament density and orientation patterns are present which are inferred to be related to the recently-determined (thrust) tectonic stress conditions in the area of recent seismic activity. Features oriented perpendicular to the maximum horizontal stress appear on all scales of imagery while those (joints ?) oriented parallel to this direction are seen only on high resolution aerial photographs. Ground-based observations of neotectonic deformation associated with recent seismicity in the Moodus area are greatly hampered by near-surface effects of recent glaciation. These approaches may provide a means of locating and characterizing zones of geologically-recent seismic activity where epicenters of pre-instrument earthquakes are poorly known.

15:45

FAULT PARAMETERS AND SLIP DISTRIBUTION OF THE 1915, AVEZZANO, ITALY EARTHQUAKE DERIVED FROM GEODETIC OBSERVATIONS

WARD, S.N., *Institute of Tectonics, University of California, Santa Cruz*. VALENSISE, G., *Istituto Nazionale di Geofisica, Roma, Italy*

This paper analyses surface displacements associated with the Avezzano, Italy earthquake (M_s=6.9) of January 13, 1915. The Avezzano event locates on a shallow normal fault centered in the Apennine mountains near a quaternary tectonic depression named "Conca del Fucino". The outward expansion of metropolitan Rome (80 km southwest) in recent years has heightened awareness of the seismic potential of the Fucino region. Although many quaternary and holocene faults can be recognized in the field, the 1915 earthquake is the only sizable event to have occurred in the area for at least two millenia. Because of a fortuitous pre-earthquake leveling survey near the fault in the mid 19-th century, good quality geodetic data exist which illuminate details of the 1915 rupture. We modelled the faulting using both uniform and variable slip planar dislocations. The best fitting focal mechanism includes pure dip slip on a plane striking 135° and plunging 63° to the southwest. This fault geometry is consistent with surface scarps and the broad scale tectonics of the region and is common to several large earthquakes of the central-southern Apennines. The uniform slip analysis estimates fault length, width, slip and moment to be 24 km, 15 km, 79 cm and 9.2×10^{18} N m respectively. Numerical simulations indicate that residuals left in the uniform slip model are not entirely random and likely represent systematically unmodelled features of fault slip. Variable slip models of the faulting significantly reduce the residual variance and reveal a broad (two-lobed) slip pattern, separating a central region of very low moment release. Resolution and stability of the results were carefully tested. Neither survey noise nor the intrinsic resolving power of the network seriously question the slip pattern's major features.

There are two simple models that may explain this correlation: (1) the Dupal anomaly represents the lower mantle composition that is not affected by upper plate motions or (2) it represents recycled and/or present-day subcontinental mantle. However, the low $^{3}He/^{4}He$ ratios of lavas from oceanic islands in the Dupal anomaly regions suggest the presence of a recycled component. Moreover, the biggest Dupal anomaly is in the Indian-South Atlantic; the lower mantle velocity minima in this region has been under a continental lithosphere for at least the last ~150 Ma. Hence, the Dupal anomaly associated with the large-scale, low seismic velocity regions in the lower mantle is most probably subcontinental mantle in origin. If this is true, then the correlation constrains mantle convection models.

T51A-11 1145H

Atlantic vs. Pacific Young Seamounts: Petrologic and Sr-Nd- and Pb- Isotopic Constraints

R. BATIZA (Dept. Geological Sciences, Northwestern University, Evanston, Ill 60201)

P. R. CASTILLO (DTM, Carnegie Institution of Washington, 5241 Broad Branch, NW, Washington, D.C. 20015)

Young seamounts near the slow spreading (35 - 40 mm/yr) MAR between 25° and 27° S latitude are similar in shapes and size distributions to those near the fast spreading (80 - 120 mm/yr) EPR between 9° and 21° N latitude. Lavas from both seamount groups are MORBs that are systematically more primitive, and display significant variations in $^{87}Sr/^{86}Sr$, $^{143}Nd/^{144}Nd$ and to a certain extent, $^{206}Pb/^{204}Pb$, than lavas from their respective adjacent ridge axes. However, MAR seamount lavas have generally higher $^{87}Sr/^{86}Sr$ (0.70260 - 0.70303) and Δ8/4 (-6 to 46) and lower $^{143}Nd/^{144}Nd$ (0.51292 - 0.51309) values than EPR seamount lava $^{87}Sr/^{86}Sr$ (0.70222 - 0.70298), Δ8/4 (-15 to 9) and $^{143}Nd/^{144}Nd$ (0.51289 - 0.51327) values, respectively.

We propose that lavas from both seamount groups are produced by the same general process - small degree partial melting of a depleted upper mantle source of MORBs containing large magnitude, small-scale heterogeneities. Lavas erupted at adjacent ridge axes are produced by large degree melting that average the chemical and isotopic characteristics of the same mantle source. The main difference lies in the composition of the small-scale heterogeneities in the upper mantle under the southern MAR and northern EPR.

Earthquakes, Geophysics, and Geology Near Moodus, Connecticut I (T51B)

Room 305 Fri AM

Presiding, C. T. Stratton

Woodward-Clyde Consultants

S. Alexander

Pennsylvania State Univ

T51B-01 0845H

Geological Setting of the Moodus, Ct. Area

J C Drobinski, P J Turner, and O Leblanc (Weston Geophysical Corporation, Post Office Box 550, Westboro, MA 01581; 617-366-9191)

Moodus is located in eastern Connecticut, a region underlain by a complex sequence of sedimentary, volcanic and plutonic rocks which range from Precambrian(?) to Late Paleozoic in age. Multiple dynamothermal orogeneses of these eugeosynclinal rocks by Appalachian/Caledonain orogenic events, have resulted in the compressional, translational, and accretionary structural and stratigraphic succession now evident in this amphibolite grade metamorphic assemblage. Post-metamorphic deformation during the Late Paleozoic (Permian) and the Mesozoic eras has produced the dominant brittle fabric of the region as expressed by dikes, joints and high angle, gouge-filled and mineralized faults. Three major tectonostratigraphic zones characterize the region immediately surrounding the Moodus Area: the Bronson Hill anticlinorium sequence, the Merrimack Synclinorium sequence, and the Avalonian Platform basement sequence. The Bronson Hill and Merrimack tectonostratigraphic zones are fault bounded. Geologic mapping in the Moodus area has identified northwest-trending fracture maxima. Evaluation of the seismicity indicates a possible north-northwest alignment of epicenters in the vicinity of a subtle northwest-trending radar lineament and gravity anomaly. The extent and significance of these northwest trends is unclear. The current understanding of stress fields in southern New England is incomplete; however, a NE-SW directed stress field is inferred. Sources of stress data indicate that in-situ stresses are common in New England; these stresses are most commonly detected during excavation activities. The observed phenomena (post-glacial offsets, offset drillholes and rock squeeze events) are most indicative of transient relief of residual stresses.

T51B-02 0900H INVITED

Geology of the Moodus Area, Connecticut: Possible Relations to Modern Seismicity

David London (School of Geology & Geophysics, University of Oklahoma, Norman, OK 73019; 405-325-3253)

Surface geologic mapping provides a new data base on ductile and brittle deformation near Moodus, CT. Brittle deformation is manifested by shear zones with chlorite mylonite and slickensides, fractures without attendant retrograde metamorphism, and rarely mylonites with and without argillic alteration. Similar features are present in core from recent scientific boreholes in the area. From surface geology, the 72° 29'W longitude emerges as an important structural boundary in the Moodus area and lies just west of the centers of recent earthquakes. The 72° 29'W longitude divides brittle faults and fractures into two distinct groups: east of this longitude, brittle deformation is pervasive along subhorizontal foliation surfaces, and especially in fracture swarms that strike N30°W with 90°-70°NE dip. West of 72° 29'W, the prevalent fracture system strikes N75°E with subvertical dip; fractures and brittle faults with NS, N30°E, and N20°W strikes are present but subordinate. Interference between N30°W and N75°E fracture systems is not conspicuous at the surface near 72° 29'W, but interpenetration of these two fracture sets occurs in two shear zones west of this longitude. The 72° 29'W longitude also delineates the trace of a regional, westward-vergent fold with horizontal, NS axis. East of the fold axis, layering and foliation in metamorphic rocks are subhorizontal; west of the axis, layering and foliation strike NS with vertical dip. The different orientations of brittle deformation may stem from variations in the regional attitudes of metamorphic layering and foliation, which result from ductile deformation. In some cases, ductile folds and faults were reactivated during brittle deformation. Projection of surface geology to depth is hindered by discontinuities introduced by numerous ductile faults.

T51B-03 0915H

Lithology and Structure Identified in a 1.5 km Borehole Near Moodus, Connecticut

P C Naumoff (Woodward-Clyde Consultants, Wayne, NJ 07470; 201-785-0700)
(Sponsor: C T Staunton)

A 1.5 km (4800 ft) borehole was drilled in the spring of 1987 near Moodus, CT. The borehole was drilled to investigate the orientation and magnitude of the regional stress field near this site of recurring seismicity in the south-central part of the state. The borehole is located roughly midway between two regional geologic features: the Willimantic dome to the north and surface exposures of the Honey Hill fault to the south. The borehole penetrated a lithologic sequence similar to those exposed at these two localities. Well-cuttings sampled at 20-foot intervals and cores recovered from every major rock unit, as well as thin section analysis of selected samples, provide the basic borehole geology. Formations encountered are:

0 to 1900 ft - Hebron Gneiss - interlayered biotite schists and calcsilicate gneiss.

1900 to 2090 - Canterbury Gneiss - pink and white granitic gneisses.

2090 to 2240 - (?) Hebron Gneiss - interlayered biotite schist and granite gneiss.

2240 to 2630 - Tatnic Hill Fm. - muscovite-biotite +- sillimanite schists and amphibole-biotite schists.

2630 to 4800 - Waterford Group Gneisses - leucocratic amphibole-bearing gneisses.

Although thin mylonite zones occur throughout the borehole, mylonitic and cataclastic fabrics associated with the Honey Hill fault zone are best developed in the Tatnic Hill Fm. Chip samples collected across the Tatnic Hill-Waterford Group contact (the traditional map position of the fault) do not appear deformed.

Preliminary observations, based on borehole televiewer and formation microscanner logs, show that the strike of borehole rock foliation is variable, but dips are generally shallow to moderate. Minor recumbent folds are evident in the Tatnic Schist at depths of around 2460 ft, and the foliation steepens considerably in the hinge areas of the folds.

T51B-04 0930H INVITED

NEOTECTONIC DEFORMATION in the HONEY HILL FAULT ZONE (Ct) by REACTIVATION of MESOZOIC NORMAL FAULTS.

Yuan-hsin Chen, Jelle Zeilinga de Boer, (Both at: Dept. of Earth & Environmental Sciences, Wesleyan University, Middletown, CT 06457-6034)

Fracture attitudes (and density) were measured in a core drilled through the Honey Hill fault zone (Haddam, Ct), using the northdipping foliation for reorientation of core segments. This data base is compared with brittle fractures exposed at the surface and provides a 3.D pattern to a depth of 1500'. While late Paleozoic deformation in the H.H. fault zone was characterized by SE thrusting-reverse faulting, Mesozoic deformation occurred by WNW-ESE and NW-SE extension along penetrative conjugate sets of normal faults. The data suggests that strain resulting from the present day E-W compression maybe released by reversal of motion along fractures of the latter group. Individual normal faults have relatively small surface areas. Reactivation could, however, make use of a conjugate system of intersecting fractures, thereby significantly increasing the area of cumulative strain release (and earthquake magnitude). The highest densities of normal faults occur in relatively narrow (100 ft) zones at depth levels 698-800 and 1076 to 1169 ft. The upper zone contains several low angle thrusts with E-W slickensides and brecciated normal faults.

T51B-05 0945H

Neotectonic, Geochemical, and Lineament Studies of the Moodus Seismic Area

CHRISTOPHER A. SHUMAN and SHELTON S. ALEXANDER (Dept. of Geosciences, Penn State, Univ. Park, PA 16802)

In an attempt to identify neotectonic features in the seismically active area near Moodus, Connecticut, a reconnaissance study was conducted consisting of: 1) a review of previous geologic research in the region for mention of features related to local seismic activity; 2) examination and sampling of the area's stream network to identify geochemical species which might show ground-water flow along faults or fractures; and 3) a study of remote sensing imagery at four scales (SLAR 1:250,000, SPOT 1:100,000, high-altitude photography 1:80,000, and low-altitude photography 1:18,000) for the presence of lineaments or other features possibly related to bedrock fractures and tectonic stresses.

No unambiguous evidence of neotectonic geologic features has previously been reported. Our limited geochemical studies in the Moodus area revealed no evidence of supersaturated conditions in 33 bottom samples and 8 water samples. Lineament analysis at the four scales produced data on lineament orientations, frequencies, and lengths. Prominent lineament orientation peaks at 060-090 and 340-330 degrees are nearly parallel and perpendicular, respectively, to the direction of the maximum compressive stress (σ_1) as determined from in situ stress and earthquake focal mechanisms which suggests a causal association with a thrust stress regime. Lineament frequency was observed to increase in the Moodus quadrangle relative to adjacent study quadrangles, suggesting an increase in fracture density in the vicinity of the seismic area. From the multi-scale lineament data, we found an exponential decay in lineament frequency per unit area and a linear increase in average lineament length with increasing spatial scale number.

T51B-06 1015H INVITED

In-Situ Stress Measurements in the Earth's Crust Near Moodus, Connecticut

M H Singh and T A Rundle (Engineers International, Inc., Westmont, IL 60559-1595; 312-963-3460)
(Sponsor: C T Stratton)

Estimation of the occurrence and severity of vibratory ground motions in the vicinity of nuclear power plants and other related facilities is significant in the rational design of these facilities, and also in the evaluation of existing facilities. In order to reduce the uncertainty in estimating seismic risk for this purpose two holes were drilled for hydrofracture tests in the Moodus area. The first, to a depth of 1,000 ft, was drilled within the "generally accepted" seismic zone. The direction of the largest horizontal stresses was determined to be nearly N48°W. The second hole was drilled approximately 8 miles to the south to a depth of 1,500 ft, hydrofracture tests in which indicated the largest horizontal principal stress direction to be N75°W. The maximum hole deviations from the vertical were 3° for the first hole and 12° for the second. Stress magnitudes in these holes were also estimated.

T51B-07 1030H

Hydraulic Fracturing Stress Measurements in the Moodus Research Borehole and Shallow Earthquakes

Mark D. Zoback, Joerg Baumgaertner, and Daniel Moos (all at the Dept. of Geophysics, Stanford University, Stanford, CA 94305)

In July 1987, 13 hydrofracture experiments were conducted in the Moodus research borehole over the depth range between 100 and 1300 m. Over the entire depth range of the tests the maximum horizontal compression is sufficiently greater than the vertical stress that N-S striking thrust faults are potentially active. This observation is in good agreement with shallow fault plane solutions in this area. At all depths the least principal stress was vertical and approximately equal to the weight of the overburden. This is confirmed by the generation of sub-horizontal fractures in three test sections at 837 m, 1184 m, and 1277 m. During these tests only the vertical stress S_v was measured as shut-in pressure. In

NRC FORM 335 (2-84) NRCM 1102, 3201, 3202

U.S. NUCLEAR REGULATORY COMMISSION

BIBLIOGRAPHIC DATA SHEET

SEE INSTRUCTIONS ON THE REVERSE

1. REPORT NUMBER (Assigned by TIDC, add Vol. No., if any)
NUREG/CR-5418

2. TITLE AND SUBTITLE
Near-Surface Neotectonic Deformation Associated with Seismicity in the Northeastern United States

3. LEAVE BLANK

4. DATE REPORT COMPLETED
MONTH: July YEAR: 1989

5. AUTHOR(S)
S. S. Alexander, D. P. Gold, T. W. Gardner, R. L. Slingerland, C. P. Thornton

6. DATE REPORT ISSUED
MONTH: October YEAR: 1989

7. PERFORMING ORGANIZATION NAME AND MAILING ADDRESS (Include Zip Code)
Department of Geosciences
Pennsylvania State University
503 Deike Building
University Park, PA 16802

8. PROJECT/TASK/WORK UNIT NUMBER

9. FIN OR GRANT NUMBER
D1150

10. SPONSORING ORGANIZATION NAME AND MAILING ADDRESS (Include Zip Code)
Division of Engineering
Office of Nuclear Regulatory Research
U.S. Nuclear Regulatory Commission
Washington, DC 20555

11a. TYPE OF REPORT
Final

b. PERIOD COVERED (Inclusive dates)
February 1985-July 1989

12. SUPPLEMENTARY NOTES

13. ABSTRACT (200 words or less)

An investigation of the Lancaster, PA seismic zone using remote sensing data, surface geology and recent seismicity has revealed that neotectonic deformation is concentrated in a NS-trending fault zone some 50 km in length and 10-20 km in width. This zone is associated with lineaments and erosion patterns, recent uplift along the Susquehanna River, and travertine deposits downstream from the inferred active fault zone. In the Moodus seismic zone it was observed that the frequency of tectonically controlled lineaments increases in the Moodus quadrangle compared to adjacent areas and that the dominant lineament directions are perpendicular and parallel to the maximum horizontal stress direction (N80-85E) as determined from borehole measurements and earthquake focal mechanisms.

One of the most important results of this study is the identification of travertine as a promising indicator of recent fault movements in areas underlain by carbonate rocks. Using this theory, travertine deposits were discovered just downstream from the Fruitville fault which is associated with the major recent earthquake activity in the Lancaster area.

14. DOCUMENT ANALYSIS - a. KEYWORDS/DESCRIPTORS

Lancaster, PA — Neotectonics
Moodus, CT — Travertines
Seismicity — Lineaments

b. IDENTIFIERS/OPEN-ENDED TERMS

15. AVAILABILITY STATEMENT
Unlimited

16. SECURITY CLASSIFICATION
(This page) Unclassified
(This report) Unclassified

17. NUMBER OF PAGES

18. PRICE

*U.S. GOVERNMENT PRINTING OFFICE:1989-262-436:00309

UNITED STATES
NUCLEAR REGULATORY COMMISSION
WASHINGTON, D.C. 20555

OFFICIAL BUSINESS
PENALTY FOR PRIVATE USE, $300

SPECIAL FOURTH CLASS RATE
POSTAGE & FEES PAID
USNRC
PERMIT No. G-67

120555139531 1 1AN1RA
US NRC-OADM
DIV FOIA & PUBLICATIONS SVCS
TPS PDR-NUREG
P-223
WASHINGTON DC 20555